AFOSR-TR. 89-0021

SC5493.FR

Copy No. 08

THERMAL DECOMPOSITION OF TNT AND RELATED MATERIALS IN THE CONDENSED PHASE

AD-A204 363

SC5493.FR

FINAL TECHNICAL REPORT FOR THE PERIOD
November 1, 1986 through September 30, 1988

Prepared for

Air Force Office of Scientific Research
Directorate of Chemical and Atmospheric Sciences
Building 410
Bolling AFB, DC 20332-6448

DTIC
ELECTE
FEB 1 3 1989
D

T.M. McKinney and I.B. Goldberg

JANUARY 1989

Rockwell International
Science Center

89 2 10 134

The Contractor, Rockwell International Corporation Science Center, hereby certifies that, to the best of its knowledge and belief, the technical data delivered herewith under Contract No. F4960-87-0003 is complete, accurate, and complies with all requirements of the contract.

REPORT DOCUMENTATION PAGE

1a. REPORT SECURITY CLASSIFICATION		1b. RESTRICTIVE MARKINGS			
UNCLASSIFIED					
2a. SECURITY CLASSIFICATION AUTHORITY		3. DISTRIBUTION/AVAILABILITY OF REPORT			
2b. CLASSIFICATION/DOWNGRADING SCHEDULE		Approved for public release; distribution is unlimited			
4. PERFORMING ORGANIZATION REPORT NUMBER(S)		5. MONITORING ORGANIZATION REPORT NUMBER(S)			
SC5493.FR		AFOSR·TR· 89-0021			
6a. NAME OF PERFORMING ORGANIZATION	6b. OFFICE SYMBOL (If Applicable)	7a. NAME OF MONITORING ORGANIZATION			
ROCKWELL INTERNATIONAL Science Center		AFOSR			
6c. ADDRESS (City, State, and ZIP Code)		7b. ADDRESS (City, State and ZIP Code)			
1049 Camino Dos Rios Thousand Oaks, CA 91360		same as 8c			
8a. NAME OF FUNDING/SPONSORING ORGANIZATION	8b. OFFICE SYMBOL (If Applicable)	9. PROCUREMENT INSTRUMENT IDENTIFICATION NUMBER			
AFOSR, Directorate of Chemical and Atmospheric Sciences	NC	CONTRACT NO. F49620-87-C-0003			
8c. ADDRESS (City, State and ZIP Code)		10. SOURCE OF FUNDING NOS			
Building 410 Bolling AFB, DC 20332-6448		PROGRAM ELEMENT NO. 61102F	PROJECT NO. 2303/B1	TASK NO. B1	WORK UNIT ACCESSION NO.

11. TITLE (Include Security Classification)
THERMAL DECOMPOSITION OF TNT AND RELATED MATERIALS IN CONDENSED PHASE

12. PERSONAL AUTHOR(S)
McKinney, T.M. and Goldberg, I.B.

13a. TYPE OF REPORT	13b. TIME COVERED	14. DATE OF REPORT (Year, Month, Day)	15. PAGE COUNT
Final Report	FROM 11/01/86 TO 09/30/88	1989 JANUARY	177

16. SUPPLEMENTARY NOTATION

17. COSATI CODES			18. SUBJECT TERMS (Continue on reverse if necessary and identify by block number)
FIELD	GROUP	SUB-GROUP	

19. ABSTRACT (Continue on reverse if necessary and identify by block number)

2,4,6-Trinitrotoluene (TNT) undergoes thermal composition by a process that permits ESR observation of two distinctly different free radical species. The initial free radical has been ascribed to intermolecular coupling of two TNT moieties to produce a nitroxide with distinctive hyperfine structure. The other species has a single featureless ESR absorption line. It appears to arise from a polymeric material which we call "Tar."

The kinetics of formation of these two species was monitored by ESR. Analysis reveals that Tar is produced at an accelerated rate early in the reaction, as compared to the autocatalytic (i.e., pseudo-first order with respect to Tar) rate observed later. TNT. (polymer)

20. DISTRIBUTION/AVAILABILITY OF ABSTRACT	21. ABSTRACT SECURITY CLASSIFICATION		
UNCLASSIFIED/UNLIMITED ☐ SAME AS RPT ☒ DTIC USERS ☐	UNCLASSIFIED		
22a. NAME OF RESPONSIBLE INDIVIDUAL	22b. TELEPHONE NUMBER (Include Area Code)	22c. OFFICE SYMBOL	
Major Larry Davis	(202) 767-4960	NC	

DD FORM 1473, JUN 86   Previous editions are obsolete.

19 ABSTRACT (Cont'd)

A series of reactions is proposed:
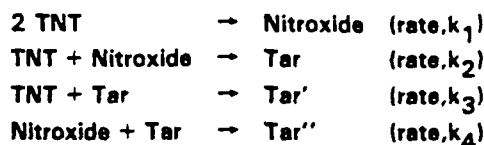
2 TNT	$\rightarrow$	Nitroxide	(rate,k_1)
TNT + Nitroxide	$\rightarrow$	Tar	(rate,k_2)
TNT + Tar	$\rightarrow$	Tar'	(rate,k_3)
Nitroxide + Tar	$\rightarrow$	Tar''	(rate,k_4)

Numerical simulations based on rate expressions for this set of simultaneous processes yield concentration-time curves with the same characteristics as the experimental curves.

Experimentally, the nitroxide concentration remains small and behaves as if nitroxide is a reactive intermediate. Known disproportionation reactions of dibenzylnitroxide provide a reasonable model for the observed behavior of the nitroxide from TNT as a participant in a dynamic reaction cycle. The nitrone that results from the disproportionation also provides a likely candidate for reactions leading to Tar-like species.

The presence of moisture in TNT promotes high nitroxide concentrations under relatively mild thermolysis conditions. It is not clear whether water enhances nitroxide production or inhibits nitroxide destruction. Moisture has negligible effect on the development of Tar.

Hexamethylbezene (HMB) and TNT react to form mixtures of spectrally similar nitroxide radicals. The kinetics can be simulated on the basis of a set intermolecular condensation reactions analogous to that of TNT.

Hexamethylbezene and 2,4,6-trintrobezene (TNB) do not provide a clean model system for the TNT reaction because many different nitroxide-like radicals are also observed. The proportions of radicals depend on reactant ratios as well as temperature of formation. The effect of charge transfer intermediates is considered to be an important route to formation of secondary nitroxides in systems containing HMB.

Trace quantities of almost any material or small changes in experimental conditions affect the course of thermal decomposition of TNT. This fact exacerbates the problem of kinetic and mechanistic studies because seemingly inconsequential changes in experimental conditions may have a significant impact on experimental reproducibility. A number of different materials were intentionally added in efforts to learn more about the nature and process of Tar production.

Nucleophiles have a profound effect on TNT decomposition. Tar formation is enhanced but the nature of the Tar, as reflected by the g-factor, depends on the individual nucleophile. Acids on the other hand appear to retard radical and Tar formation. The effect is more pronounced with phosphoric acid. This may warrant further investigations as a means for desensitizing TNT and extending its storage life. Oxidants, reductants, and spin traps were also studied.

Known products of TNT oxidation include 2,4,6-trinitrobenzyl alcohol, 2,4,6-trinitrobenzaldehyde, and 2,4,6-trintrobenzoic acid. These compounds produce distinctive ESR spectra depending on whether they are thermolysed in the pure state, in benzene solutions, or in the presence of TNT or hexamethylbenzene. Several of the spectra have been assigned on the basis of numbers and kinds of magnetic nuclei, but molecular structures have not been verified.

TABLE OF CONTENTS

TABLE OF CONTENTS (Continued)

Accession For

NTIS   CRA&I   ✓
DTIC   TAB
Unannounced
Justification

By
Distribution

Dist

A-1

QUALITY
INSPECTED
4

LIST OF FIGURES

LIST OF FIGURES (Continued)

LIST OF FIGURES (Continued)

LIST OF FIGURES (Continued)

LIST OF FIGURES (Continued)

LIST OF FIGURES (Continued)

I. HISTORICAL BACKGROUND

The thermal decomposition of TNT has been a subject of military and technological interest for decades. It was first synthesized in 1863 by Wilbrand. It has long been recognized that prolonged storage produces deterioration which diminishes the stability of TNT and leads to unpredictable behavior. A better understanding of the processes responsible for such degradation could provide a rational foundation for selecting appropriate additives and storage conditions that would help to stabilize military and industrial explosives.

Researchers have noted the presence of free radicals during the course of thermal decomposition of TNT.[1,2,3] The significant features of such observations include the early observation of a complex ESR spectrum comprising many hyperfine lines followed by exponential growth of a progressively dominating species with only a single line as shown in Fig. 1. Even without detailed knowledge of the identity of the initial species a large effort was expended in investigating the kinetics of formation of the secondary species.[2]

Prior to the initiation of this Contract we collaborated with personnel at the F.J. Seiler Laboratory of the USAFA and the result of this cooperation was a proposed reaction scheme and identification of the initial radical.[4]
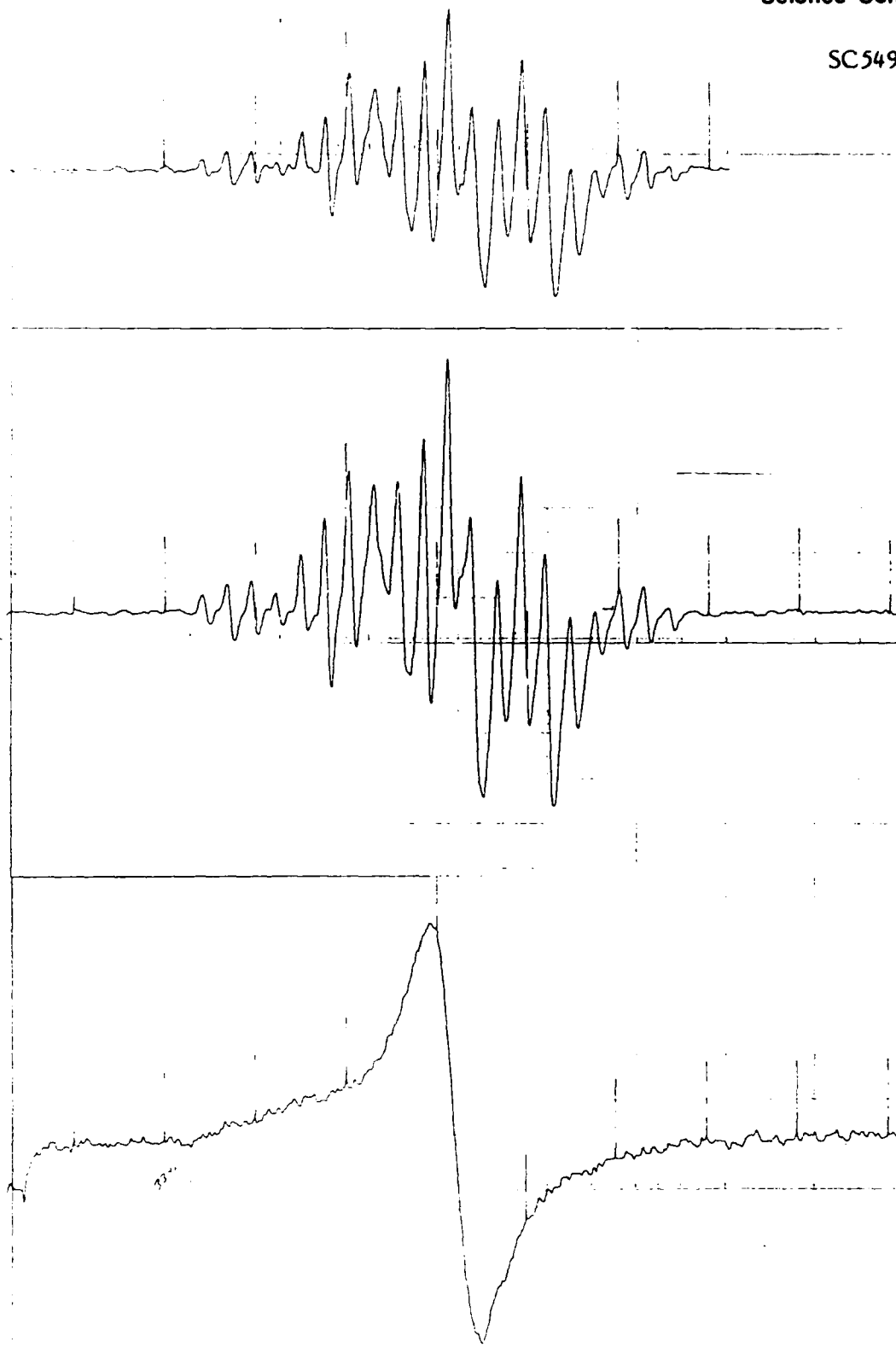
Fig. 1 Time evolution of ESR spectra during thermolysis of TNT.

$$2 \text{ (2,4,6-trinitrotoluene)} \longrightarrow \text{CH}_3\text{-(ArNO}_2\text{H)} + \text{CH}_2\text{-(ArNO}_2\text{)}$$

$$\text{CH}_3\text{-(ArNO}_2\text{H)} \longrightarrow \text{OH}^\bullet + \text{CH}_3\text{-(ArN=O)}$$

(1)

$$\text{CH}_3\text{-(ArN=O)} + {}^\bullet\text{CH}_2\text{-(ArNO}_2\text{)} \longrightarrow \text{CH}_3\text{-Ar-N(O}^\bullet\text{)-CH}_2\text{-Ar-NO}_2$$

1
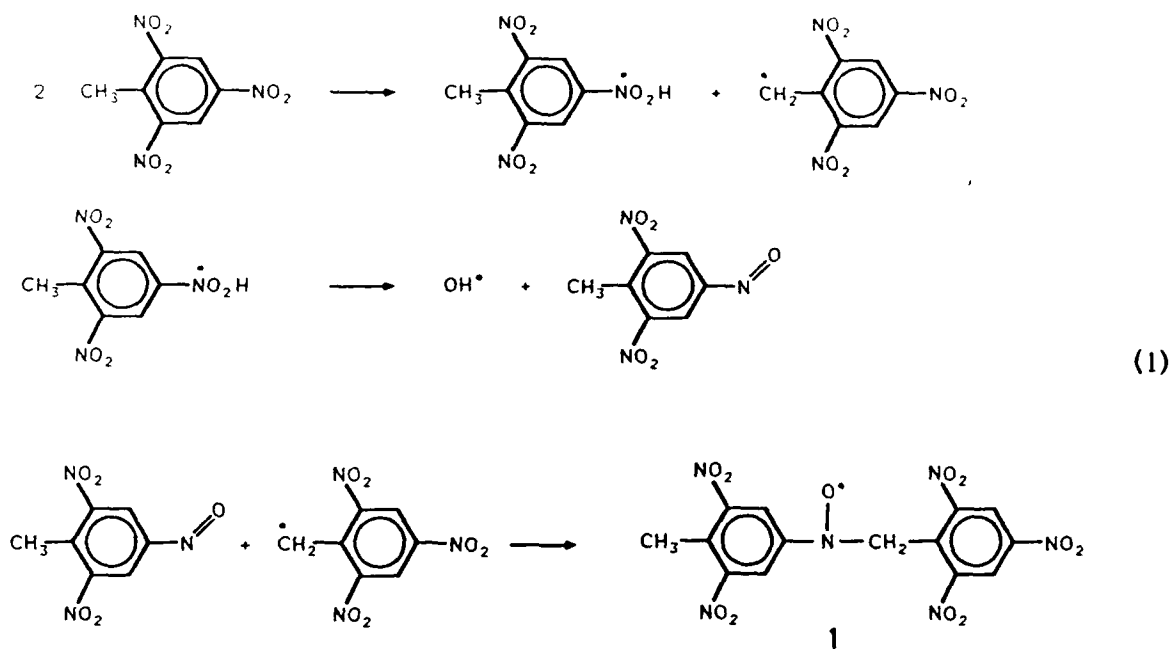
These suggestions have been widely accepted in the high energy materials community and constitute the basis for much current research activity.

It would be extremely useful to find an inert solvent in which to pursue kinetic studies of TNT decomposition and make systematic studies of concentration effects. Two different materials were proposed and used in the period prior to our involvement in the program, when the TNT decomposition was thought to proceed primarily by an intra-molecular pathway. One diluent was 1,3,5-trinitrobenzene which, lacking an oxidizable methyl group, was presumed to be inert under the reaction conditions. The other puta-tive diluent was hexamethylbenzene which, lacking any nitro substituents, was presumed to be unreactive. It was recognized from the earliest experiments using HMB that some unexpected reaction was occurring because the nitroxide species was formed much more readily and at much lower temperatures than with neat TNT decomposition reactions.

We subsequently showed in,[4] that TNB and HMB each readily couple with TNT and also couple with each other in the absence of TNT. These observations were in fact the foundation for the above reaction scheme and nitroxide radical structure determination. However, later in the present Report we will describe additional

observations that reveal deeper levels of complexity in the reactions of TNB and HMB which suggest that even this supposedly straightforward system is subject to competitive reaction pathways.

The reactivity of TNB and HMB toward TNT precludes their utilization as inert solvents. But on the other hand, a better understanding of these reactions and evaluation of the kinetics can also be used to gain insights into the fundamental chemistry of TNT itself.

Of course, it would still be useful to find a truly inert solvent for TNT that would permit evaluation of concentration effects. A number of different candidates have been screened but none meet the necessary criteria of chemical inertness and TNT solubility. We found that in general the reaction between nitro- and alkyl-aromatic compounds follow the general reaction

$$Ar-NO_2 + CHR_2-Ar' \rightarrow Ar-N-CR_2-Ar' \qquad (2)$$

to form a nitroxide radical analogous to nitroxide 1.[5] Even aliphatic hydrocarbons react with nitroarmatics to form a variety of nitroxide products. Benzene appears to be an adequately inert solvent at temperatures below 250°C, but the absence of nitroxide formation indicates that the mechanism requires that two TNT molecules must be in close proximity for the reaction to occur. Consequently, kinetic studies continue to be clouded by the inability to investigate concentration dependence.

II. PRESENT WORK

A. Description of the Spectra

The earlier work by Davis[2] et al indicated that the radicals formed during TNT thermolysis appear in stages. Initially, after an induction period, a species with rich hyperfine structure is observed. This is the radical that we have since identified as nitroxide 1. After a longer induction period the spectrum begins to appear progressively more asymmetric and is ultimately dominated by a single, broad line. This line grows at an exponential rate. The kinetic behavior of this single-line species was the subject of most of the earlier studies.

In the interest of verbal economy in this report, we shall indulge in a colloquialism and refer to this single-line species as "Tar." The intensity of the ESR signal from this material correlates well with the degree of discolorization of the sample and so Tar is probably an ill-defined polymeric material, related to the pyrolysis of TNT and its decomposition products.

Figure 2 shows an ESR spectrum observed early in a TNT thermolysis experiment. A distinctive feature of the spectrum is the grouping of the lines into five main branches having intensities in the ratio 1:3:4:3:1. Each of these branches is further split into lines having intensity ratios of 1:5:10:10:5:1, although the outer lines of these sextets overlap between contiguous branches. It was shown in[4] that the 5-branch pattern can arise from nitroxide 1, with the splitting of the nitroxide nitrogen atom being accidentally equal to that of the two benzylic hydrogen atoms. The sextet splitting arises from three methyl protons and two ortho ring protons having the same hyperfine splitting constants as is a general feature of aromatic nitroxides.[5,6]

Early in the program we began to refer to the pertinent ESR spectral lines by a set of arbitrary identifiers, Line 1, Line 2, .., Line 8 as shown in Fig. 3. As the program continued, it became clear that Lines 1, 5, and 8 were the most important in terms of interpretation of kinetics. Unfortunately, our numbering scheme is at odds with the earlier scheme used by Guidry and Davis et al (who also had to revise their original scheme when better quality spectra were obtained).[2]

SC5493.FR
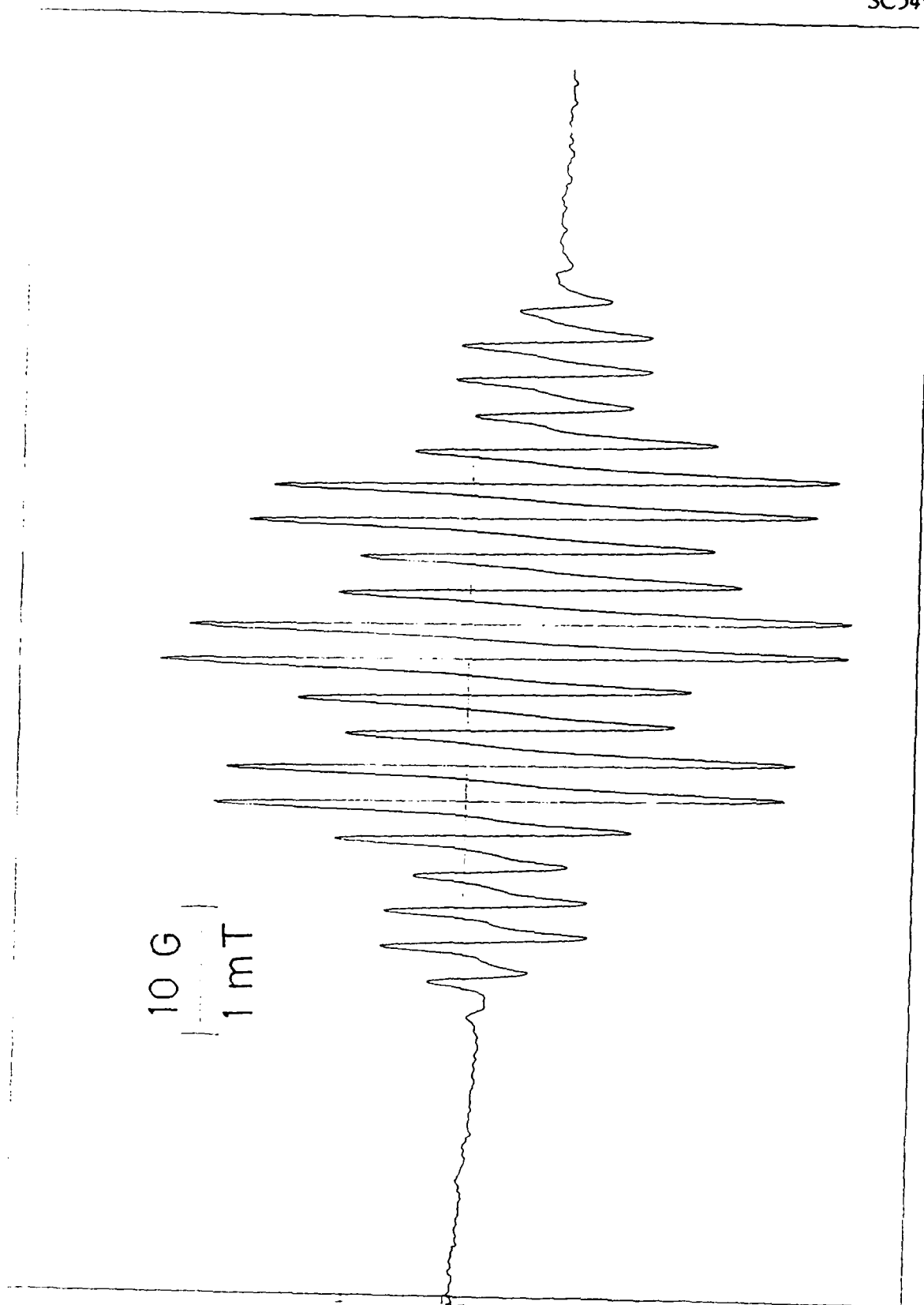
Fig. 2 ESR spectrum of TNT heated at 195° for 800 sec.

10 G
1 mT

Figure 3 shows a stick spectrum with all the pertinent numbering schemes identified. Since the opportunity for confusion is rampant, we shall use the letters A, B, and C to identify the lines that will be important to our analysis. As will be shown below, the difference between the amplitude of lines C and B is an important quantity for evaluations of the early kinetics of tar formation.

The magnetic field at the line-center of the Tar absorption occurs about 3.0 G above the midpoint of the nitroxide spectrum. It is coincident with Line C of the nitroxide spectrum. In the absence of any polymeric radical, the intensity (measured as peak-to-peak amplitude of the first derivative line) of any two symmetrically disposed lines above and below the field center should be identical, neglecting anomalous line width effects. (Even if there were significant line width variation, it should be time-independent for isothermal experiments and consequently would have no effect on the following analysis.) Thus, in principle, any one of the nitroxide lines could have been used to monitor the nitroxide kinetic behavior, so long as it is well separated from the magnetic field at which Tar exhibits significant absorption. However, there is less chance for signal-to-noise measurement error when strong lines are chosen. Consequently, Line A, which is is the strong line with the greatest separation from Tar absorption was taken as best representing the kinetic behavior of the nitroxide species. The corresponding line at the high-field end of the spectrum would be less satisfactory because in addition to being closer to the Tar absorption, it is also anomalously broadened by relaxation processes associated with incomplete averaging of hyperfine and g-tensor anisotropies.

The overlap of lines in the nitroxide spectra and the fact that Tar lineshape overlaps much of the nitroxide spectrum preclude the use of double integration of the derivative lineshape as a means of determining the nitroxide and Tar concentrations. Although double integration is more accurate, it has too many experimental difficulties to be applied to this problem.

The nearly-equal values of a_N and $a_{\beta-CH_2}$ for the nitroxide radical[4] introduces some uneasiness about the utility of using other hyperfine lines from the more intense members of the 1:3:4:3:1, 5-branch pattern to track the nitroxide kinetics. Any small differences between a_N and $a_{\beta-CH_2}$ readily distorts this pattern to non-integral ratios. There is such a wealth of examples of temperature-dependent hyperfine ESR splittings
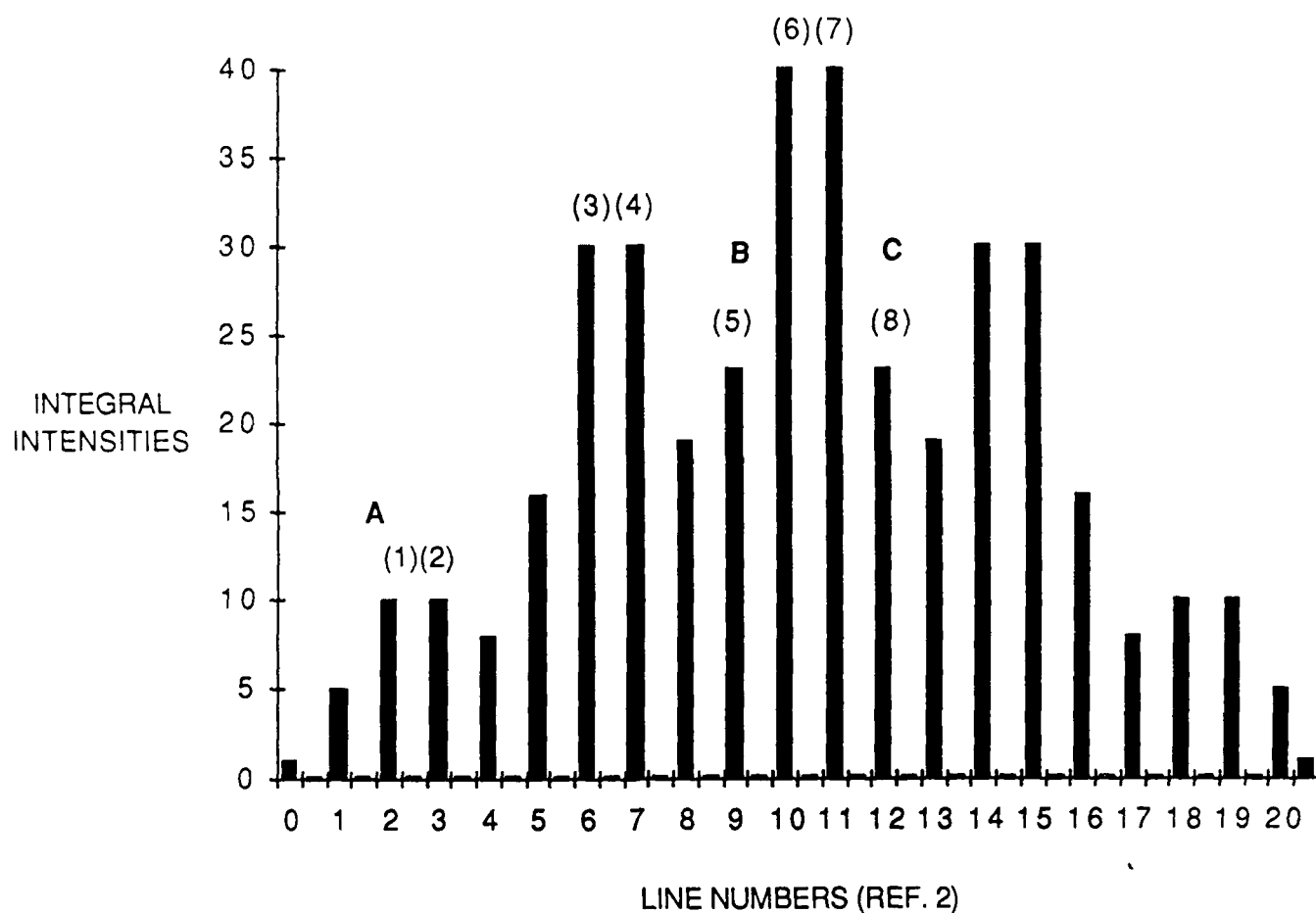
Fig. 3   Stick diagram of ESR line positions from radical 1. Ordinate reflects number-
ing scheme of Ref. 1.   Identifiers in parenthesis were used in our early
analyses.   Letters A, B and C identify lines important to arguments in this
report.

that it is unrealistic to assume that the TNT-nitroxide species is immune to such variations. Nonetheless, meaningful kinetic data can be gleaned from this less-than-ideal situation. Lines B and C are identified as the penultimate (intensity = 5 in a 1:5:10:10:5:1 sextet pattern) members of the major, central branch. The Tar absorption eventually appears at the position of Line C while the kinetics of Line B tracks quite closely the early behavior of Line A.

However, over the course of a reaction, B decreases faster than A. This is due to "intensity borrowing" from line B when the broader Tar line starts to interfere destructively with B. This is brought out rather well in Fig. 4 by looking at all the strong lines in the central branch, (lines that were once called "5", "6", and "7") in a run such as 1.A.1. It is noted that the lines closer to the Tar absorption (once called line "8") fall off faster than those nitroxide lines farther away because the growth of the broader Tar line obscures nearby lines.
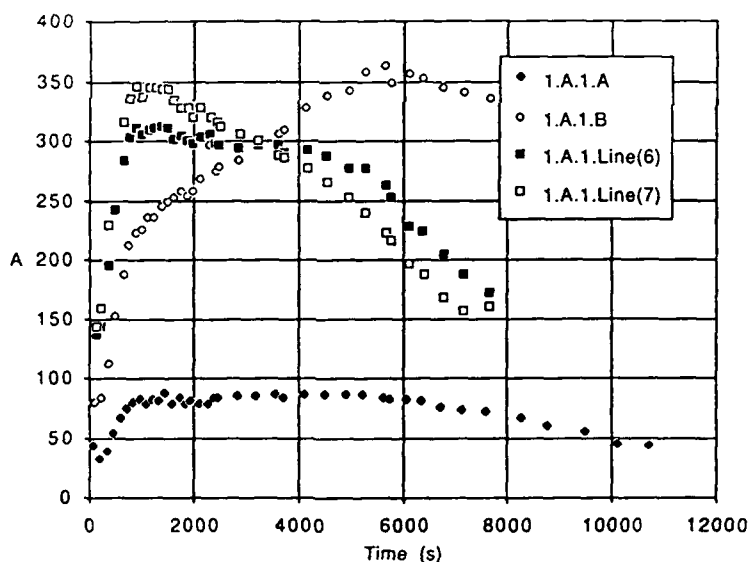
Fig. 4   Nitroxide behavior during the thermal decomposition of TNT at 228°C as indicated by different lines of the spectrum.

It is tempting to consider analyzing the Tar kinetics on a more rigorous basis, grounded in assumptions about the theoretical intensity ratios of the various lines. One such approach would involve the approximations that the absorption due to Tar, A_T, can be evaluated as the amplitude of line C minus twice the ample of line A,

$$A_T = A_C - 2A_A. \tag{2}$$

rather than using lines C and B,

$$A_T = A_C - A_B \tag{3}$$

However, A_B is seldom precisely $2A_A$ even in the earliest stages of the reaction because of either the aforementioned slight inequality of a_N and $a_{\beta-CH_2}$, or the ubiquitous problem of anomalous relaxation which produces unequal line widths in nitrogen-containing radicals.

The line width of the Tar absorption itself introduces even greater difficulties for a rigorous comparison of Tar and nitroxide kinetics. The Tar absorption has a significantly larger line width due to factors such as unresolved hyperfine contributions and anisotropies that are incompletely averaged as the polymeric species becomes heavier and more immobile. Since all of the data-analyses described below estimate the Tar concentration on the basis of peak-to-peak amplitude measurements, they tend to underestimate the absolute rate of Tar growth. Double integration of the spectrum is not a tenable option, however, because of the impossibility of accurately subtracting the nitroxide contribution. Furthermore, we show later that the situation becomes even more complicated due to the presence of several different nitroxide radicals.

In order to gain new insights into the kinetics of Tar formation, the spectra were analyzed by measuring the amplitudes of lines B and C as a function of time. Being symmetrically disposed about the center, the difference (A_C-A_B) should be constant until the formation of Tar begins to add intensity to the absorption falling at the position of line C. It was enlightening to find that this analysis indicates that Tar formation occurs from the very earliest stages of heating TNT (Fig. 5) based on the fact that the linear portion of the log plot does not extrapolate to zero. Discussion of this aspect of the problem will be deferred until later.

B.   Summary of Experiments Performed

Many kinetic ESR experiments have been performed during this program. In order to simplify references to the particular experiments they are given individual
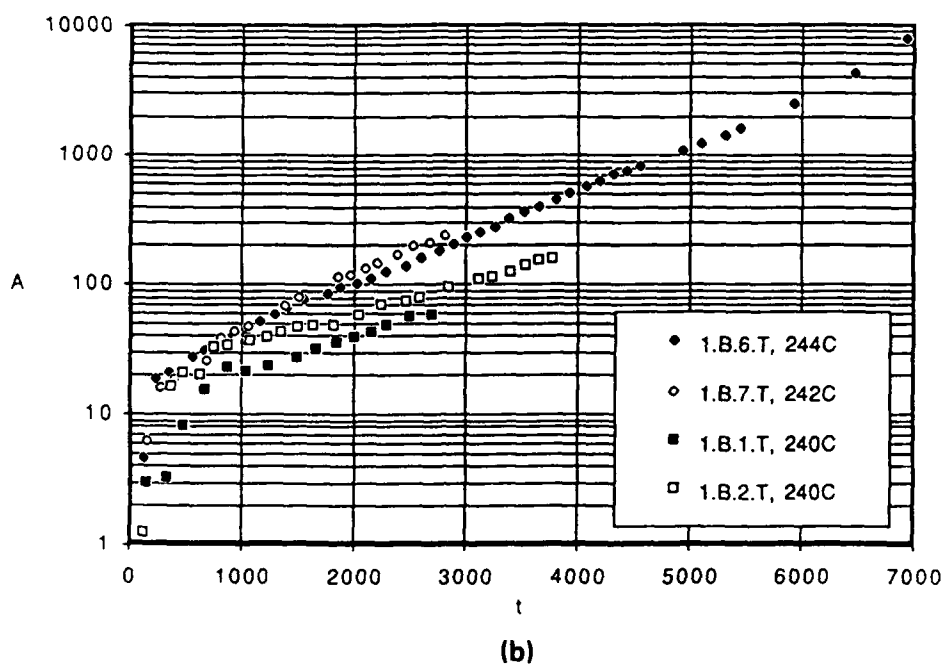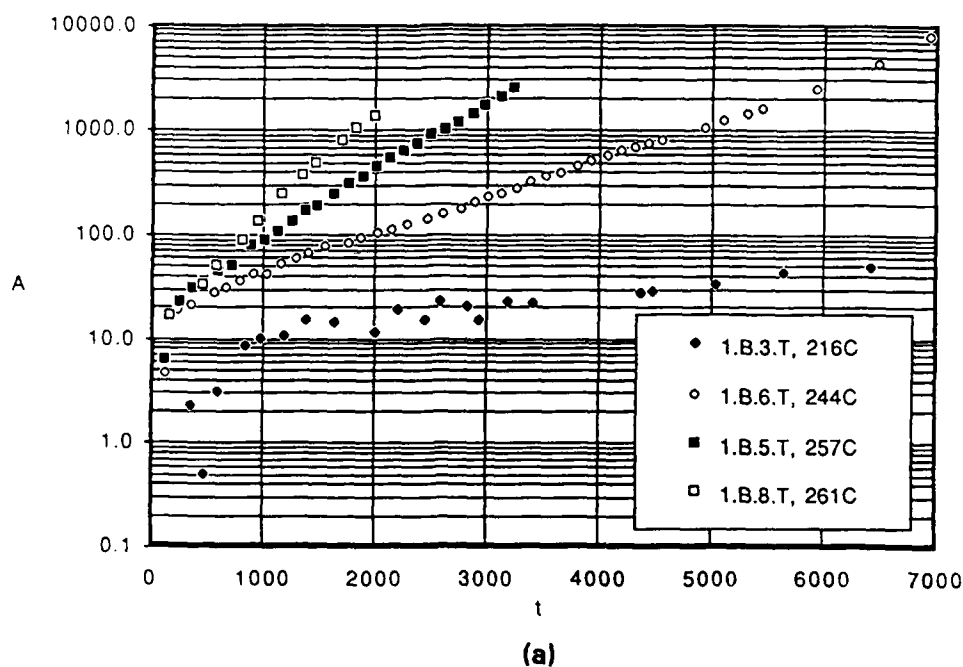
Fig. 5   Tar growth during TNT thermolysis at several different temperatures: (a) wide temperature range, and (b-d) narrower temperature ranges showing more detail than a.

(a)

(b)
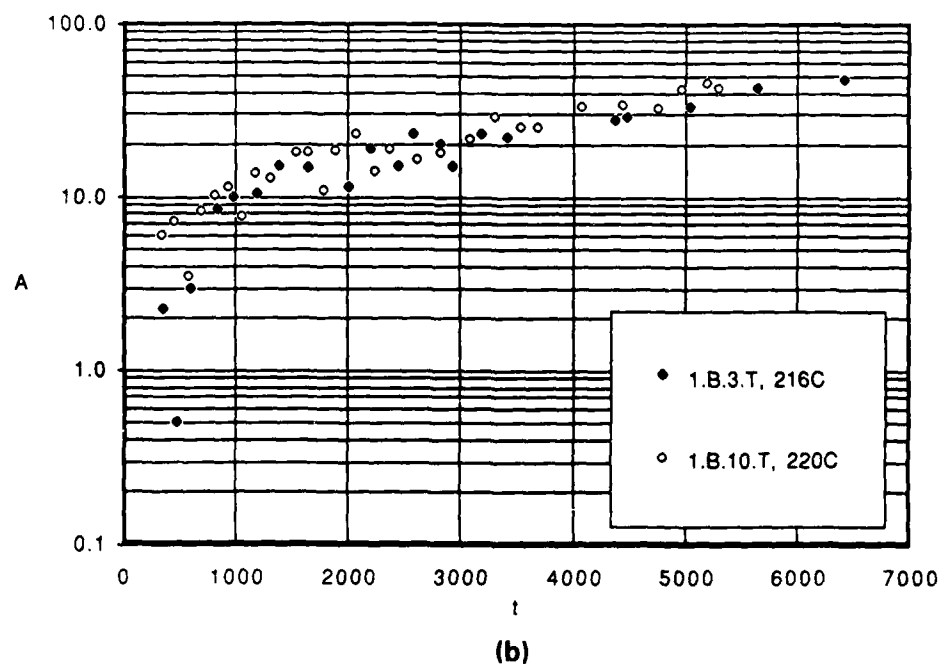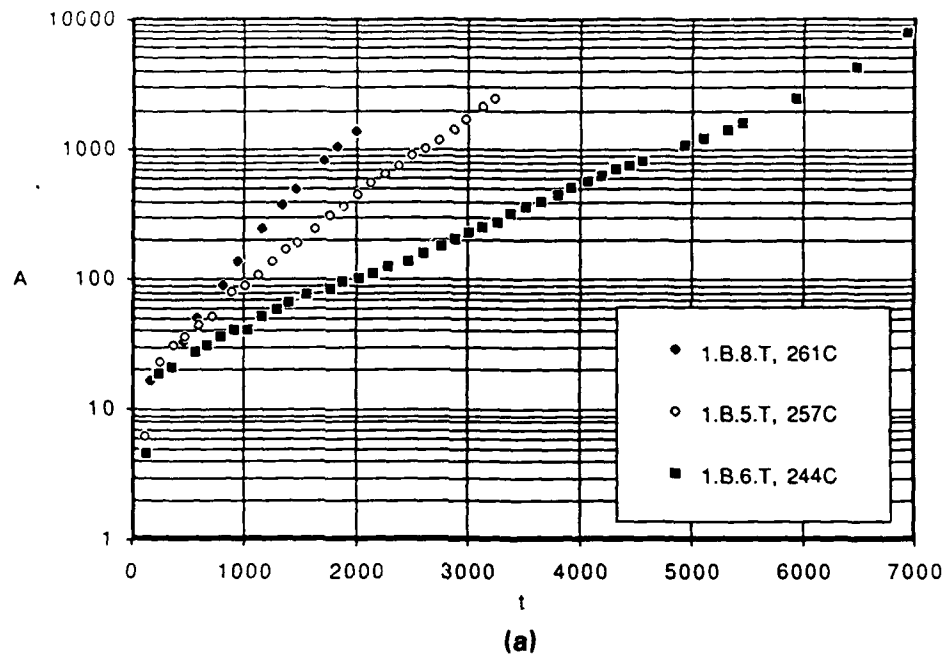
Fig. 5 (Continued)

identifiers of the form N.L.n.l according to the scheme outlined in Table 1. The first number and letter refers to a particular chemical compound or mixture of compounds while the subordinate number indicates a serial identifier; occasionally, in the figures and discussions that follow, a subordinate letter is appended to identify behavior of a particular spectral line, as in the case of Tar ($= A_C-A_B$) behavior in Fig. 5.

Table 1

Identification Scheme for TNT Kinetic Experiments

1. Neat TNT
   - A.　Initial material, subjected to preliminary purification
   - B.　More highly purified material
2. TNT plus water
   - A.　Initial material, subjected to preliminary purification
   - B.　More highly purified material
3. TNT plus HMB (hexamethylbenzene)
   - A.　5 mol % TNT
   - B.　10 mol % TNT
   - C.　10 mol % TNT plus water
   - D.　20 mol % TNT
   - E.　50 mol % TNT
   - F.　95 mol % TNT
   - G.　TNT reactions with HMB-d_{18}
4. Trinitrobenzene (TNB) plus HMB
   - A.　5 mol % TNB
   - B.　95 mol % TNB
   - C.　50 mol % TNB
   - D.　Reactions with HMB-d_{18}
5. Miscellaneous additives
   - A.　"Coke"; other fractions from TNT reactions
   - B.　Solvents and other amendments
   - C.　TNT with reductants, nucleophiles, and bases
   - D.　TNT with mineral acids
6. Systems with 4,6-Dinitroanthranil (DNAnth)
   - A.　Neat
   - B.　Benzene solvent
   - C.　TNB solvent
   - D.　TNT/DNAnth 4:1
   - E.　TNT/DNAnth 1:1
   - F.　TNT/DNAnth 9:1
   - G.　DNAnth/HMB
7. Detonation mixtures
   - A.　TNB-CHO/Benzene
   - B.　TNT/DNAnth/Benzene
   - C.　TNB-CH_2OH/Benzene

Table 1 (Continued)

8. Reactions with Phenyl-t-butyl nitrone

9. TNB Reactions

    A. Neat

    B. $TNB/Ca(OH)_2$

10. $TNB-CH_2OH$ Reactions

    A. Benzene solvent

    B. HMB

    C. TNT

11. TNB-CHO Reactions

    A. Benzene solvent

    B. HMB

    C. TNT

    D. Neat

12. Miscellaneous HMB Reactions

    A. HNO_3

13. Toluene solvent

    A. TNB-CHO

    B. TNT

14. TNT in Benzene

Table 1 is expanded in Appendix A to list all the kinetic reactions carried out on this project. In some instances, the data for a given run have not been analyzed due to instrumental problems; but the run has been retained in the reaction log in case it may yet be found useful.

C. TNT Kinetics

1. Qualitative Observations on Nitroxide Kinetics

The kinetics of the nitroxide species indicate that it plays the role of an intermediate in a more complex overall reaction scheme. Figure 6 shows plots of the

intensity of the nitroxide line A, A_A, versus time at many different temperatures ranging from 204-261°C. The following points should be noted:

(1)   The nitroxide concentration peaks at times inversely related to the temperature of the decomposition reaction.

(2)   The initial slopes and peak times are only moderately reproducible (as shown in Fig. 6b for the series of reactions done at 240°C).

(3)   At the lower end of the temperature range (Fig. 6c), there is an initial decrease in nitroxide intensity, followed by a rise to a plateau value which continues for a long interval.

This behavior suggests competition between nitroxide-forming and nitroxide-destroying reactions. It could also suggest an equilibrium between the paramagnetic nitroxide and a diamagnetic precursor which is depleted early in the reaction, but discussion of this point will be postponed.

These observations indicate that the nitroxide kinetics involve processes other than the basic steps outlined in Scheme 1.

A further curious feature of Fig. 6a is the observation that the rate of increase of A_A appears to be essentially independent of temperature over the range 216-261°C. This also appears to support the idea of either a diamagnetic precursor in equilibrium with nitroxide or of competitive production/destruction reactions. The fact that the nitroxide spectrum eventually decays is clear evidence that some destruction process ultimately prevails.

2.   Nitroxide Kinetics

One of the striking features of thermal decomposition of nitro-compounds as studied by ESR is the fact free radicals (as contrasted to Tar) are never present at very high concentrations. An upper limit for concentration is approximately 6×10^{-5} M under any circumstances. The experimentalist is usually pushing the spectrometer to its performance limits in an attempt to get well resolved spectra at a reasonable signal-to-noise values. Moreover, in kinetic studies, the need to sweep the spectrum repeatedly at short intervals in order to obtain the time dependence precludes use of signal averaging.

(a)

(b)
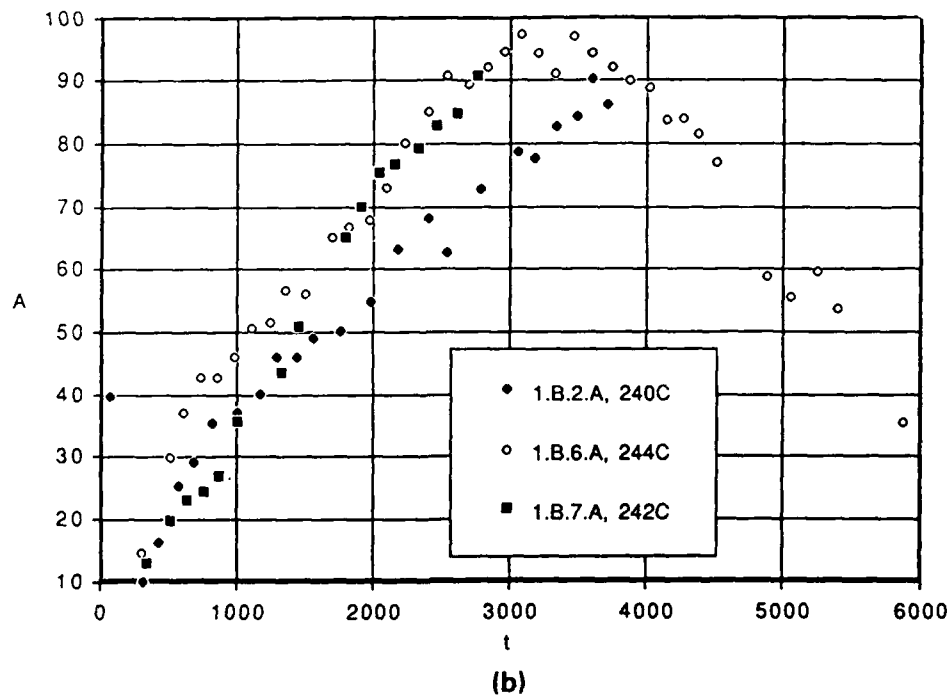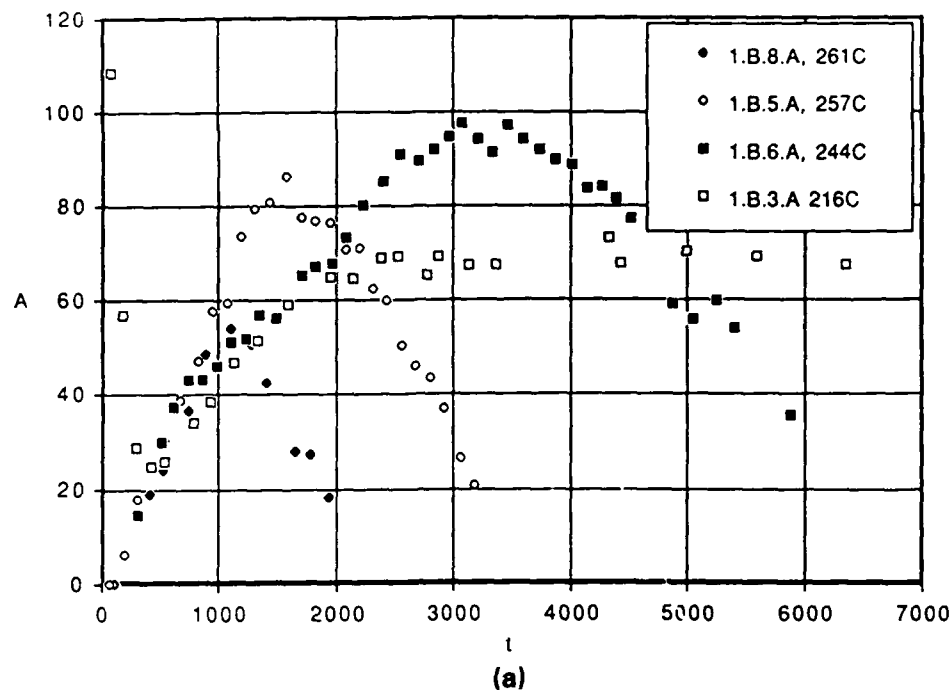
Fig. 6   Amplitude of the nitroxide signal as a function of time at different temperatures: (a) broad range of temperatures, and (b-c) narrower range showing more detail.

(c)
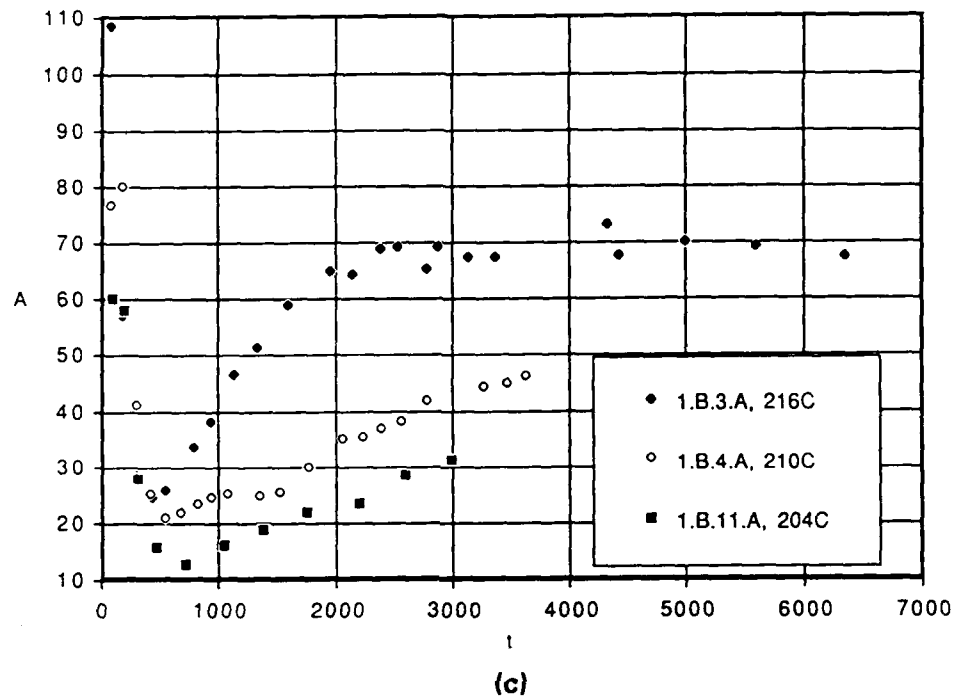
Fig. 6 (Continued)

The need to use small damping time constants to prevent distortions by overdamping is also deleterious to the signal-to-noise ratio.

The small concentration of nitroxide alone is sufficient foundation to state that the nitroxide radical observed in TNT thermolysis probably exists as a quasi-steady state intermediate in a more complicated set of chemical transformations. Taken together with the kinetic plots summarized in Fig. 6, this conclusion takes on additional credibility. This raises the obvious question about what sort of competing reactions could occur in this system to prevent buildup of a large concentration of nitroxide radicals.

Product identification was not one of the main goals of this program so we rely mainly on results of earlier work in the following discussion. Other studies of thermolysis of bulk samples of TNT have revealed the presence of tetranitro-azoxytoluene, 2,4,6-trinitrobenzaldehyde, picric acid and other unknown components when the polymeric "explosive coke" is subjected to thin layer chromatographic analysis with polar solvents.[7] With nonpolar solvents such as benzene, at least seven mobile aromatic components have been resolved and the two major components were identified as 4,6-dinitroanthranil and 2,4,6-trinitrobenzaldehyde.[4] Other workers have also identified the presence of 2,4,6-trinitrobenzyl alcohol, 2,4,6-trinitrobenzoic acid, and 1,3,5,-trinitrobenzene.[8,9]

The presence of these latter derivatives of TNT in which the methyl group has been oxidized are easily explained on the basis of a series of transformations related to the process already suggested in Scheme 1

$$CH_3ArNO_2 + CH_3Ar'NO_2 \rightarrow CH_3ArNO(OH\cdot) + \cdot CH_2Ar'NO_2 \qquad (4a)$$

$$\rightarrow CH_3ArNO + \cdot OH + \cdot CH_2Ar'NO_2 \qquad (4b)$$

$$\rightarrow NO_2Ar'CH_2OH \qquad (4c)$$
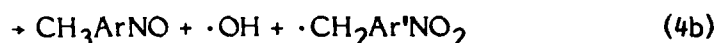
Subsequent reactions can likewise produce the more highly oxidized members of the series,

$$CH_3ArNO_2 + NO_2Ar'CH_2OH \rightarrow \rightarrow [NO_2Ar'CH(OH)_2] \rightarrow NO_2Ar'CHO + H_2O \qquad (5)$$

$$NO_2Ar'CHO + NO_2Ar'CH_2OH \rightarrow \rightarrow NO_2Ar'COOH \rightarrow NO_2Ar'H + CO_2 \qquad (6)$$

The presence of 4,6-dinitroanthranil can be explained formally by a simple dehydration reaction of TNT, but this begs the question of mechanism.

As a class, nitroxides tend to be quite stable (at room temperature), particularly when compared to most other free radicals.[10] While much of the stability of nitroxides arises from the fact that the valencies of nitrogen and oxygen are essentially satisfied,[11,12] the degree of steric protection around the nitroxide function can further enhance the stability. In general, primary alkylarylnitroxides (such as 1) are not sufficiently stable for isolation,[10] but are often detected by ESR during oxidation of alkylarylamines or hydroxylamines to the corresponding nitrones.[13,14]

Dibenzylnitroxide is known to undergo a disproportionation reaction,

$$2C_6H_5CH_2-N(\cdot O)-CH_2C_6H_5 \rightarrow C_6H_5CH_2-N(OH)-CH_2C_6H_5 + C_6H_5CH_2-N^+(O^-)=CHC_6H_5$$
$$(7)$$
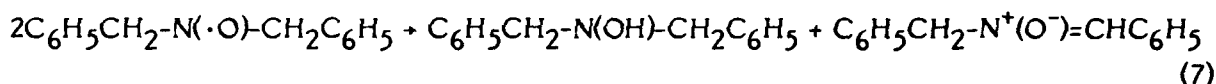
to produce a hydroxylamine and a nitrone. The rate constant for this reaction was found to be of the order of $10^4 M^{-1}s^{-1}$ in hydrocarbon solvents at room temperature[15] while a much slower rate constant of $10^{-3}M^{-1}s^{-1}$, was reported for alkaline aqueous ethanol solutions.[16] The reliability of this value was questioned since its value was so much lower.[17]

It is interesting to speculate that the initial alkylarylnitroxide, 1, formed in TNT thermolysis is also capable of undergoing a similar disproportionation reaction. The hydroxylamine formed by disproportionation can easily be oxidized by another TNT molecule back to the nitroxide. Oxidation of hydroxylamines is a major synthetic route to nitroxides[10] and nitroaromatic compounds such as TNT are certainly reasonably good oxidizing agents. The byproducts of such oxidative cycling between nitroxide and hydroxylamine would produce additional nitrosobenzenes and hydroxyl radicals which are expected to participate in further radical-forming reactions (see Scheme 2).
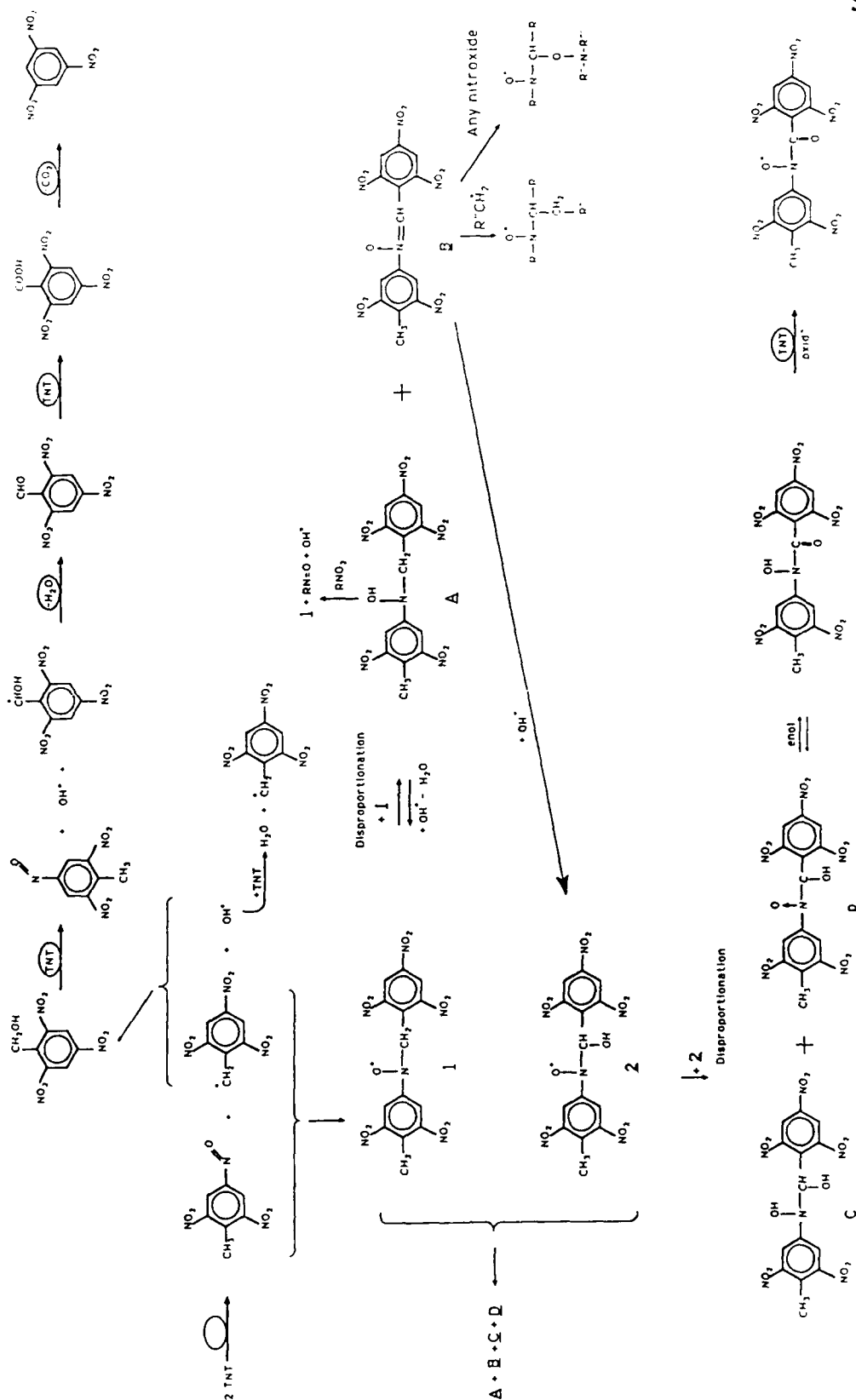
Scheme 2: Nitroxide disproportionation and follow-up reactions

25

Moreover, the nitrone produced in the disproportionation reaction could also scavenge a great variety of radicals to produce different nitroxides, few of which would be expected to survive at elevated temperatures. This reaction sequence might ultimately be the source of the materials responsible for the Tar absorption.

This set of reactions provides a reasonable explanation for the fact that nitroxide radicals are never present at high concentrations, but rather appear to exist in a dynamic steady-state condition. It is also consistent with the observation that the time at which the nitroxide concentration peaks is inversely proportional to the reaction temperature (Fig. 6a).

3. Tar Formation

During the course of TNT thermolysis at elevated temperatures (>230°C) the TNT-melt gets progressively darker and more viscous. When an experiment is interrupted at this stage the viscous fluid is stable to supercooling and may remain transparent at room temperature for hours or days, unless solidification is induced by mechanical shock. However, if the melt is subjected to continued heating it becomes almost black and eventually begins to undergo minor detonations. The growth of the Tar ESR absorption is roughly exponential until this stage is reached, but once the "bumping" or detonations start, material is expelled from the sensitive portion of the ESR cavity and no further quantitative measurements can be obtained. Consequently, the sound of "popping corn" generally signals the end of a kinetic run. (This is the reason for the short run-times in data obtained at the higher temperatures.)

Some representative data for the Tar formation during the decomposition of neat TNT are shown in Fig. 7. The increase of the Tar signal is roughly exponential, indicative of a first-order or pseudo-first-order process. (These data for the kinetics of Tar formation were all evaluated as described above by subtracting the nitroxide absorption, Line B, from the Tar absorption, Line C.) Careful examination of the kinetic data shows that the log plots are not precisely linear. Rather, they show enhanced rates in the early interval of the reaction period, followed by a long interval of linear growth, and often succeeded by yet another segment of accelerated rate which ushers in the minor detonations mentioned earlier.

(a)

(b)
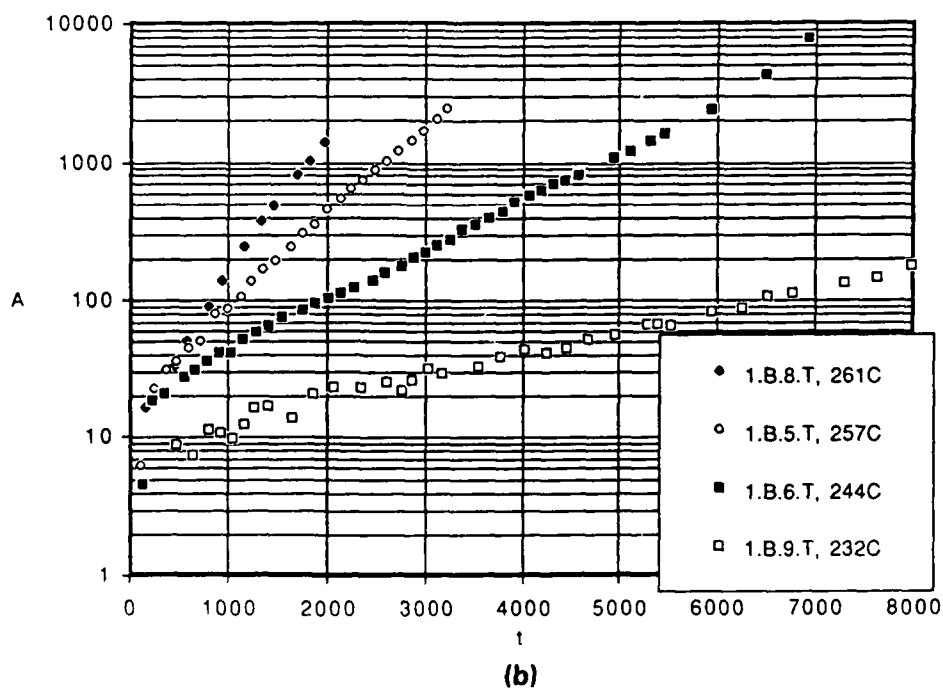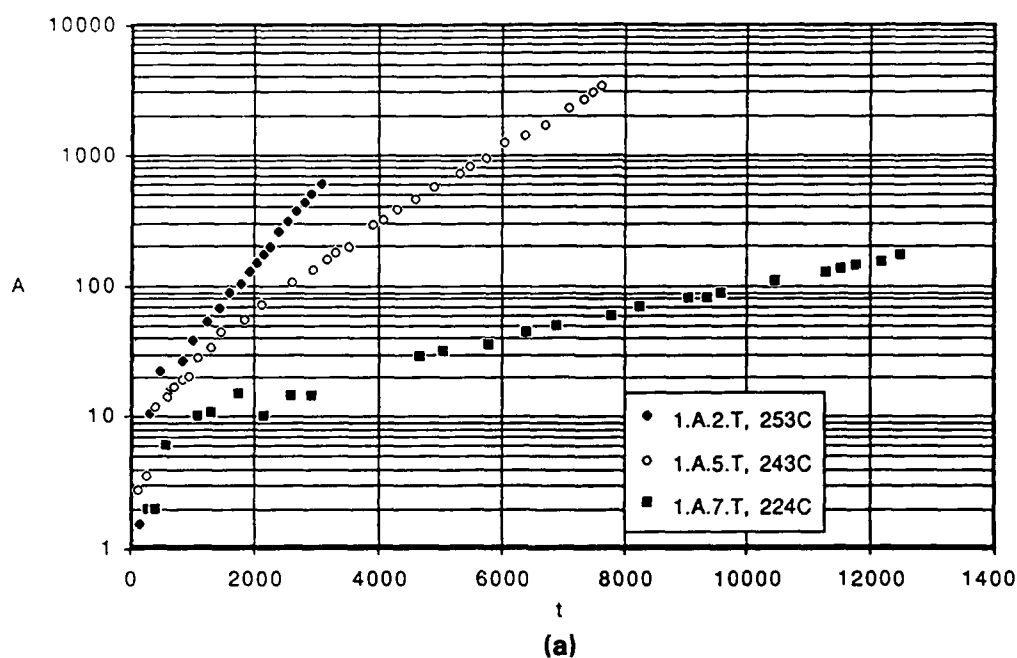
Fig. 7   Amplitude of the Tar ESR signal as a function of time at various temperatures
(a) early sample, (b) more highly purified sample.

While the growth of the Tar absorption follows roughly first order kinetics, the obvious departures from strictly exponential growth at the early and late periods of experiments warrants discussion. A hypothesis for this behavior can be drawn from analogies from the field of polymer kinetics where a chain forming sequence consists of initiation, propagation, and termination reactions.

In the case of well studied reactions such as vinyl polymerization, the initiator is usually a material that decomposes to the radicals that carry the reactive chain

$$\text{Initiator} \rightarrow 2R\bullet \qquad (k\text{-dec.})$$

These radicals then react with "monomer," M, to initiate polymerization through monomer-derived radical $M_n\bullet$

$$M + R\bullet \rightarrow RM\bullet \qquad (k\text{-initiation})$$
$$M + M_n\bullet \rightarrow m_n M\bullet \qquad (k\text{-propagation})$$

Ultimately, monomer-derived radicals couple to produce polymer

$$2M_n M\bullet \rightarrow P \qquad (k\text{-termination})$$

(See for example Ref. 18.)

It is conceivable in our TNT case that some exogenous material which is rapidly consumed in the early stages of the reaction acts as an initiator (in addition to the radicals formed by nitroxide-forming processes)

$$In \rightarrow R\bullet$$
$$R\bullet + TNT \rightarrow T\bullet$$

If this is true, the reaction rate would accelerate during the early stage until either (a) the initiator is all consumed or (b) the initiation process achieves a steady stage. Then in the intermediate stage of the reaction, the observed "autocatalytic" behavior (pseudo-first-order kinetics) would prevail

$$T\bullet + TNT \rightarrow TNT-T\bullet$$
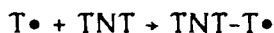
and the observed linear portion of the log [T] vs plot is well behaved. We and the other researchers have also noted that the temperature rises during the final accelerating stages. Thus, this part of the reaction may only be caused by the inability of the sample to dissipate the internally generated heat.

The nitroxide molecule, 1, possesses important reactive functionalities beyond those outlined in Scheme 2. The presence of aromatic nitro groups and methyl and benzylic hydrogen atoms leaves this compound open to a variety of additional attacks such as outlined in Scheme 1.

The fact that the analysis (according to T = C - B) shows Tar to be formed from the earliest stages of the reaction led us to suggest that Tar may actually be a polymeric species, formed by successive additions of TNT moities to any of the reactive sites (methyl- or nitro-groups) of a nitroxide-like substrate. This led us to suggest a possible reaction sequence

2 TNT	$\rightarrow$	Nitroxide	(rate, k_1)	(7a)
TNT + Nitroxide	$\rightarrow$	Tar	(rate, k_2)	(7b)
TNT + Tar	$\rightarrow$	Tar'	(rate, k_3)	(7c)
Nitroxide + Tar	$\rightarrow$	Tar"	(rate, k_4).	(7d)
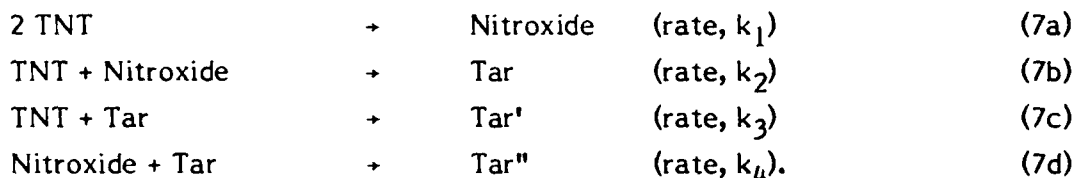
A set of simultaneous kinetic rate equations based on this scheme is too complicated for a simple, analytic solution. But it is possible to subvert a spreadsheet program, such as Microsoft Excel, to perform scientific calculations. The advantage of using such a packaged program is that the facility for rapid, interdependent calculations is already available without having to invest any significant programming time. When this approach is used it is fairly simple to obtain numerical simulations for such a kinetic scheme.

Some very crude, order-of-magnitude estimates of absolute rates can be obtained from some reasonable assumptions and from the experimental data. No great credence should be attached to these numbers; they are intended solely to provide a starting point for some calculations based upon the foregoing kinetic model to see if it

has any validity when compared to the experimental kinetic curves. The particular experiment chosen as the basis for these ballpark-calculations was 1.B.1 because it was run at 240°C, a temperature that has been used as the norm in many other studies; this run made use of more highly purified TNT than earlier studies; and the nitroxide growth broke into two distinct segments corresponding to initial growth rate and a secondary, slower growth rate after the competitive process set in, see Fig. 8.

The initial slope of the kinetic curve for nitroxide as indicated by Line B was 0.055 mm/s while in the subsequent, competitive segment the slope was 0.031 mm/s. A set of assumptions can be based on the following reasonable values:

(a)   The early line width of Tar has a value of 0.1 mT, but nitroxide has a line width of 0.08 mT.

(b)   The values are normalized to a spectrometer gain value of 1×10^6 and at this setting a line of 5 mm amplitude has a signal-to-noise ratio of at least 2, adequate for recognizing the presence of an ESR line.

(c)   The density of molten TNT is 1.47 g/cc,[19] so that a standard 100 mg sample has a volume of about 0.06 cc and, regardless of the quantity, the initial concentration of TNT is about 6.5 molar.

(d)   The spectrometer sensitivity is 10^{13} spins/ΔH (mT), for a time constant of 0.2 s, modulation amplitude of 0.5 G, power of 15 db, and Q of about 1000-1500.

Under these assumptions, Tar should be detectable at a concentration of

$$[Tar] = 10^{14} \text{ spins}/(6 \times 10^{23} \text{ spins mol}^{-1} \bullet 6 \times 10^{-5} \text{ l})$$
$$\sim 2.8 \times 10^{-6} \text{ M.}$$

But this assumes a line amplitude of 5 mm, so the incremental measure of Tar concentration would be about 5.6×10^{-7} M/mm.

In the case of the nitroxide concentration, the estimate must be compensated both for the degeneracies of the hyperfine lines and for the sharper line shape of nitroxide. Accordingly, Line A contains 10/384 of the total spectral intensity while

(a)

(b)
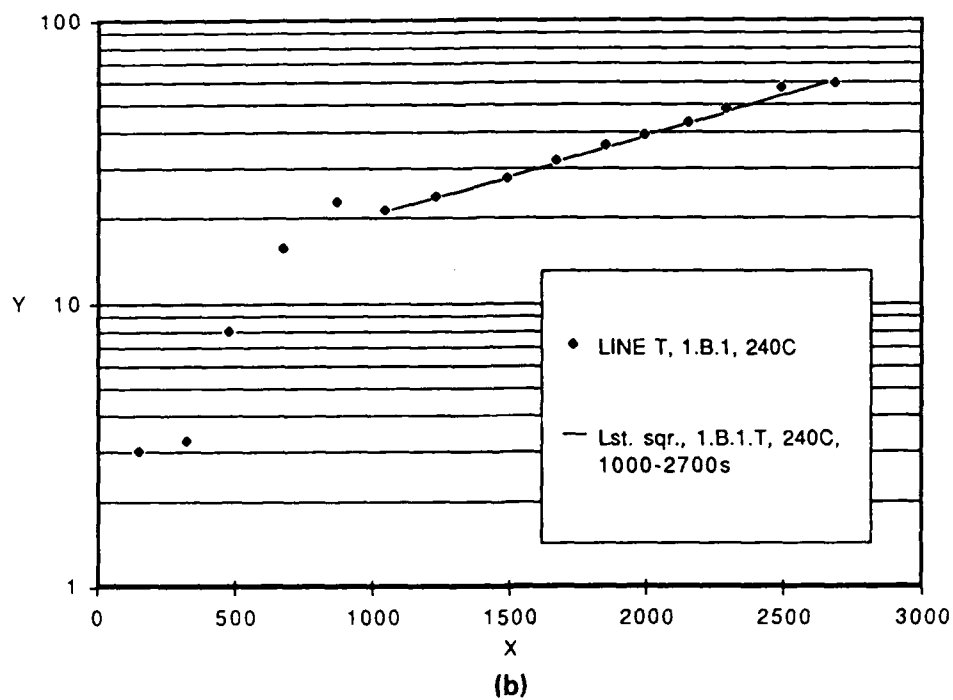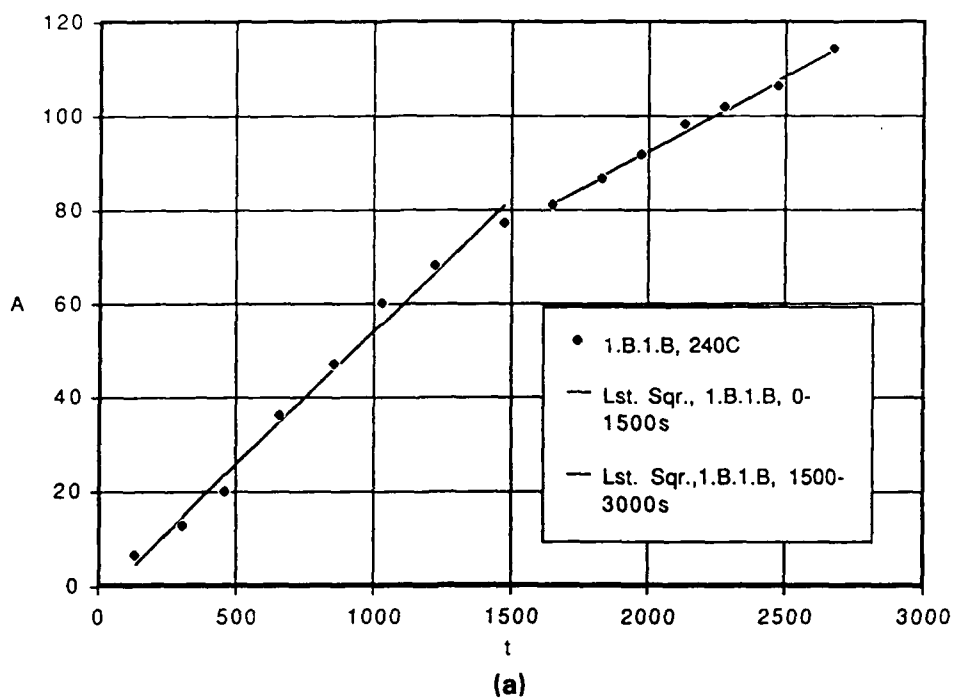
Fig. 8 Growth of (a) nitroxide and (b) Tar signal in Expt 1.B.1, neat TNT at 240°C.

Line B contains 20/384. The simple method for comparing radicals with different line widths approximates the quantity of radical as

$$\text{Quantity} = \text{Amplitude} \times (\Delta H)^2 \tag{8}$$

so that for two different single-line species having linewidths of 0.1 and 0.08 mT, respectively, lines of equal amplitudes would correspond to quantities $Q_{0.08} = 0.64\ Q_{0.1}$ so that the detection sensitivity is greater for the narrower-line width species. Incorporating the hyperfine degeneracy factors, the net results for Lines A and B of the nitroxide spectrum are:

(Line A): $(5.6 \times 10^{-7}\ \text{M/mm}) - (0.64) - (384/10) = 1.4 \times 10^{-5}\ \text{M/mm}$,

(Line B): $(5.6 \times 10^{-7}\ \text{M/mm}) - (0.64) - (384/20) = 6.8 \times 10^{-6}\ \text{M/mm}$,

while Line T sensitivity is $5.6 \times 10^{-7}\ \text{M/mm}$.

Using the rate expressions derived from the foregoing reaction scheme and the slopes exhibited by Line B in Fig. 8, crude estimates of rate constants are obtained. The initial rate of growth of Line B is

$$d[N]/dt = 0.055\ \text{mm/s} = k_1\ [TNT]^2$$
$$(0.055\ \text{mm/s}) \times (6.8 \times 10^{-6}\ \text{M/mm}) = k_1 (6.5\ \text{M})^2$$
$$k_1 = 9 \times 10^{-9}\ \text{l mol}^{-1}\ \text{s}^{-1}.$$

In the secondary region

$$d[N]/dt = 0.031\ \text{mm/s} = k_1\ [TNT]^2 - k_2\ [TNT]\ [N].$$

From the data in Fig. 8 it appears that the nitroxide concentration produces a Line B amplitude of ~80mm when the secondary process begins and this corresponds to a concentration of $[N] = 80\text{mm} \times 6.8 \times 10^{-6}\ \text{M/mm}$ or $5.44 \times 10^{-4}\ \text{M}$. Making the appropriate substitutions in the above rate equation

$$k_2 = \{(0.055 - 0.031)\text{mm/s}\} \cdot (6.8 \times 10^{-6}\ M/\text{mm})$$
$$(6.5\ M)(\ 80\ \text{mm} \times 6.8 \times 10^{-6}M/\text{mm})$$
$$= 3.5 \times 10^{-5}\ l\ \text{mol}^{-1}\ s^{-1}.$$

There are some pitfalls associated with numerical modeling. For example, consider the simplest case of first-order growth, $dx/dt = kx$. When this is modelled numerically the differentials must be approximated by intervals of the form

$$\frac{x_i - x_{i-1}}{\delta} = kx_i \tag{9}$$

where x_i is the concentration at some time and x_{i-1} is the concentration at the preceding time separated by δ, the time increment used in the simulation. If the usual initial condition of $x_0 = 0$ at $t = 0$ is used, x is forever fixed at zero. So some small but finite value of x_0, must be included as an initial condition. Another, more isidious, problem arises when the sampling interval is too large because the calculations can rapidly "run away" and violate not only the conservation of mass balance but also the mass of the Universe. This creates a problem within the limitations of display routines used with personal or laboratory computers because calculations at small increments rapidly consume the relatively small number of points available for plotting. However this shortcoming can be circumvented by "combing" through the calculated value table and just plotting every nth point.

Some of the calculations are shown in Fig. 9.

The curves of Fig. 9d-f were calculated under the assumption of the following rate equations

$$d[N]/dt \qquad = k_1[TNT]^2 - k_2[TNT][T] - k_4[T][N] \tag{9}$$
$$d[T]/dt \qquad = k_2[TNT][N] + k_3[TNT][T] + k_4[T][N]$$
$$d[TNT]/dt \qquad = -(2k_1[TNT]^2 + k_2[TNT][N] + k_3[TNT][T])$$

or

$$[N]_{i+1} \qquad = [N]_i + \delta\{k_1[TNT]_i^2 - k_2[TNT]_i[N]i - k_4[T]_i[N]_i\} \tag{10}$$
$$[T]_{i+1} \qquad = [T]_i + \delta\{k_2[TNT]_i[N]i + k_3[TNT]_i[T]_i + k_4[T]_i[N]_i\}$$
$$[TNT]_{i+1} \qquad = [TNT]_i + \delta\{2k_1[TNT]_i^2 + k_2[TNT]_i[N]_i + k_3[TNT]_i[T]_i\}$$

(a)
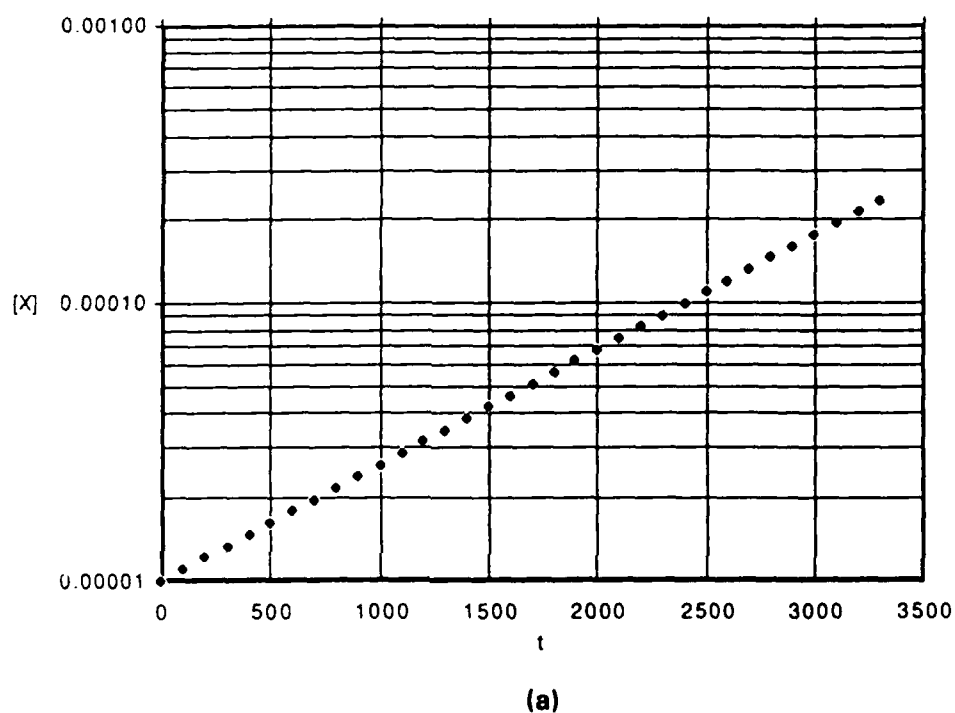
Fig. 9a.   Simulation of simple first order process, Eq. (9) to demonstrate validity of simulation procedure. $[X]_0 = 10^{-5}$ M, $k_1 = 10^{-3}$ s^{-1}, $\delta = 100$ s.

(b)

(c)
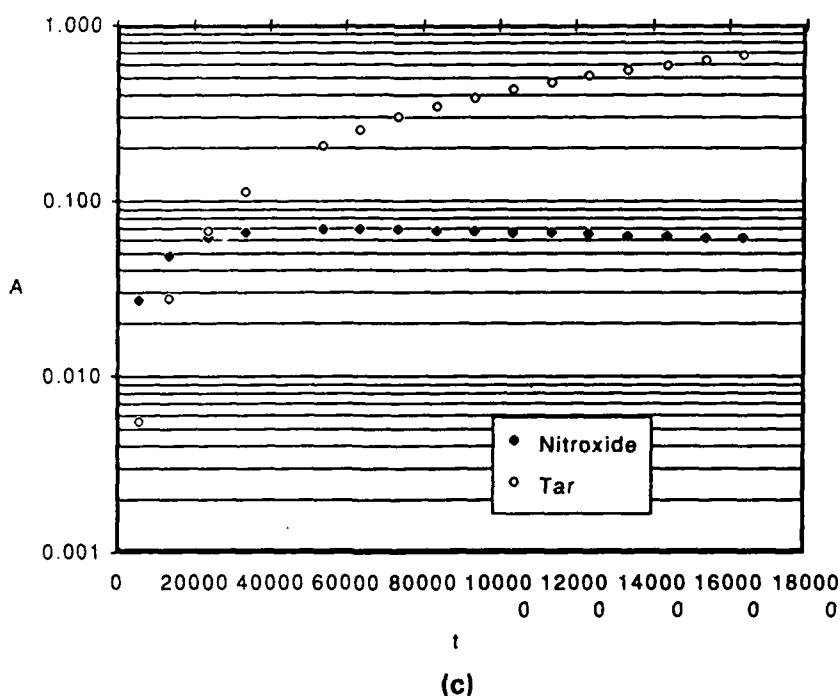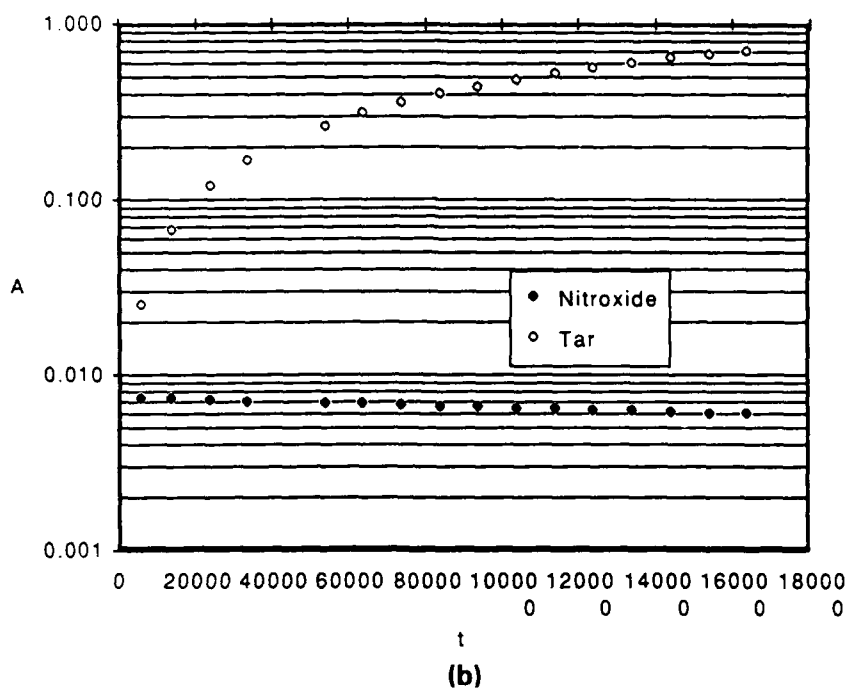
Fig. 9b,c. Simulations based upon only the first two steps (k_1 and k_2) of Eq. (7):
(b) $k_1 = 1 \times 10^{-7}$, $k_2 = 1 \times 10^{-4}$,
(c) $k_1 = 1 \times 10^{-7}$, $k_2 = 1 \times 10^{-5}$ ℓ mol^{-1}s^{-1}.
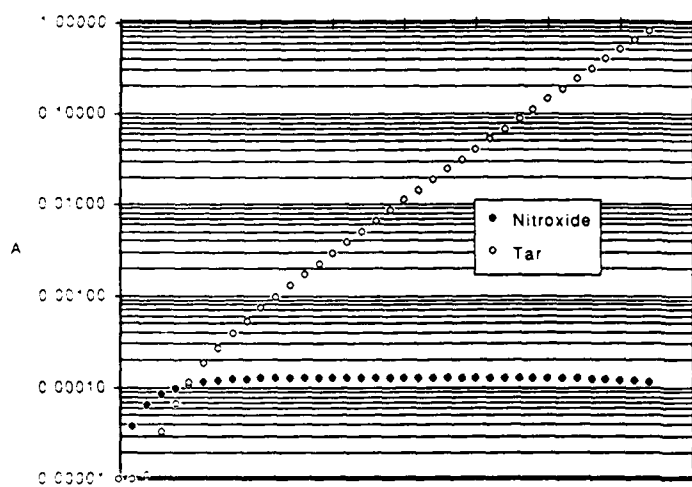
(d)
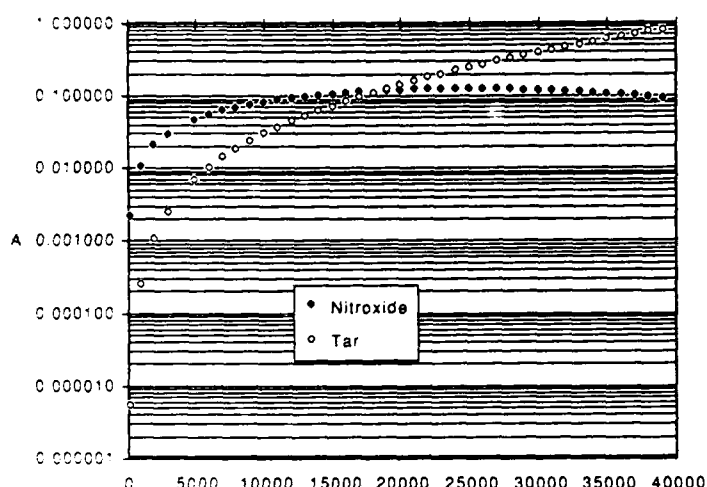
(e)
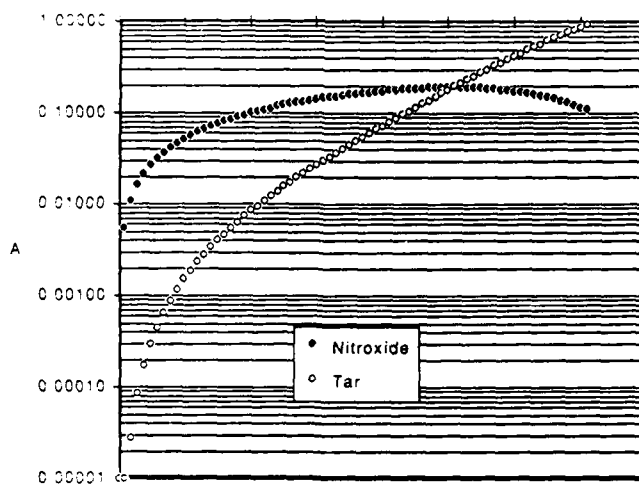
(f)

Fig. 9d,e,f.   Simulations based on all four steps of Eq. (7):
(d) $k_1 = 7 \times 10^{-9}$, $k_2 = k_3 = k_4 = 4 \times 10^{-4}$,
(e) $k_1 = 2 \times 10^{-7}$, $k_2 = 7 \times 10^{-6}$, $k_3 = 1 \times 10^{-5}$, $k_4 = 1 \times 10^{-4}$, and
(f) $k_1 = 1 \times 10^{-6}$, $k_2 = 7 \times 10^{-6}$, $k_3 = 1 \times 10^{-4}$,
and $k_4 = 1 \times 10^{-3}$, $\ell\ mol^{-1}s^{-1}$.

This set of calculations reflects three important aspects of the experimental data:

1. Nitroxide concentration builds up to a steady state value and remains constant.
2. There is an early, accelerated stage of Tar production.
3. Later, there is a well behaved pseudo-first order stage of Tar production.
4. This latter segment extrapolates back to an initial Tar concentration greater than zero.

It is gratifying that the proposed kinetic equations simulate the broad features of the experimental curves without having to invoke the presence of an exogenous free radical initiator reactant.

One of the surprising results of this simulation effort was the discovery that certain reasonable combinations of simulation rate constants produced significant temporal oscillations in the nitroxide concentration. When some of the experimental data were later reexamined, kinetic runs which had been disallowed because of excessive experimental scatter were found to be interpretable in terms of similar temporal oscillations in nitroxide concentration. Some of the appropriate simulations and experimental data are presented together as Fig. 10. While the oscillations in Fig. 10a may be an artifact of the relatively crude simulation procedure, there are enough instances of otherwise unexplained experimental irregularities to raise the question of concentration oscillations.

We are the first to admit the folly of extrapolating thermal decomposition data to detonation conditions, but we cannot surppress the speculation that such oscillatory behavior (on a far faster time scale) could lead to a resonant shock wave. And while speculation is rampant, this could also explain why TNT is a deflagratory explosive and requires physical confinement to yield its full brissance potential.

(a)

(b)
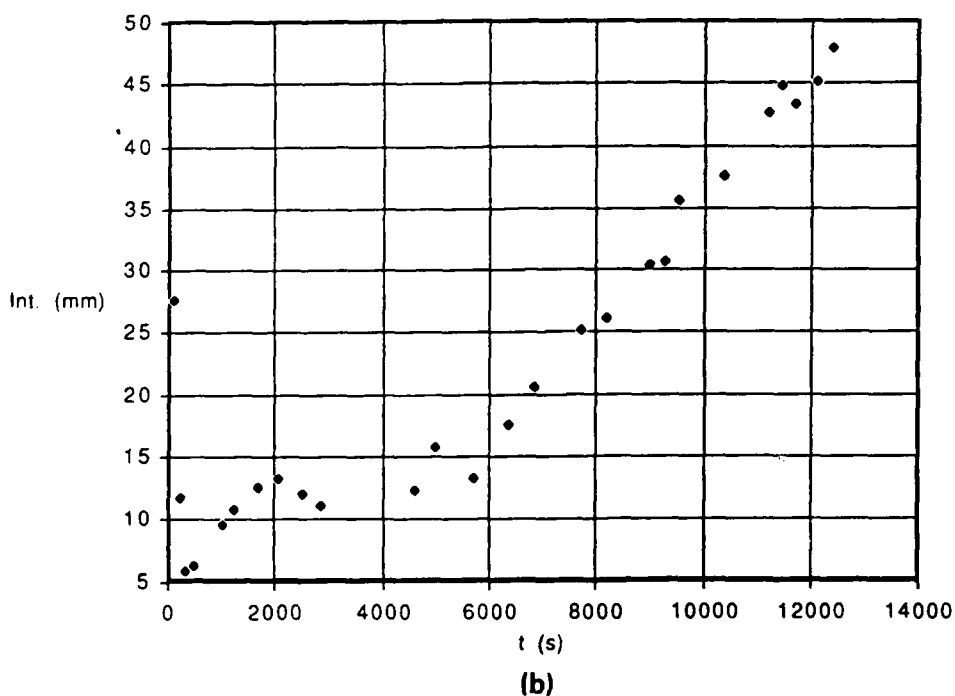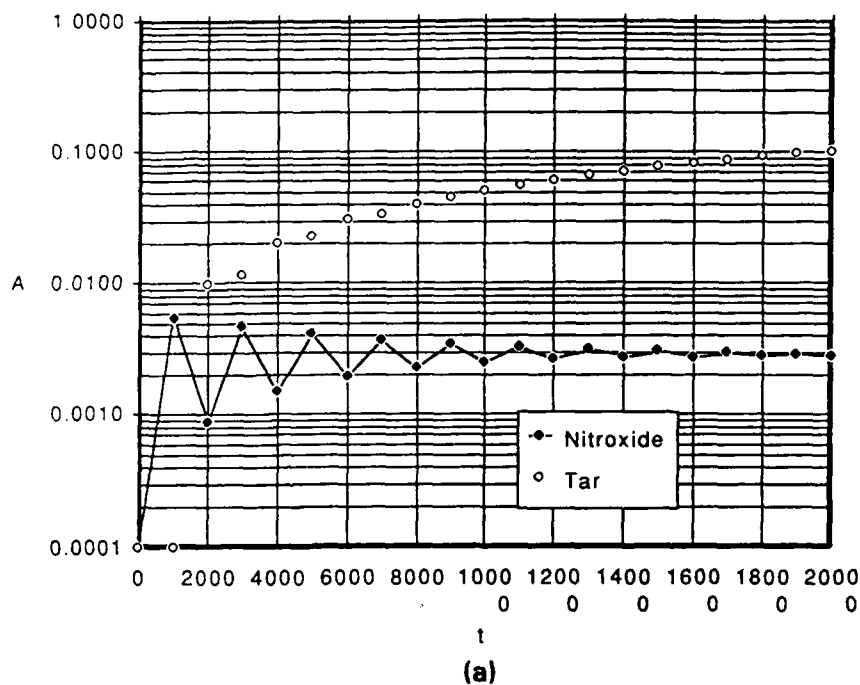
Fig. 10   Examples suggestive of oscillatory nitroxide behavior. (a) Simulated behavior
$k_1 = 1 \times 10^{-7}$, $k_2 = k_3 = k_4 = 2.5 \times 10^{-4}$ ℓ mol^{-1}s^{-1}; experimental behavior in
dry TNT (b) Expt. 1.A.7 and moist TNT (c) Expt. 2.B.3 and (d) Expt. 2.B.7.

(c)

(d)
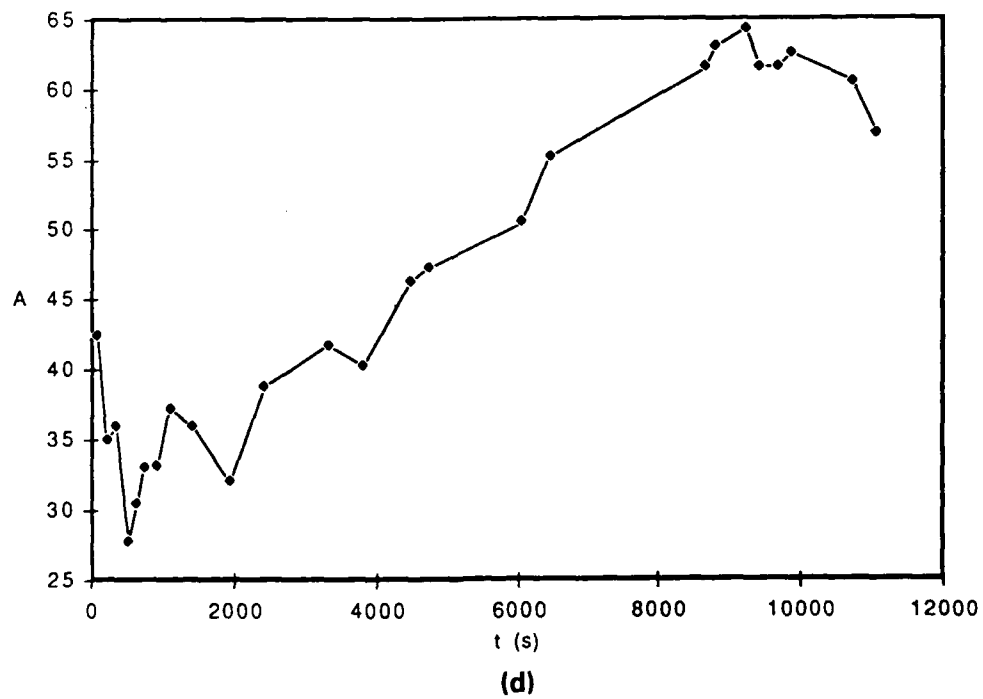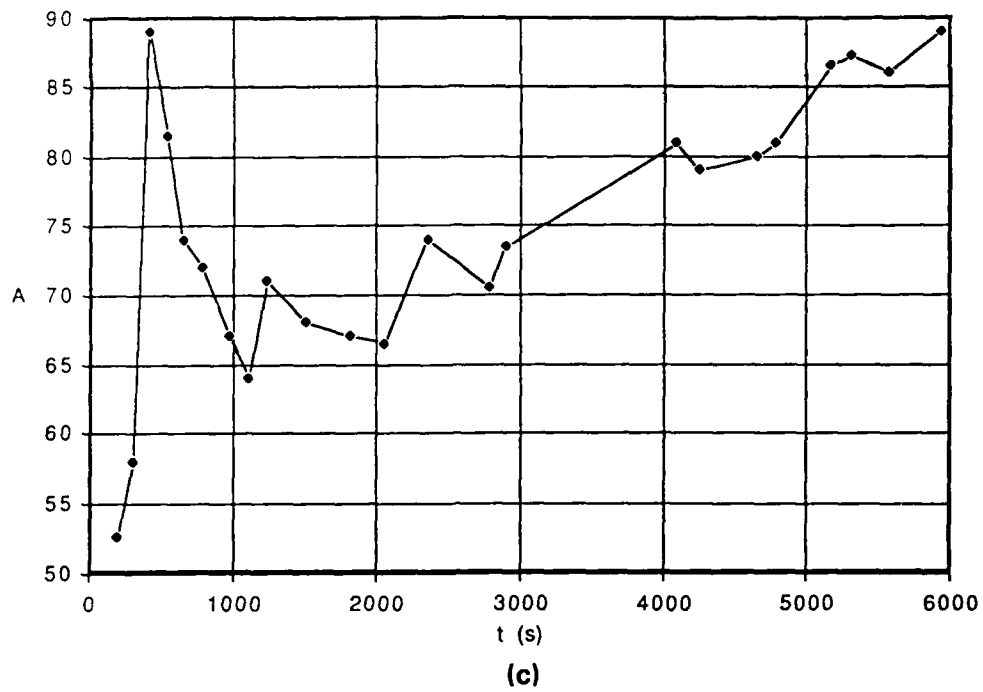
Fig. 10 (continued)

4. TNT Thermolysis with Added Water

We made the serendipitous observation that small quantities of water appear to promote the formation of the TNT-nitroxide during an independent investigation of the effect of ultrasound on chemical reactions of TNT. This has significant implications for the long-term stability of TNT-based explosives and propellants. (Recognize that water is added to samples of TNT for laboratory use to inhibit explosive decomposition. However, based on these results, the water may also promote slow degradation at ambient temperatures.) Accordingly we carried out a number of thermolysis experiments on TNT doped with small quantities of deionized water. The water was first introduced into the bottom of the ESR tube with a fine capillary dropper drawn from soft glass.

All the thermolysis reactions were carried out at temperatures well above the boiling point of water. Consequently most of the water rapidly vaporized out of the active region of the ESR cavity and recondensed in the upper, cooler region of the ESR tube. It was not possible to make ESR observations until this process was completed because of the erratic microwave coupling problems during steam expulsion. The molten TNT subsequently settled to the bottom of the tube and observations could be monitored routinely. The experimental conditions are listed in Appendix A.

The most noteworthy effect of added water was the appearance of extremely strong nitroxide signals at temperatures well below the values required to produce radicals in the early kinetic experiments with dry TNT. Figure 11 displays the nitroxide behavior for several reactions of moist TNT in the temperature range of 150-170°C.

Little significance can be attached to comparison of the absolute amplitudes of a nitroxide line between the various runs because of the different quantities of material, the problem of irreproducible tube placement within the cavity, and the amount of TNT that may have been spattered out of the sensitive region during steam expulsion. However it must be noted that nitroxide is formed in significant quantities in approximately 10 minutes at these low temperatures as compared to hours in the absence of water (see below).

Another important result of these experiments is the absence of Tar formation. Figure 12 shows data derived from the standard (T=C-B) analysis. There is tremendous scatter in the resulting "Tar" concentrations but the reason is clear when a least-squares line is added; the "Tar" concentration is essentially zero and invariant at
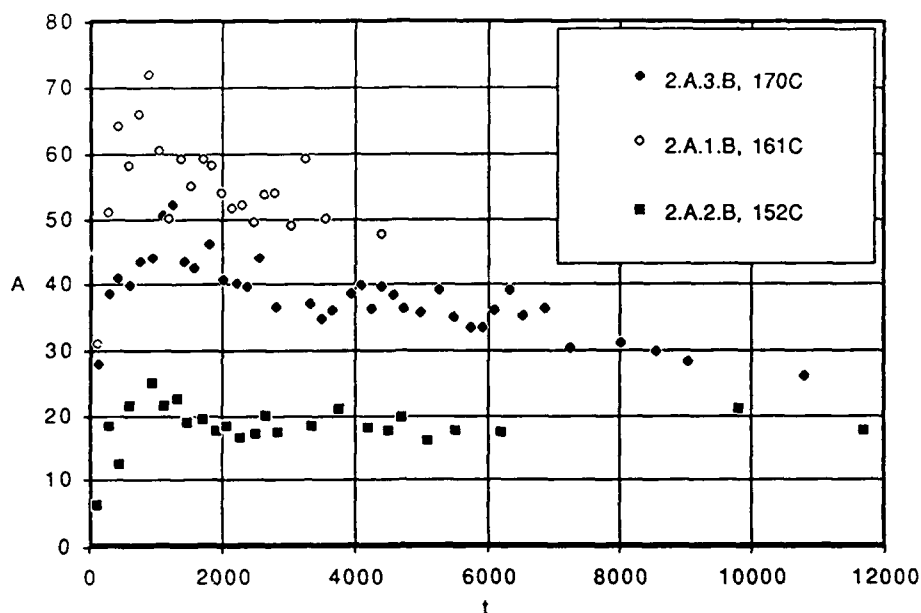
Fig. 11   Very low temperature evolution of nitroxide during thermolysis of TNT with water initially added.

these low temperatures. The scatter results from the insignificant difference between amplitudes of lines B and C.

At higher temperatures, above 200°C, Tar production begins to occur as in the case of neat TNT thermolysis. At this temperature, the water has probably evaporated completely from the TNT and condensed in the cooler regions of the sample tube. Figure 13 displays the logarithm of the Tar signal vs time for a number of different experiments. The relatively short total reaction times at elevated temperatures reflect the onset of decrepitation. The results are plotted separately for the two different batches of TNT that were used in these studies.

Figure 14 compares the growth of Tar between dry (Series 1) and wet (Series 2) samples at different temperatures. In three of the four cases the slopes are essentially parallel, indicating that water has no effect on the kinetics of Tar formation at elevated temperatures.

(a)

(b)
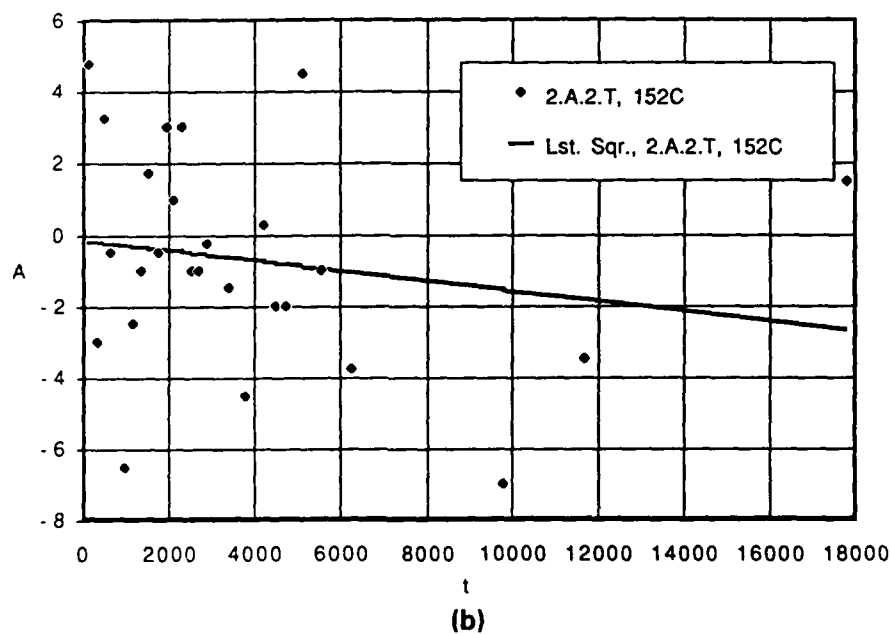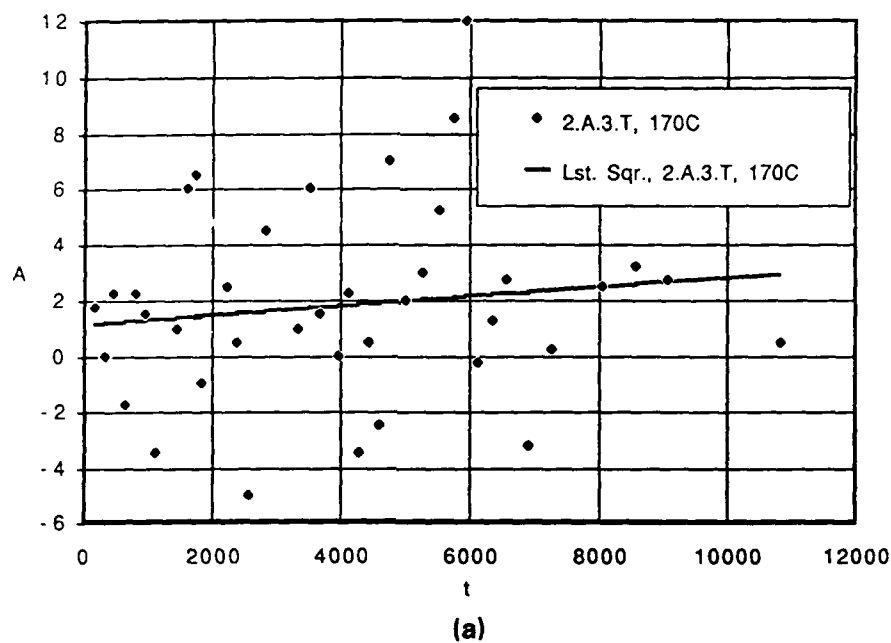
Fig. 12   Two experiments at low temperature: (a) 170°C, (b) 152°C showing absence of Tar formation.
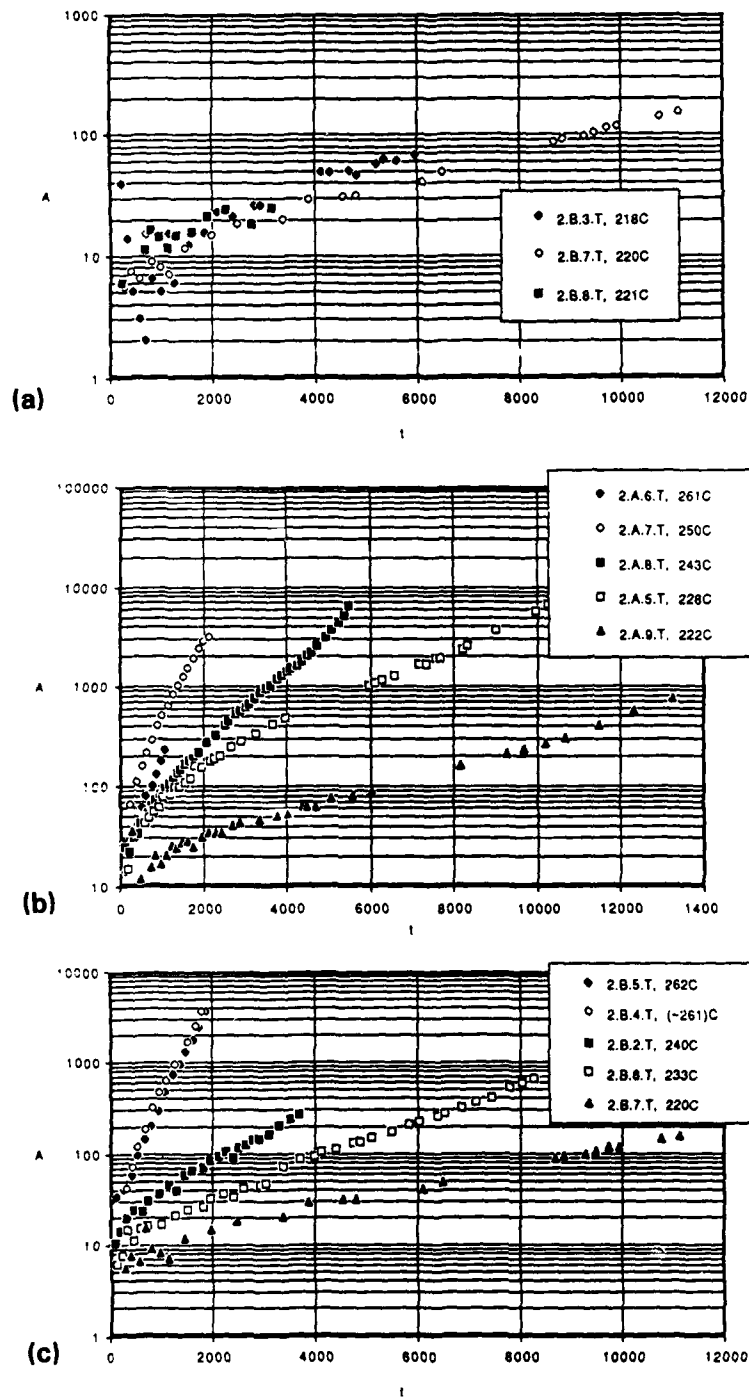
Fig. 13   (a) Superposition of three experiments near 220°C, showing reproducibility,
(b) Tar production in moist TNT, (c) Tar production in more highly purified
moist TNT.

(a)

(b)
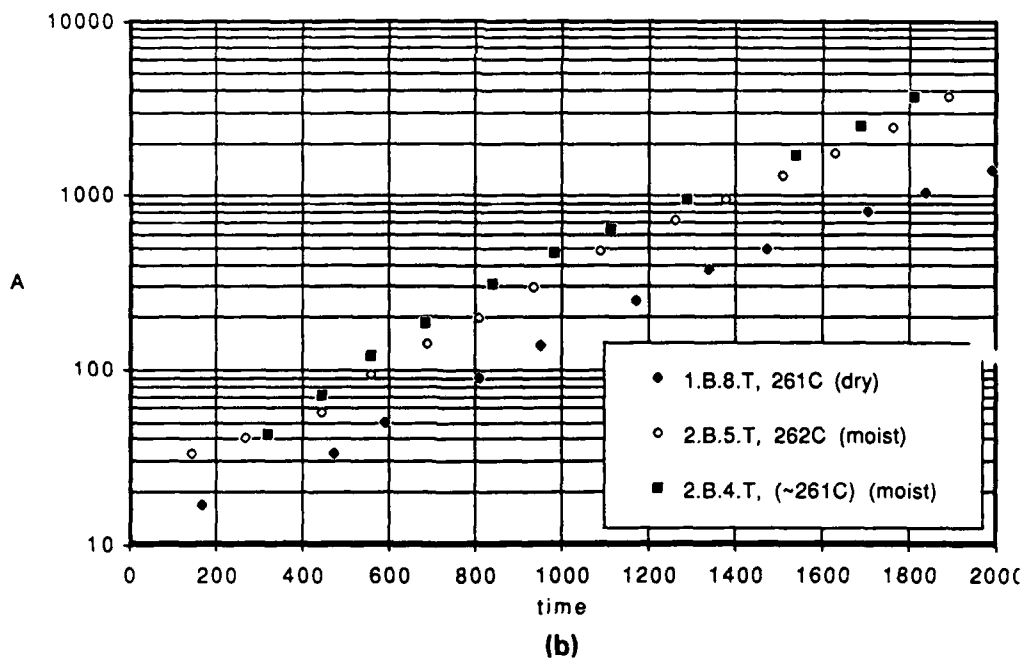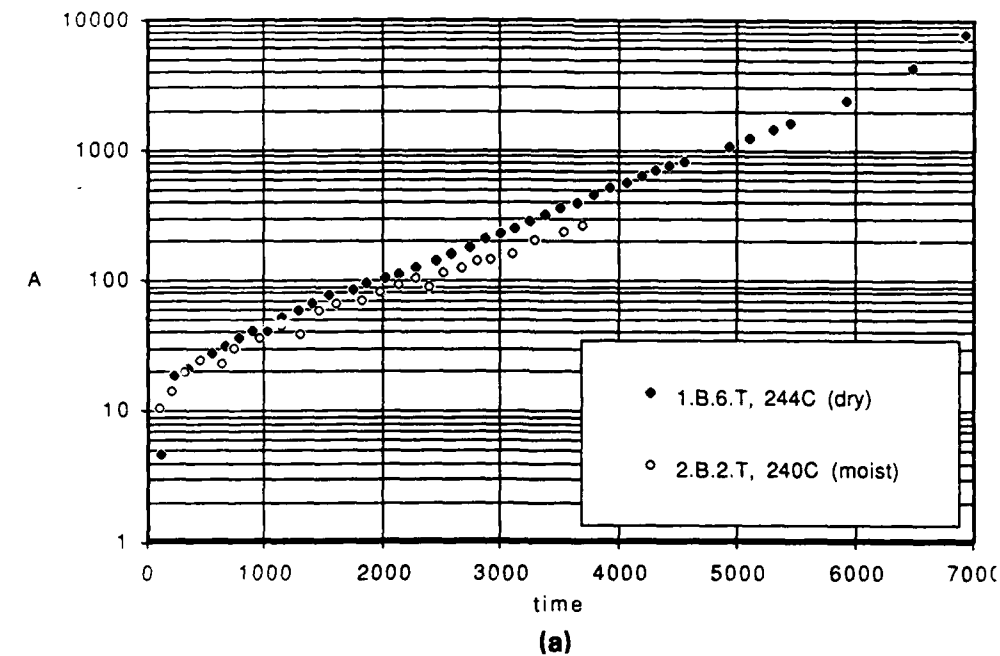
Fig. 14   Approximate isothermal comparisons of the logarithm of the tar signal vs time
for experiments which were carried out for dry (Series 1.B) and wet (Series
2.B) TNT. (a) ~ 240°C, (b) ~ 260°C, (c) ~ 230°C, (d) ~ 220°C.

(c)

(d)

Fig. 14 (Continued)

C9636DA/ejw
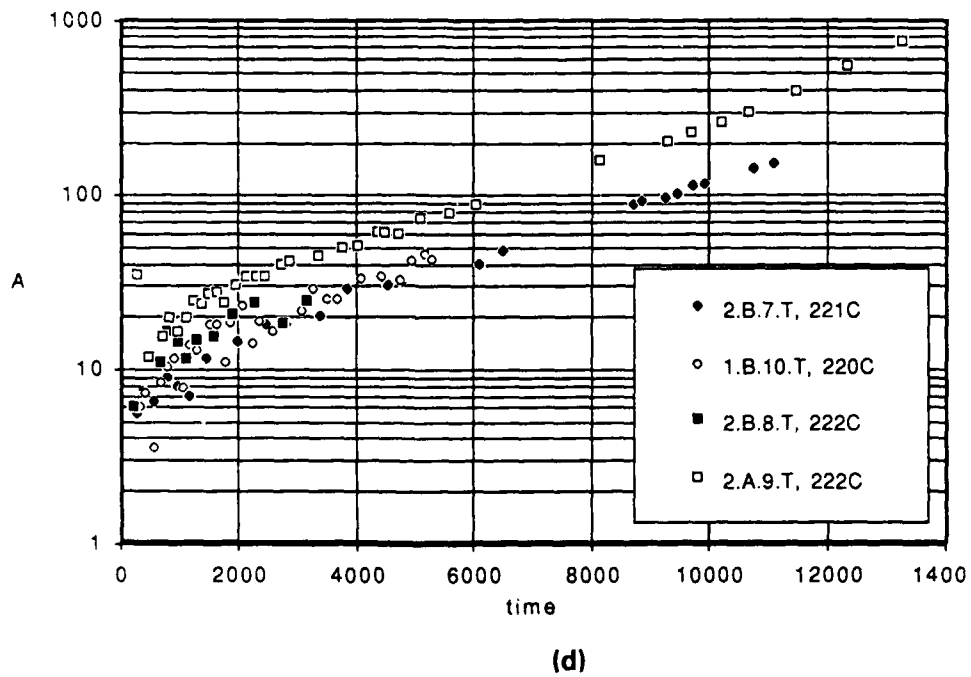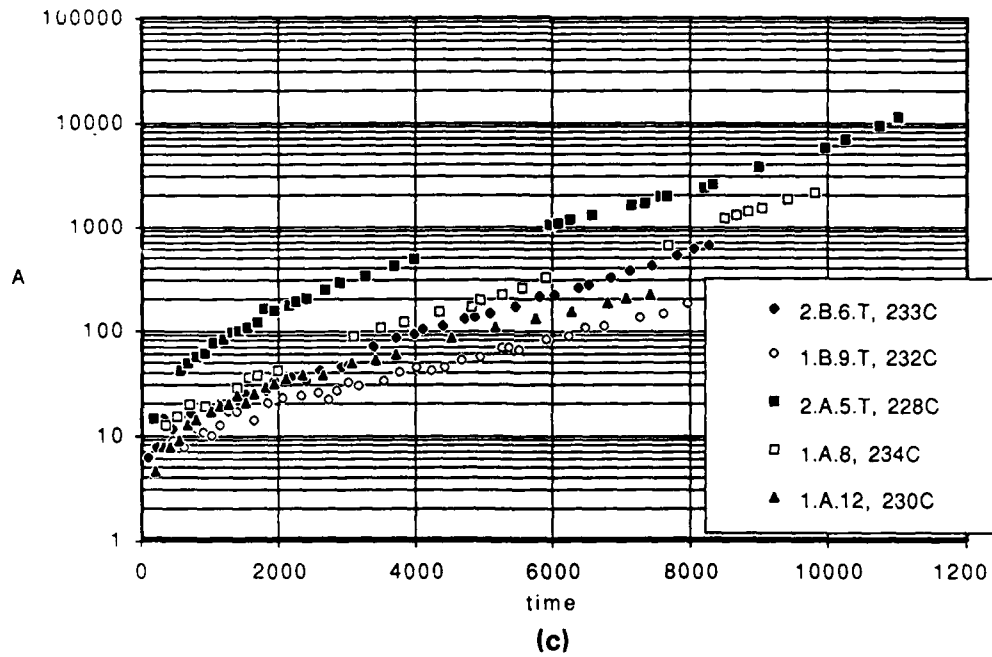
It appears that water has a significant impact upon nitroxide formation and that the effect is more pronounced at lower temperatures. Figure 15 presents comparisons of nitroxide behavior in dry and moist TNT at several temperatures. At these higher temperatures there is little difference betwen the dry and moist samples. But Fig. 16 exhibits different behaviors at lower temperature. This type of divergent behavior was observed in several other comparisons. The charts in Fig. 17 limit attention to the first 2000 seconds of reactions to emphasize these differences. But Fig. 17 also demonstrates that there is too much variability in the behavior of the nitroxide kinetics for moist TNT at moderate temperatures to attempt any quantitative assessment of the significance of these observations. However, the respected occurrence of incongruent behavior between dry and moist TNT samples at moderate temperatures as well as the enhanced nitroxide signal in moist TNT at low temperatures argues forcefully for some important role of moisture.

It is difficult to justify any firm conclusions from the curves in Fig. 17 because the contrasts between dry TNT (solid data point markers) and wet TNT (open data point markers) are not fully consistent. One fact worth noting is that in every case of dry TNT thermolysis at intermediate temperatures the nitroxide concentration (as measured by Line A) initially falls and then subsequently rises. But in a large number of reactions of moist TNT at comparable temperatures the nitroxide concentration increases at the outset of the run, just as it was seen to do at much lower temperatures. However, there are also enough examples (such as Fig. 17c,d) of an early decrease in nitroxide content during thermolysis of wet TNT that conclusions must be suspended about a meaningful difference based on the presence or absence of water.

It is clear that water alters the course of nitroxide formation. Two possibilities are obvious:

- Water enhances formation of nitroxide.
- Water inhibits destruction of nitroxide.

The later possibility appears more tenable in view of the initial decrease of nitroxide signal during the early stages of dry TNT thermolysis at intermediate temperatures. However, the other possibility is supported by the spectra shown in Figs. 18 and 19. Samples of wet and dry TNT were heated at 160°C. The wet sample showed a
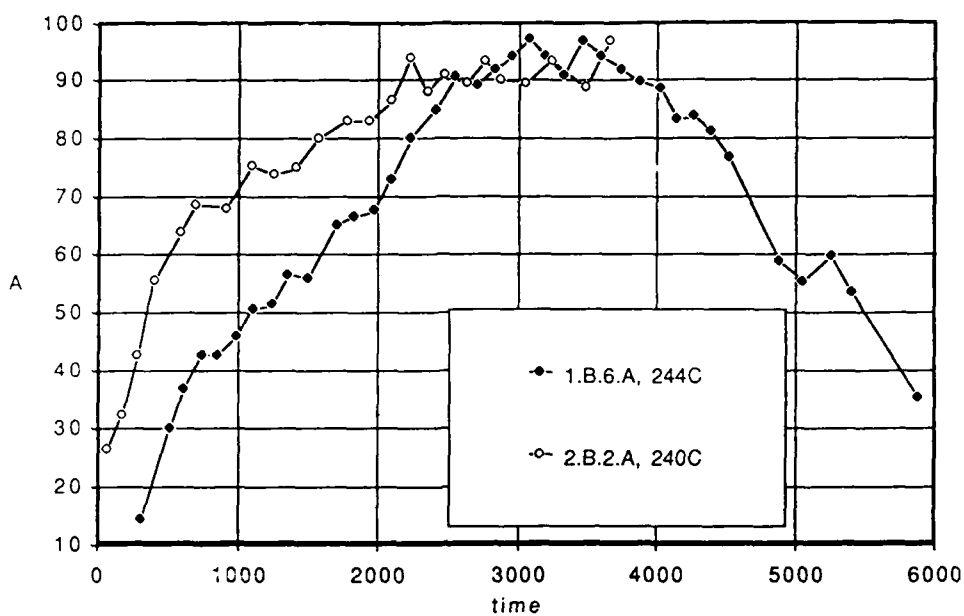
(a)
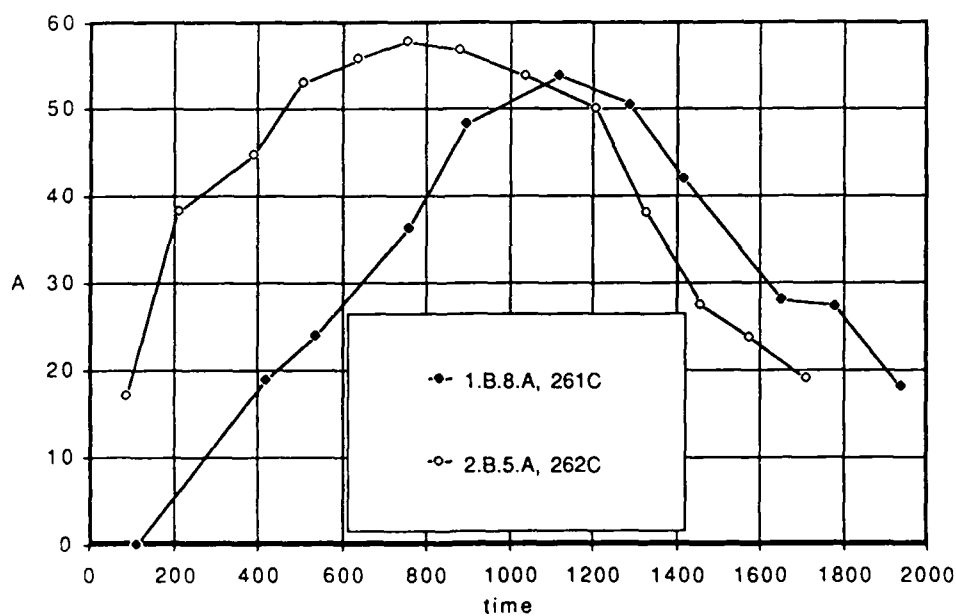
(b)

Fig. 15   Comparison of nitroxide formation and decay for moist and dry TNT samples at approximately 240°C (a) and 260°C (b).

(a)

(b)
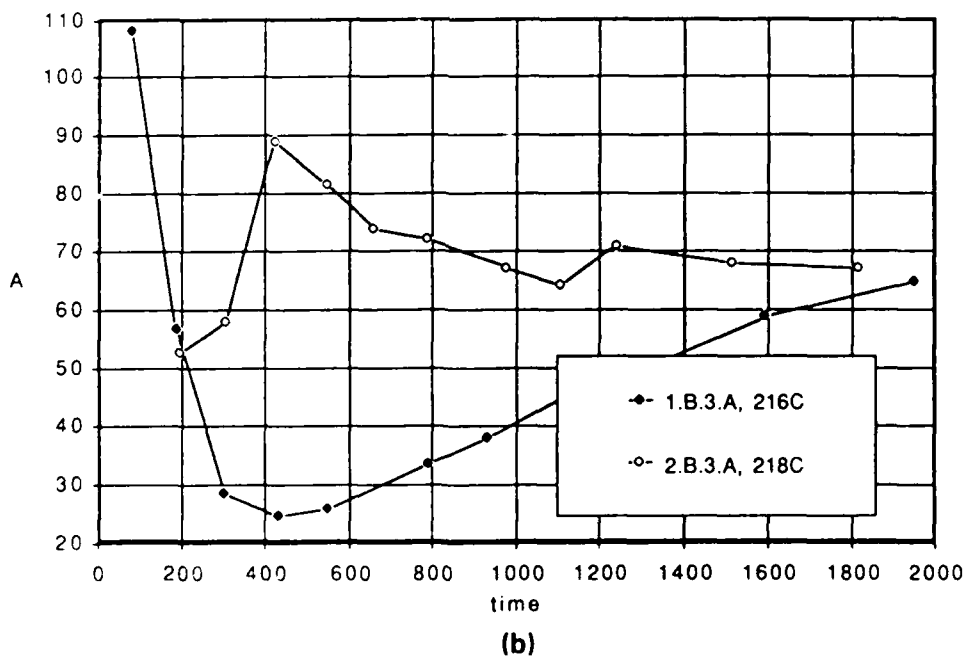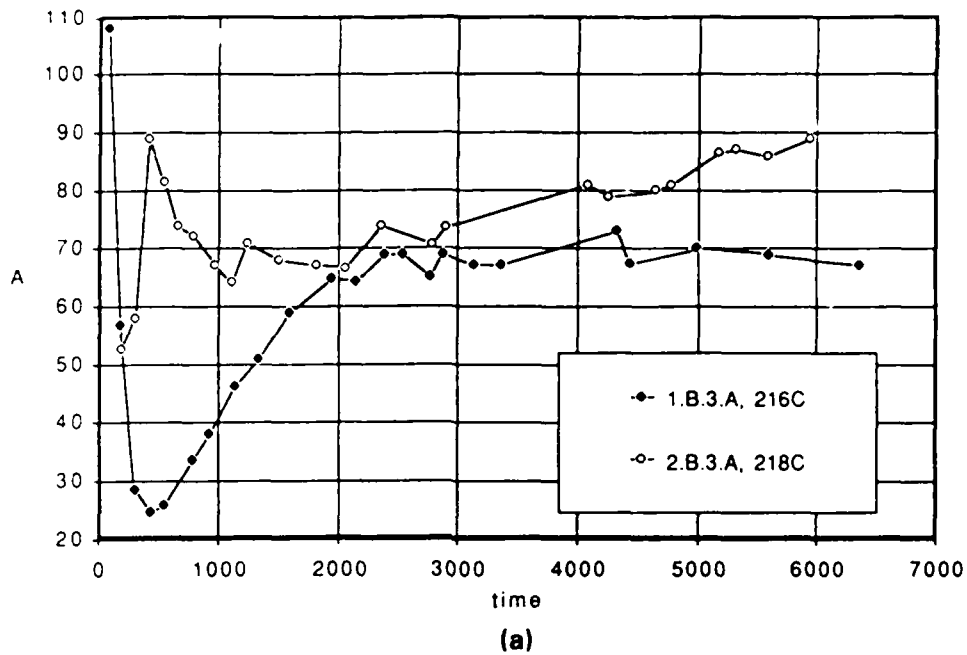
Fig. 16   Comparison of nitroxide decay and formation in moist and dry TNT samples at approximately 218°C.   (a) Entire data set; (b) expanded scale, restricted to initial 200 s.

(a)

(b)
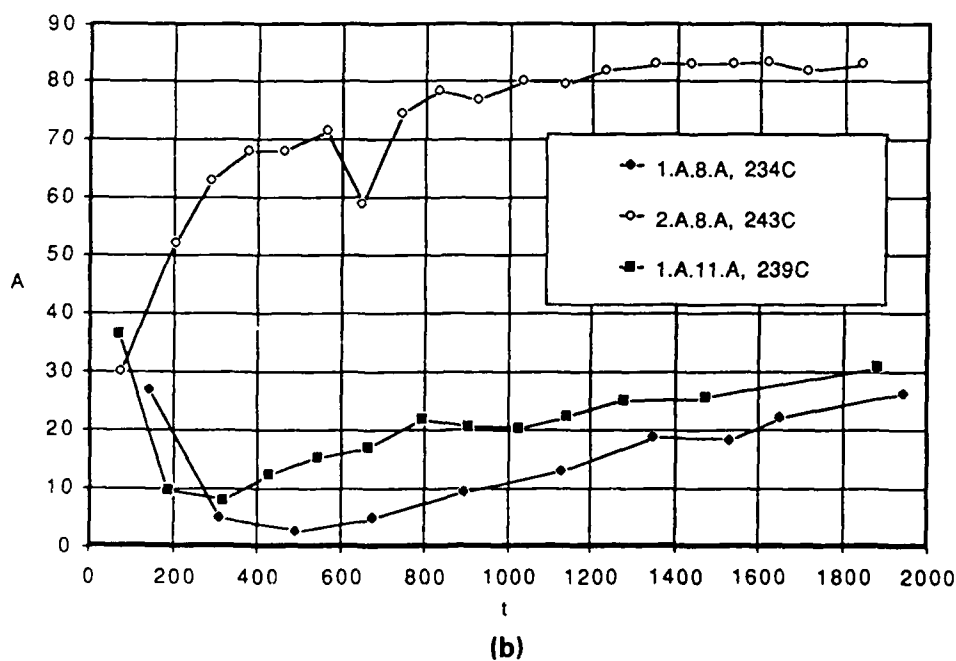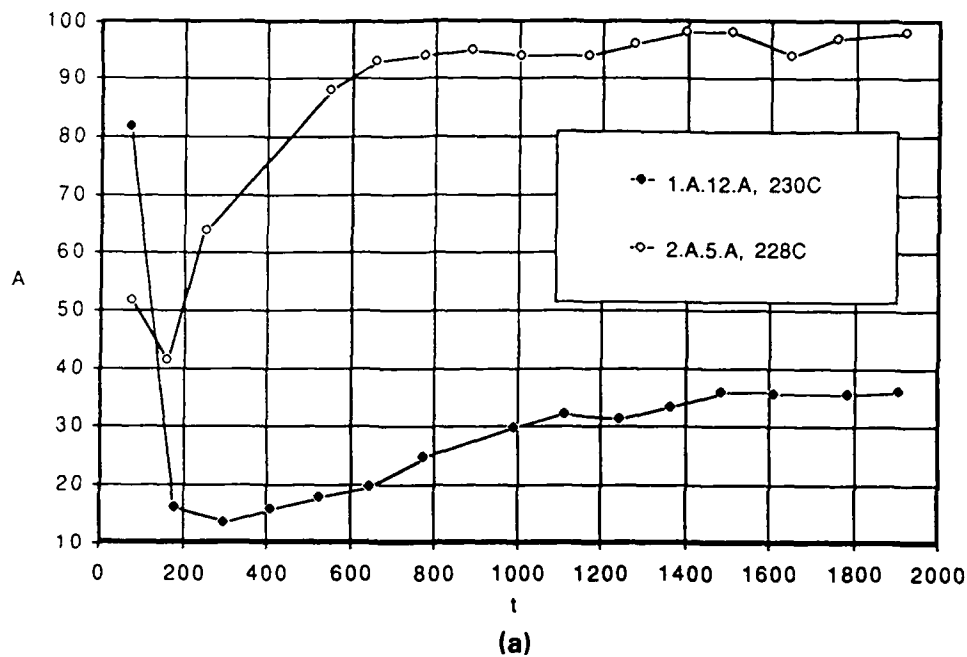
Fig. 17   Comparison of nitroxide behavior in moist and dry TNT samples during early
stage of thermolysis reactions.

(c)

(d)

Fig. 17 (Continued)

SC5493.FR

10 G
1 mT.
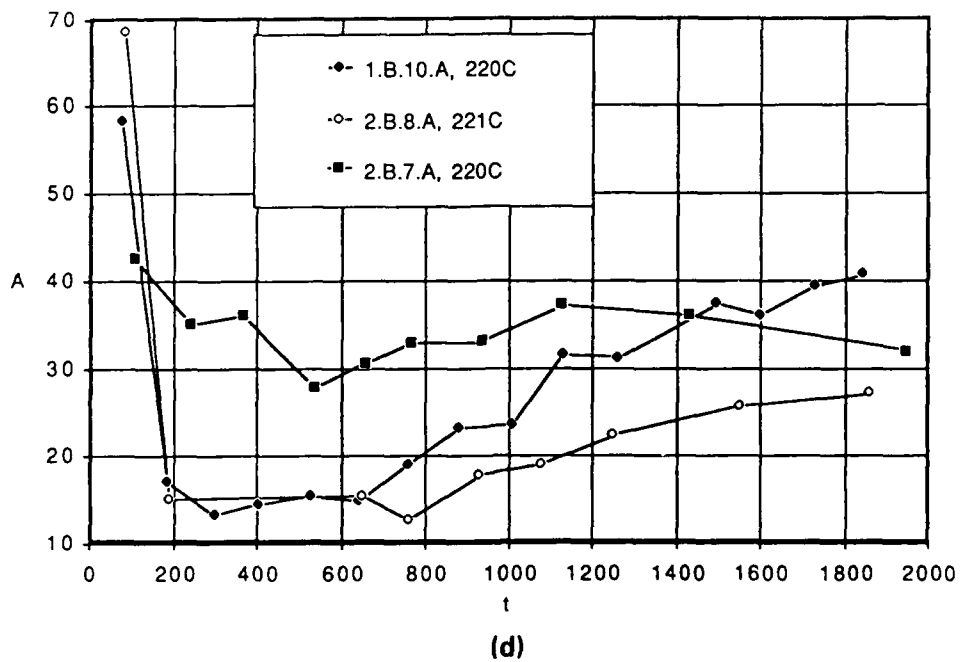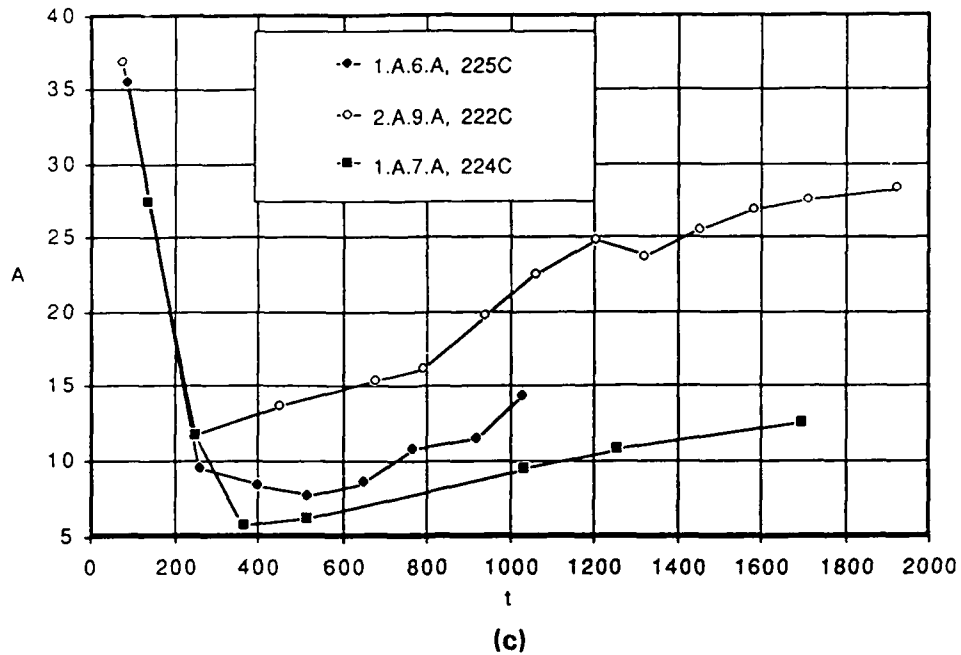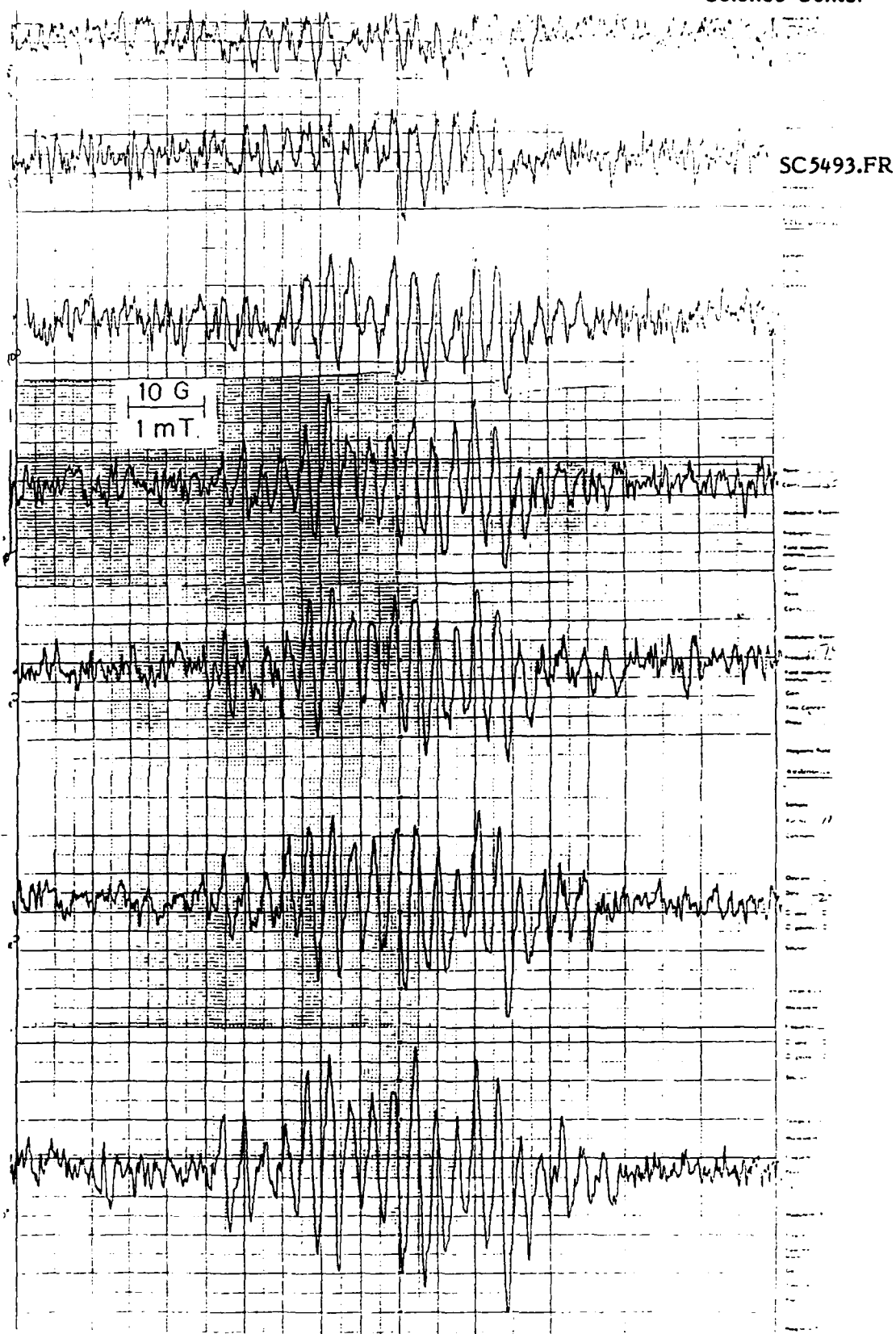
Fig. 18   Time dependence of the nitroxide spectra from dry TNT at 160°C.   Traces
recorded at 3300 (top), 6200, 9400, 11800, 12500, and 1500 s (bottom).

SC5493.FR

10 G

1 mT
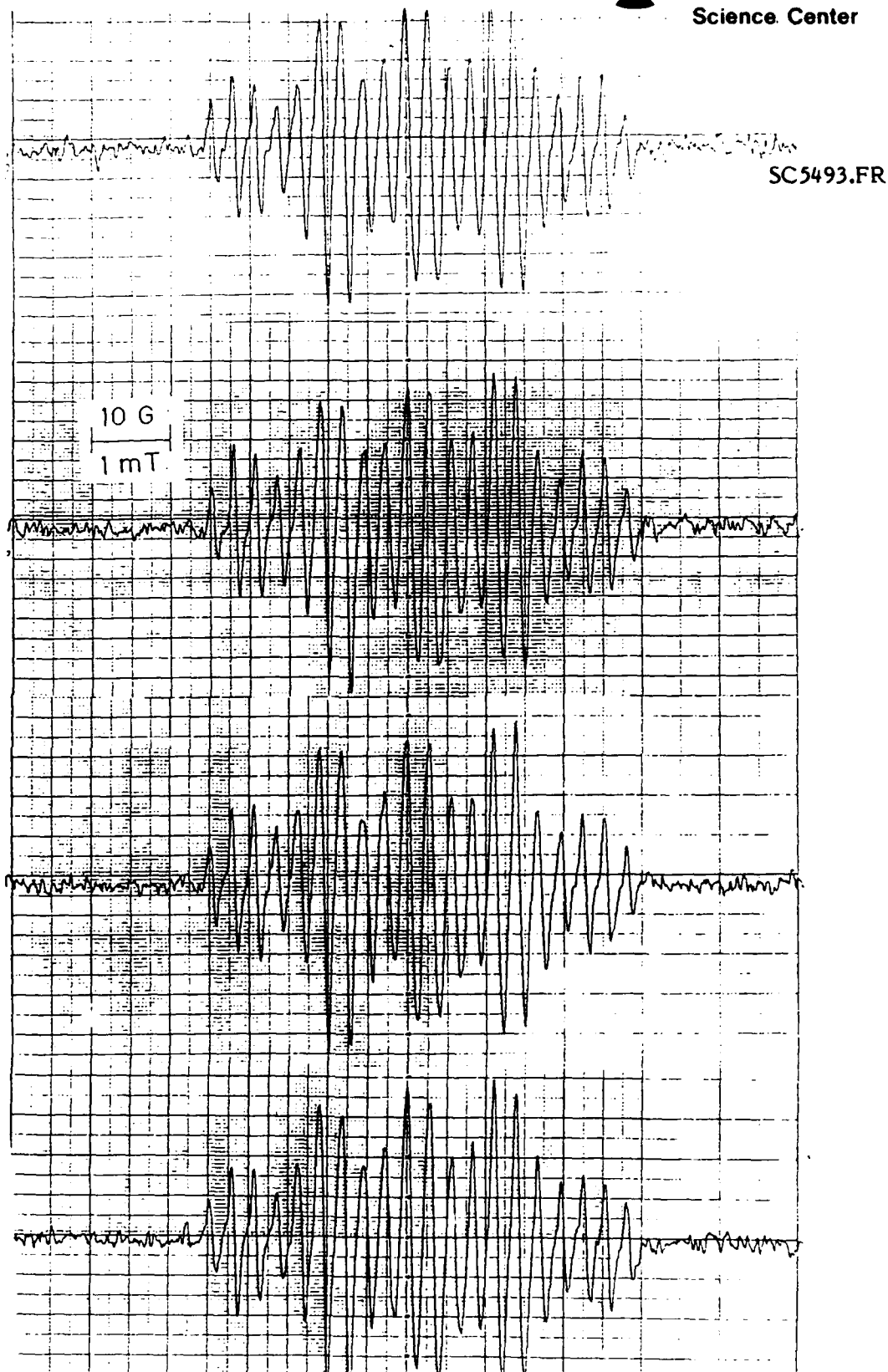
Fig. 19 Time dependence of the nitroxide spectra from moist TNT at 160°C with instrumental gain of one-half that of Fig. 18. Traces recorded at 500 (top), 1100, 1600, and 3600 s (bottom).

strong, stable nitroxide signal from the start whereas the dry sample did not exhibit any appreciable signal for nearly 2½ hours. Eventually the nitroxide level became significant.

Two reactions shown in Scheme 2 suggest that water is produced along with the known products such as trinitrobenzaldehyde. Consequently, the eventual appearance of nitroxide in Fig. 17 may result from interactions with the water byproduct formed during other reactions.

In many thermolysis experiments, liquid condensed in the cool upper portion of the ESR tube and this was shown by NMR to contain significant amounts of water.

Data from a number of different runs have been reduced to the slopes d[N]/dt and d ln[T]/dt and these are plotted versus 1/T in Fig. 20.

In many cases these rates are faster at the start of the experiment and then change to a slower secondary rate for the duration of the experiment (see Fig. 8). Rather than using a least squares slope for all the data points, we chose instead to separate the early data from the subsequent data in those experiments where there was a discrete break in the slopes. This improved the least squares correlation coefficients of the individual segments to greater than 0.95 for 42 of 44 segments. Only the later slopes or overall slope (when there was no discrete break) were used in Fig. 20.

The least squares lines of the data in Fig. 20 suggest that water appears to have an essentially negligible effect on the Arrhenius plots. That is, whatever the reason for the increased nitroxide concentration at low temperatures in the presence of water, it is not due to an activation process.

It might be useful to consider the following speculative hypothesis as additional experiments are designed and performed: Water may play some role in displacing an equilibrium between nitroxide and a diamagnetic precursor. It would be very useful to have a demonstration of the existence of such a precursor. Possibly the introduction of microliter quantities of water into a TNT-saturated toluene solution would produce nitroxide at room temperature and lend some credence to this idea. However, when such an experiment was performed, no ESR signal was observed.

Schemes 1 and 2 propose the formation of hydroxyl radicals in several different steps. These short-lived intermediates might be expected to react with oxidizable functions such as the methyl group of TNT:

$$R\text{-}CH_3 + \cdot OH \rightarrow R\text{-}CH_2\cdot + H_2O \qquad\qquad\qquad (11a)$$

Hydroxyl may also be reduced to hydroxide ion and if so, there is a rich chemistry open to reactions of this species with TNT. The formation of Meisenheimer complexes between nucleophiles and nitroaromatic compounds is well documented.[20,21] The reactions of methoxide and ethoxide ions with TNT have been studied both by visible spectroscopy[22] and by NMR.[23] Such studies have revealed the formation of sigma-bonded Meisenheimer complexes, 3, acid base interactions, 4, and reactions of 4 with TNT to produce Janovsky complexes such as 5 (where B⁻ is used to represent a general base or nucleophile, such as methoxide). Kinetically, the formation of Meisenheimer adducts is the fastest of these processes.
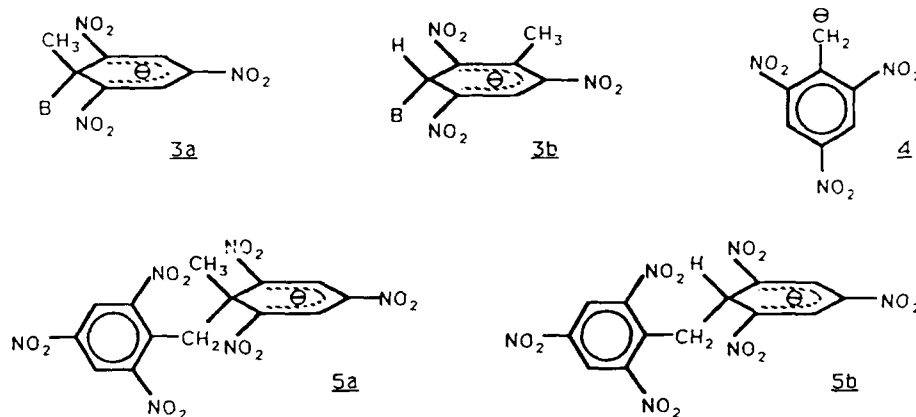
The effect of added bases upon the ESR spectra of nitroarenes will be considered later. But it is appropriate to introduce Meisenheimer and Janovsky complexes here, in conjunction with the observations on the effect of water upon nitroxide production in TNT.
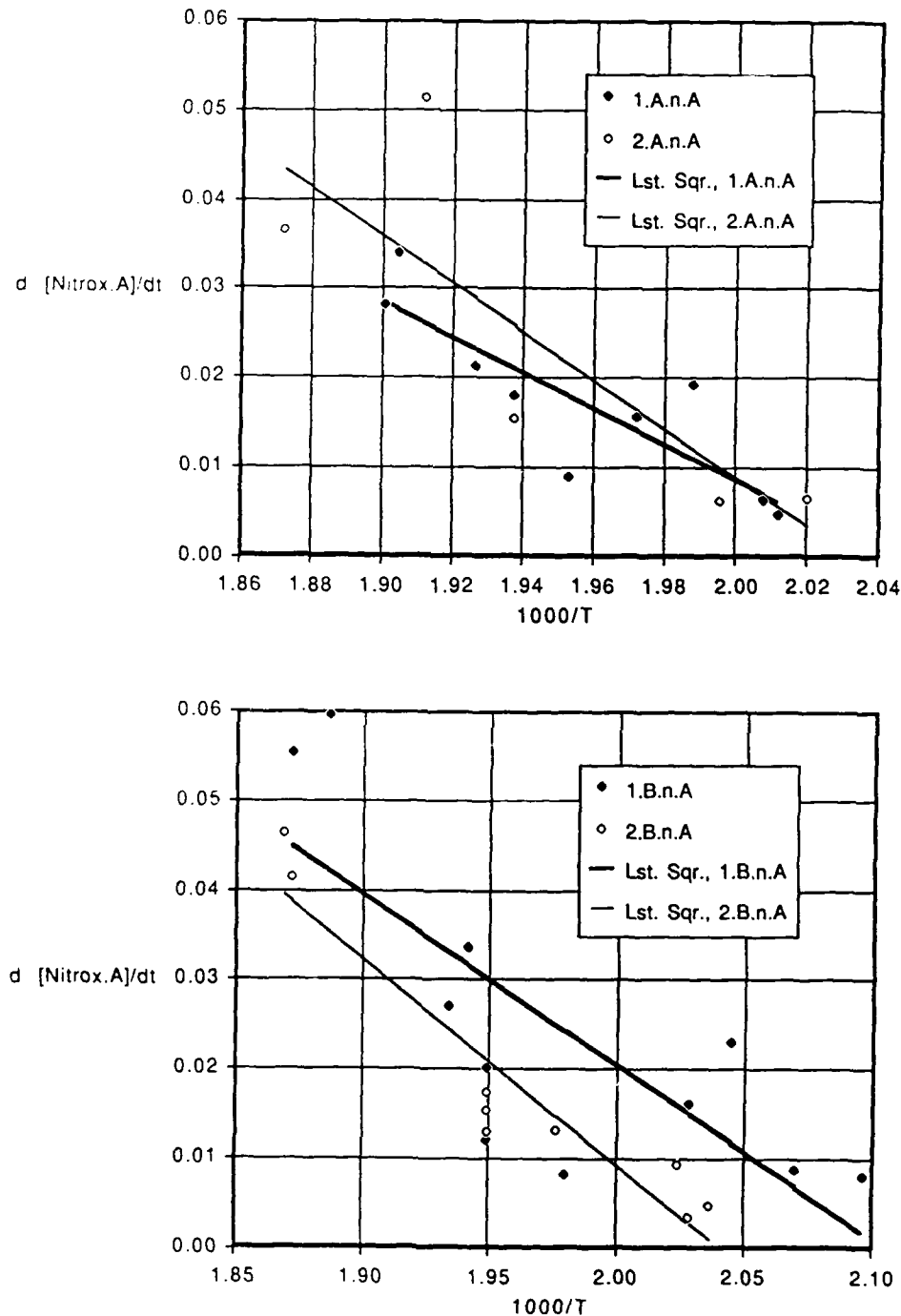
Fig. 20 Comparison of least squares analysis of the rate versus reciprocal temperature plots in two different samples (A and B) of dry and moist TNT (1 and 2, respectively). Comparison of nitroxide behavior (a,b) and Tar behavior (c,d). Comparison of all four least squares lines for nitroxide (e) and Tor (f).
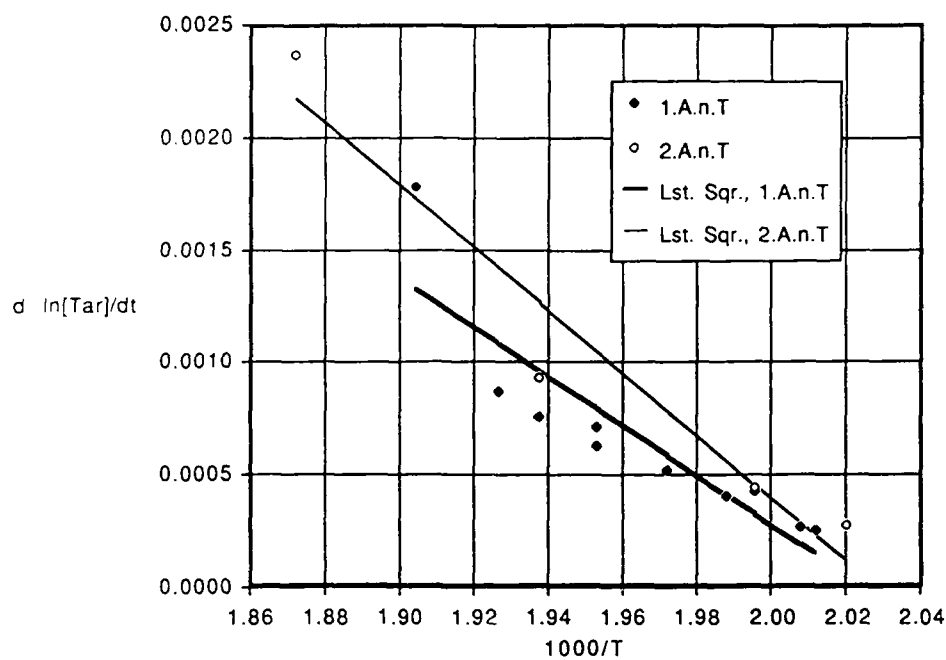
(c)

(d)

Fig. 20 (Continued)

(e)

(f)
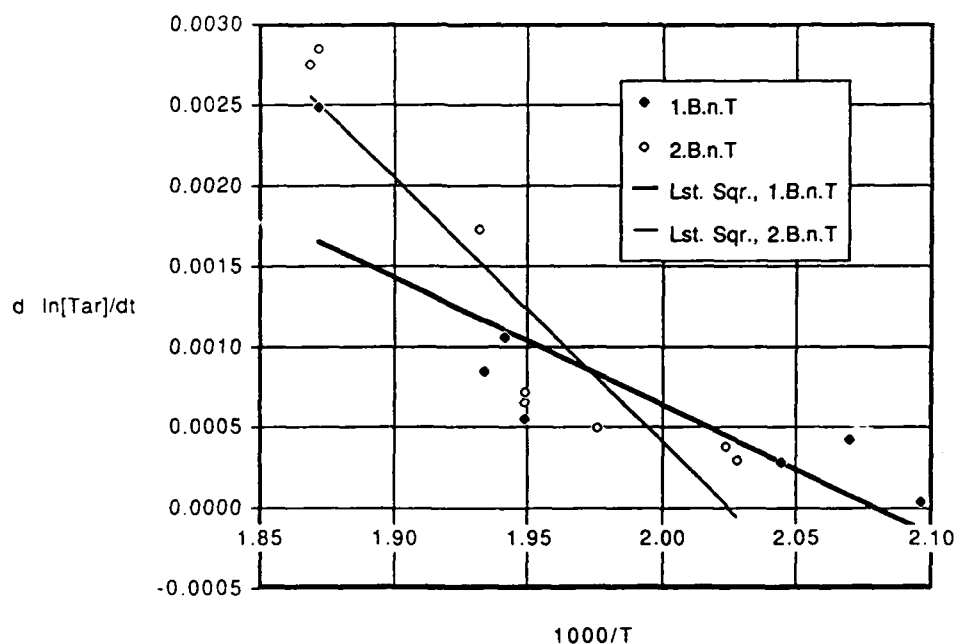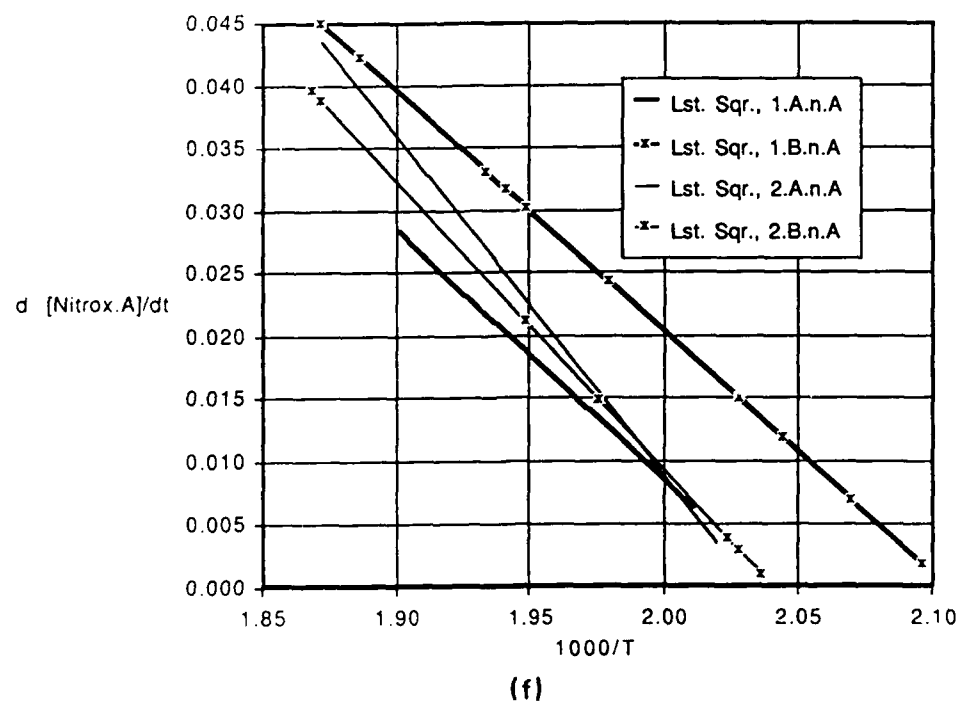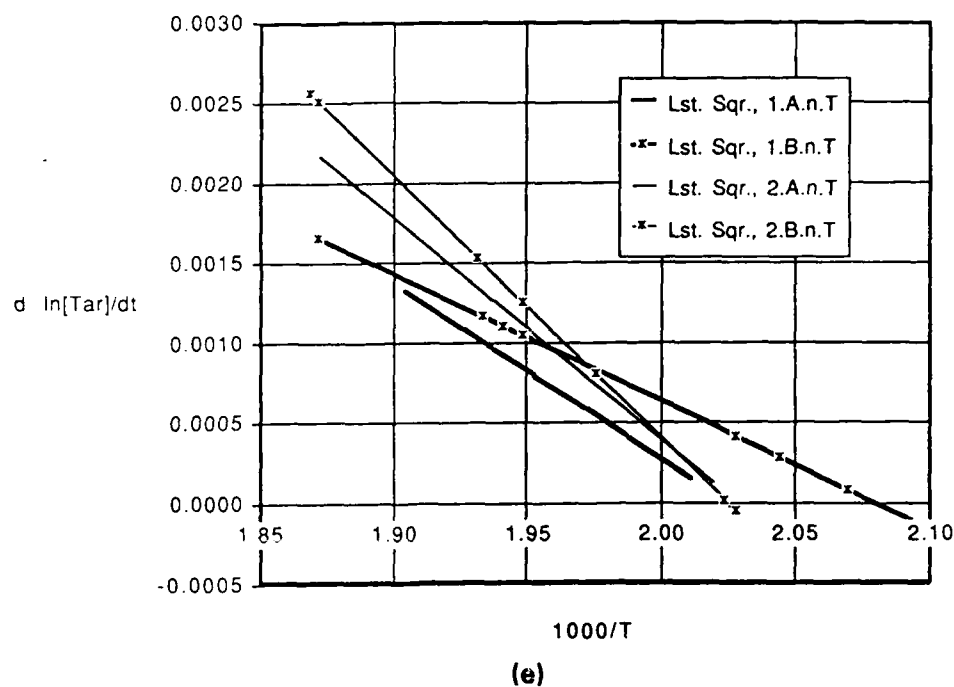
Fig. 20 (Continued)

D. Reactions of Hexamethylbenzene with TNT

Years ago, hexamethylbenzene was proposed as a candidate for an inert solvent in which to study the concentration dependence of TNT decomposition kinetics. Surprise was expressed at that time because radical formation ocurred at much lower temperatures in the presence of HMB than in neat TNT. We now understand that HMB can couple to TNT by a process similar to Scheme 1 and produce spectra that are essentially identical with radical 1:

TNT + TNT → <u>1</u>

TNT + HMB →

(12)
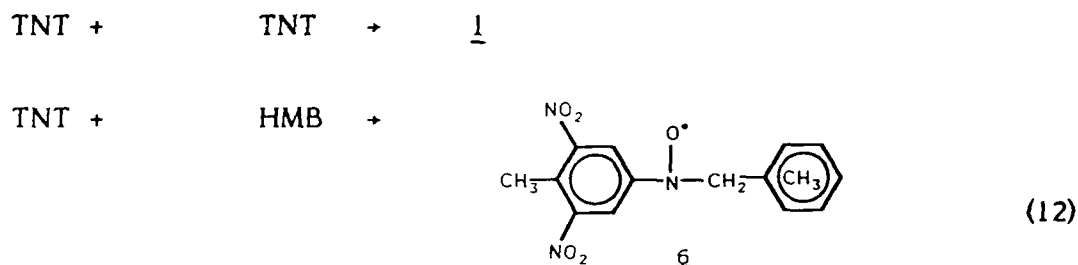
A yellow-to-orange color is observed whenever HMB is ground with a polynitro aromatic compound such as TNT or TNB. This color has been ascribed to a charge transfer complex of the form HMB^+TNT^-. In view of our proposed mechanism for the production of nitroxide species in TNT it is understandable that a charge transfer complex of this type would be predisposed to the formation of $(CH_3)_5C_6C \cdot H_2$ and $(NO_2)_2CH_3C_6H_2NO \cdot)OH$ radicals and consequently permit observation of the nitroxide coupling product at lower temperatures.

The protonated nitroaromatic anion radical intermediate $(NO_2)_2CH_3C_6H_2N(O \cdot)OH$ could eliminate either OH^- or $OH \cdot$ which would then proceed to enter into other reactions. Such elimination would leave $Ar-N^{\cdot+}=O$ or $Ar-N=O$, respectively. Nitrosobenzene is known to scavenge radicals to produce nitroxide radicals.

However, efforts to exploit the TNT/HMB reaction to gain further insights into TNT kinetics have been frustrated by the appearance of multiple radical species that complicate the ESR spectra to such an extent that it is very difficult to extract any meaningful kinetic data. When we voiced our dismay at the complexity of this system, workers at the Seiler Lab shared a technical report[24] that showed that our two groups had observed precisely reproducible effects. They had also speculated that the multiple species might arise from competitive processes that produce coupling of two TNT molecules as well as cross coupling between TNT and HMB. The kinetic behavior of asymmetric mixtures were vastly different, depending on whether TNT or HMB was the excess reactant.

We report here some results on the reactions of binary mixtures of TNT and HMB conducted as Series 3 (see Table 1 and Appendix A). The kinetic analysis was clouded by the appearance of multiple radical species as suggested above and in Fig. 21.

These spectra appear quite different but measurement indicates that all three have the same total span. Consequently the differences appear to arise from the presence of a mixture of radicals, with the mixture comprising different proportions of the same radicals as the reactant concentrations are varied. Other experiments (Appendix A) indicate that the radical ratio in a given mixture also changes when the reaction takes place at different temperatures.

A simplistic explanation for the presence of such multiple species lies in the obvious possibility of competing processes leading to simultaneous formation of radicals 1 and 6.

However our independent studies[25] of reactions between different hydrocarbons and nitroarenes argues against any significant difference in the splitting constants of radicals 1 and 6, so this explanation is not satisfactory. (These unpublished studies show that the splittings of ortho and para protons on the aryl group of radicals such as 1 or 6 have a value close to 0.26 mT in a great variety of nitroxides, regardless of the aliphatic substituent. The protons on the aliphatic carbon attached to the nitroxide function do exhibit considerable variablity, depending upon the steric requirements of the substituent. But in a large number of examples, hexamethylbenzene produces a nitroxide with a large benzylic hydrogen splitting having the same magnitude as the nitroxide nitrogen splitting.)

10 G
1 mT
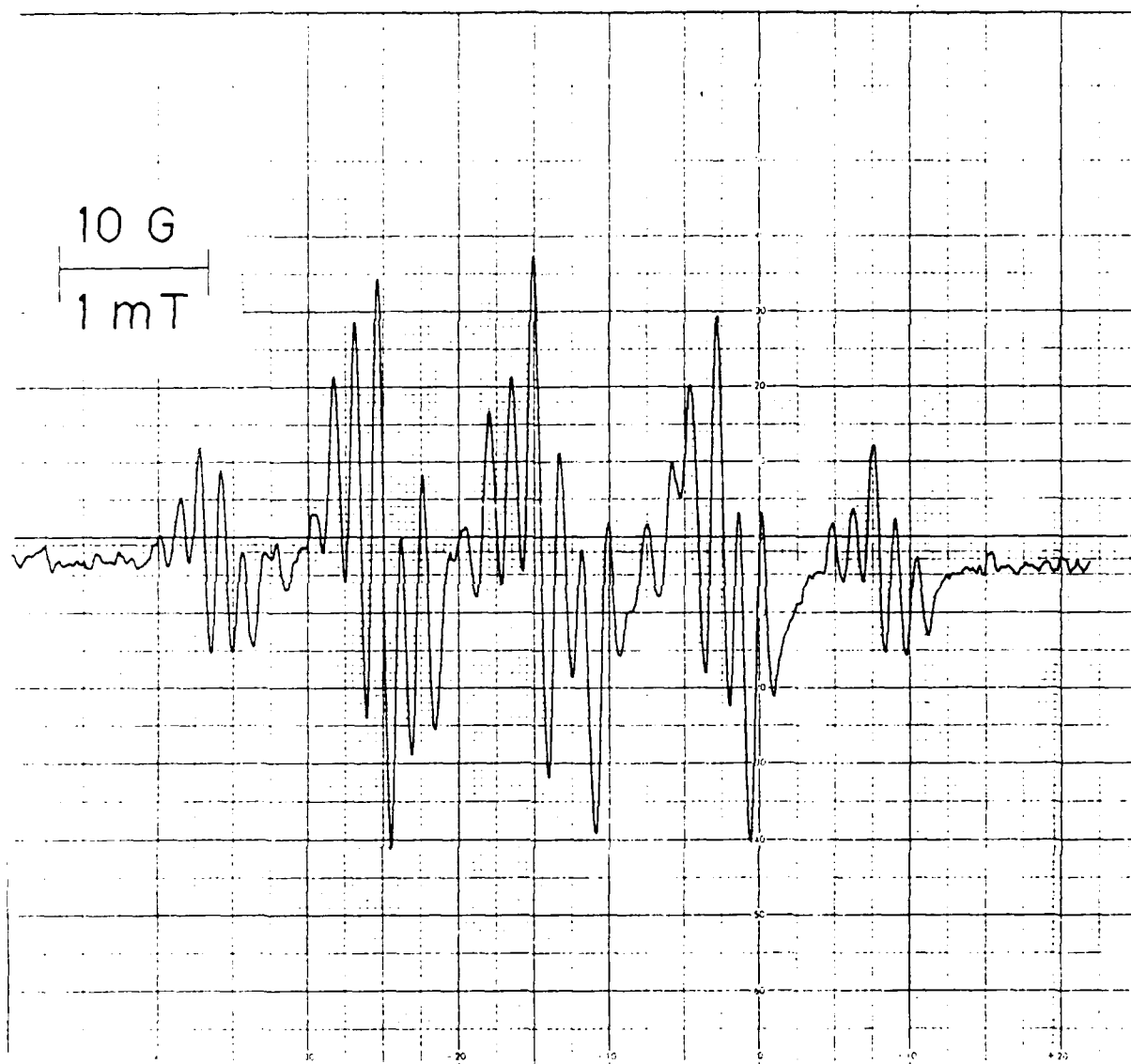
Fig. 21 Spectra indicative of multiple radical species present in thermal reaction between TNT and HMB near 175°C. (a) 5% TNT/HMB (Expt. 3.A.3) at 280 s, (b) 20% TNT/HMB (Expt. 3.D.5) at 255 s, and (c) 50% TNT/HMB (Expt. 3.E.1) at 250 s.

10 G

1 mT

Fig. 21 (Continued)

10 G
——
1 mT

Fig. 21 (Continued)

C9636DA/ejw
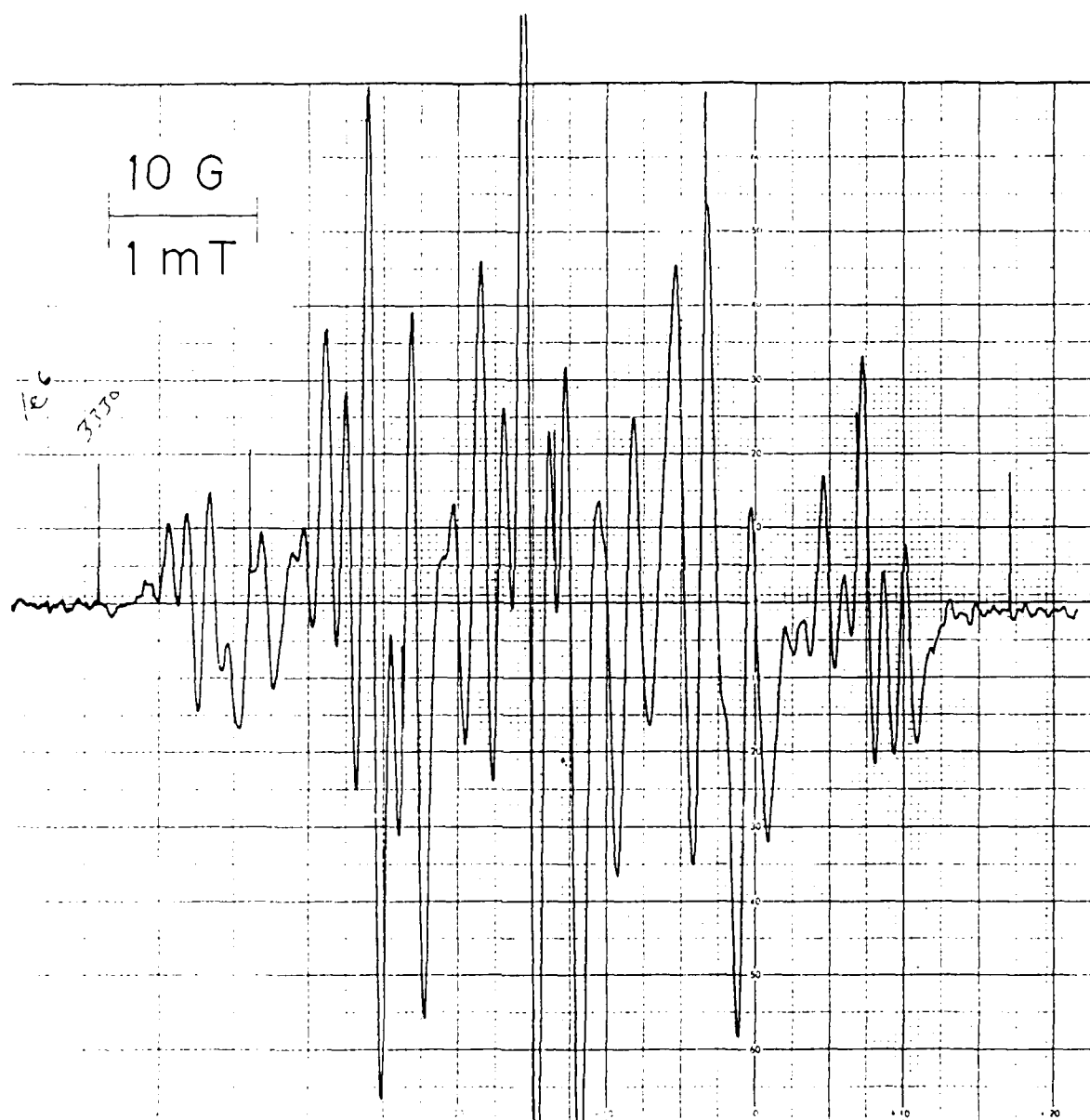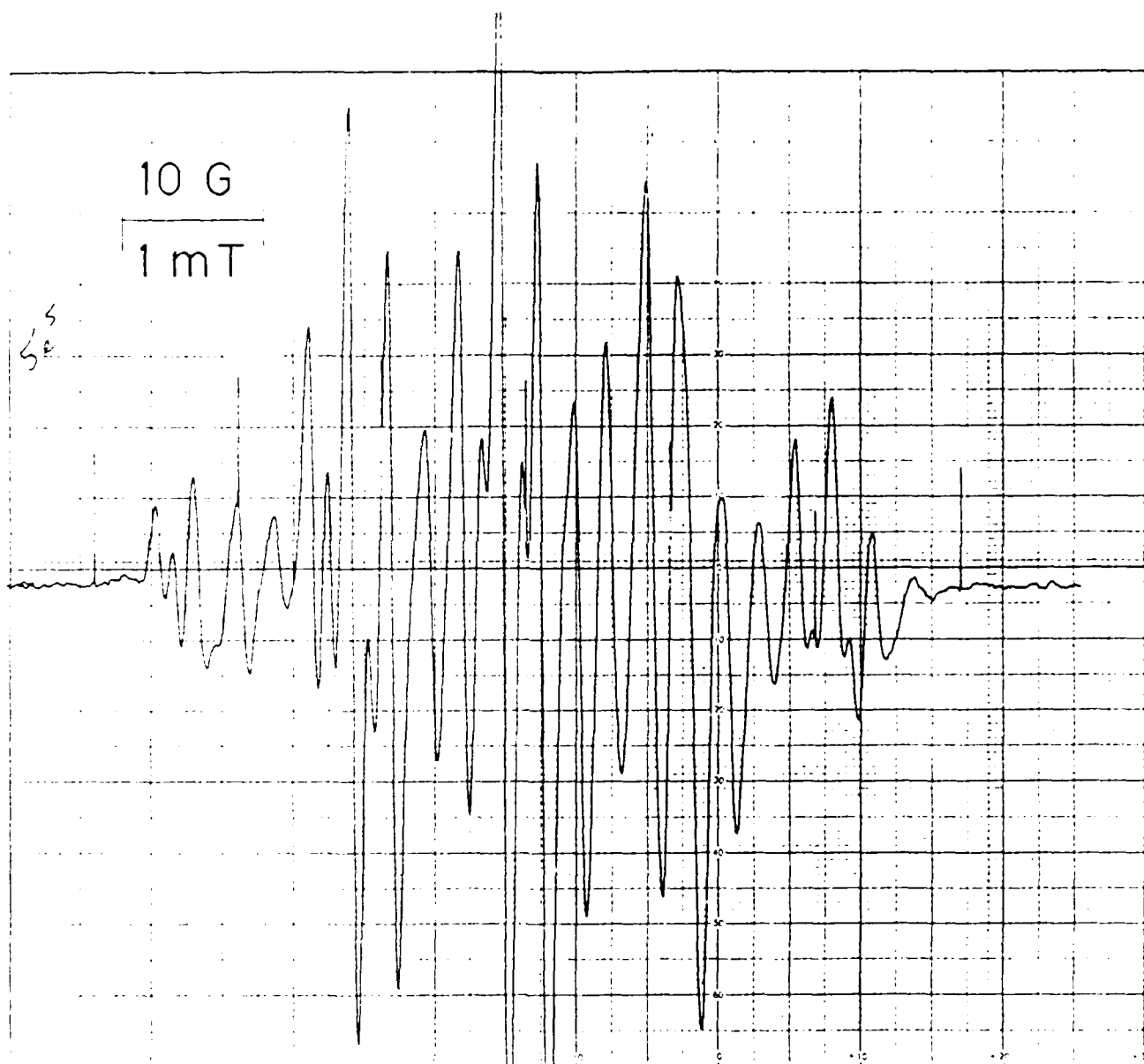
It is worth noting that the multiple species are evident at low temperatures (170°C) and in non-stoichiometric mixtures of reactants. It is perplexing that the secondary radicals remain unidentified. Without such knowledge, the overlap of the spectra makes it difficult to determine which lines might be suitable for a more meaningful evaluation of kinetic data.

An effort was made to extract kinetic data from the set of TNT/HMB reactions listed in Appendix A, even though the understanding of the underlying spectra is incomplete. In many instances it was not possible to identify the positions of lines B and C during the early stages of the reaction because of the spectra were complicated by multiple species. But once significant intensity began to build in the Tar line it was possible to measure from it to identify the line analogous to line B in the spectrum of 1. Then it was possible to follow the evolution of these two lines back in time to the beginning of the experiment. (It was not possible to analyze experiments occurring at temperatures below 210°C because Tar formation was not observed at lower temperatures.) The charts that follow use the same assessment of Tar intensity, $A_T = A_C - A_B$, that was used in the TNT data analysis. Unfortunately it is too difficult to measure the intensity of line A in these mixtures, so information about the nitroxide behavior is limited to the changes in line B.

There are several different variables to discuss in this set of experiments: (a) The behavior of Tar and (b) the behavior of nitroxide at (c) a given temperature as a function of sample composition or (d) in a given sample mixture as a function of temperature. Moreover, the effect of added moisture was studied for one sample mixture (10% TNT/HMB).

It is worth summarizing the reactions of Series 3 (see Appendix A) here to aid understanding of the following discussion. Five different mixtures of TNT/HMB were studied. The mole-percentages of TNT in the mixtures were 5% for set "A", 10% for sets "B" and "C", 20% for set "D", and 50% for set "E"; set "B" differed from set "C" in that the samples in set "C" were moistened with water. There are several distinguishing features between this set of experiments (Series 3) and the experiments of Series 1 and 2:

- The formation of Tar appears to occur as a zero order reaction.

- Nitroxide does not achieve a steady state concentration. Rather, it peaks early in the reaction and then diminishes. The rate of decay may be exponential, but the data show some curvature on a log plot.

- The rate of Tar formation and the rate of nitroxide disappearance are both strongly dependent upon the fraction of TNT in the sample, occurring faster at higher mole fraction of TNT.

Figure 22 shows plots of Tar kinetics at different temperatures for two diferent mixtures It is uncertain how much significance can be attached to the earliest portions of these plots since the total radical concentrations were changing rapidly. The apparent dip in Tar intensity may simply be an artifact of the methods used to separate Tar from nitroxide intensity contributions. However the later development in Tar intensity appears to approximate a linear increase, rather than the exponential growth that was observed in the reactions of Series "1" and "2".

Figure 23 compares the rate of Tar formation in different mixtures under approximately isothermal conditions. This rate is obviously strongly influenced by the proportion of TNT in the sample, being much faster at high concentrations of TNT. This observation adds credence to the idea proposed above that Tar is produced by reaction of TNT with some intermediate such as nitroxide.

Figure 24 compares the rates of Tar formation in dry and moist samples of 10% TNT/HMB at two different temperatures. It is difficult, on the basis of such limited data, to draw firm conclusions about the effect of water on Tar formation in this system. But it appears that water may have a acceleratory effect since the slopes of the lines for the moist samples are each slightly greater than those for the corresponding dry samples. This interpretation is at variance with the conclusions based upon a larger number of experiments in the Series "1" and "2" reactions. But lacking additional data for Series "3", these results are simply reported without interpretative comment.

Examination of Fig. 25 reveals the reason for the difficulty of evaluating the early Tar behavior in these experiments. It shows the corresponding behavior of nitroxide (as measured through line B). In each of the two samples of Fig. 25 the nitroxide intensity peaks early and then declines for the remainder of the experiment.

(a)

(b)
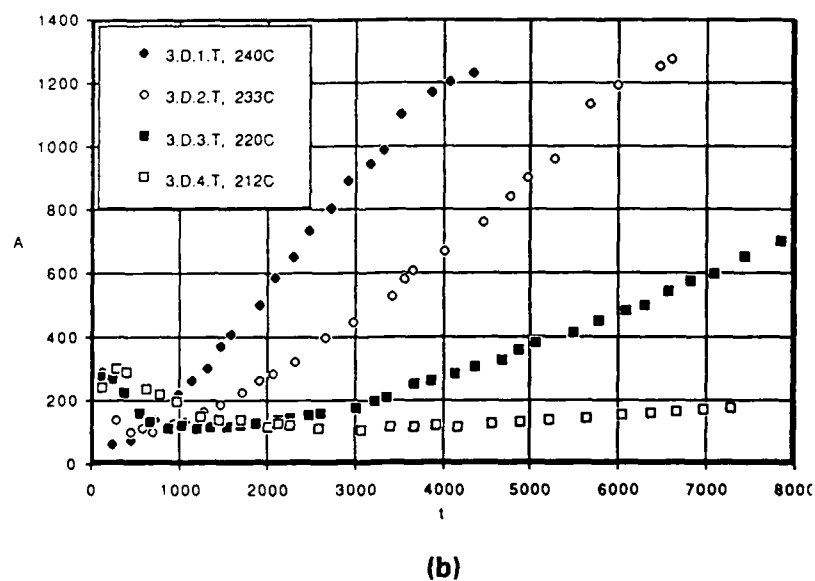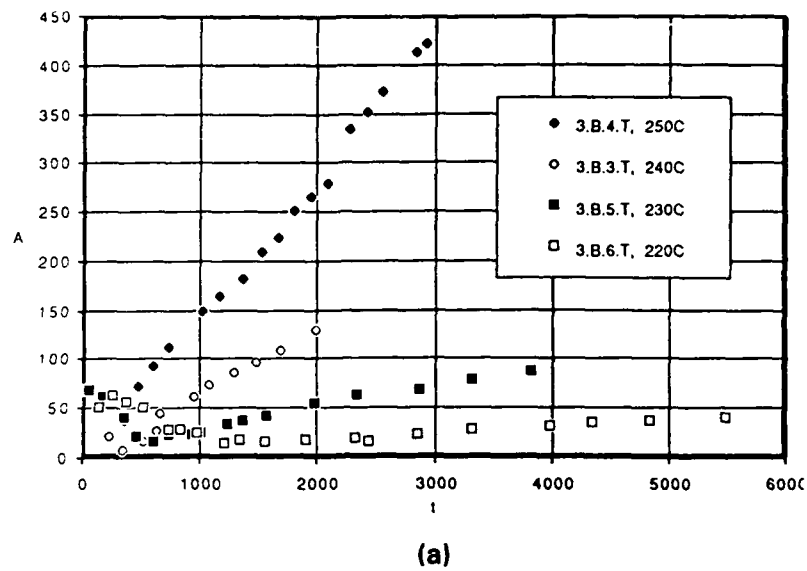
Fig. 22   Tar formation in (a) 10% TNT/HMB and (b) 20% TNT/HMB at several different temperatures.
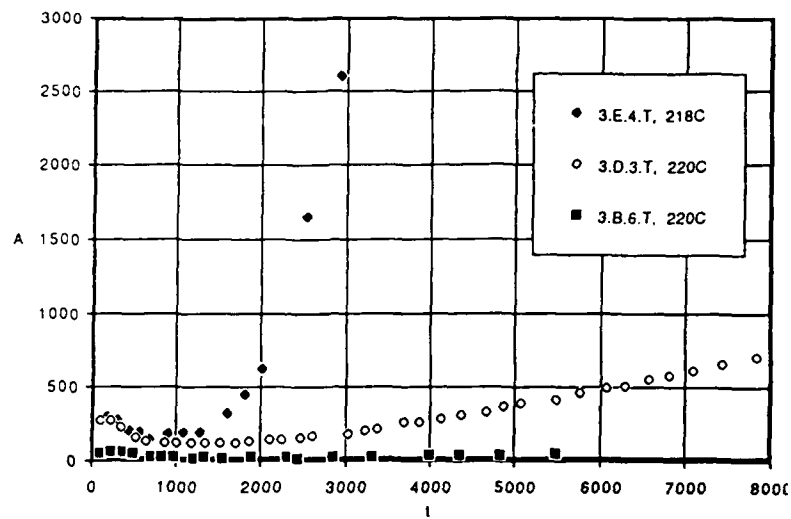
(a)
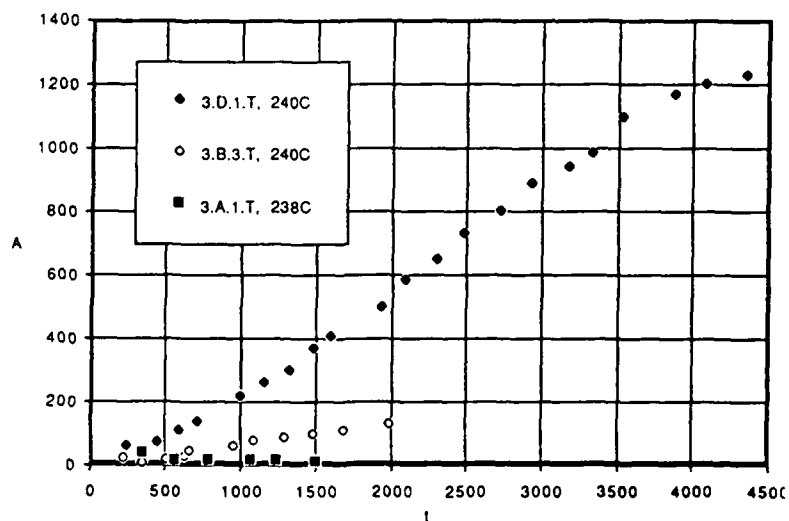
(b)

Fig. 23   Tar formation in TNT/HMB mixtures: A=5%, B=10%, D=20% and E=50% TNT in HMB. Reactions near (a) 220°C and (b) 240°C.
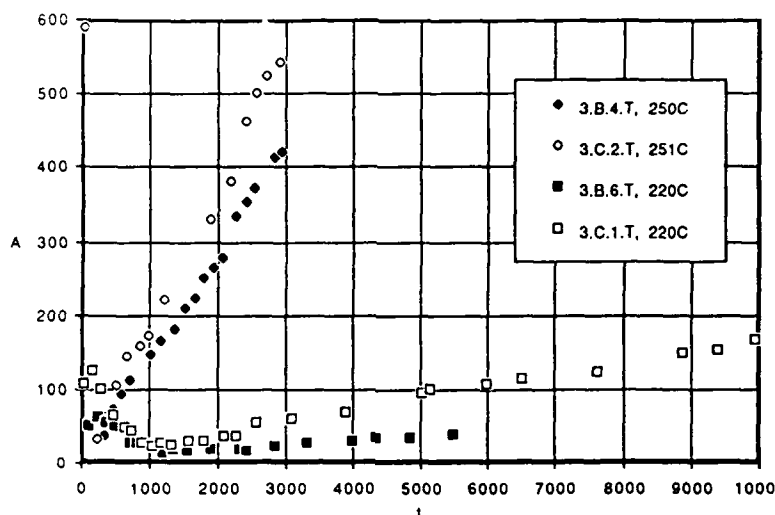
Fig. 24   Tar formation in 10% TNT/HMB mixtures. "B" samples were dry while "C" samples were moistened with 15-20 mg quantities of water prior to heating. Comparisons at 250°C and 220°C.

The time required to reach the peak intensity of nitroxide in inversely related to the temperature of reaction, longer times being required at lower temperatures. This is similar to the behavior observed in Series "1" and "2", again suggesting competitive nitroxide formation and destruction reactions, with the latter dominating at higher temperatures and longer reaction times.

The decay portions of these curves appear exponential, but the logarithmic plots of Fig. 25c and d reveal considerable divergence from pure exponential behavior. This may reflect complications due to a multiple step reaction sequence (similar to Scheme 2) or it may simply underscore the measurement difficulties encountered in trying to analyze kinetics from spectra arising from multiple species.

Figure 26 compares the effect of sample composition under approximately isothermal reaction conditions. (It should be reiterated that the data analysis attempts

(a)

(b)
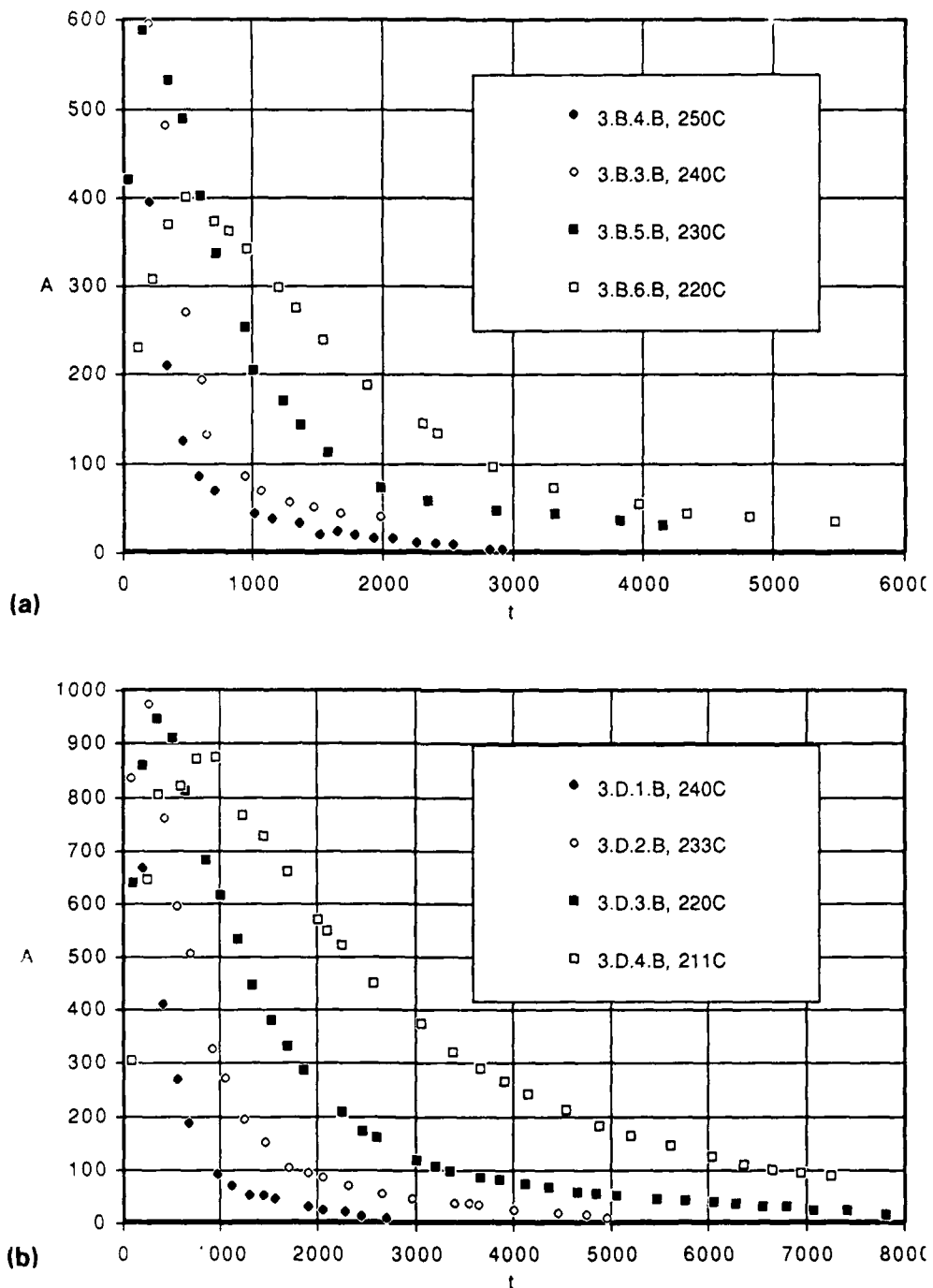
Fig. 25   Nitroxide behavior in (a) 10% TNT/HMB and (b) 20% TNT/HMB at several different temperatures.   Plots (c) and (d) display the same data on a logarithmic intensity scale.

(c)

(d)
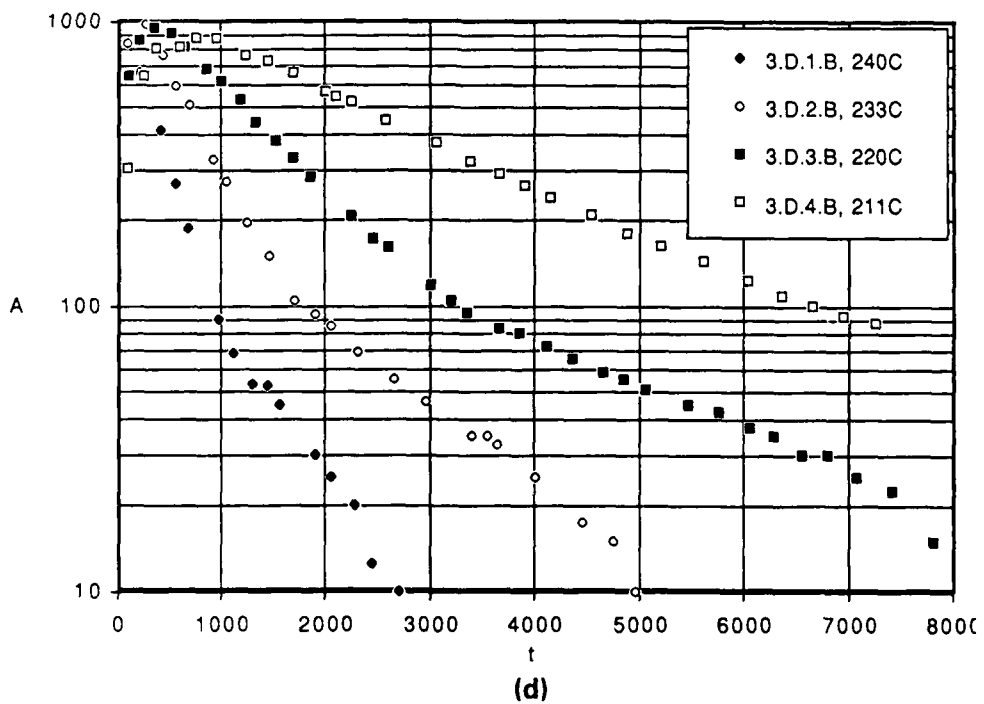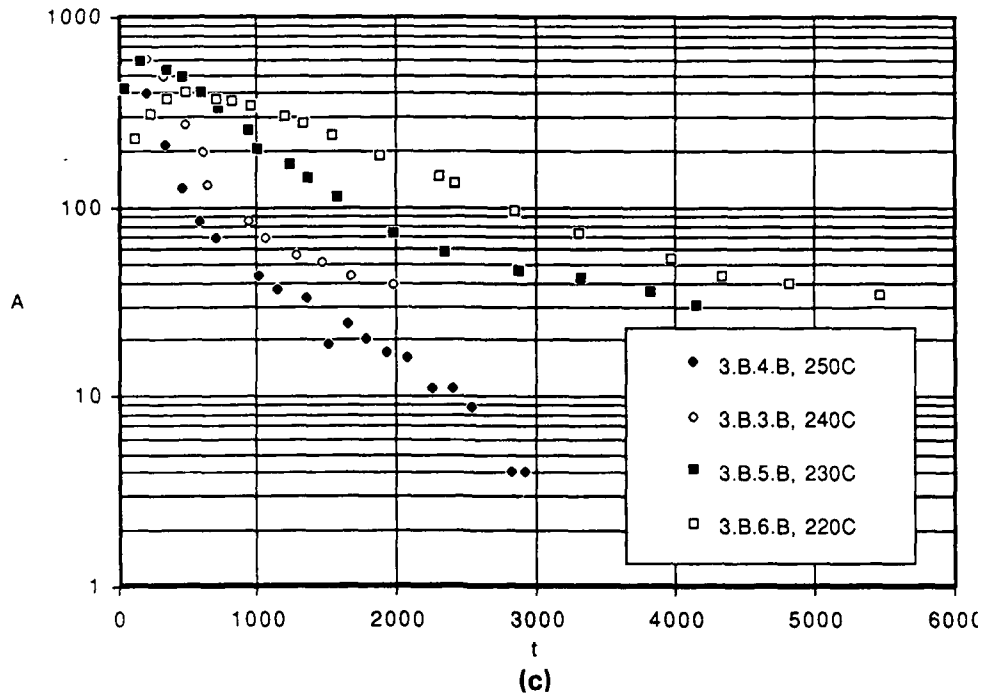
Fig. 25 (Continued)

intentionally to discriminate against the secondary, unidentified radical which is presumably also a nitroxide species.) At each temperature, the highest nitroxide concentration is observed at the highest proportion of TNT in the sample. This is as expected since the rate of formation of 6 is proportional to the product [TNT] [HMB], Eq. (12), which is maximized at 50 mole percent. There is another observation consistent with the greater ease of formation of Radical 6 as compared with Radical 1 in mixtures of TNT and HMB. When data for neat TNT are similarly displayed (Fig. 6a), there is a greater spread in the intervals at which the peak nitroxide concentration occurs, as compared to Fig. 25. Moreover, there is also an initial drop in nitroxide intensity at the lower temperatures (Fig. 6c) which is not observed in the TNT/HMB mixtures. While there is not yet any detailed understanding of the latter effect, these differences are not inconsistent with the greater ease of formation of radical 6 as compared with radical 1.

Comparison of the behavior of nitroxide in the the moistened samples reveals (Fig. 27) that water appears to promote nitroxide formation in the TNT/HMB system, just as it did in the pure TNT experiments. At the lower temperature, the nitroxide intensity peaks to a higher value and then proceeds to track the behavior of the dry sample after the water has been either consumed or ejected. At the higher temperature, the different samples are essentially indistinguishable.

It is futile to attempt to fit the TNT/HMB rate data to a reaction scheme until some plausible reactions can be linked to the experimental observations. One of the fundamental problems in this endeavor is the lack of knowledge about the nature of the multiple radicals observed during reaction of binary mixtures of TNT and HMB. However, evaluation of the rate data as described above leads to a working hypothesis about formation and nitroxide and Tar in the TNT/HMB system.

The linear growth of Tar during the late stages of the reaction appears to be approximately zero order and it described by the rate equation

$$d[Tar]/dt = k_a \qquad\qquad (13a)$$

Recognizing that a true zero order reaction would be bizarre in this system, a logical candidate for a pseudo-zero order equation is

$$d[Tar]/dt = k_a^*[TNT] \tag{13b}$$

where [TNT] remains roughly constant. Similarly, the nitroxide intensity declines approximately exponentially as in the equation

$$d[Nitrox]/dt = -k_b[Nitrox] \tag{14a},$$

but is more likely a pseudo-first order process, approximated as

$$d[Nitrox]/dt = -k_b^*[Nitrox][TNT] \tag{14b}.$$

Equations 13b and 14b are consistent with the experimental observations that the rates are enhanced at higher concentrations of TNT.

A set of reactions can be hypothesized by analogy to Equation 7

HMB + TNT	→	6	k_1	(15a)
6 + TNT	→	Tar	k_2	(15b)
Tar + TNT	→	Tar'	k_3	(15c)
6	→	Diamag.	k_4	(15d)

and when rudimentary simulations are performed, the resulting curves are similar to the experimental curves.

Such a set of simulations is presented in Fig. 28. For consistency with the designations used in experiments of Series "3", the simulations (Series "S") are coded with the letter "A" for 5/95 proportions (TNT/HMB ratio), "B" for 10/90, "D" for 20/80, and "E" for 50/50. These letters are followed by the value of k_4 used in the simulation (zero or 5×10^{-4} s^{-1}), and this in turn is followed by the letter B or T to indicate nitroxide (as in experimental line B) or Tar behavior. This set of simulations was performed using rate constant values (l mol^{-1} s^{-1}) of 10^{-4} (k_1), and 5×10^{-4} (k_2 and k_3).

The curves in Fig. 28a concur that nitroxide intensity should be greater for greater initial TNT concentrations, in conformity with the experimental facts. Incorporation of an additional nitroxide-destroying step, Fig. 28b, hastens the onset of
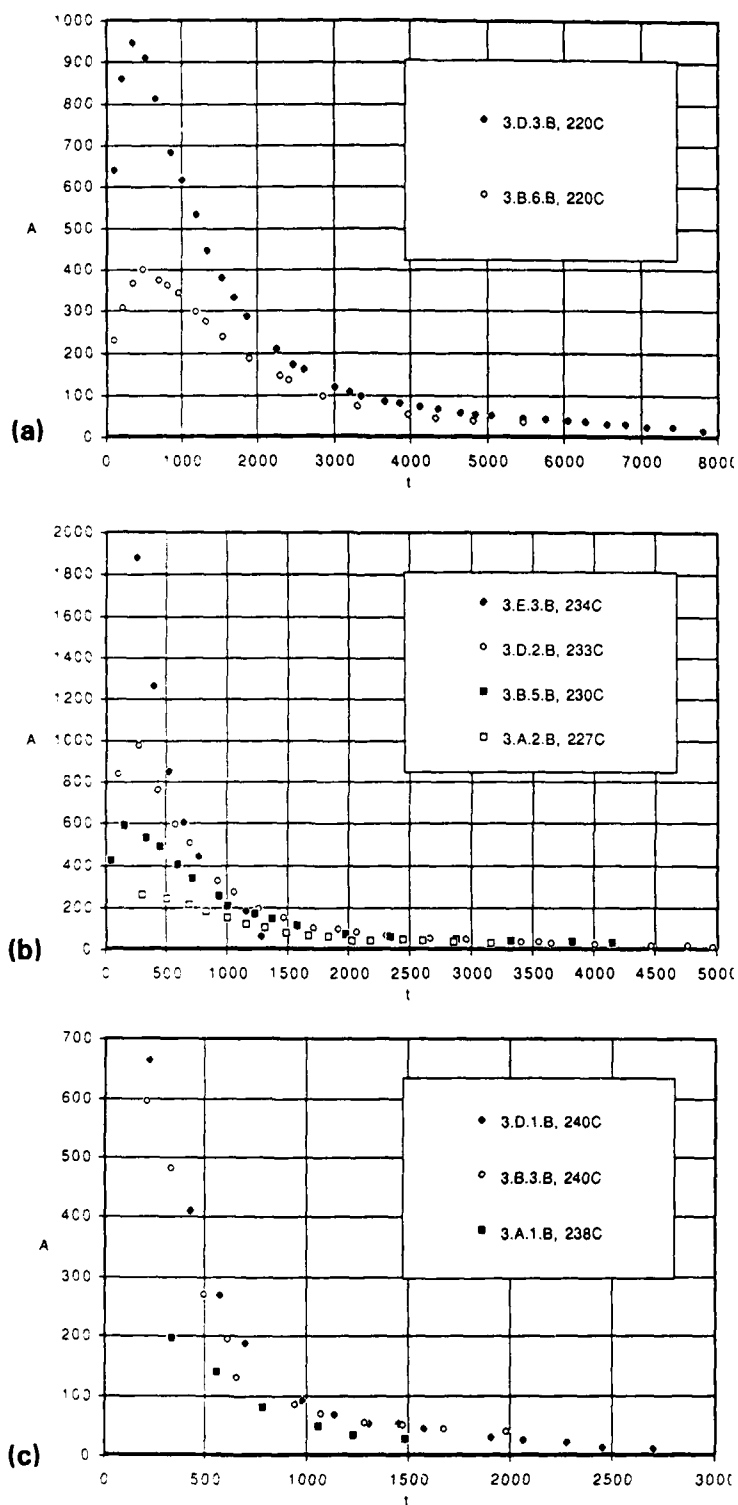
Fig. 26   Nitroxide behavior in TNT/HMB mixtures: A=5%, B=10%, D=20% and E=50% TNT in HMB. Reactions near (a) 220°C, (b) 230°C, and (c) 240°C.
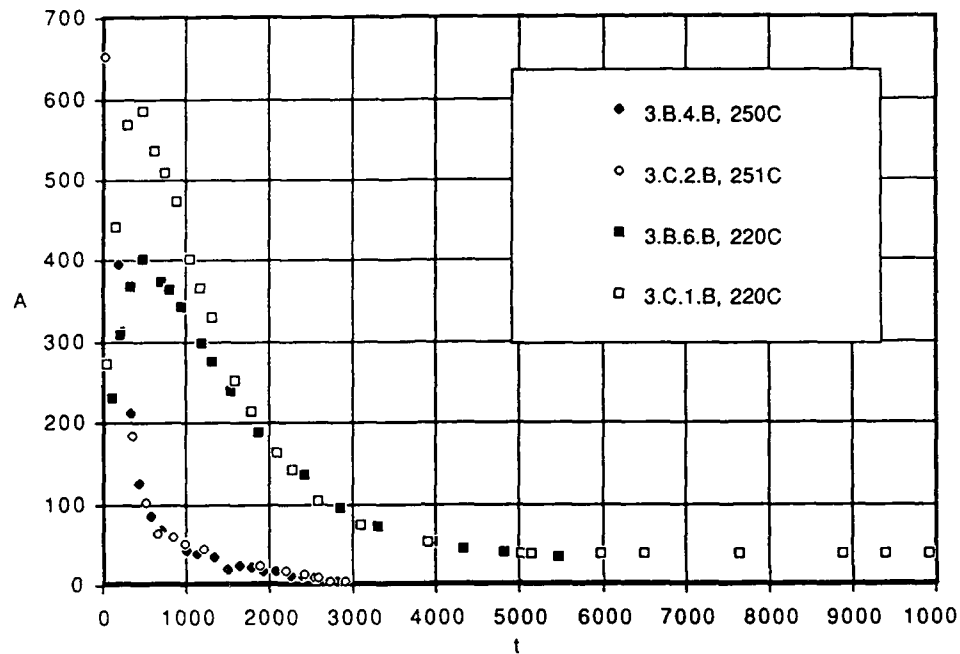
Fig. 27   Nitroxide behavior in 10% TNT/HMB mixtures. "B" samples were dry while "C" samples were moistened with microliter quantities of water prior to heating. Comparisons are at (a) 250°C and (b) 220°C.

(a)

(b)
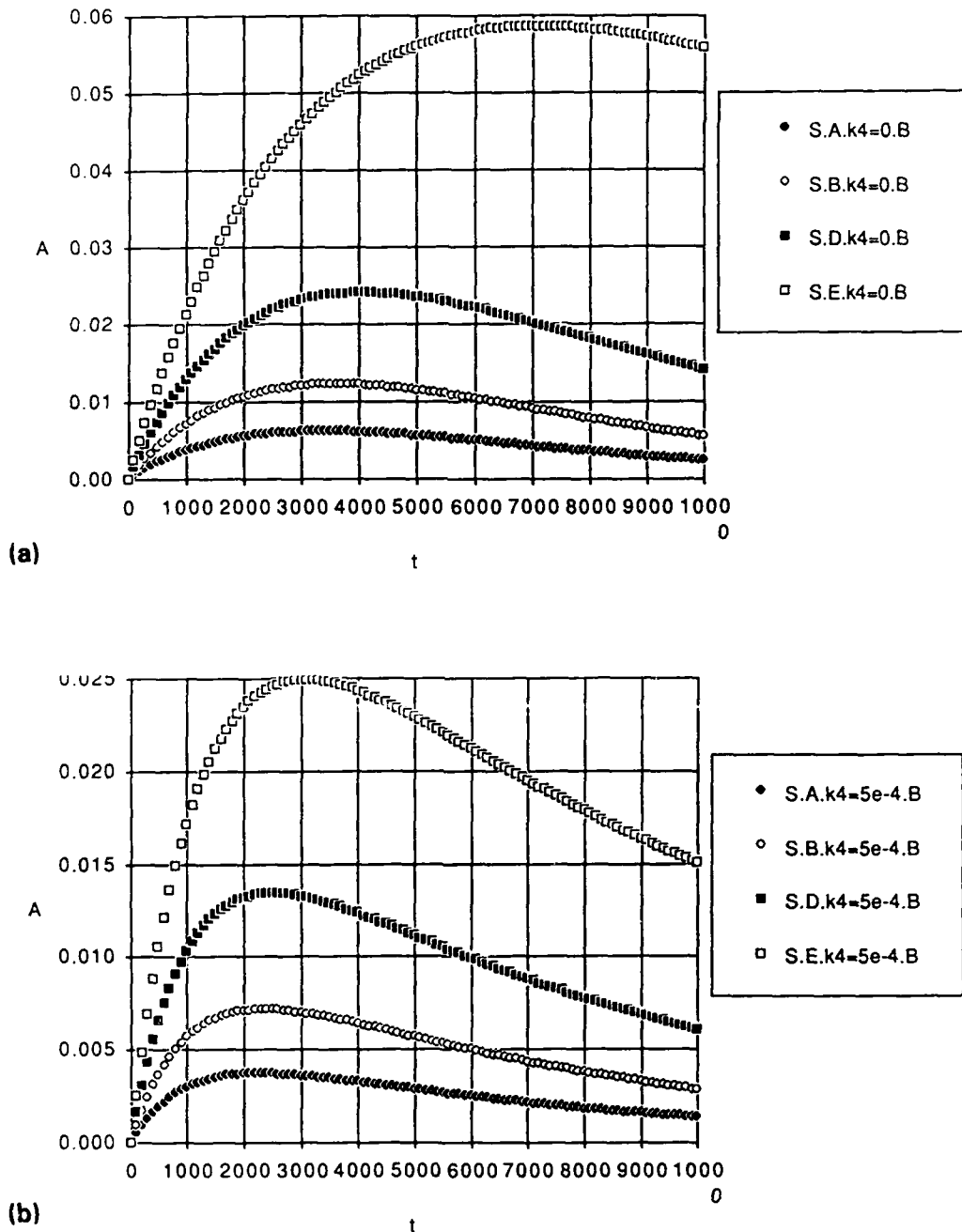
Fig. 28   Simulations based on Equation 15.   (a)   Nitroxide behavior, three-step mechanism; (b)   nitroxide behavior, four-step mechanism; (c)   Tar behavior, three-step mechanism; (d)   Tar behavior, four-step mechanism.

(c)

(d)
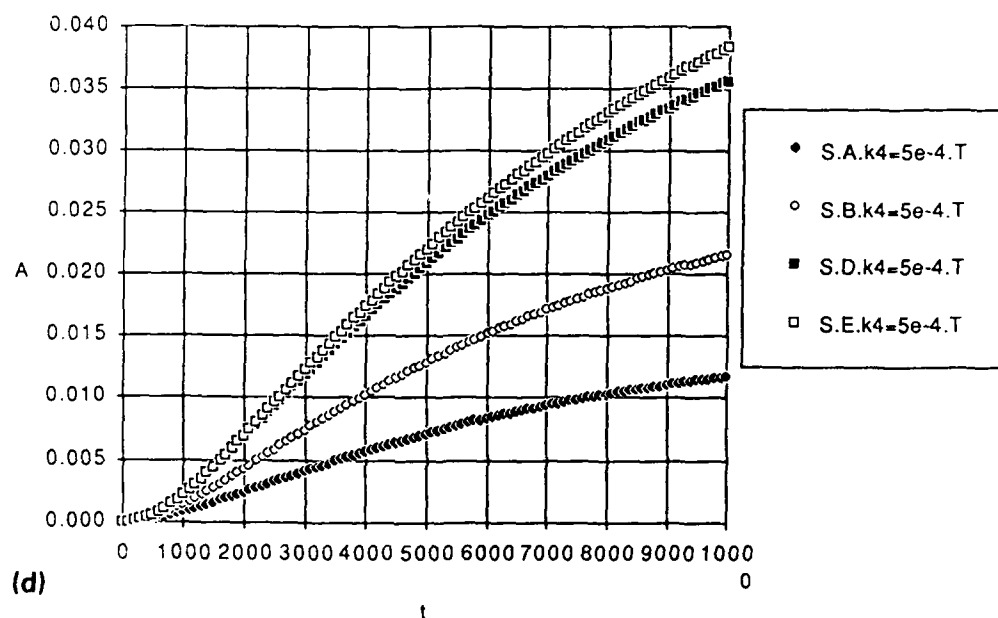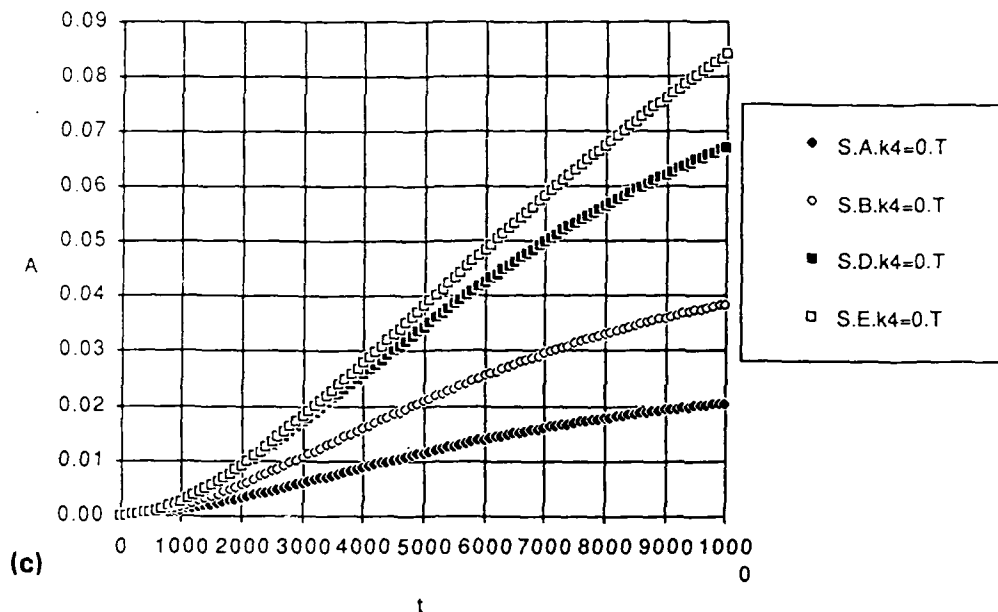
Fig. 28 (Continued)

the exponential decay portion of the curves, which more closely aproximates the experimental behavior. The Tar behavior in Fig. 28c is similar to the experimental curves in that it is roughly linear and has larger slopes at greater TNT proportion. However, when the nitroxide destruction step is incorporated, the effect of TNT concentration becomes less distinct at high values of [TNT], in contrast to the experimental curves, so this casts doubt upon the validity of the particular form of reaction 15d in this crude, trial set of simulations. It would be profitable to be able to devote more effort to testing other reasonable models in an effort to fit the experimental curves more closely. Regretably, there has not been an opportunity to simulate the effects of more complicated reaction sequences such as those suggested in Scheme 2 and such models might be expected to be more fruitful than the rudimentary ones used to date.

E.   Reactions of Hexamethylbenzene and TNB

Parallel studies were made on mixtures of TNB and HMB in an effort to preclude some of the possibilities for multiple radical species (Experiments 4.A-D.n). It was anticipated that the high symmetry of the reactants would produce clean spectra of the radical (7)
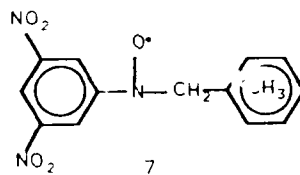
formed by coupling of TNB and HMB. The spectrum shown in Figure 29 was observed from a mixture of 40% TNB/60% HMB at 180°C (Expt. 4.C.2). Superficial examination indicates that this spectrum is consistent with the structure of radical 7. (The spectrum has a small quartet splitting of 0.26 mT arising from the three ring protons and the larger five branch pattern arising from accidental equivalence of the nitroxide nitrogen and benzyl hydrogen nuclei, as in the case of radical 1.) However, more careful scrutiny reveals that some of the lines are misshapen and this indicates that another radical is also present.
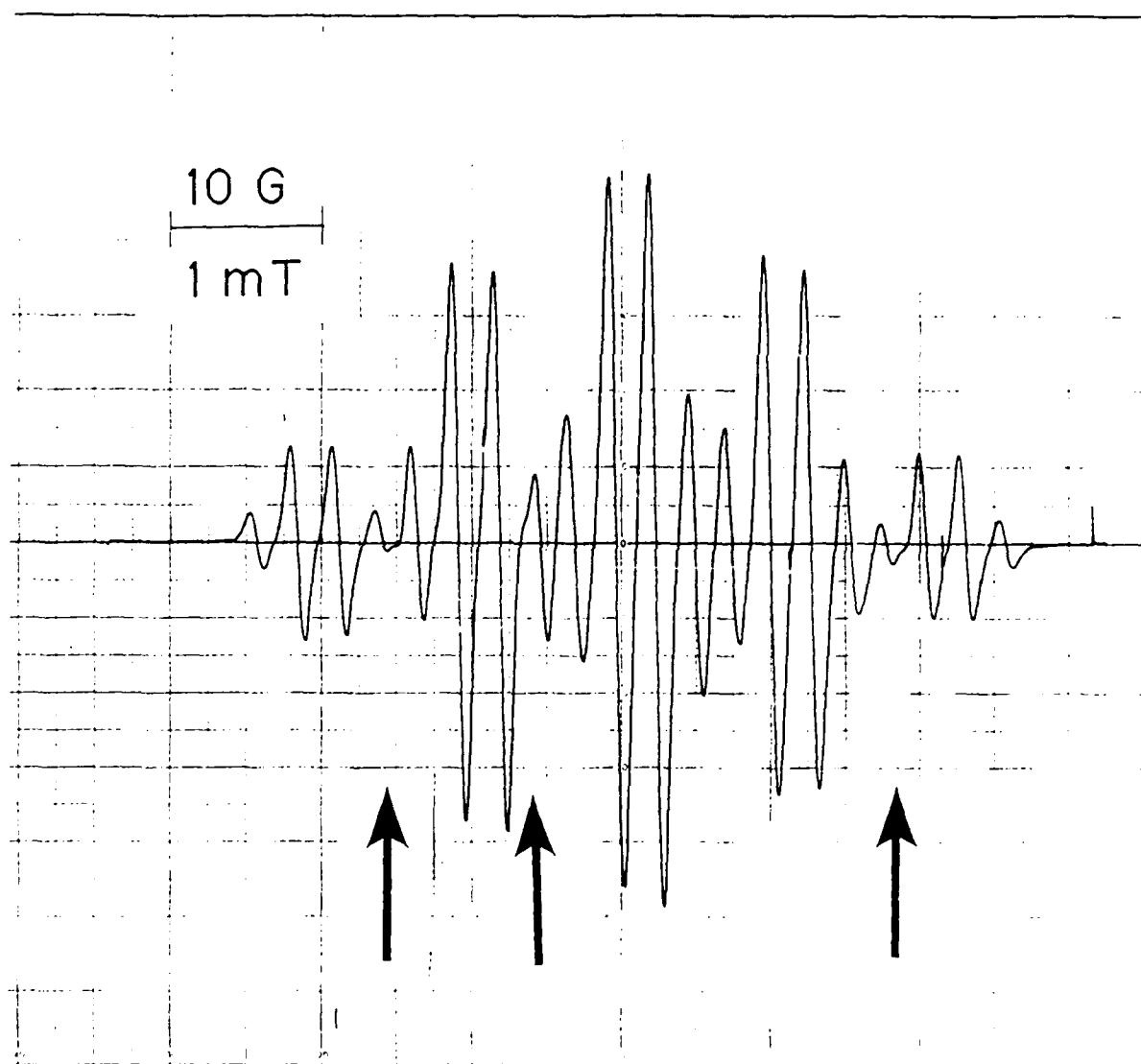
Fig. 29   ESR spectrum of a mixture containing 40% TNB in HMB at 180°C.   Arrows
indicate lineshape anomalies suggestive of a sut sidiary radical.

Figure 30 shows spectra of two other samples in which there is a great excess of one reactant. Depending upon whether TNB or HMB predominates, there are significant differences between the spectra.

The changes between Fig. 30a and 30b may arise from the temperature difference of the two experiments. It is instructive to follow the effect of changing temperature on a given sample, as is shown in Fig. 31 for Expt. 4.A.1.

The spectrum shown in Fig. 31a was essentially unchanged after 5600 s of heating at 175°C. Instrumental malfunction caused the temperature to fall to room temperature, and when the experiment was resumed, the temperature was elevated to 244°C. Additional lines began to appear and the overall span of the spectrum increased by 0.28-0.3 mT. (This behavior was replicated in Expt. 4.A.2, but without the intermediate cooling step.)

This quantity is close to the value of 0.26 mT that has been observed repeatedly for the ortho and para ring and methyl protons in a wide variety of similar nitroxide radicals.[25] But there is no reasonable way to increase the number of ortho and para protons from three to four, so this does not provide a reasonable explanation for the change in spectral span. Rather, it argues for production of a new species differing from the original one by having different values of the nitrogen or benzylic hydrogen splittings. This cannot be ascribed to anything so simple as a temperature dependent hyperfine splitting since the various species are observed simultaneously.

Table 3 summarizes the observations on this unexpectedly complicated system in the course of this work.

As noted earlier, the spectra observed in Experiment 4.B.1 (95%TNB/5%HMB, 220°C) were asymmetric (Fig. 30b), but the relative strengths of the lines remained esentially constant through the run. The radicals appeared quickly and decayed slowly. This contrasts with the behavior of spectra in Expt. 4.A.3 (5%TNB/95%TNB, 220°C) where the species with the greater span formed at the expense of the species with the lesser span. (But neither species had a span as large as that in 4.B.1). Moreover, second derivative presentations of these spectra had a pronounced baseline roll in the region of the Tar g-value although a discrete Tar line never developed in the first derivative display.
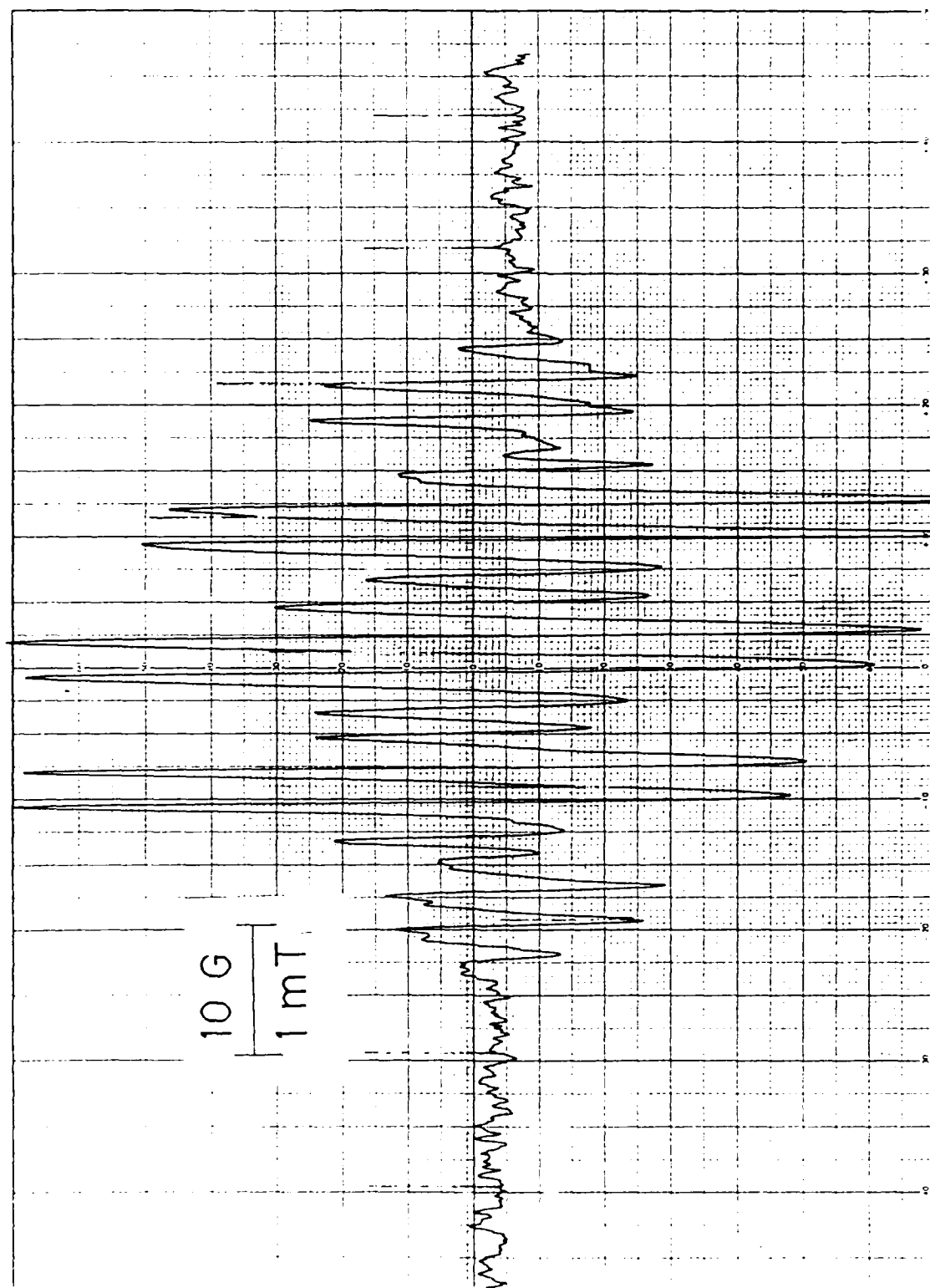
Fig. 30 ESR spectra of mixture of TNB and HMB: (a) 5% TNB/in HMB at 170°C.
(b) 95%TNB with 5%HMB at 220°C.
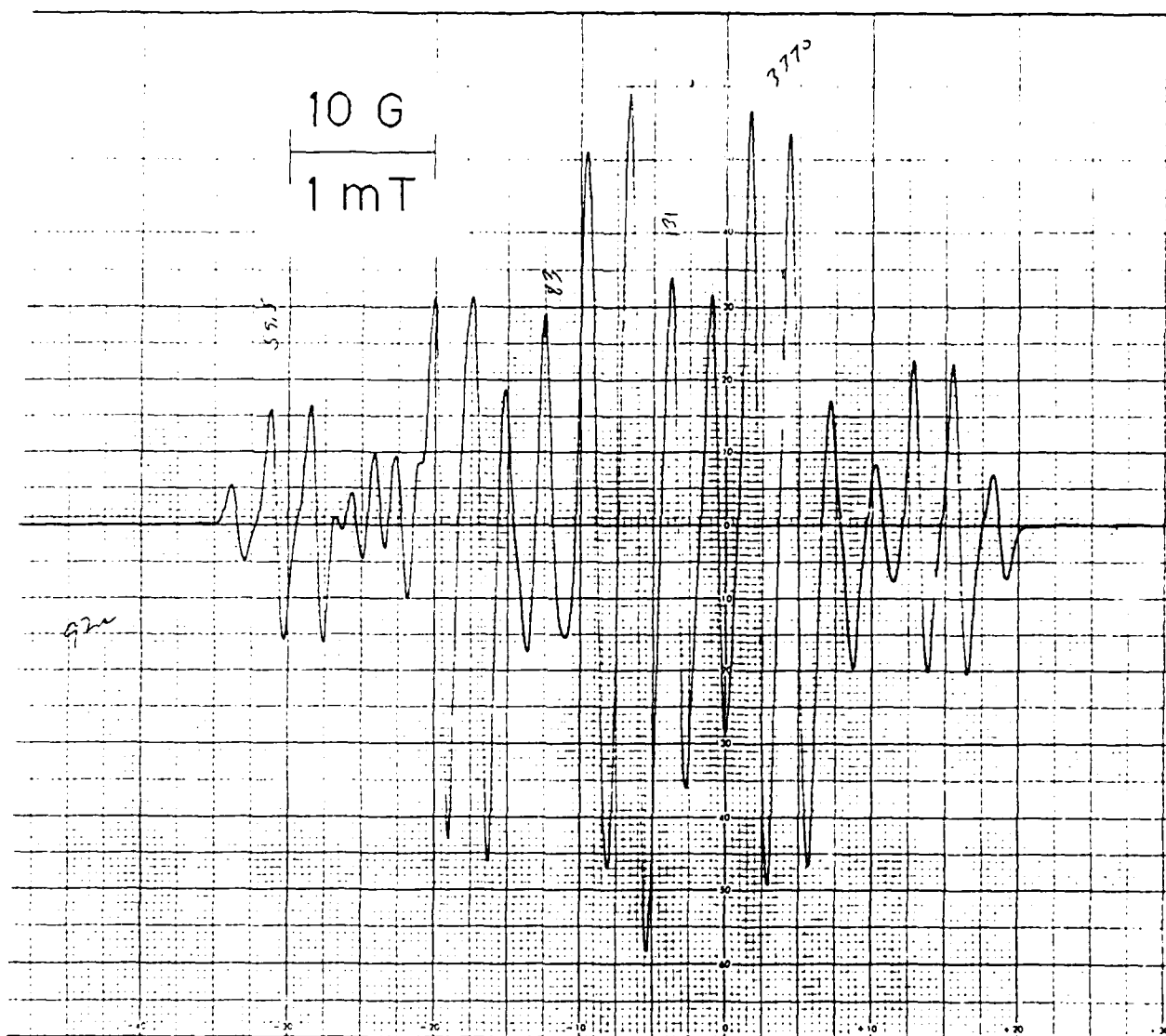
Fig. 30 (Continued)

SC5493.FR
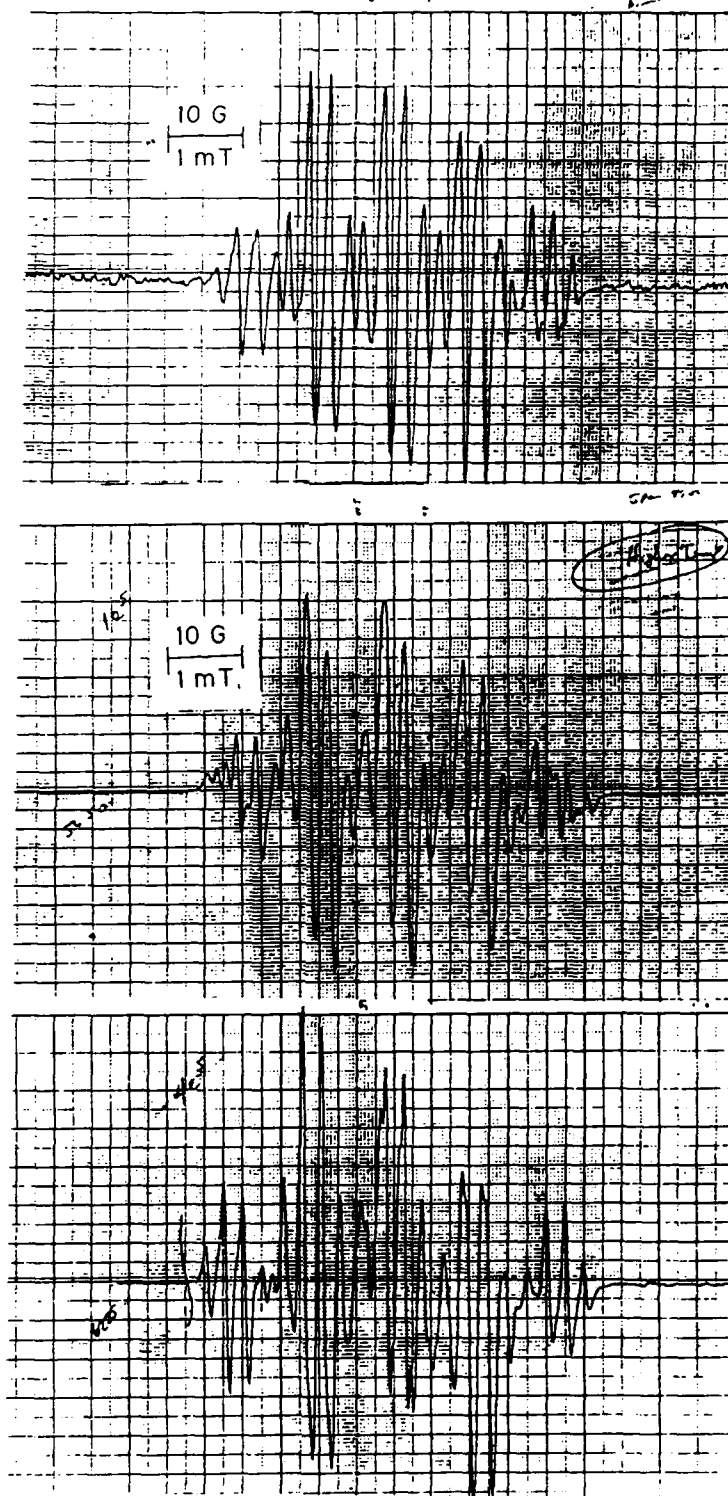
Fig. 31   ESR spectra of 5% TNB in HMB: (a) at 175°C after 300 s; sample was heated for 5600 s at 175°C, and then cooled to room temperature. Subsequently spectrum (b) was recorded after elevating temperature to 244°C, (c) same sample after heating an additional 600 s at 244°C.

Table 3

Experimental Conditions and Description of ESR Spectra
Obtained from Heated Samples of TNB and HMB.

Expt.	Composition TNB/HMB	Temp. (°C)	No. species	Overall Span (mT)
4.A.1	5:95	175	1(+)[a]	4.586
		244	2[b]	4.876-4.90
4.A.2	5:95	170	1(+)[a]	4.576
		203	2[b]	4.879
		220	2(+)[c]	4.90
4.A.3	5:95	220	1(+)[a]	4.611 (initial)
			2(+)[d]	4.891 (2700 s)
			1(+)[a,d]	4.895 (4680 s)
4.B.1	95:5	220	2[e]	5.003
				(4.793)[e]
4.C.1	50:50	223	1	4.824 (75 s)
				4.806 (1000 s)
4.C.2	50:50	180	2(+)[f]	4.9.14
				4.817

[a]Line shapes suggest presence of an additional species; evident in second derivative display at 2440 s.

[b]Second species evident as soon as temperature was raised. The original species was largely supplanted by second species after about 700 s at 244.

[c]Conversion to second species essentially complete. However, lineshapes of outer lines point to beginnings of yet another species with greater span.

[d]Second derivative spectra late in experiment show a "hump" suggestive of Tar.

[e]Extra lines between the two low-field branches indicate presence of second species. Second derivative presentations reveal additional lines from the secondary species. The span of these weaker lines encompasses 4.793 mT. Proportions of the two species remain roughly constant as decay commences during latter stages of experiment (>6000 s). No evidence for Tar formation.

[f]Lineshape distortion between the two low-field branches indicate presence of second species. Elevated temperaure to 245 °C and conversion to Tar was almost complete within about 400 additional seconds.

These mixtures display deeper layers of complexity than had heretofore been suspected. Taken together, these observations point to the conclusion that TNB and HMB are capable of reacting at 220°C to produce at least three different free radical species. Explanations for the appearance of these species must be able to accommodate the following observations:

- The aromatic proton splittings are nearly constant among the various species.

- The different spectral spans appear to stem from differences in a_N and a_{CH_2} but there is no clear cut way to rationalize possible structures for these discrete species without accurate values for the hfs.

- The stabilities and proportions of the various species depends on the reactant ratio (at a given temperature).

- They also depend on the temperature (for a given reactant ratio).

These observations totally undermine the original prediction that TNB/HMB would be a clean system that should produce a single product and thus could shed light on the complexities of the TNT/HMB reaction. Quite the contrary!

Yet another complication results from an experiment (9.B.1) carried out on neat TNB. When it was heated at 172°C, it gave no ESR signal; however, when water was added, a spectrum was observed and it had a span of 3.17 - 3.2 mT (g = 2.0057) which is significantly smaller than the total spans listed in Table 3. A pronounced 1:3:3:1 quartet pattern of ~ 2.5-2.65 G was evident at the ends of the spectrum, but there was enough asymmetry to suggest the presence of multiple species, Fig. 32.

The radical species decayed over time and by 5500 sec only a weak spectrum remained. It however displayed asymmetry suggestive of the "Tar" signals seen in other experiments. (See, for example, later discussion of reactions with $Ca(OH)_2$.) This experiment supplies some additional facts concerning the free radical thermochemistry of TNB:
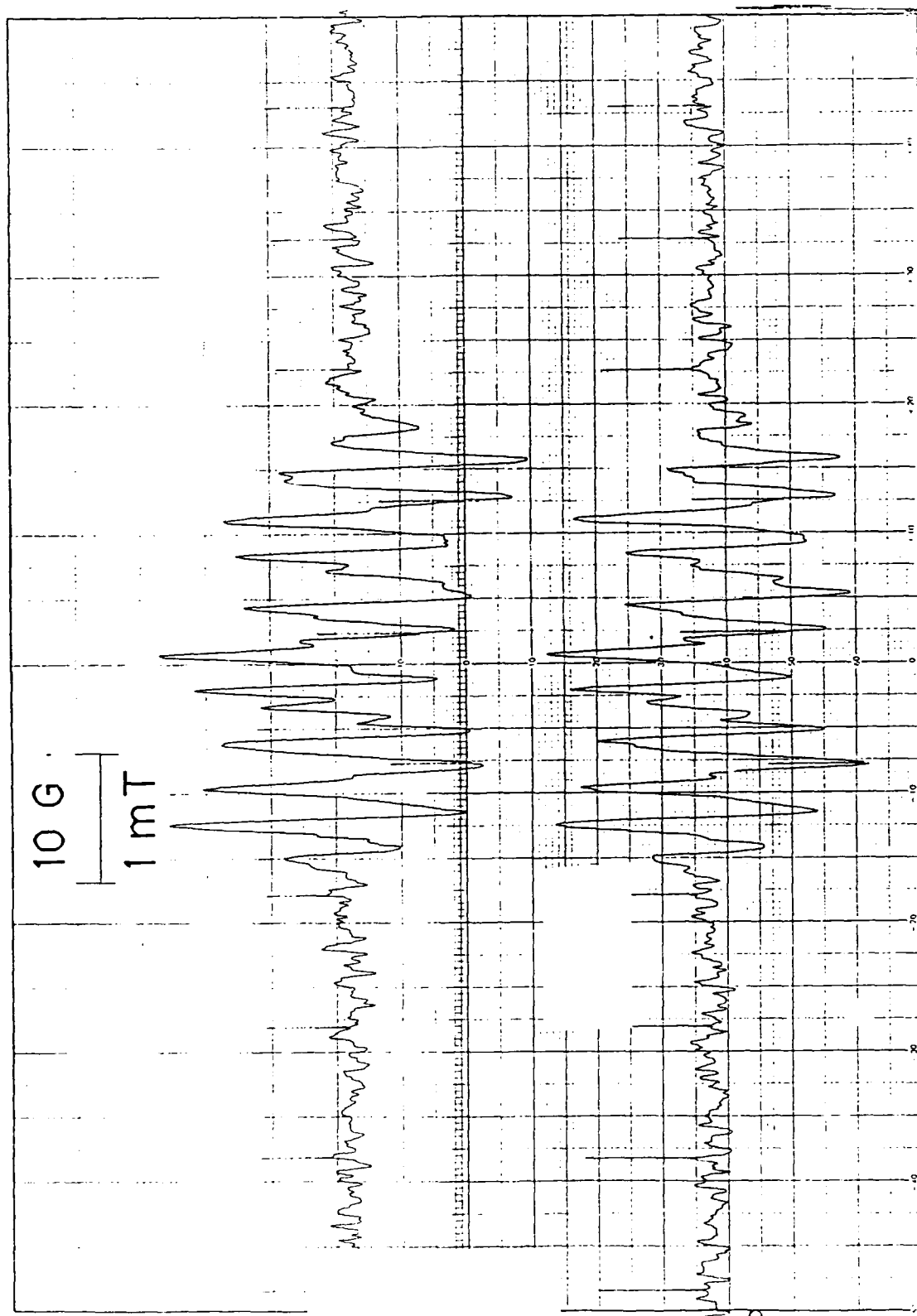
Fig. 32 ESR spectrum of TNB at 172°C with water added. Traces recorded at 3550 (bottom) and 4250 s (top).

- Neat TNB is thermolytically stable.

- Water promotes radical formation in TNB even though the water quickly vaporizes from the sample.

The smaller total span of the spectrum in Fig. 32 and the suggestion of a three-branch splitting of about 1.0 mT is suggestive of a diarylnitroxide such as 8, although the spectra of of such poor quality that no definitive conclusions are possible. Scheme 3 suggest a series of reactions in which water could play a catalytic role in formation of a nitroxide radical from TNB.

SCHEME 3:
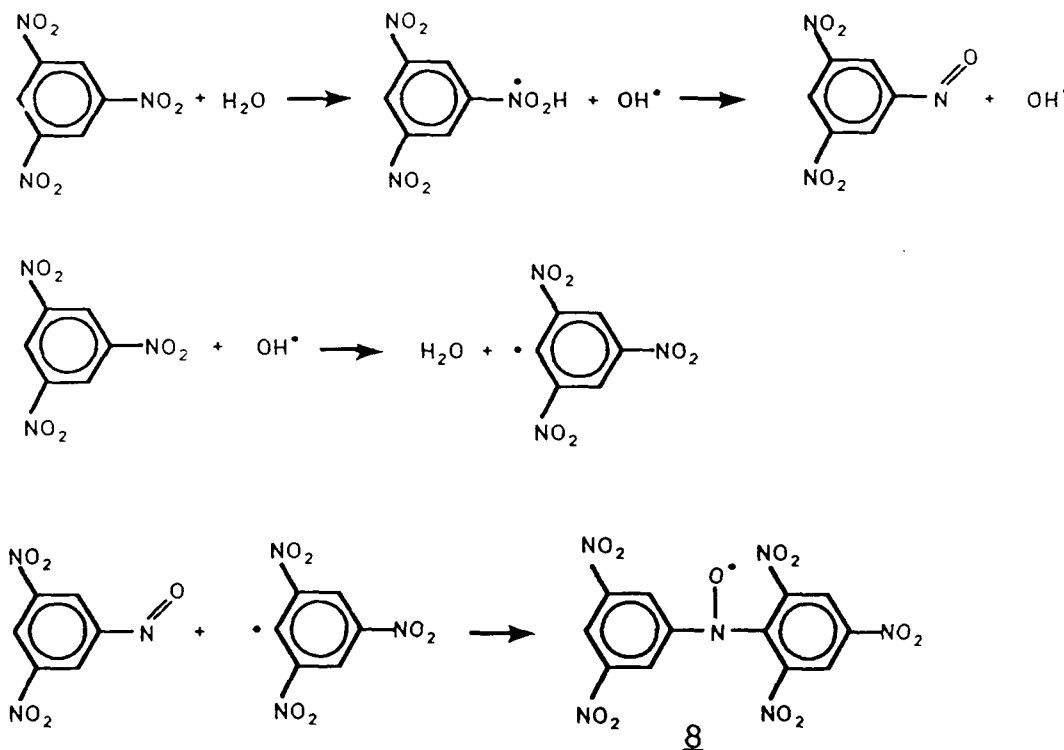
A great deal of effort could profitably be spent in better characterizing the species that occur in systems involving reactions of TNB. At the present time we have little insight into the nature of these free radicals or the reactions which produce them.

Some speculations follow: It is conceivable that the TNB/HMB system produces polyradicals. with multiple nitroxide attachments to a single alklybenzene nucleus. For example, 9
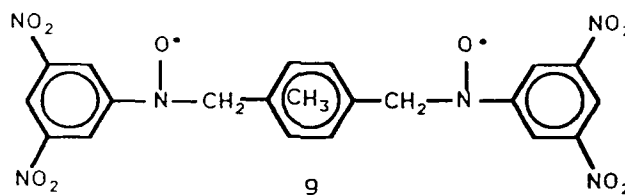
This would provide considerable separation of the electron dipoles and prevent exchange interactions. The benzylic carbon linkages would prevent delocalization of unpaired spin density into the alkylbenzene ring. But the separation would be sufficiently efficient that it is not clear why the nitrogen and/or benzyl splittings should differ between mono-, di-, and tri-radicals.

The presence of a charge transfer complex between TNB (or TNT) and HMB is almost certainly the phenomenon responsible for the observation of strong nitroxide ESR signals at temperatures significantly lower than those required for nitroxide formation from TNT alone.

Scheme 4 suggests how charge transfer complexation could facilitate formation of a pentamethylbenzyl radical and a protonated nitroaromatic anion radical under mild conditions. The decomposition of the latter species into a hydroxyl radical and the nitrosodinitrotoluene derivative would not only lead to the expected nitroxide coupling product, but it could also initiate a set of competitive coupling reactions which would lead to other types of radicals responsible for the extra species observed in the experiments of series 4.

Furthermore the facile charge transfer complexation between electron deficient nitroaromatic compounds and electron rich alkylaromatic nuclei is expected to carry over to each end of the nitroxides such as 6 and 7 above. It is conceivable that such C/T complexes with the nitroxide products are sufficiently stable to explain the presence of multiple species. It is certainly consistent with the fact that the species ratio is temperature dependent and that the total span of hyperfine lines depends

(Scheme 4)
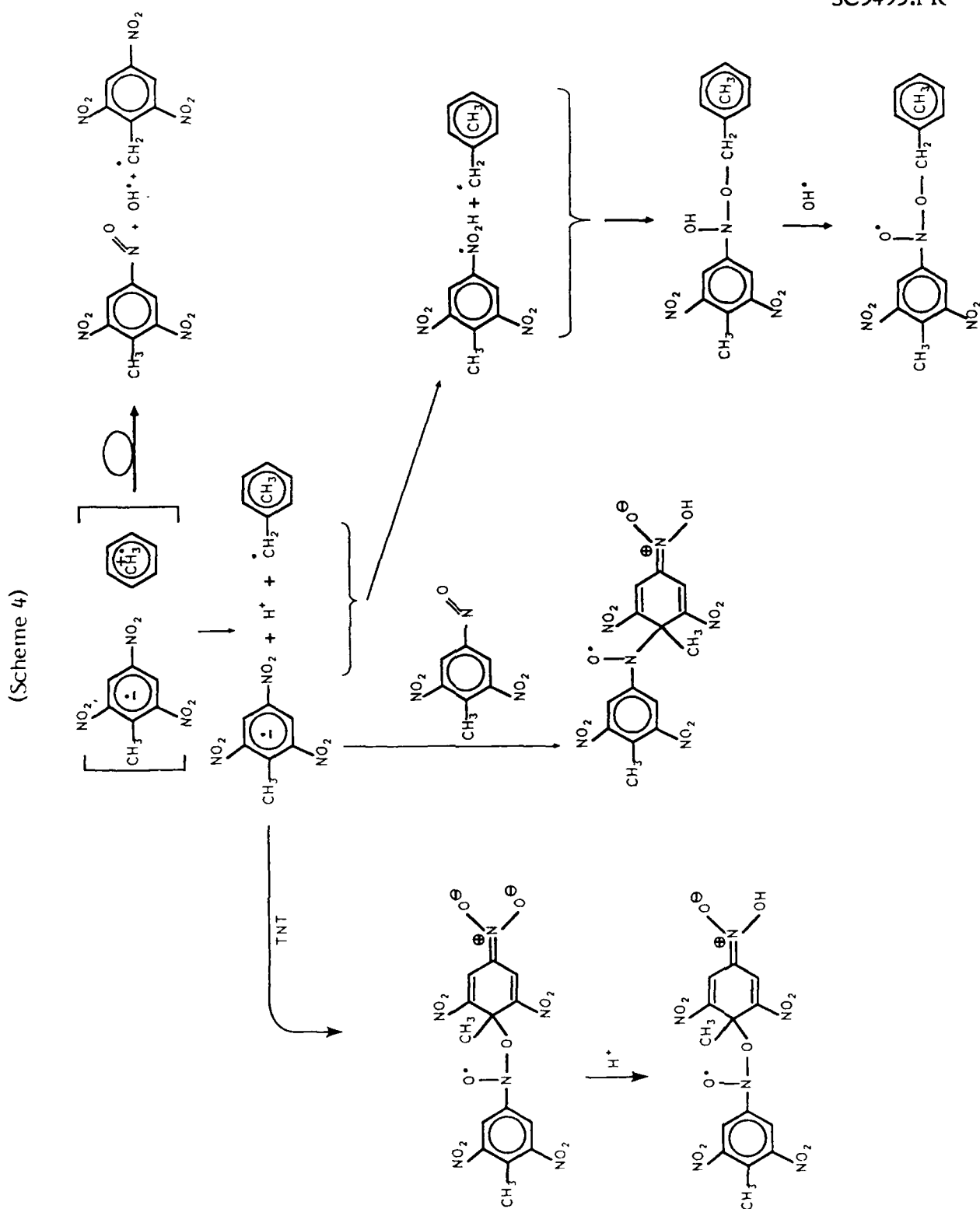
strongly on the starting ratio of reactants. However charge transfer complexes may also lead to formation of additional covalent bonds to either end of the initial nitroxide structure.

Only a limited number of experiments were run in Series 4 but one conclusion is indicated from this data. The formation of nitroxide, like the production of Tar is most efficient when the reactants, TNB and HMB, are present at equal concentration, as opposed to mixtures in which one reactant is present in large excess. Figure 33 summarizes this effect for low (ca. 175°C) and moderate (c. 220°C) temperatures. The fact that Tar production is more important when the nitroxide concentration is greater (i.e., when the reactant ratio favors nitroxide formation) lends suport to the idea that nitroxide is a precurssor to Tar production.

F. Speculations about Nitroxide "Storage"

The observation of an initial decrease in nitroxide concentration during reactions of TNT at moderate temperatures (Fig. 6c) tends to raise questions about the completeness of the reaction mechanism suggested in Ref. 4 and summarized as Scheme 1. Such an initial decrease in nitroxide intensity implies some type of competitive reaction sequence that destroys as well as produces nitroxide at different rates, depending on the reaction conditions. However, it could also suggest the existence of some type of nitroxide precursor, as in the form of a dimer molecule, which dissociates to produce a large initial value of nitroxide when the temperature is first elevated.

We have observed behavior similar to that reported by Guidry and Davis[2] in that when the temperature of a TNT sample is cycled between high and low values the nitroxide signal disappears when the temperature is dropped, only to reappear undiminished when T is restored to its original value. They speculated that nitroxide was "stored" at low temperature, but they did not venture a storage mechanism.

One of the characteristics of nitroxide radicals is their stability against dimerization reactions at the nitroxide site:[10] The Linnett hypothesis[11,12] argues that the nitrogen and oxygen atoms each have eight effective electrons and therefore achieve octet stability. Any chemical dimerization, such as formation of a peroxide linkage, would maintain such octet configurations, but would be less stable due to electron
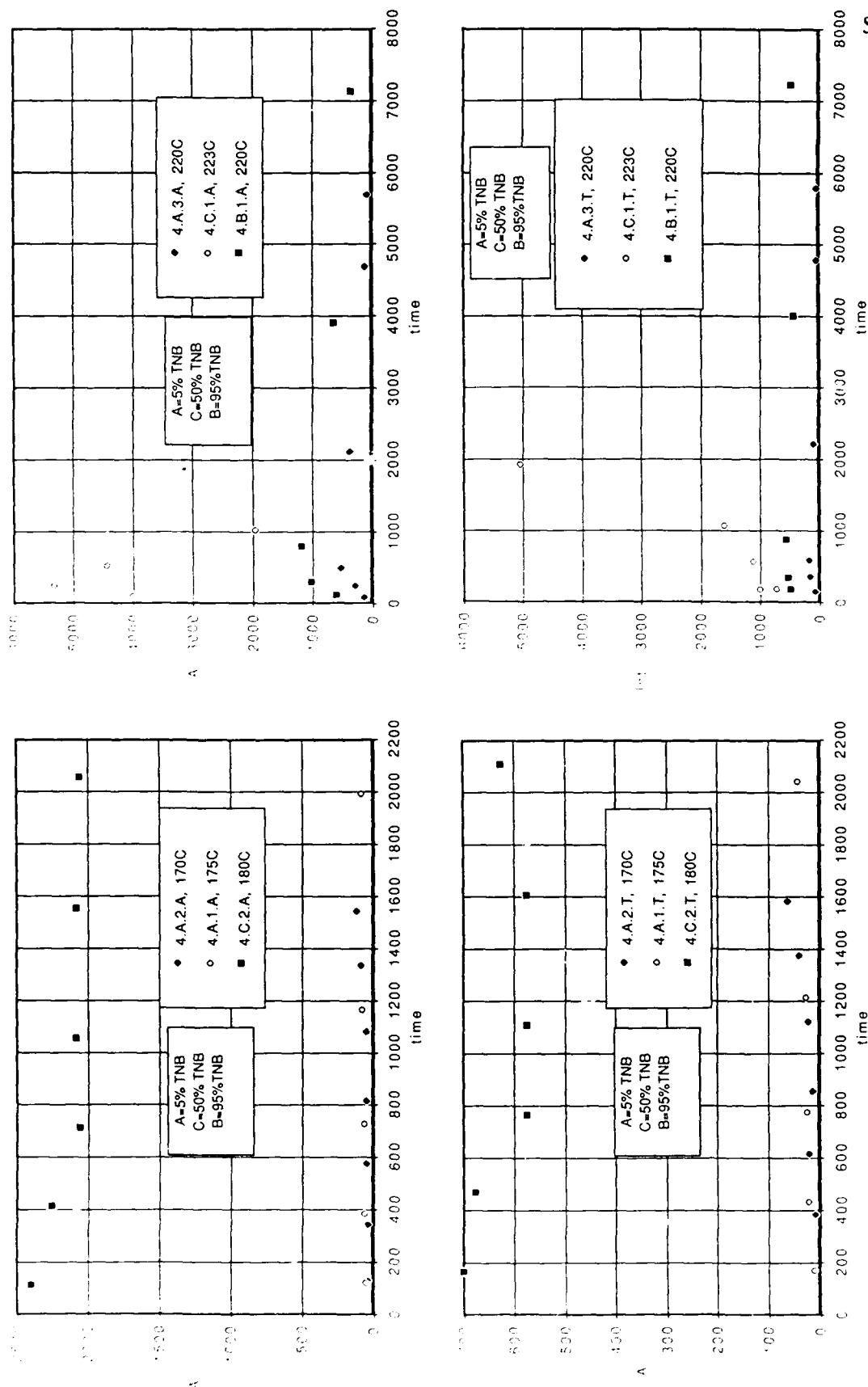
Fig. 33   Comparison of nitroxide and Tar behavior at various ratios of TNB/HMB. Nitroxide at (a) low temperature, and (b) moderate temperature; Tar at (c) low temperature and (d) moderate temperature.

repulsion terms. This is a fairly straightforward explanation when the discussion is confined to NO, but for nitroxide species with extended substituents attached to the nitrogen, dimerization may occur at some remote site in the substituent. One dimer possibility for nitroxide 1 is
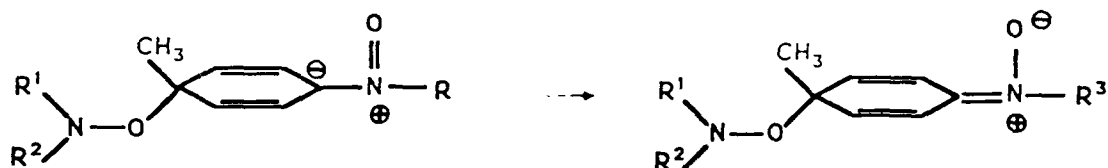
Another possibility is electron correlation to form a "singlet" state of the two unpaired electrons on different nitroxide radicals when the oxygen atoms approach each other.

A set of experiments done very late in the program sheds additional light on the disappearance of the nitroxide signal when the reacting melt is cooled. These experiments indicate that the disappearance of nitroxide signal is the result of line broadening in the solid rather than due to electron pairing through dimerization or electron correlation. Samples exhibiting moderately strong nitroxide spectra were quenched in ice water and the resulting solids were then extracted with either benzene or toluene. The yellow solutions were transferred to clean sample tubes and weak, but recognizable nitroxide spectra were recorded, along with Tar-like absorptions.

Over a period of several hours a complex set of transformations occurred and eventually a spectrum such as shown in Fig. 34 resulted. While it is impossible to feel comfortable with proposing a unique assignment for a spectrum such as this, the interpretations suggested in the figure offer some interesting points. There appear to be two different groups of lines centered on different g-factors. Significantly, these g-factors

of 2.0059 and 2.0036 are seen repeatedly under a wide variety of reaction conditions. The larger value occurs repeatedly in a great variety of systems (as shown in Appendix B) exhibiting nitroxide spectra while the lower value is closely associated with Tar absorptions.

The transformation of the nitroxide spectrum of Fig. 34a into a set of lines that might be associated with several different nitroxides lends credence to the nitroxide disproportionation reactions suggested in Scheme 2. The appearance of several different sets of lines associated with a Tar g-factor is also suggestive of the fact that the Tar radicals have an electronic structure different from that of nitroxides and that many different such compounds can arise in the TNT reactions. It is quite interesting that data in Appendix B indicates that radicals derived from trinitrobenzyl alcohol also have g-factors in this same range.

We reviewed data from our studies prior to this program to find other conditions that might yield additional insights. For instance, the reaction between HMB-d_{18} and 2,4,6-triphenylnitrobenzene produced a radical which exhibited a "powder spectrum" at room temperature for at least 4 days. Presumably the steric protection afforded by the phenyl groups does not permit decomposition or subsequent reactions so that at least an order of magnitude greater concentration is obtained.

One experiment was conducted on neat TNT at 100°C. A weak spectrum was observed for an extended period (>10,000 s) which appeared to be similar to the familiar nitroxide species except that $a_N \neq a_{CH_2}$ and consequently the 1:3:4:3:1 intensity pattern was not observed. The gain level was about four times greater than usual, so there is nothing contradictory with other observations of low nitroxide concentration and high tar concentration when the temperature is lowered in a normal heating experiment. This could argue for dissociation of a dimer species or it could simply indicate that nitroxide spectra are observed only when molecular tumbling is possible, as in a molten sample state. The one aspect of this experiment which is problematic is that a radical signal was observed so early in the run: an ESR signal recognizable as a spectrum was observed after 360 s.

The hypothesis that Tar is formed by subsequent reaction or polymerization of nitroxide through remaining reactive sites gains support from an experiment with trinitromesitylene. When 92 mg was heated to 226°C, a single line with only a hint of

SC5493.FR
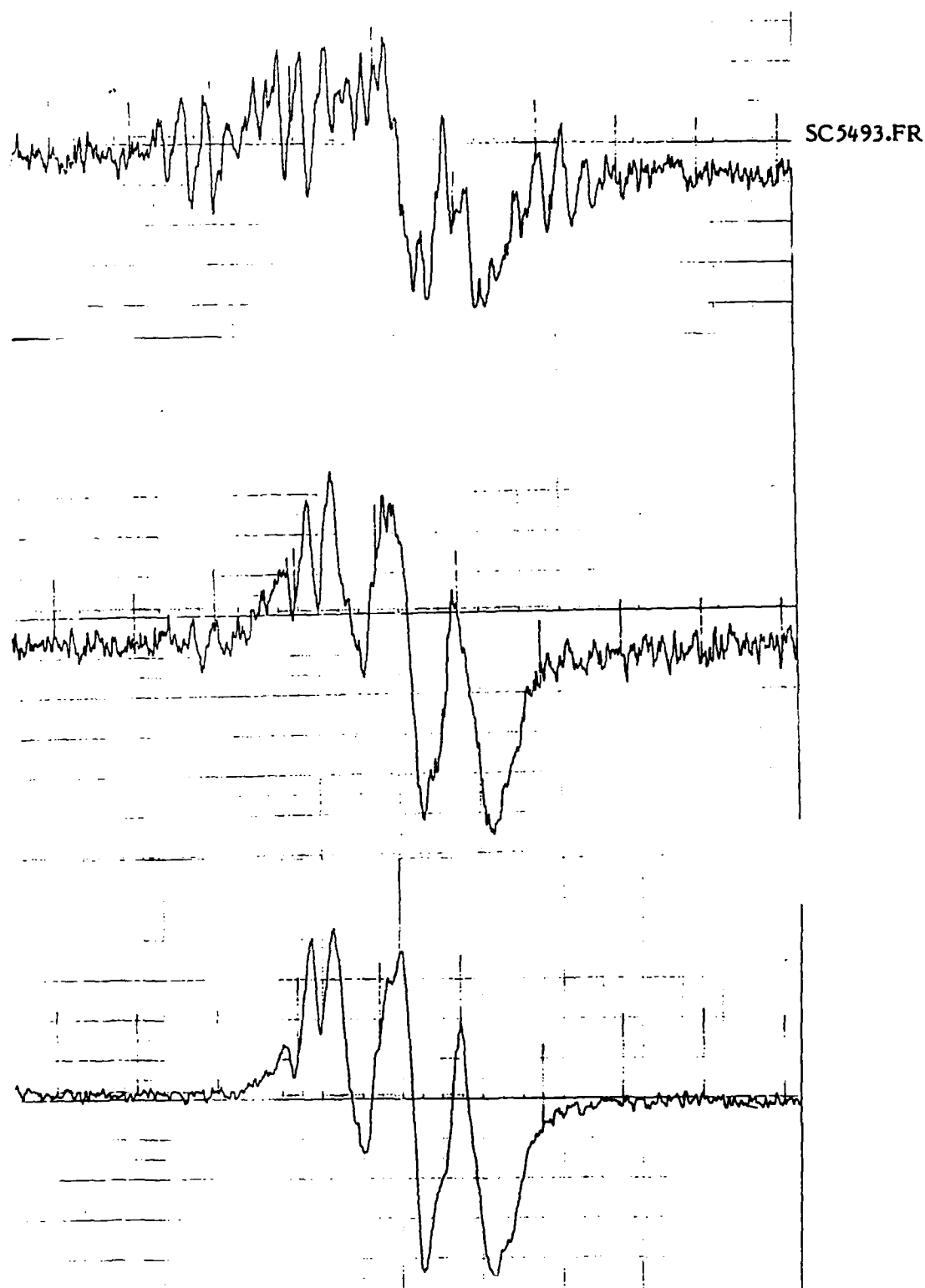
Fig. 34   Evolution of the ESR spectra of a benzene extract from a TNT reaction mixture leading to absorptions at two different g-factors: (a) evolution over approximately 1 h, at room temperature (earliest trace at top), (b) expanded spectrum showing "stick plot" of two superimposed spectra.

10 G
1 mT
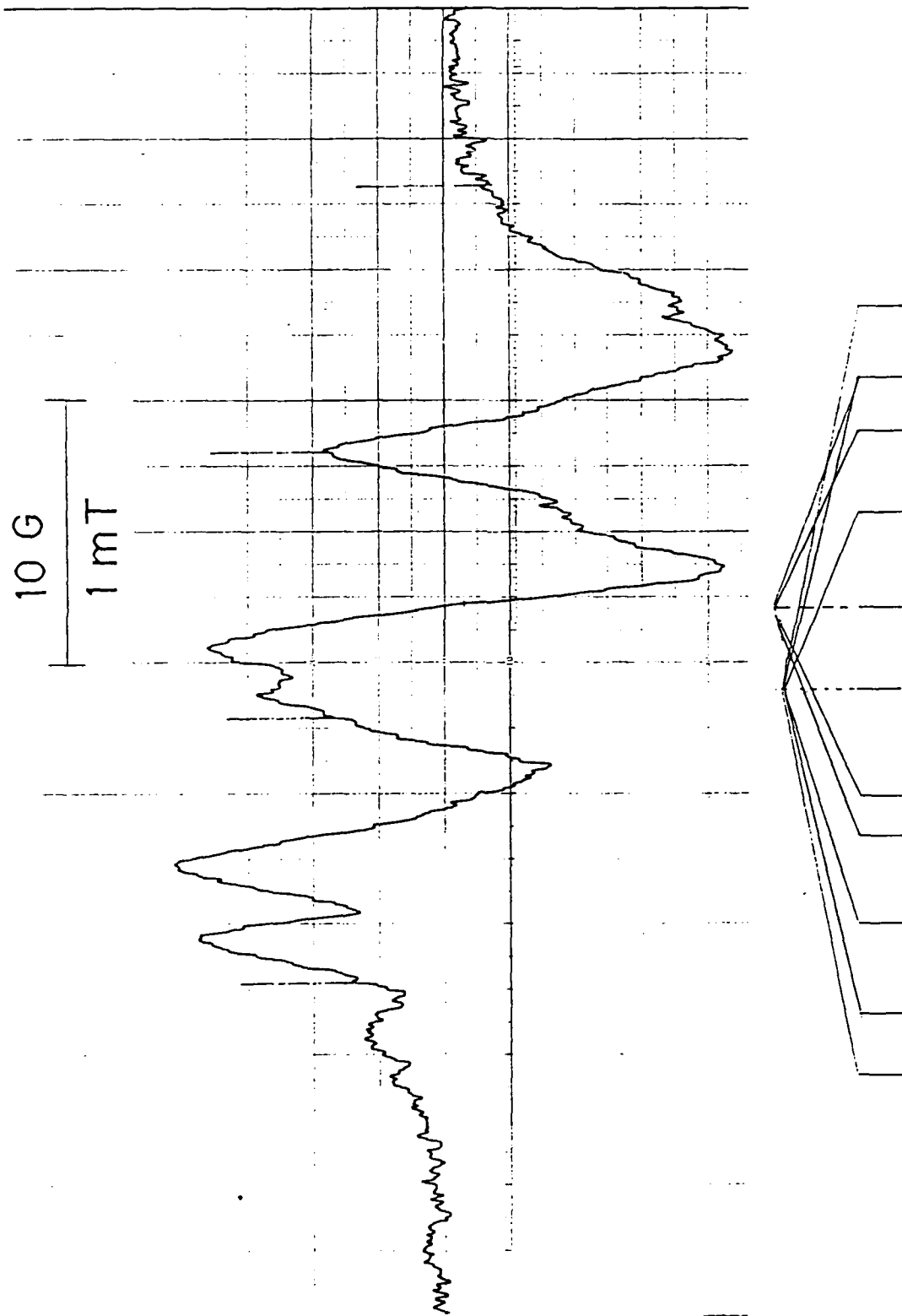
Fig. 34 (Continued)

HFS appeared rapidly. This spectrum was still present at room temperature. Another experiment with ~ 1:2 TNM:HMB produced an initially complex spectrum, followed by conversion to a mixture of Tar plus another species having a_N ~ 1.4 mT and a_{CH_2} ~ 0.85 mT. This implies that the early, complex spectrum probably contained species from intramolecular or bimolecular coupling of TNM, which rapidly converted to Tar, leaving only the Tar and bimolecular product of TNM/HMB--assuming that the methyl groups of TNM-moiety do not produce splittings. Figure 35 indicates that the lines are rather sharp (ca. 0.15mT) and this casts some doubt on this hypothesis. However, this line width is about twice the value for TNT-nitroxide so the residual radical may actually have unresolved splittings and be the structure shown in Scheme 5. The steric interactions would probably force the nitrated ring out of conjugation with the nitroxide group which might decrease the methyl splittings so that they are unresolved.

G.   Effect of Reactive Additives

1.   Oxidizing and Reducing Agents

A paper on wartime RDX research[26] pointed out the surprising role of Cl⁻ in the formation of nitramines: Chloride is oxidized to Cl_2 or HOCl by nitric acid and it was speculated that perhaps molten TNT might produce a similar effect. If such an effect occurred, then the effect observed for water might actually result from trace chloride. These species should readily react with the methyl hydrogen atoms. Also, the proposed hydroxyl should also be facile at oxidizing chloride to more positive states.

An experiment with added NaCl produced a normal development of nitroxide plus Tar. A second experiment with more carefully controlled conditions (5.C.2) did not reveal any behavior drastically different from normal kinetics. This rules out any chance that the effect observed with added water was actually due to to to a trace of chloride impurity rather than water itself.

Another experiment was run using oxalic acid as a potential reductant to see if that would have any effect on the Tar line, that is, does Tar have any redox chemistry that would give us a clue as to its identity. The kinetic behavior was not significantly different from that of undoped TNT. However, a puff of steam was noted in the early moments of heating, so some pure oxalic acid was heated in a separate experiment. At
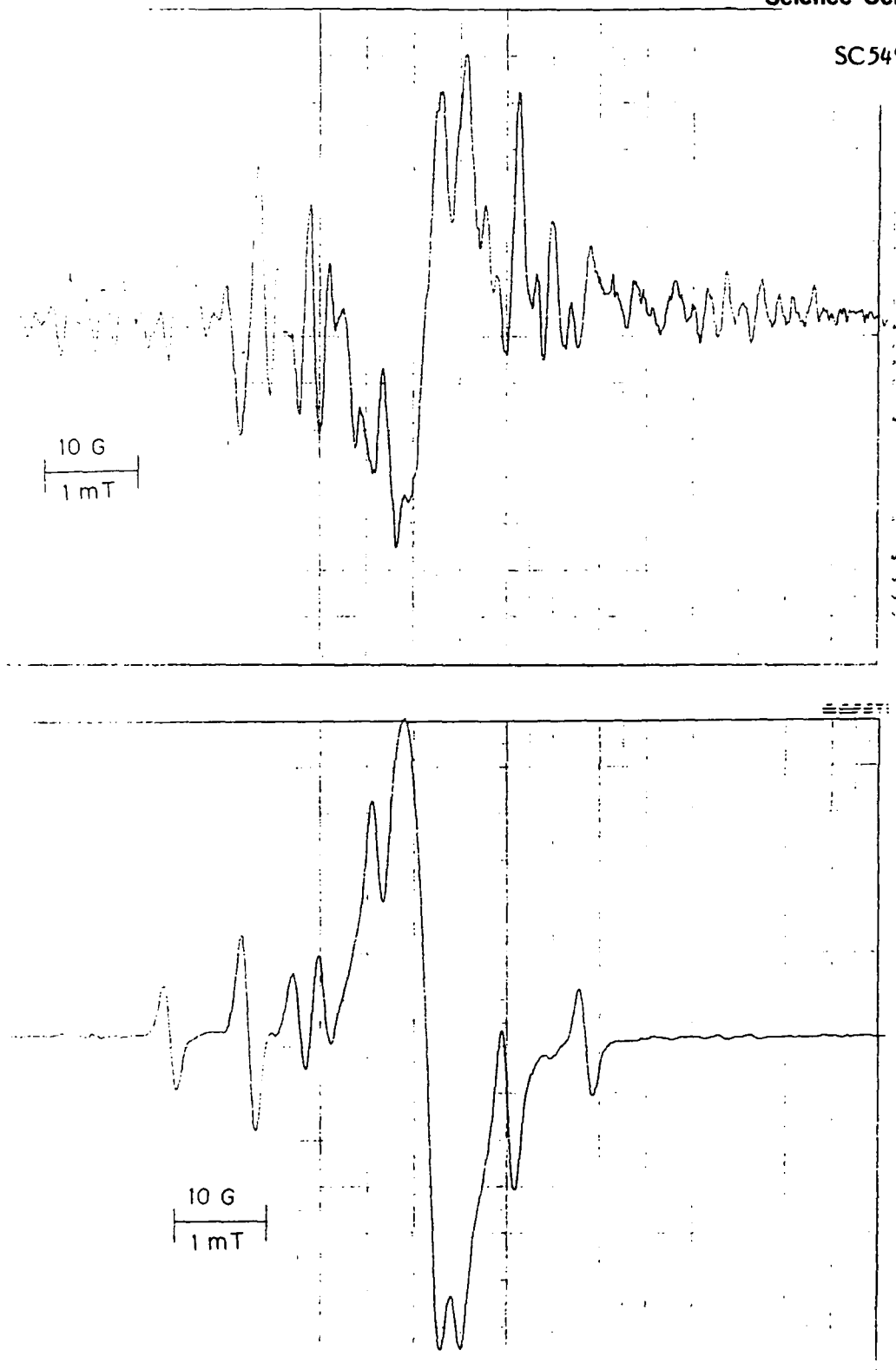
Fig. 35   Trinitromesitylene and HMB at 243°C. (a) 1300 s reaction time (note reversed phase) and (b) 3500 s reaction time (normal reference phase).

Scheme 5
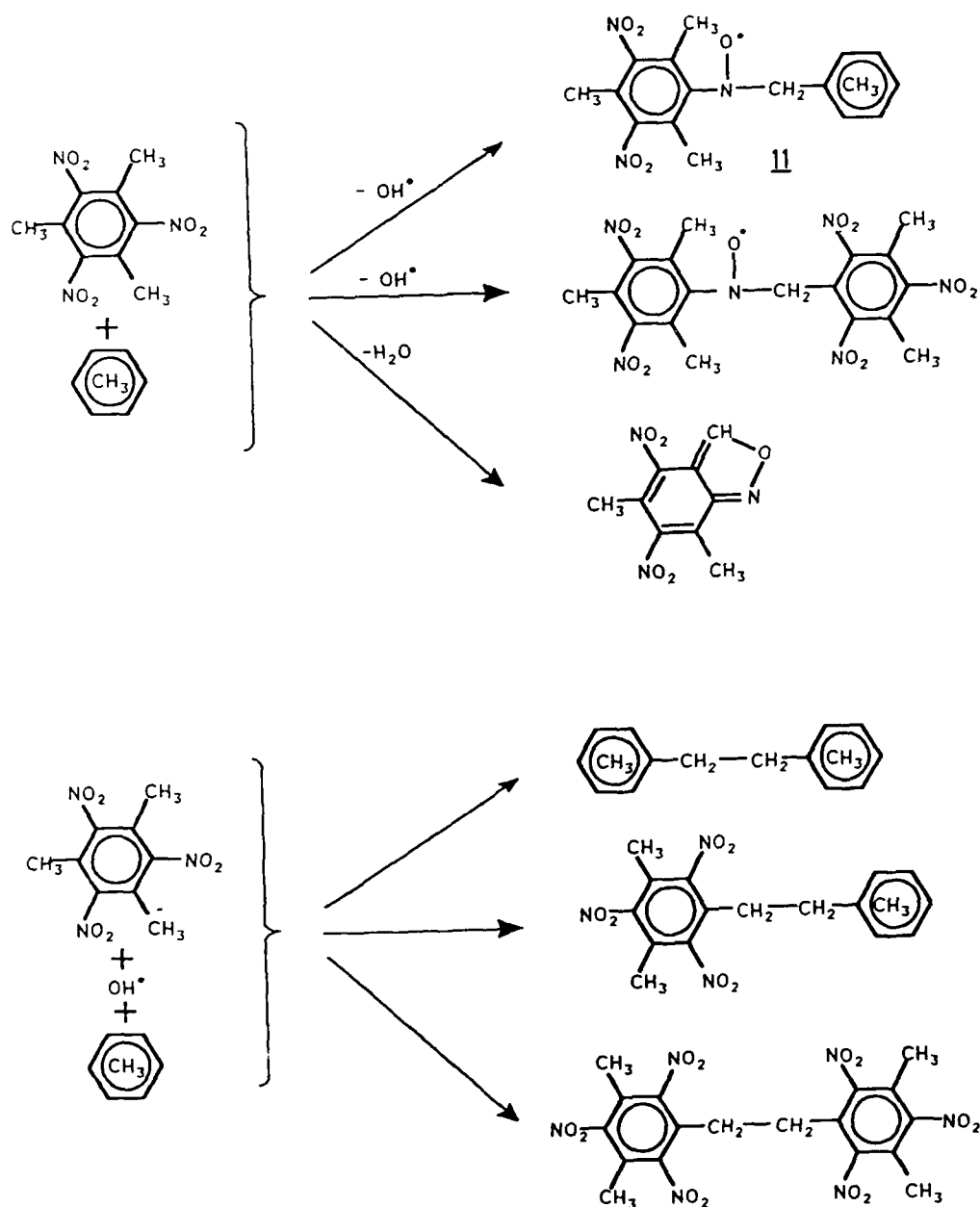
242°C oxalic acid undergoes air-oxidation quite rapidly to produce water and carbon dioxide, so it is not a suitable reductant for this system. But it might be mentioned that this is an alternative way of introducing water into the TNT system and it might be worthwhile exploring this reaction at the lower temperatures where water appears to have such an acceleratory effect.

An alternate reducing agent, sodium dithionite, was then used to pursue the redox question. There was a hint of nitroxide-like material present after 120 s (242°C), but the spectrum was totally dominated by a Tar-like signal, Fig. 36. In this experiment, the NMR gaussmeter was not in use, so g-factors were not computed. There was vigorous gas evolution and a noticeable odor which may be the result of escaping SO_2. To complicate the picture further, trinitrobenzene and dithionite were mixed and run at 236°C The resulting anisotropic spectrum was complicated by hints of isotropic HFS, Fig. 37.

2.   Spin Traps

The spin-trap phenyl-t-butyl nitrone (PBN) was mixed with TNT and run at 92°C. A straightforward nitr -derived nitroxide spectrum (a_N ~ 14mT, a_H ~ 3.5mT) was observed (Fig. 38) but it decayed quickly, probably because of air oxidation at the elevated temperature. Addition of water to a sample mixture had no appreciable effect. Addition of dithionite in another experiment with PBN increased the intensity of the early signal, but not dramatically.

In another experiment some trinitrobenzene and PBN were mixed and the spectrum indicating a mixture of simple nitroxide radicals (Fig. 39) was obtained. This result is superficially surprising, but probably results from oxidation of the t-butyl groups by the TNB nitro groups to produce a "real mess." In another run TNB and PBN were mixed with dithionite. The spectrum was dominated by an asymmetric pattern similar to Fig. 39 but there were also several HFS components that appeared similar to the PBN-derived nitroxide spectra.

On the other hand, TNT, PBN, and dithionite produced only the PBN-nitroxide spectrum. Superficially, this might suggest that TNB is a stronger oxidant than TNT but there is no evidence for this reflected in electrochemical E_0 values. Alternately, the

SC5493.FR
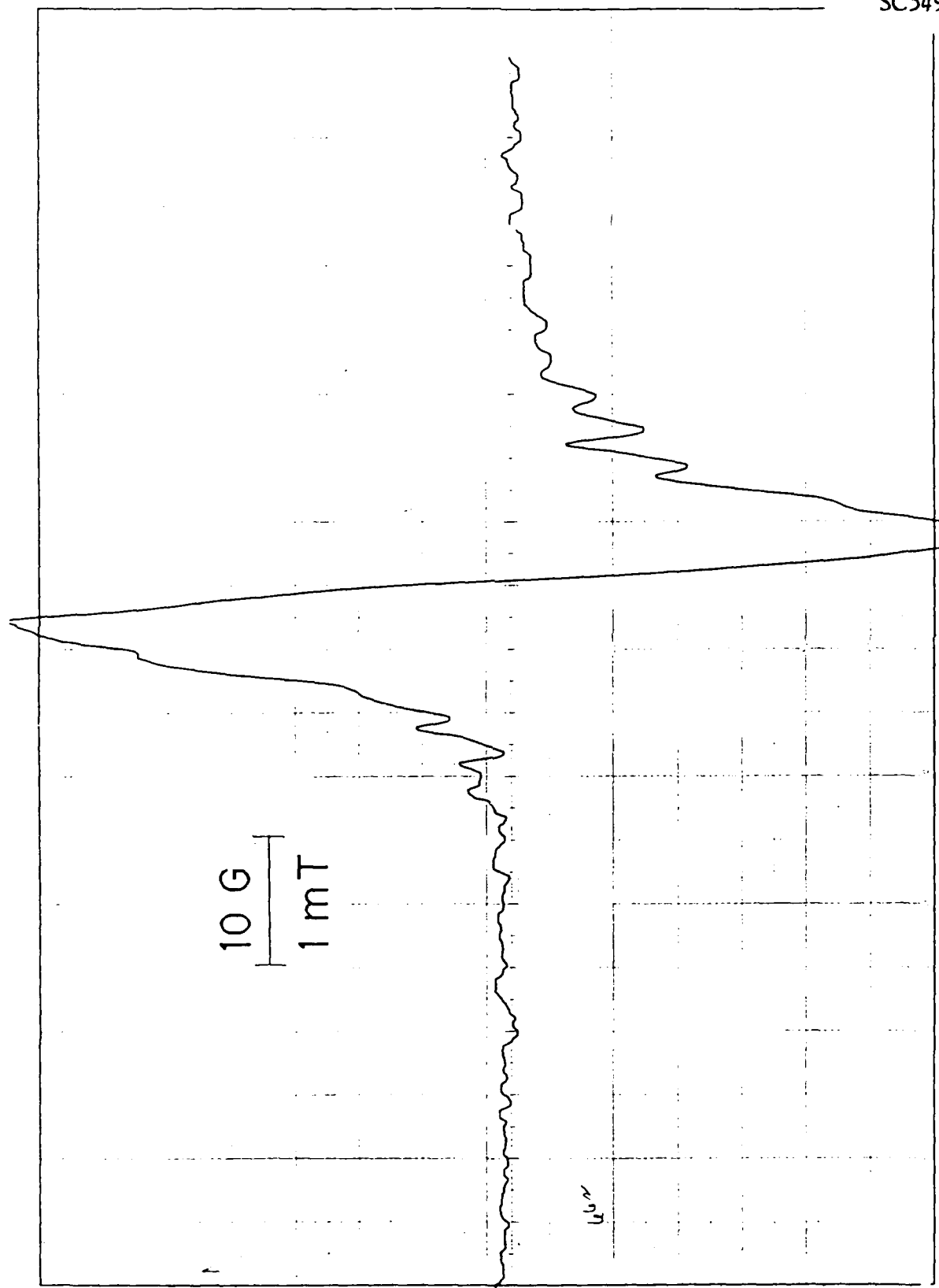
Fig. 36 ESR spectra of the reaction mixture of TNT with sodium dithionite at 240°C.

10 G
1 mT

10 G / 1 mT
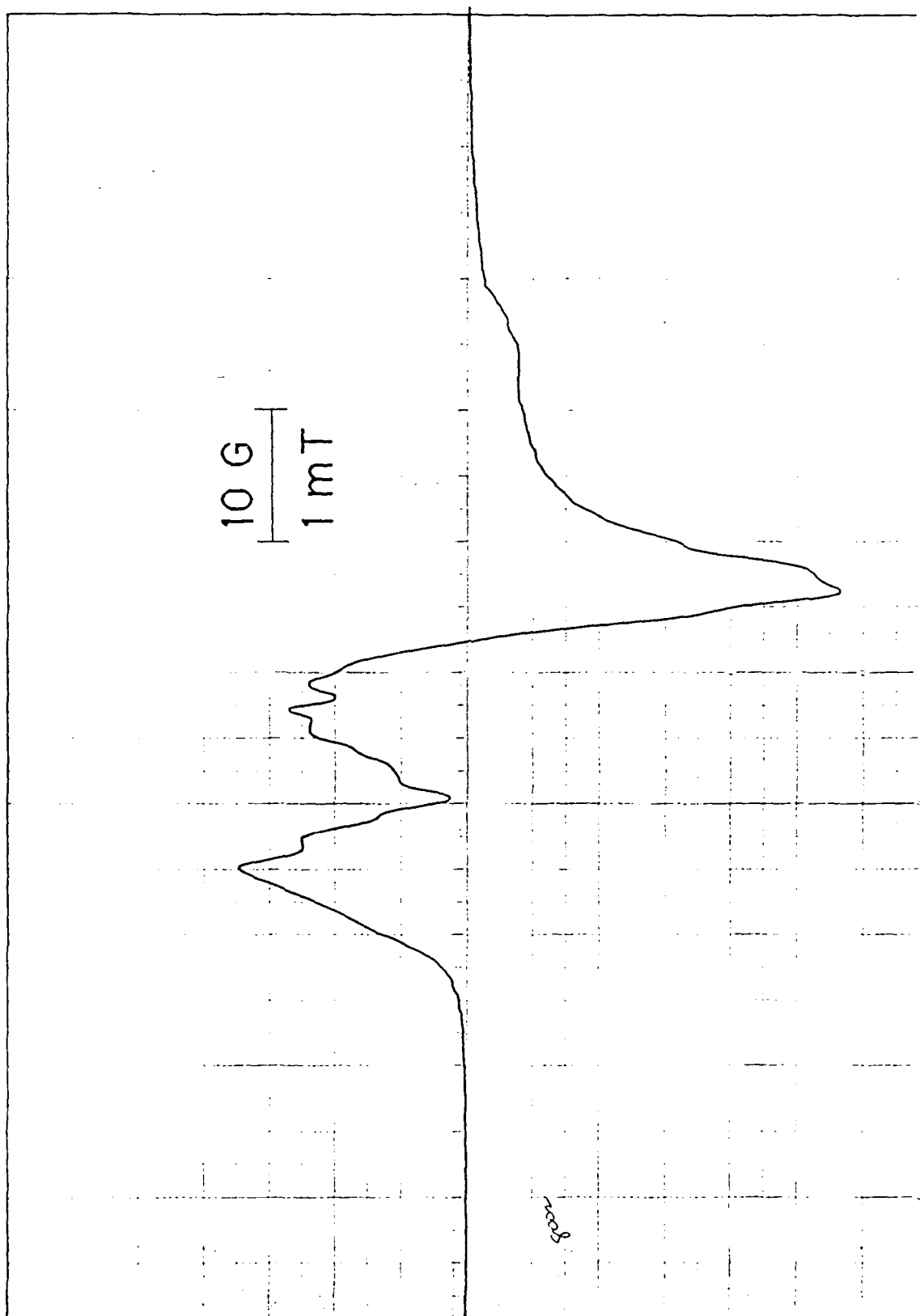
Fig. 37 ESR spectra of the reaction mixture of TNB with sodium dithionite.

SC5493.FR
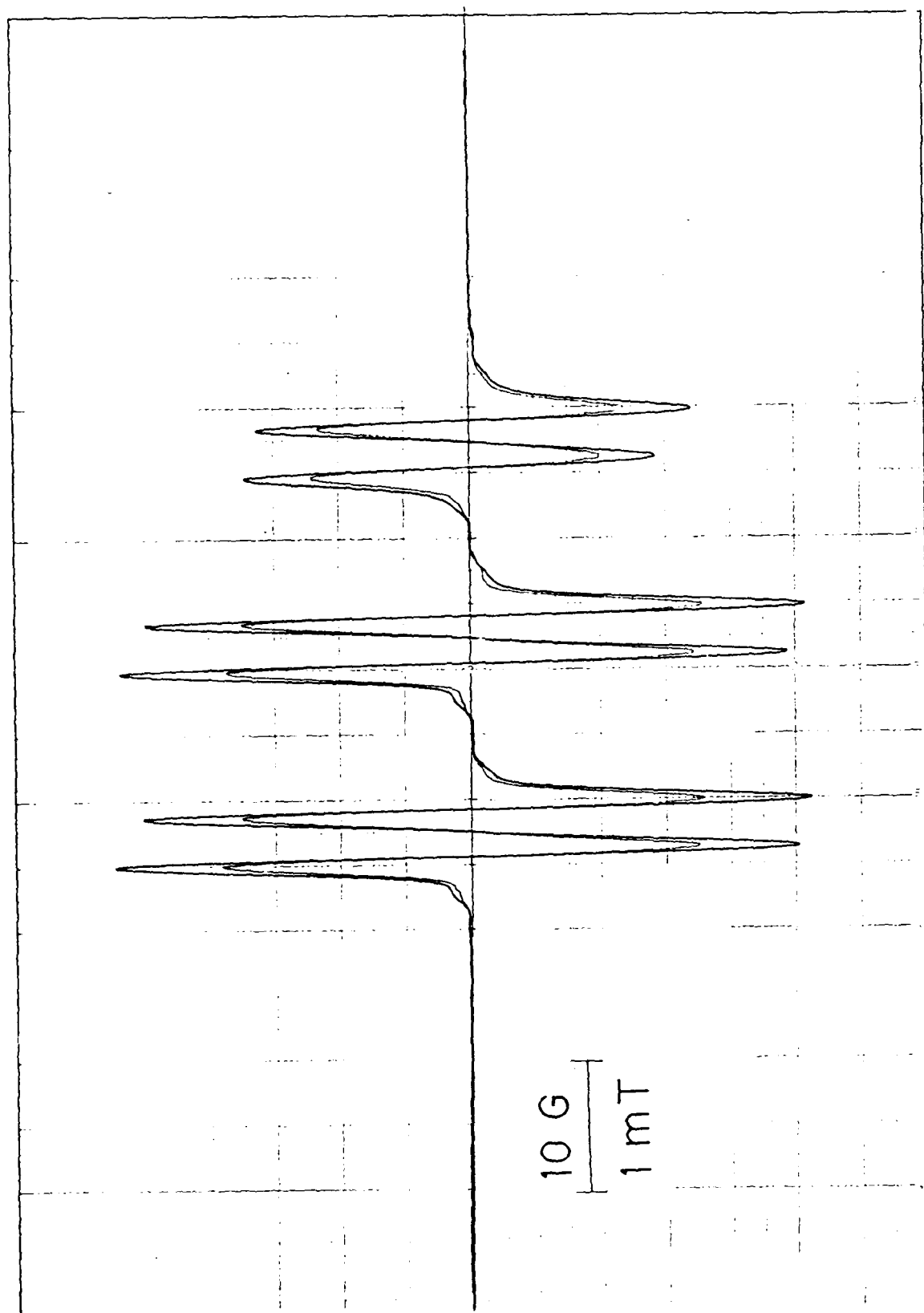
Fig. 38   ESR spectra of the reaction mixture of TNT with phenyl-t-butyl mixture at 92°C.

10 G
1 mT

SC5493.FR

10 G
1 mT
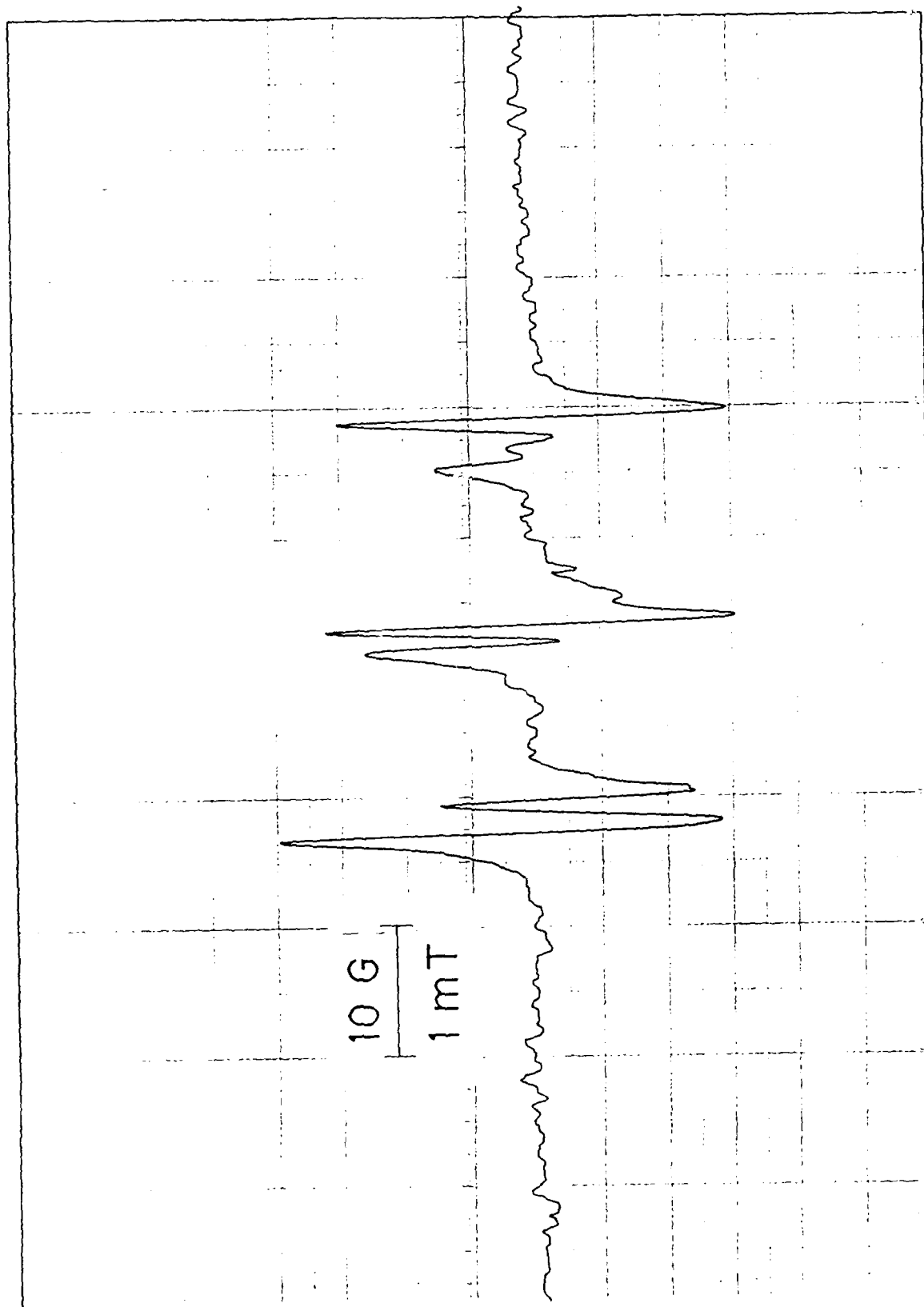
Fig. 39   ESR spectra of the reaction mixture of TNB with phenyl-t-butyl-mixture at 90°C.

presence of the TNT methyl group may make it more vulnerable and open an easier reaction pathway for production of radicals that can be trapped by PBN. This is the more tenable interpretation.

3.   Bases

In an effort to gain insight into the water effect, several reactions were carried out using added basic materials. The reason for this approach was a speculation that OH^- might be the culprit in hastening the nitroxide formation through Meisenheimer-type complexes, 3. Meisenheimer colors were observed under extremely mild conditions, such as the layering of TNT and $Ca(OH)_2$ into a sample tube at room temperature. In the cases described below, the Tar formation was greatly accelerated and the nitroxide was extremely transitory. It is noteworthy that in the $Ca(OH)_2$ experiment (5.C.5) the "Tar" line coincided not with Line C but rather with the nitroxide line once removed downfield from Line C so that this early Tar species is distinctly different from the normal material.

Buncel's[20] review mentions that hydride can also add as a Meisenheimer complex. Some $NaBH_4$ of questionable purity was mixed with TNT. When the sample tube was inserted in the hot cavity, sufficient gas was evolved to eject a portion of this sample. This ejected material was red colored. The material that remained in the heated portion of the tube turned quite black and produced the spectrum shown in Fig. 40a. Unlike the "explosive coke" formed during neat TNT thermolysis, this material was not soluble in acetone; but it was soluble in water. Another portion of the $TNT/NaBH_4$ sample was subjected to milder treatment at 100°C. It also turned red and produced the spectrum shown in Fig. 40b which is significant because of the much greater line width.

In another set of experiments (5.C.8a and b) sodium sulfide (nonahydrate) was used as the base. The rationale for using this material was founded on the idea that if the Meisenheimer precursor plays a role in Tar formation then the presence of a sulfur atom in the Meisenheimer quinoid structure (Eq. (3)) would be reflected in a g-factor larger than that of the corresponding hydroxy compound. When TNT and sodium sulfide nonahydrate were ground together a red color indicative of the Meisenheimer complex was observed. The spectrum of Fig. 41a was recorded when the sample was heated to

100°C. The g-factor of this asymmetric line was approximately 2.0038 which is not significantly different from the g-factors of the Tar line in reactions of neat TNT. It is conceivable that the water of hydration present with the strongly basic sodium sulfide favors Meisenheimer addition of hydroxide rather than bisulfide. As seen in Fig. 41a, the line width is narrower than that observed for the $NaBH_4$ adduct. The sample charred badly, even at 100°C. A fresh sample was inserted in a room temperature dewar and additional components (other than the three anisotropic components) were observed, Fig. 41b.

Addition of calcium hydride to TNT also results in a strong ESR signal at room temperature (Fig. 42). This spectrum exhibits an unusual phase shift in the modulation reference to obtain maximum signal intensity. This may be due to interference because of high sample conductivity, saturation transfer effect, or modulation sidebands. The latter speculation does not explain why it also occurs with the wider line width material produced during reaction with Na_2S. The g-factor of the line in Fig. 42 was evaluated as 1.9999. This is the lowest value of any species observed and is significantly different from the usual Tar g-factors which were generally close to 2.0035. Such observations are consistent with enhanced electrical conductivity.

In another series of experiments (9.B.n), the effect of Meisenheimer complexes was investigated by doping TNB with $Ca(OH)_2$. When solid $Ca(OH)_2$ and TNB were layered in a sample tube (Expt. 9.B.2&3), a mixed-species spectrum was observed at 244°C. It displayed a 1:3:3:1 quartet hfsc of 0.2265 mT, an overall span of 3.633 mT and a midpoint g-value of 2.00599. Another strong single line (which eventually evolved into a Tar-like absorption had a g-value of 2.00497. (At the end of the run, this appeared to be partially resolved into an anisotropic g-parallel/g-perpendicular pattern, but it was too distorted by residual isotropic hfs to permit evaluation.)

When water is placed in the bottom of the tube, prior to adding the solid TNB and $Ca(OH)_2$ (Expt. 9.B.4) the hyperfine structure lasts longer and the Tar formation is considerably delayed.

In Expt. 9.B.5, the effect of Meisenheimer complex formation was investigated by adding an aqueous slurry of $Ca(OH)_2$ to TNB to effect a more uniform distribution. A somewhat better resolved spectrum was then observed at 166°C, Fig. 43. The wings showed the familiar quartet splitting and the overall span was 3.664 mT. The resolution

10 G
1 mT

(a)

10 G
1 mT

(b)
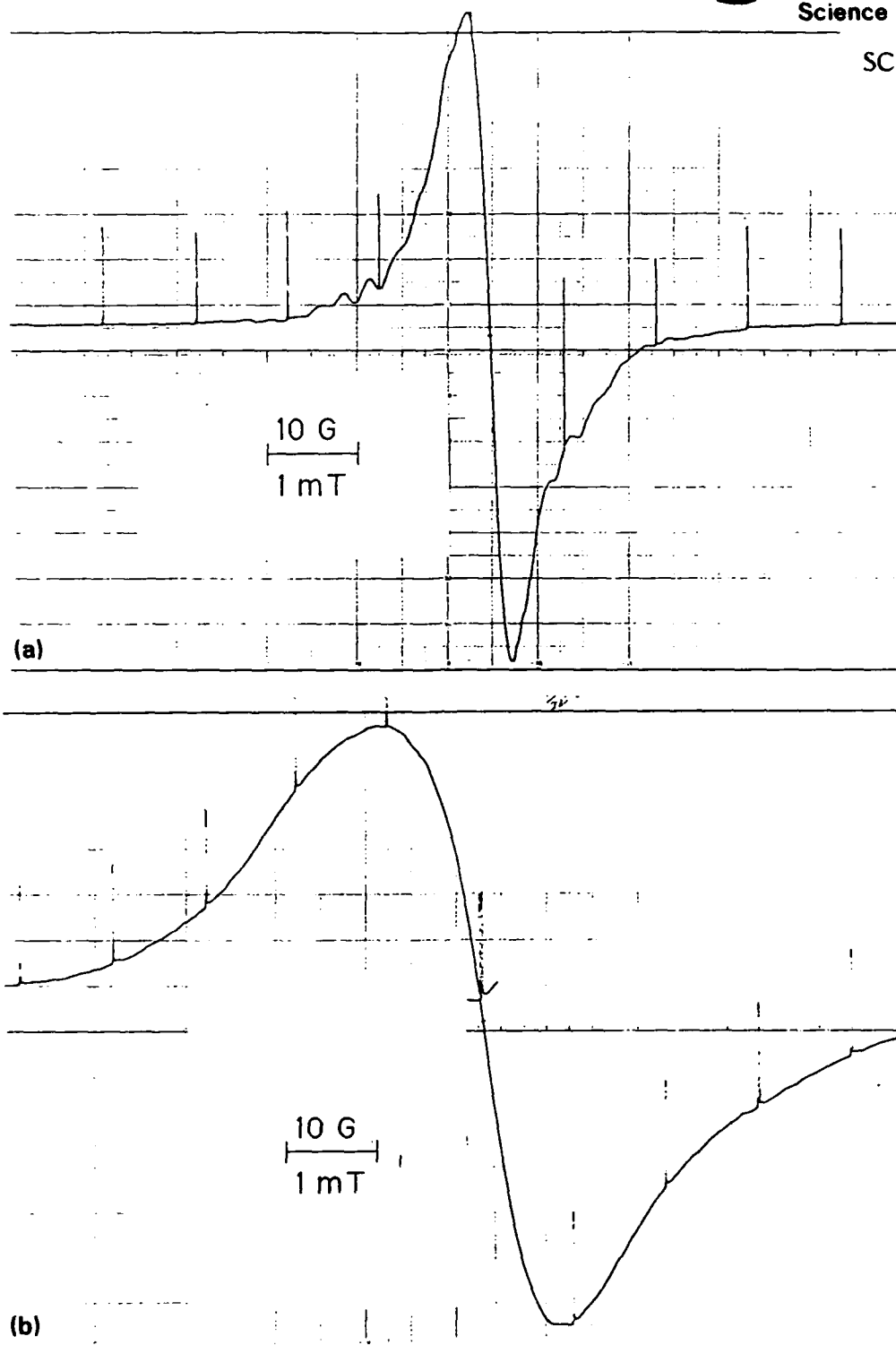
Fig. 40   ESR spectra observed during heating of mixtures of TNT and NaBH4.
(a) sample heated to 232°C (Expt. 5.C.6); (b) sample heated to 100°C
(Expt. 5.C.7).
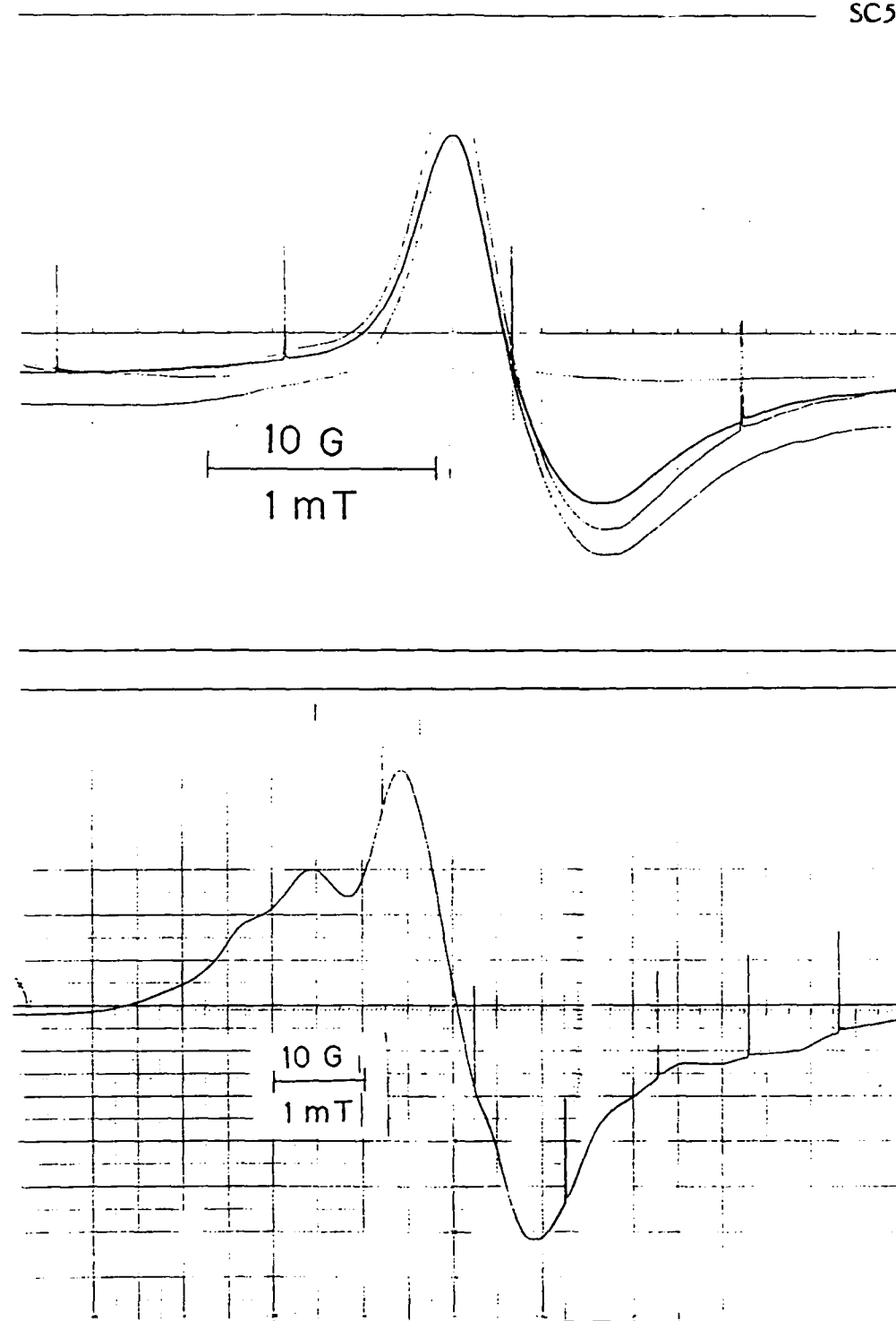
Fig. 41   (a) Spectrum of TNT and sodium sulfide at 100°C. (b) Spectrum of an unheated
sample at room temperatu e. Note the large number of anisotropic hyperfine
components.
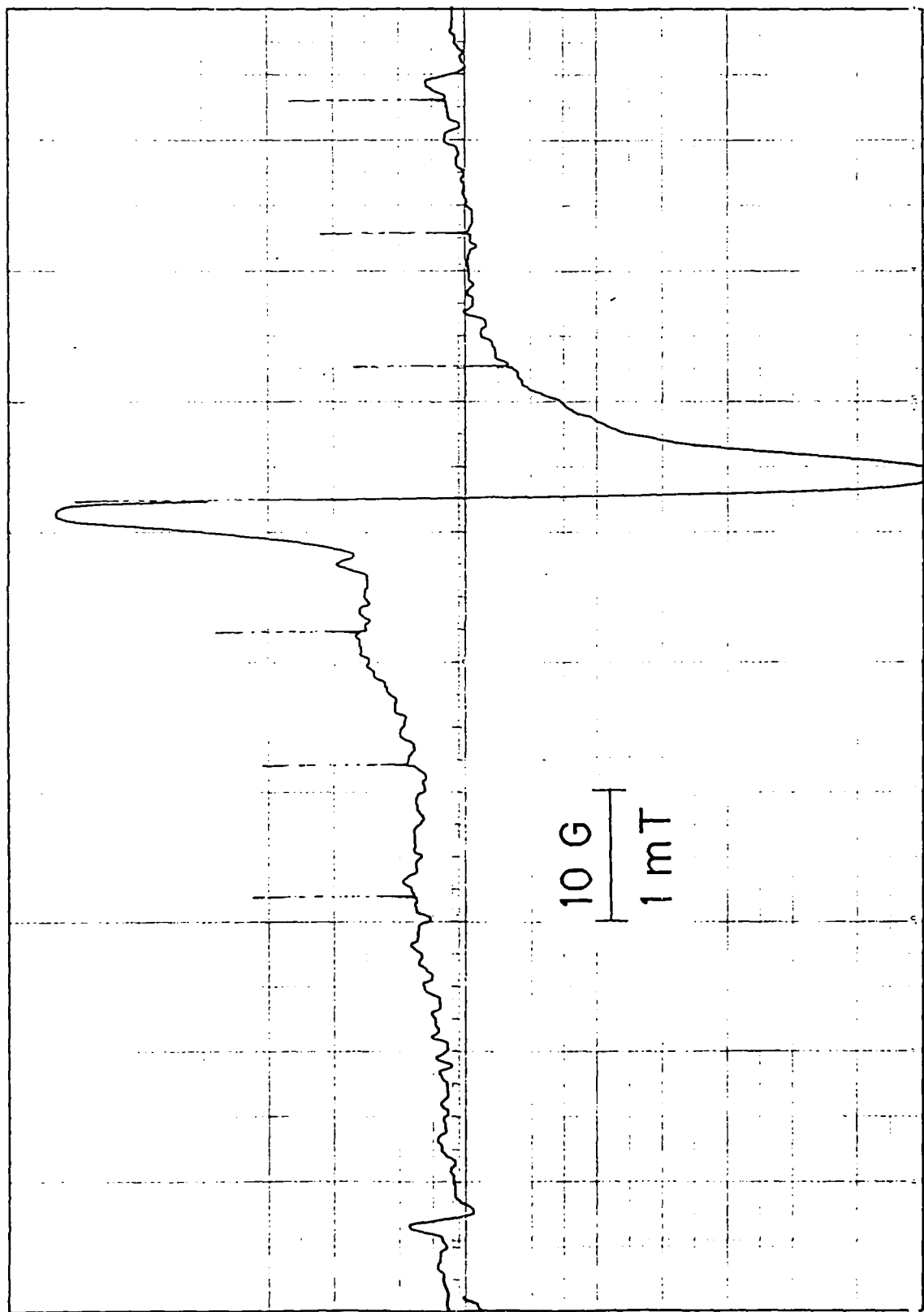
Fig. 42 ESR spectrum of unheated mixture of TNT and CaH$_2$.

10 G

1 mT

in the interior of the spectra was enhanced in comparison to spectra obtained in the presence of solid $Ca(OH)_2$. The spectrum is tentatively assigned as consisting of the aforementioned quartet of 0.264 mT, a nitrogen splitting of 0.846 mT and a proton doublet of 1.18 mT. This would be consistent with a structure such as 12.

12
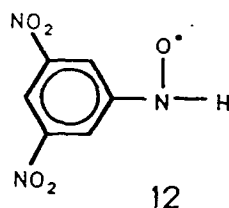
Many different monoarylnitroxides have been reported to have similar values of a_N, $a_{H(NH)}$ and $a_{o,p}$ (Ref. 6, pp. 538-555).

The g-value (midpoint, uncorrected) for this species was 2.0059. An additional, single, sharp line occurred at g = 2.0049 which conferred asymmetry on the overall spectrum. This lower g-factor suggests the presence of Tar. However, it is not so low as the g-factors observed in TNT thermolysis reactions (ca. 2.0035); moreover, it remained sharp throughout the experiment and did not grow appreciably. Only toward the end (6000 s) did it begin to dominate due to loss of intensity in the multiple line species. Consequently, the species responsible for this absorption is probably distinctly different because TNB lacks the "bifunctionality" (methyl as well as nitro substituents) of TNT and consequently lacks a ready pathway for polymerization.

The radicals observed for wet TNB with and without $Ca(OH)_2$ appear to be closely related. (Compare Figs. 32 and 43.) But there is an unexplained difference in the overall spans of the spectra—36.6 vs 32 G, respectively. It will be necessary to do simulations to see wherein the difference occurs. It may be due to (a) a large hydrogen splitting or (b) a smaller splitting by two hydrogens.

This series of experiments suggests several conclusions:

• Water behaves as a weak nucleophile (in the Meisenheimer sense) and facilitates nitroxide formation in neat TNB which is otherwise inert. Tiny quantities of Tar appear to survive after the nitroxide disappears.

• A stronger base (aq. Ca(OH)$_2$) promotes formation of greater quantities of nitroxide and Tar and the latter survives after the former begins to disappear.

• The Tar formed from TNB in the presence of Ca(OH)$_2$ has a higher g-factor than Tar formed without added base.

• A large proportion of base (solid Ca(OH)$_2$) produces a transitory nitroxide radical and a large Tar residue.

• It does not appear that the nitroxide is capable of reacting autocatalytically with TNB to accelerate formation of Tar. Rather, the Tar appears to be formed by the process

$$TNB + OH^- \rightarrow Nitroxide \rightarrow Tar + other\ products.$$
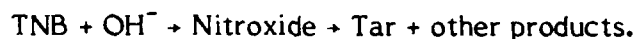
4. Mineral Acids

By way of symmetry, it seemed reasonable to check the effect of acids on the TNT decomposition. Approximately 1M solutions of mineral acids were prepared by non-quantitative dilutions. The acids used were HCl, HNO$_3$, H$_2$SO$_4$, and H$_3$PO$_4$. In an effort to be semiquantitative, the samples were prepared by introducing a weighed quantity of acid into an EPR tube, followed by a weighed quantity of TNT. All the experiments were run at the same nominal temperature of 245°C.

Three experiments with added HCl were performed. In each case there was slow development of a weak, messy spectrum of TNT nitroxide. By the time the spectrum was fairly well developed, the asymmetry caused by the Tar was already evident (Fig. 44).

HNO$_3$ additive was distinguished by the initial slow growth of an ill-resolved 3-line spectrum, $a_N \sim 0.9$mT, followed by a fairly rapid appearance of a strong nitroxide spectrum that was fairly clean, except that Tar was already evident. In the case of one experiment using concentrated HNO$_3$ rather than 1M acid, the three-line species lasted longer before being replaced by the nitroxide. A given intensity of Tar signal occurred

SC5493.FR
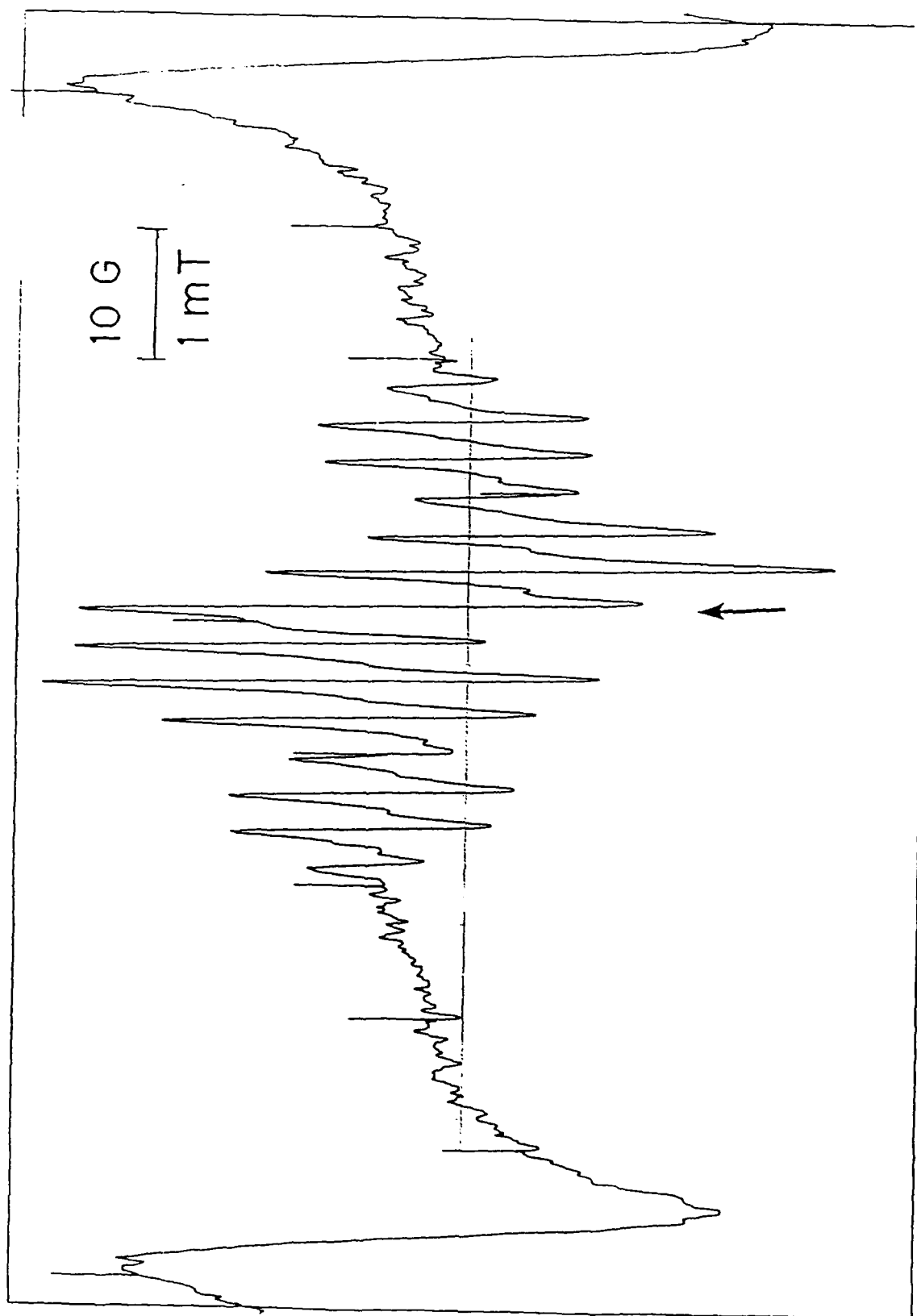
Fig. 43 Trinitrobenzene heated at 166°C with an aqueous slurry of Ca(OH)$_2$. Arrow indicates position of Tar absorptions that remained after hfs deteriorated. Broad lines at extremities of the recorded trace are due to manganese impurity in the calcium hydroxide.

10 G
1 mT
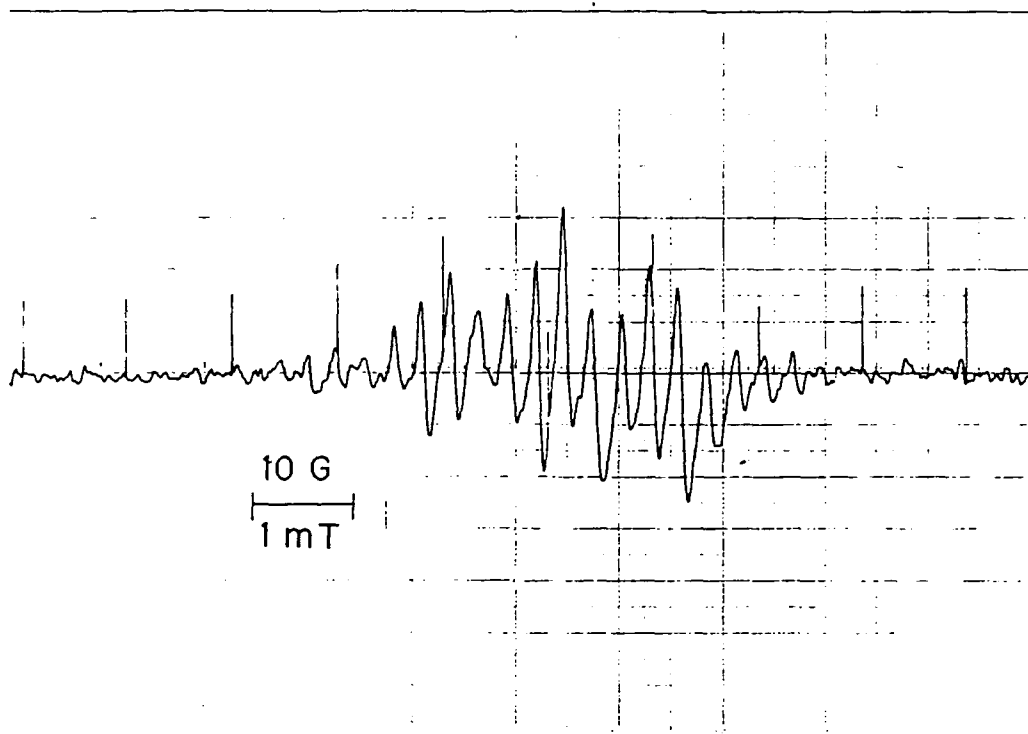
(a)
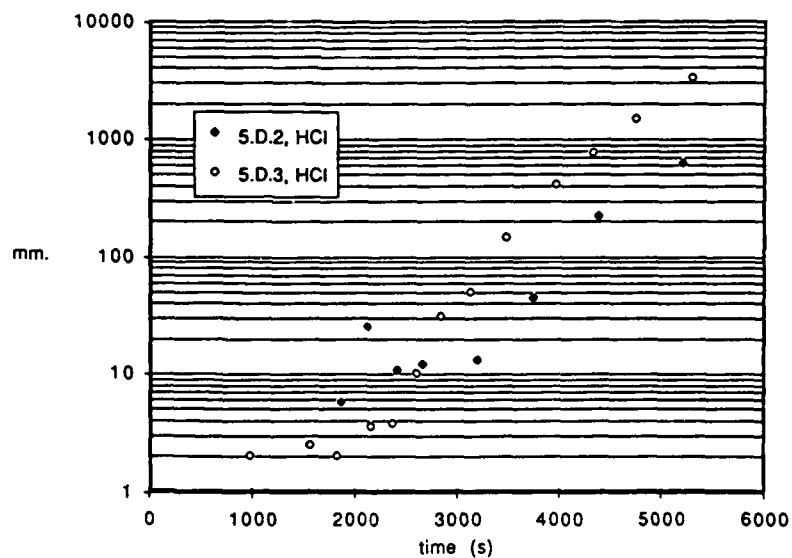
(b)

Fig. 44 (a) Spectrum of TNT at 241°C with aqueous HCl added. (b) Rate of Tar formation with added HCl.

10 G

1 mT
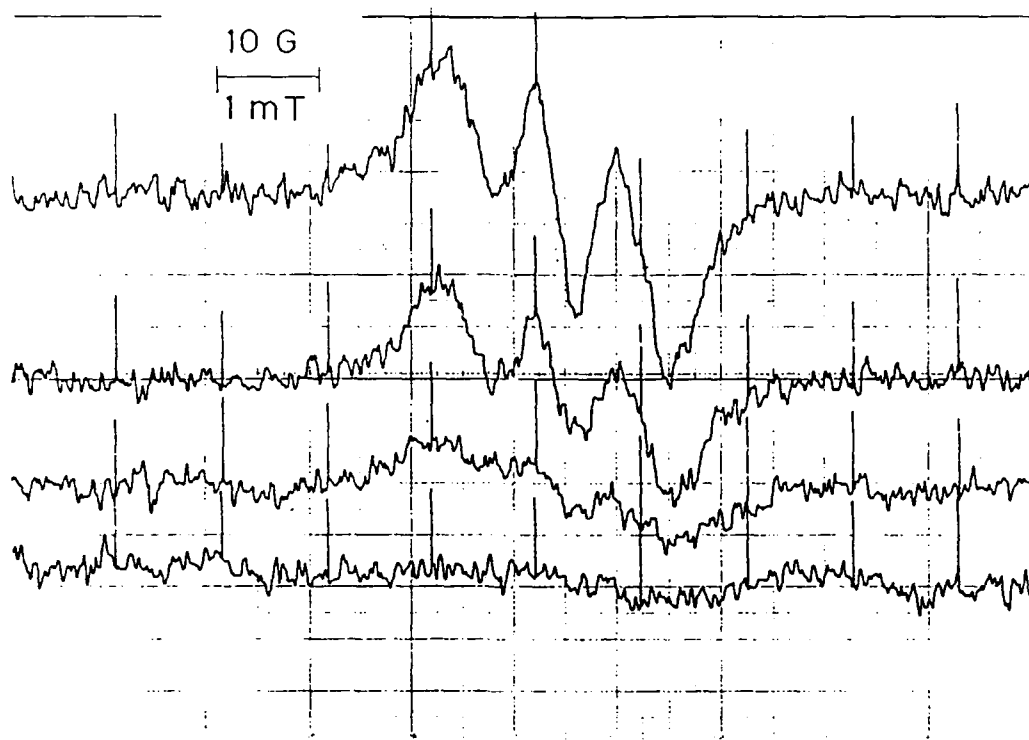
(a)
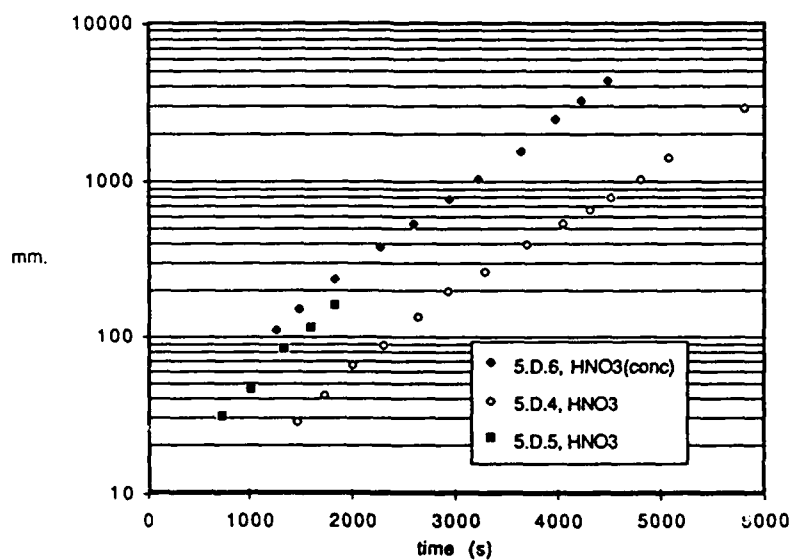
(b)

Fig. 45   (a) Spectrum of TNT at 245°C with aqueous HNO_3 added. (b) Comparison of
Tar rates with concentrated and dilute HNO_3.

sooner in this experiment than in those with dilute acid, but the overall rates were identical (Fig. 45).

The species initially observed when H_2SO_4 was added was a weak "iminoxyl"-type spectrum consisting of three sharp lines with $a_N \sim 3.2mT$. The outside lines disappeared quickly and a single line in the central portion grew steadily, but not exponentially (Fig. 46). The g-factor of the Tar absorption is similar to that of the early "iminoxyl" species (Table in Appendix 2, lines 347 and 353.) Concentrated H_2SO_4 is too lossy and too immiscible with TNT for quantitative work.

H_3PO_4 additive gave intriguing and most puzzling results. Two nearly-identical, replicate runs were made. For some inexplicable reason the induction period before the appearance of nitroxide was about 8000 s in the first (5.D.9), but only about 4000 s in the second (5.D.10). In both cases, the initial spectra were weak, ill-resolved versions of the nitroxide species, augmented by another species having sharp lines and smaller line separations than the out-lying nitroxide components. This spectrum appears to span only the area encompassed by the central three branches of the nitroxide species and it may arise from a radical that lacks the benzylic hydrogens (Fig. 47). It might be worth the effort to use a dry-box to prepare samples of TNT and P_2O_5 to investigate the effect further.

There is no obvious explanation for the variance in the induction times of these two experiments. However, the fact that they are both relatively long compared with that for other additives may have some implication for TNT stabilization efforts. (The same capillary was used to introduce the acid in both experiments; likewise, other capillaries were reused in the other experiments which also displayed shortened induction periods. One speculation is that there is an acid-leachable component to borosilicate glass that causes a delay in the tar formation step.)

Analysis of the kinetic data yields some interesting observations for this set of experiments involving mineral acids. With HCl added, the induction period before the formation of Tar is about 2000 s (Fig. 44b), but the nitroxide development seemed fairly normal, even if somewhat delayed. In the presence of sulfuric acid, the usual nitroxide is not observed (see above). Moreover, the "Tar" growth is closer to zero-order than first-order (Fig. 46b).
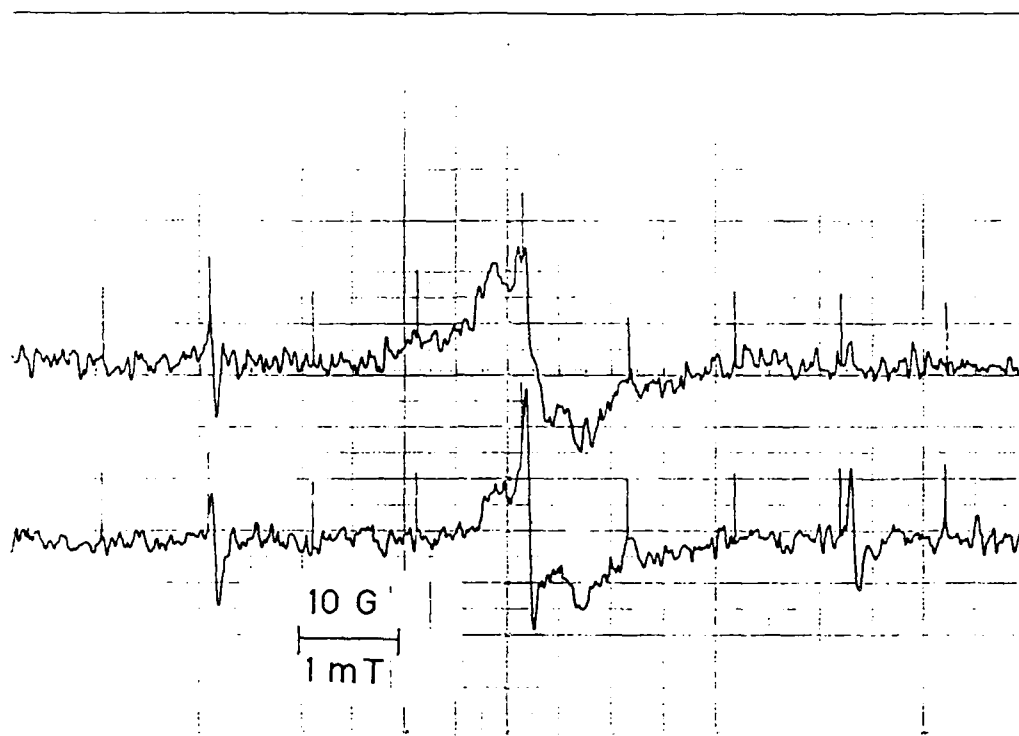
(a)
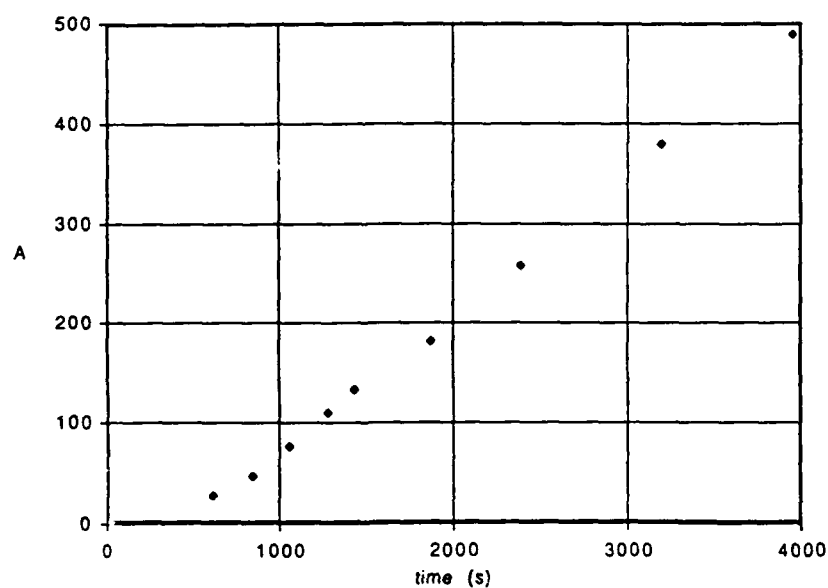
(b)

Fig. 46   (a) Spectra of TNT at 245°C with added aqueous H_2SO_4.   (b) Rate of Tar formation with added H_2SO_4.
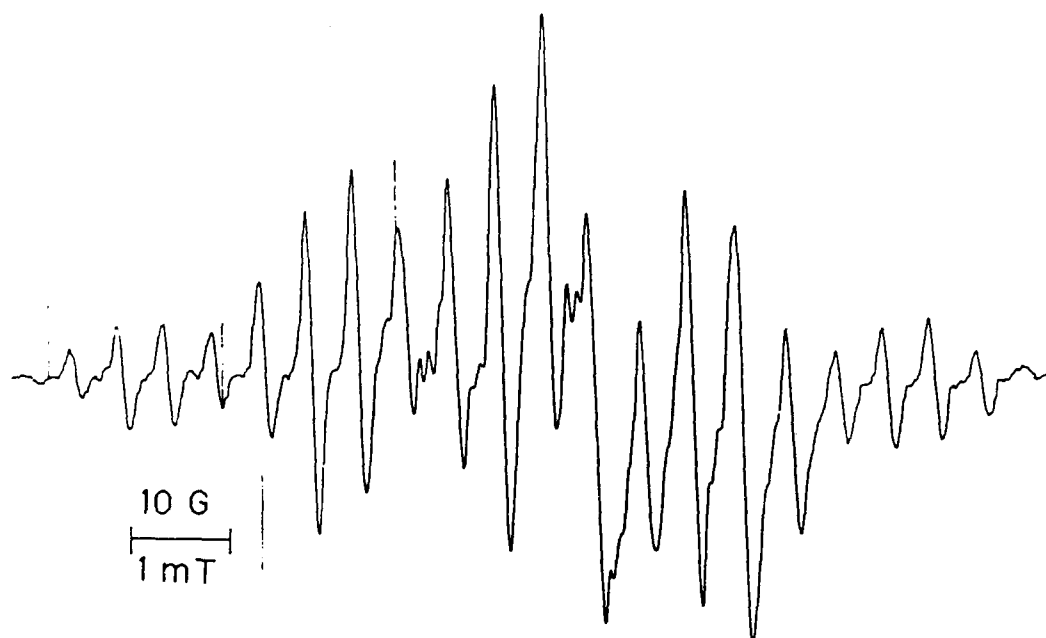
(a)
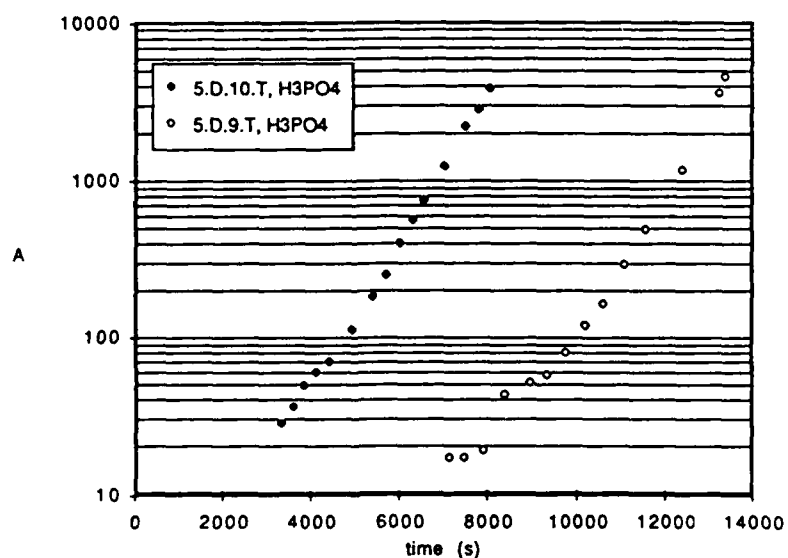
(b)

Fig. 47   (a) Spectrum of TNT at 245°C with added aqueous H_3PO_4.   (b) Rate of Tar formation with added H_3PO_4.

Since this entire series of experiments was purposely done at ~ 245°C it is interesting to compare the slopes of the Tar kinetic plots, Fig. 48. While the HCl and H_2SO_4 data are irregular, the HNO_3 and H_3PO_4 plots are intriguing in that the slopes are all essentially identical to that of a run with water being the only additive. The comparison of nitroxide and Tar development in the HNO_3 and H_3PO_4 experiments also appeared to be quite normal, Fig. 49. The noteworthy aspect of these experiments is the increased induction time required for the appearance of Tar.

On the basis of the limited data available from this exploratory work, it appears that nitric and phosphoric acid affect the evolution of free radical species in TNT only by increasing the induction time required before the onset of decomposition. Once the decomposition process starts, the evolution of nitroxide and Tar appears to follow the same course as in the absence of the acids. This behavior contrasts sharply with that observed in the presence of added bases.

With this knowledge that basic impurities promote thermal decomposition and that some mineral acids appear to delay the process, it would be reasonable to pursue further work in this area. Some preliminary experiments done in conjunction with our independent research and development programs have suggested that boric acid also has a retarding effect on radical production in TNT. Both borates and phosphates are known to behave as combustion inhibitors and these observations may be useful in desensitizing TNT formulations. While the crossover region from bimolecular thermal decomposition to unimolecular detonations cannot be addressed here, it should not be difficult for a weapons facility to test the effect of added phosphate or borate on impact sensitivity and detonation yields.

H.   Effect of Additives Derived from TNT

1.   2,4,6-Trinitrobenzyl Alcohol (TNB-CH$_2$OH)

When this alcohol was reacted at 150°C in benzene, a well-developed, symmetric spectrum resulted (Expt. 10.A.1). It had a span of 2.411 mT at 149°C (Fig. 50). The stability of these radicals was nothing short of remarkable: after a full week at room temperature, this radical from TNB-CH$_2$OH in benzene still exhibited an intense, highly symmetric spectrum shown in Fig. 51. The g-factor of 2.0040 was
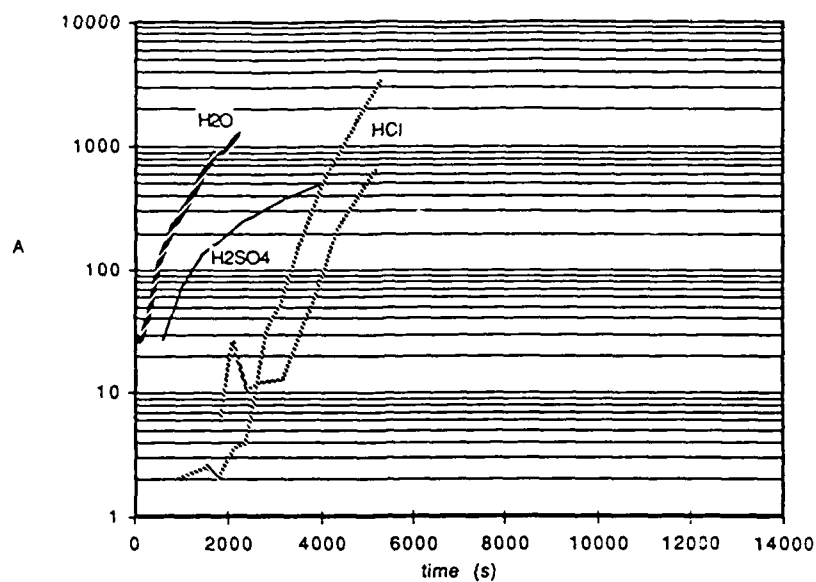
(a)
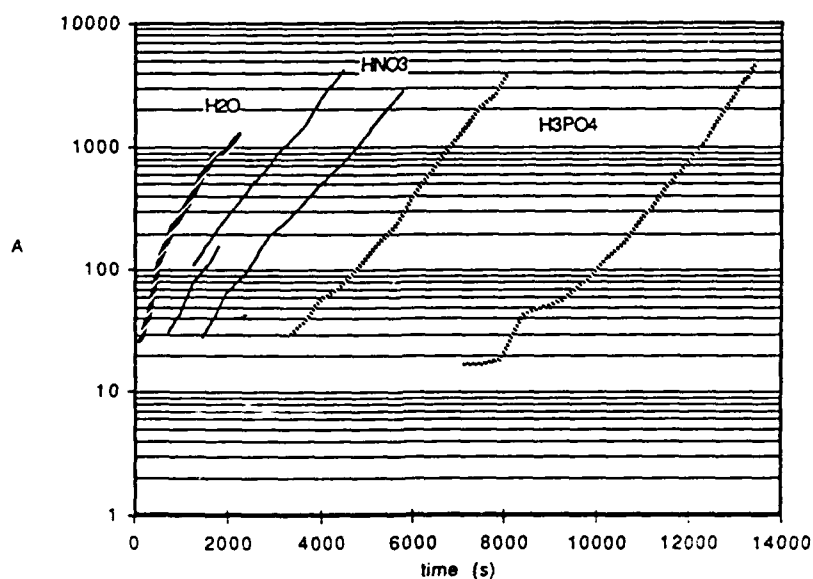
(b)

Fig. 48   Comparison of Tar formation in moist TNT near 245°C with added (a) sulfuric or hydrochloric acid or (b) nitric or phosphoric acid.
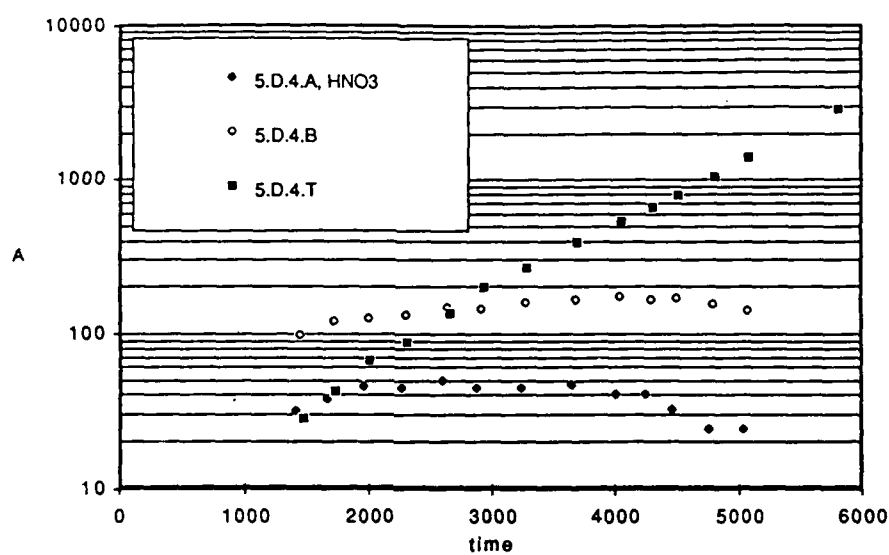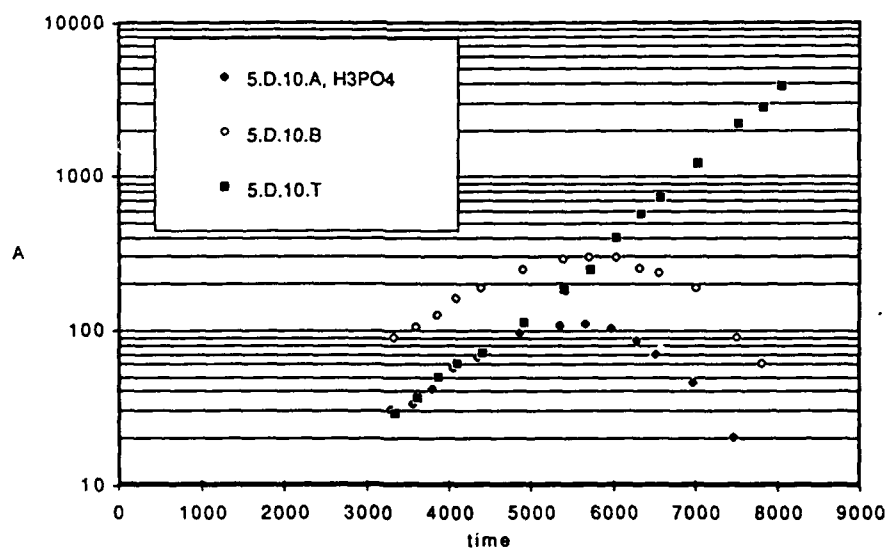
Fig. 49   Display of rate data for formation of nitroxide (lines A and B) and Tar at
245°C in TNT moistened with 1 M (a) nitric acid or (b) phosphoric acid.

noteworthy in that it was significantly lower than values observed for nitroxides derived from molten TNT thermolysis (see Appendix B), yet higher than values observed for Tar in those systems. This g-factor is comparable to that observed in the reaction of TNB with calcium hydroxide.

After storage, the total span had diminished to 2.383 mT but this may be due largely to temperature-dependent hfsc: The nitrogen splitting changed from 0.817 at 150°C to 0.808 mT at room temperature. There is a 1:1 correspondence between the original and week-old lines, although the patterns reflect some differences in overlapping interferences. As good as the resolution is in this aged material, it is still not good enough to make a straightforward assignment. There are small, symmetric "blips" that are evidently legitimate elements of the spectrum. However, the resolution is insufficient to allow any guess about the intensity ratios of the outside lines.

Quite late in the program an experiment was performed using neat TNB-CH_2OH. It was heated initially at 127°C but after recording a strong spectrum, the temperature was dropped to 106°C to prolong the life of this interesting species. The spectrum is shown in Fig. 52. It can be ascribed to two ring protons having the usual hfsc of 0.26 mT, a unique hydrogen of 1.11 mT and a nitrogen splitting of 0.82 mT. The g-factor is 2.0060, which is close to the values measured for many other radicals that are presumed to be nitroxides formed by intermolecular condensations such as indicated in Scheme 1. It is tempting to assign the radical responsible for Fig. 52 to a structure such as 13a. But if this were the correct structure, one would expect the benzylic protons para to the nitroxide function to produce significant splittings and the nitrogen splitting would be expected to be about 1.0-1.1 mT. The spectral parameters are actually more consistent with structure 13b in which the para substituent has been oxidized to an aldehyde (assuming that the aldehydic proton does not produce a resolved splitting). But it is difficult to envision this process occurring during the 200 seconds reaction time that elapsed before the first strong spectrum was recorded.

(a)

10 G
1 mT

(b)

10 G
1 mT
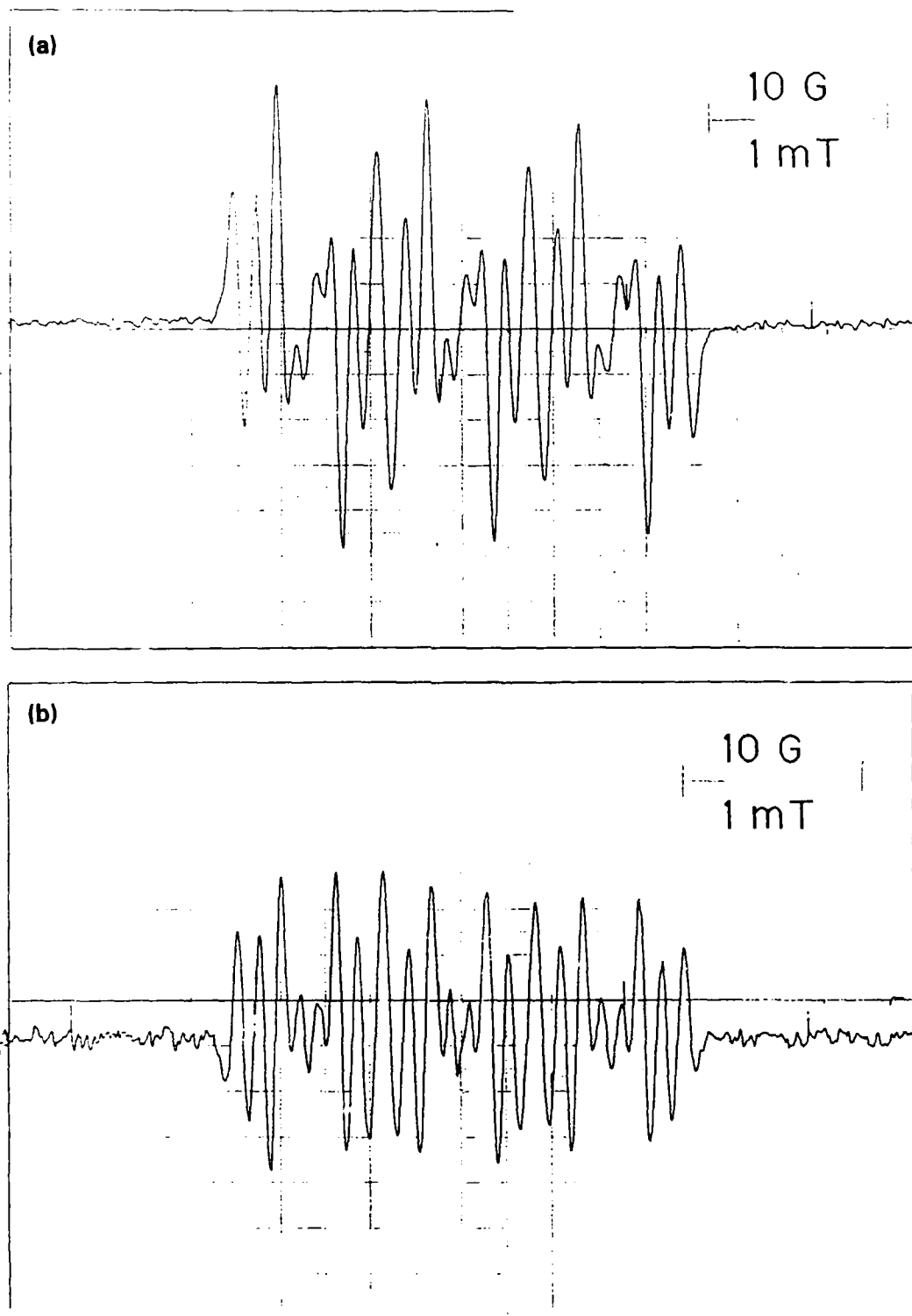
Fig. 50   TNB-CH$_2$OH in benzene (sealed tube) at 149°C.   (a) First derivative and
(b) second derivative ESR spectra.
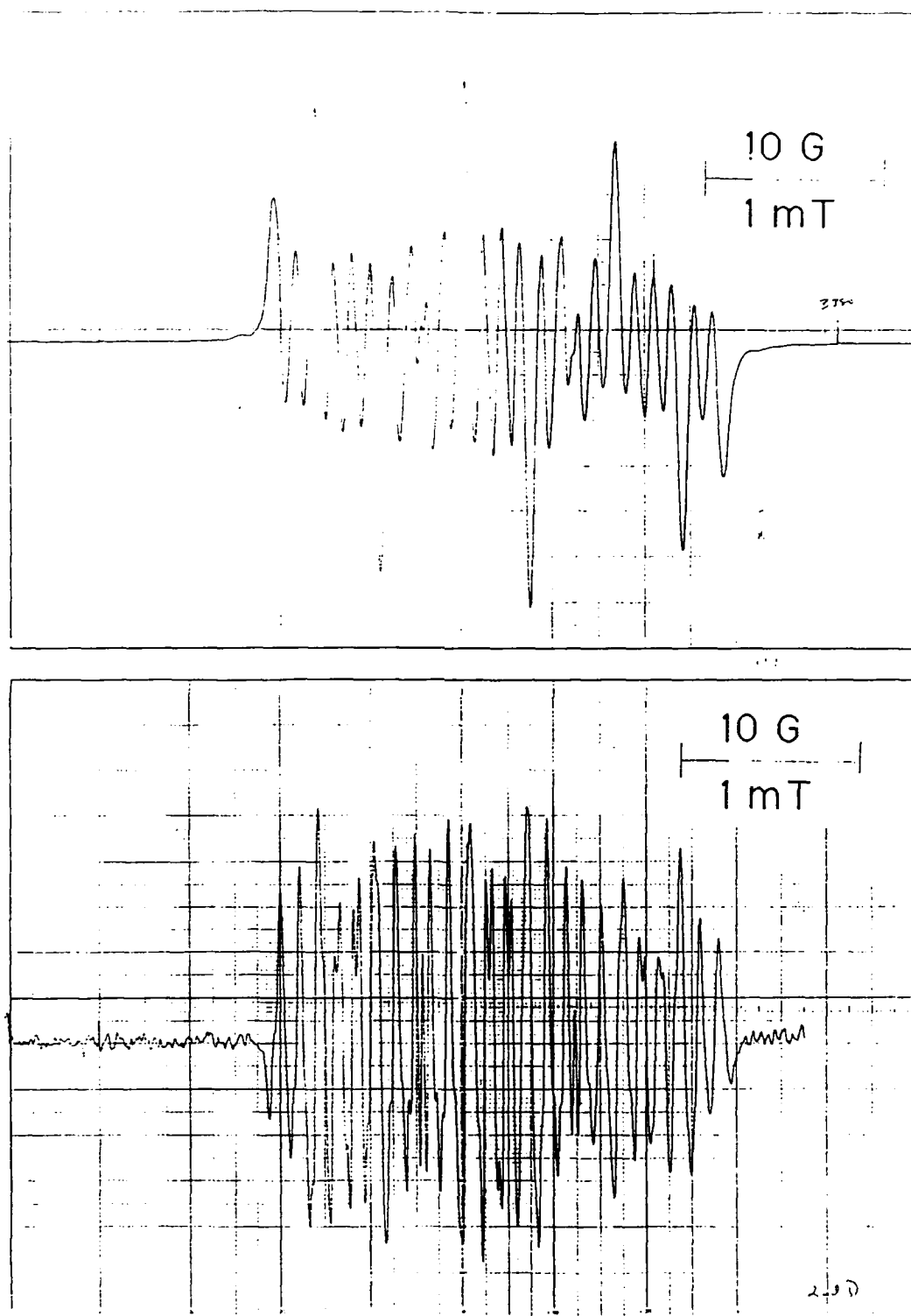
Fig. 51   Same sample as in Fig. 50 after standing at room temperature for one week.
(a) First derivative and (b) second derivative ESR spectra.

10 G
1 mT
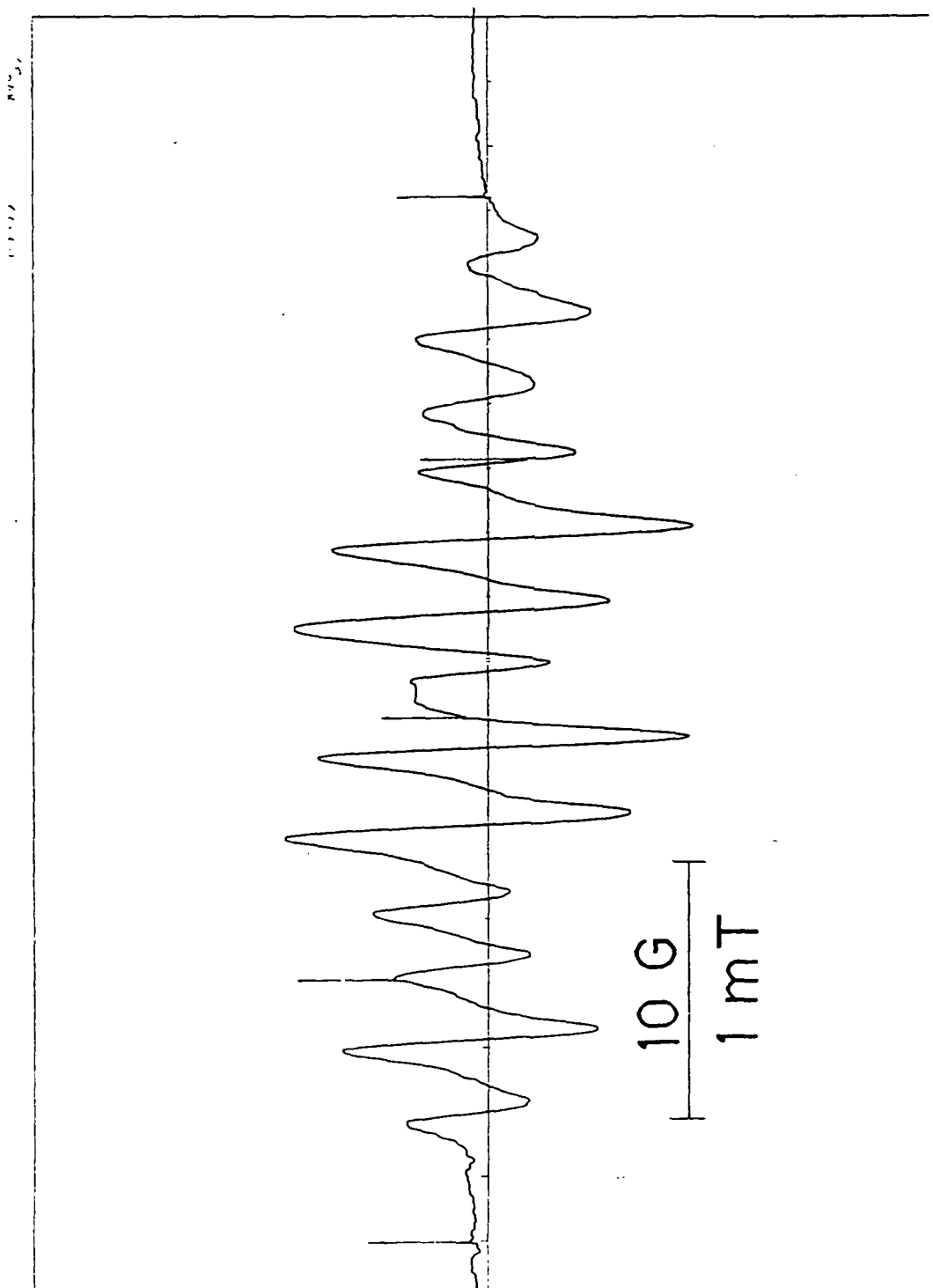
Fig. 52   ESR Spectrum of neat TNB-CH2OH reacted initially at 127°C and recorded at 106°C.

It is curious that the g-factor of the species formed in a dilute solution in benzene is so much lower than that of the species formed in a neat sample while the nitrogen splittings of these two different species are so similar (and smaller than the usual values of 1.0-1.1 mT).

TNB-CH$_2$OH was also reacted with HMB (Expts. 10.B.1&2) and with TNT (Expt. 10.C.1). These were not "clean" reactions in that the resulting asymmetric spectra underwent time evolution that reflected differing proportions of various free radical species.

The spectra from HMB reactions were notable for the large overall span and 5-branch pattern characteristic of benzylnitroxide free radicals. But there is severe asymmetry even in the wings of the spectra, Fig. 53.

Since the span of TNB-CH$_2$OH/benzene radicals is only about half that of TNB-CH$_2$OH/HMB radicals, the former cannot be responsible for the wing asymmetry of the latter. One possible explanation for the observed wing asymmetry is that two different benzylnitroxide radicals result from coupling of HMB with the two different types of nitro groups present in TNB-CH$_2$OH. Such radicals would be expected to be distinguished by subtly different g-values and slightly different ring proton splittings. (There is evidence supporting this statement in the data for TNB-CHO discussed below.) The change in relative intensities of some of the inner lines of these spectra probably reflects differences in long term stability of the two different nitroxide radicals. (The final spectra in this series had the same sort of overall asymmetry among the 5-branch pattern, Fig. 53b, that is so often seen in reactions of 2,4-dinitrotoluene. This molecule also has two distinctly different kinds of nitro groups.)

Reaction of TNB-CH$_2$OH with TNT also produced spectra that evolved over time and reveal some interesting insights, Fig. 54.

Early in Experiment 10.C.1 the overall spectral span indicated presence of a benzylnitroxide radical. But the wing intensity diminished rapidly and within 5 minutes (at 100°C) the spectrum was dominated by an asymmetric three-branch pattern characteristic of a nitrogen splitting ($a_N \sim 0.83$ mT). After more complete decay of the benzylnitroxide signal much of the asymmetry of the remaining 3-branch pattern could be ascribed to motional line broadening effects. However, careful examination of the relative intensities of the wing lines revealed that the spectrum was still evolving due to

(a)

10 G

1 mT

(b)

10 G

1 mT
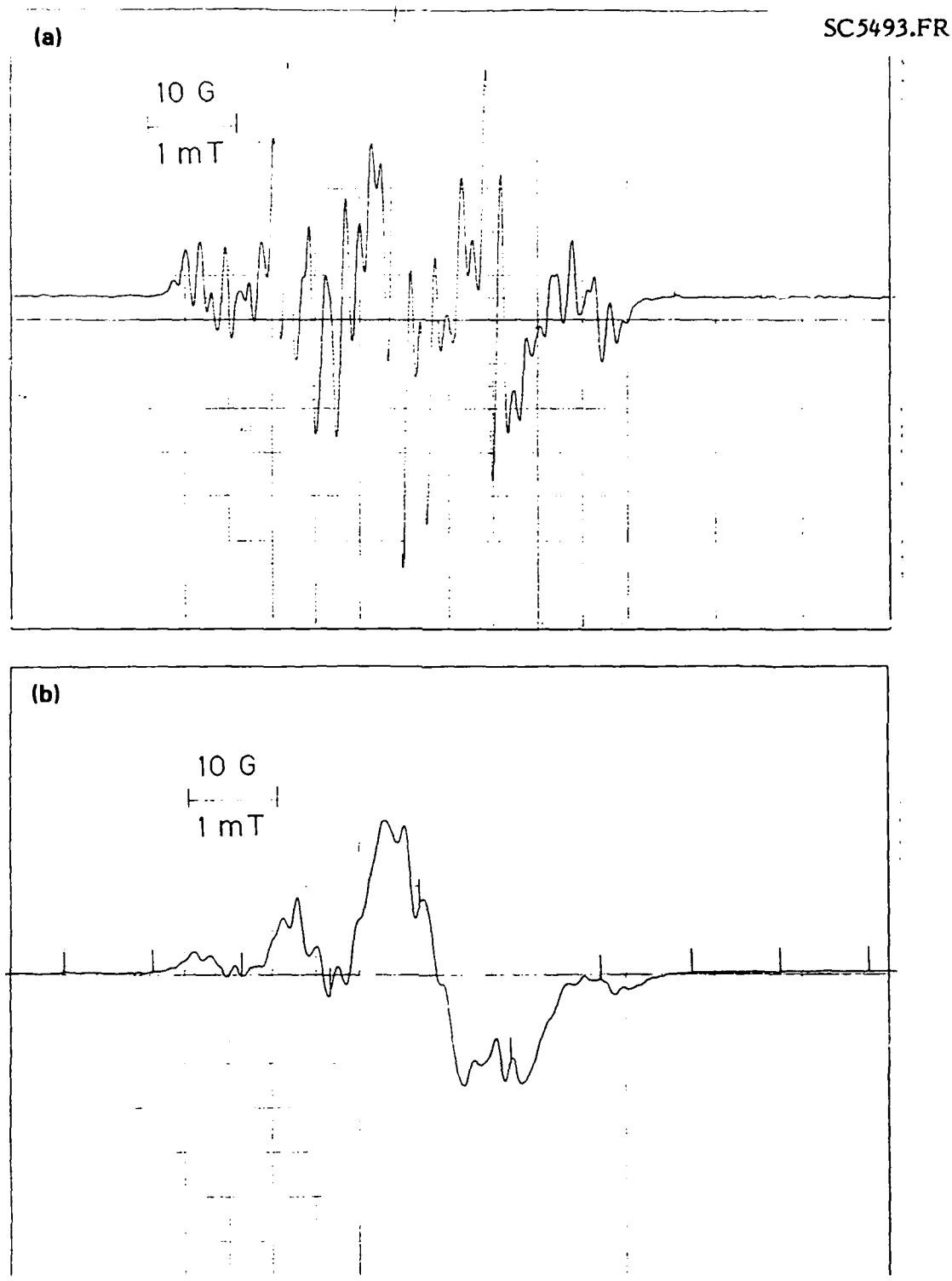
Fig. 53   ESR spectra observed during reaction of TNB-CH2OH and HMB at 198°C.
(a) Early spectrum at 330 s and (b) later spectrum at 1800 s.
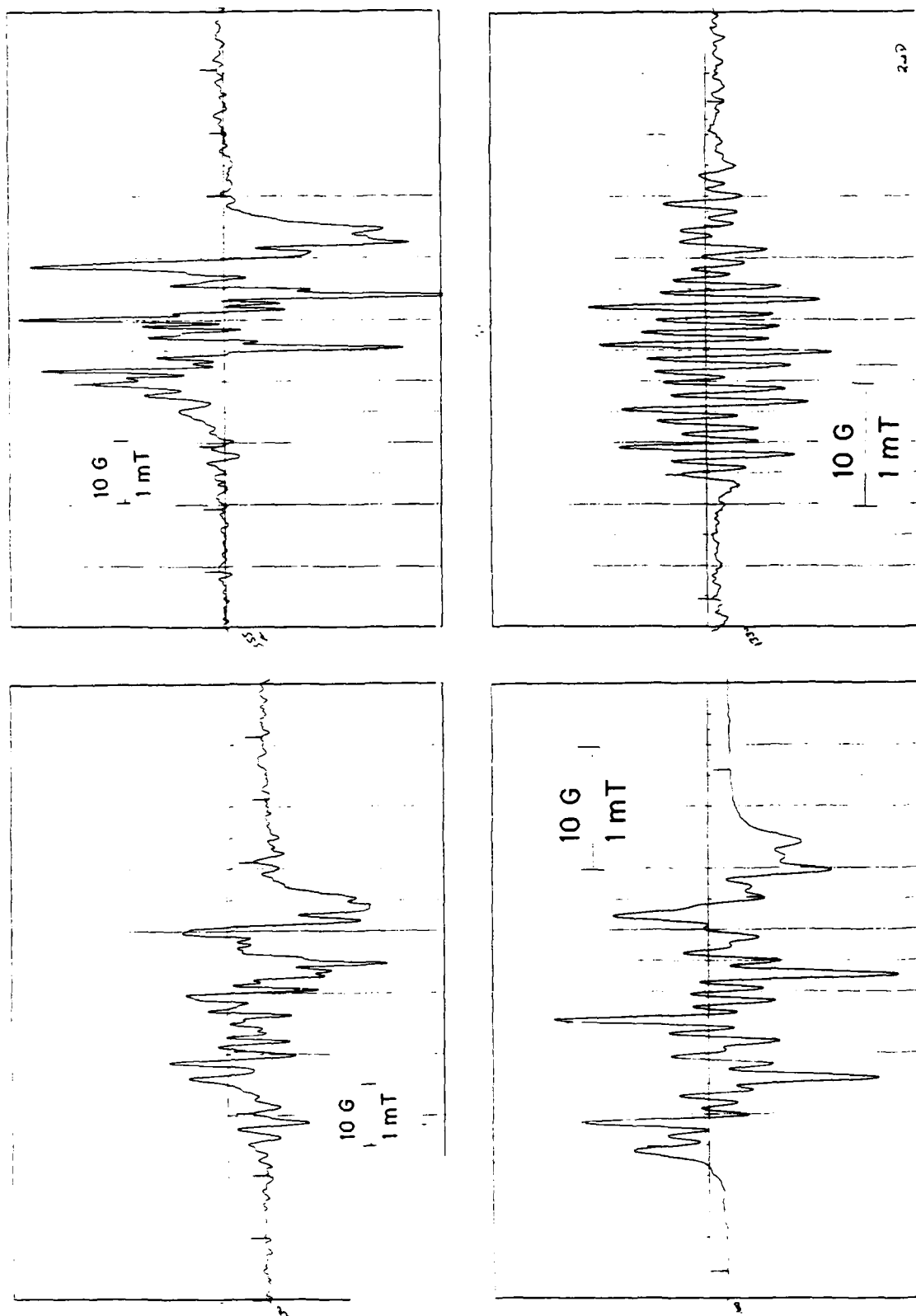
Fig. 54   ESR spectra of TNB-CH₂OH reacted with TNT at 100°C. Early spectra at (a) 130s and (b) 550 s, showing decay of a benzylnitroxide species. It is ultimately supplanted by the three-branch pattern shown in (c) at 1700s and as a second derivative presentation in (d).

decay of one member of a pair of radicals with essentially identical g-values. The hydrogen hfsc of the dominant radical appears to consist of a(2H) = 0.212 and a(1H) = 0.31 mT. The g-value is 2.0039.

This spectrum has many features in common with that observed for TNB-CH_2OH in benzene. This may argue for a nitroxide radical formed by intramolecular cyclization which outlives the benzylnitroxide produced through intermolecular condensation.

One reasonable experiment was never performed: TNB-CH_2OH inTNB. But since TNT did not produce a different radical(except for the transitory benzylnitroxide), TNB would not be expected to behave differently.

The TNB-CH_2OH/HMB reaction (Expt. 10B.1, 198C) was run at a somewhat higher temperature than the other TNB-CH_2OH reactions and this in itself may be reason for the conversion to Tar, see Fig. 53b. But it is interesting to observe the transformation to Tar in this case because the spectrometer gain was essentially constant throughout the experiment. As the presence of Tar becomes more evident, there is a corresponding broadening of the hfs components of the benzylnitroxide spectrum--far removed from the Tar line position. This could be due either to changes in the bulk viscosity of the medium as the reaction proceeds or possibly it might reflect hindered tumbling of the nitroxide radicals due to association with the heavier Tar particles. Most likely, it is the former effect because in many TNT reactions, the final product was a charred solid and when the reaction mixture was removed sooner, it appeared to be a viscous oil.

Another reaction between TNB-CH_2OH and HMB (Expt. 10.B.2, 150°C) was conducted at lower temperature and did not lead to Tar formation. When the spectrum of this material (Fig. 55) is superimposed on that of TNB-CH_2OH in benzene at 149C, many lines coincide, so it is likely that the product of intramolecular coupling is present. (Unfortunately, g-values were not determined because the frequency counter was not available.) However, it is noteworthy that there is also strong asymmetry between the outer wings of the HMB species--well beyond the region of overlap with the presumed intramolecular coupling product. So there are yet other species present.
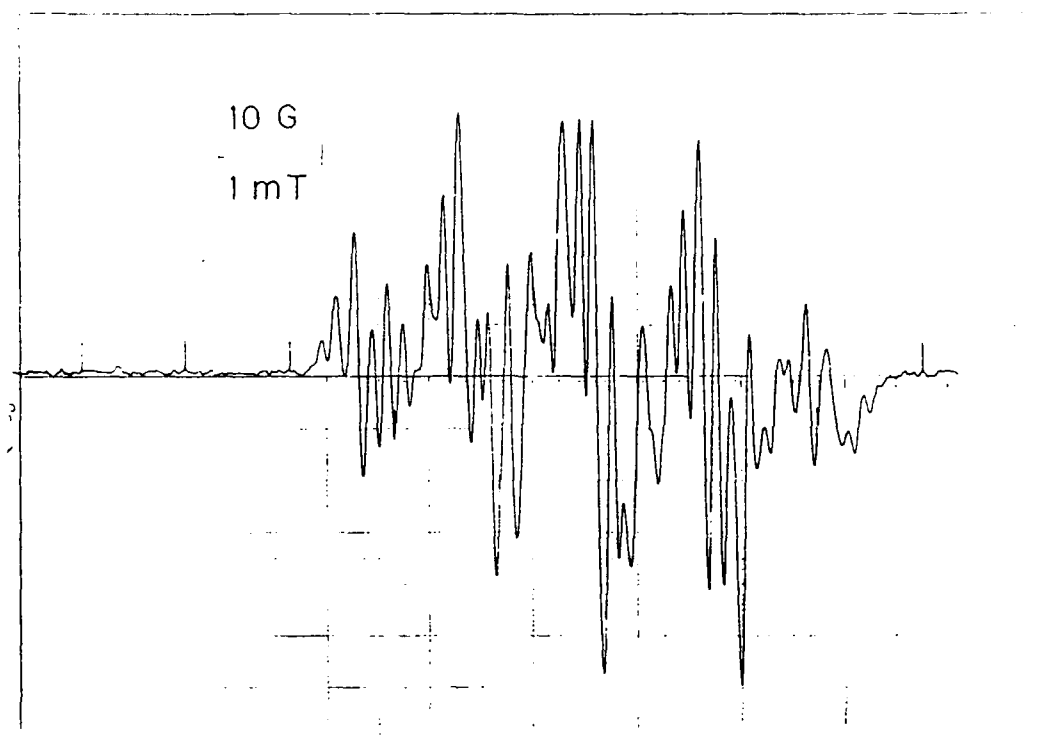
Fig. 55 ESR spectrum of TNB-CH2OH and HMB reacted at 150°C for 10,700 s.

After long storage on the shelf the TNB-CH$_2$OH had discolored. It was dissolved in toluene/methylene chloride and passed through a silica gel column. Fractions were collected and blown down to dryness with nitrogen. A portion of Fraction 3 was prepared in benzene in a sealed tube and heated to 254°C (Expt. 10.A.3). The spectral span was essentially identical to 10.A.1 (149°C); but there was far more hfs at the higher temperature, Fig. 56. When this material was cooled to room temperature, much of this hfs structure disappeared, leaving an asymmetric spectrum with rather broad lines (ca. 0.12 , vs. about 0.06 mT in most "normal" spectra.), Fig. 56b. When superimposed on the high temperature spectrum, the low temperature spectrum appeared encompass a smaller span (ca. 2.52 vs ca. 2.72 mT) and to consist of at least two different species having different g-values and line widths. (The NMR gaussmeter was not functioning at the time of these experiments, so no determination of g-values was possible.) Reheating to 209 C once again produced the sharp-lined species with

complicated hfs, Fig. 56c; however the resolution was not so good as originally observed and some of the very broad lines that had been present at the extreme low-field end of the spectrum were missing upon reheating. After about 20 m of heating at 209°C the temperature was again dropped to room temperature. A symmetric pattern of 10 broad lines replaced the complicated asymmetric pattern. This low-temperature spectrum, Fig. 56d, got more intense with time, although the resolution became somewhat poorer.

After standing overnight at room temperature (ca 14.5 h) the spectrum of Fig. 56d remained although the relative intensity was somewhat diminished. After recording several traces (including second derivatives) the tube was opened and aerated with a capillary bubbler. The resolution deteriorated but the envelope still superimposed on the high temperature spectrum.

2. 2,4,6-Trinitrobenzaldehyde (TNB-CHO) Reactions

A sample consisting of 20 mg TNB-CHO in 540 mg benzene exceeded solubility at room temperature. It was heated at progressively higher temperatures until a spectrum was finally observed at 199°C (Expt. 11.A.2). The spectrum was asymmetric, Fig. 57a, and consisted of two different species which are characterized as "weak" (span = 30.78 mT, with well-separated 1:2:(1) patterns at ends, a_H= 0.261 mT) and "strong" (span = 2.025 mT, approximately 1:4:6:4:1 outside patterns, a_H = 0.209, and a_N = 0.539 mT) species which developed differently with time. The "weak" species had decayed sufficiently by 7000 s, Fig. 57b, to permit the "strong" species to be clearly distinguished. When the temperature controller blew a fuse at 7450 s the temperature dropped from 198 to 30°C and the "strong" species survived with spectacular resolution of additional hyperfine structure, Fig. 58. The line widths were on the order of 0.02 mT and the pattern that earlier appeared to arise from 4 equivalent hydrogens now appeared to be due to three different sets of one, one, and two nuclei having nearly equal splittings. There was additional hyperfine structure which is readily interpreted as due to two previously unresolved, unique hydrogens, a_H = 0.054 and a_H = 0.04 mT.
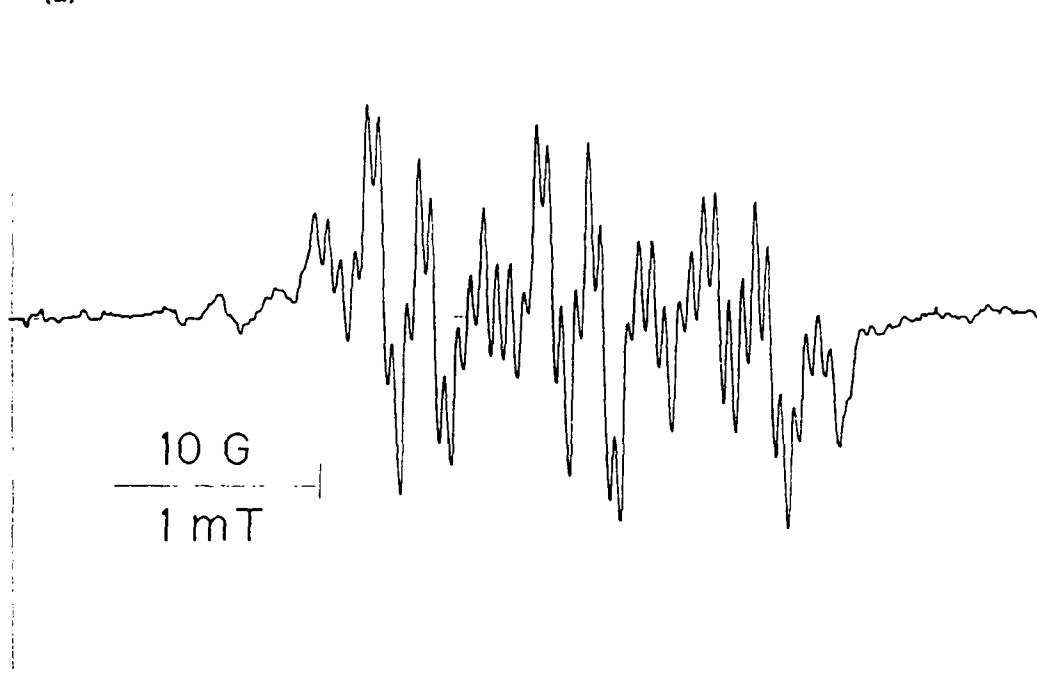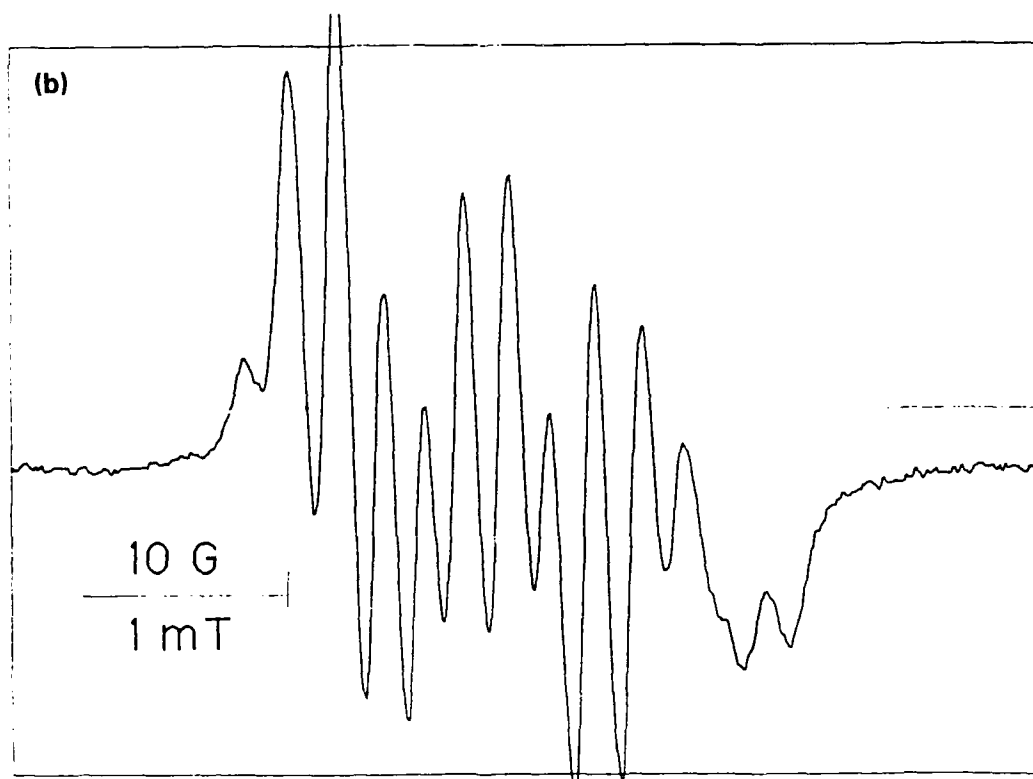
Fig. 56   ESR spectra of TNB-CH$_2$OH in benzene recorded at (a) 254°C, (b) room
temperature, (c) 209°C, and (d) again at room temperature.

10 G
1 mT

10 G
1 mT
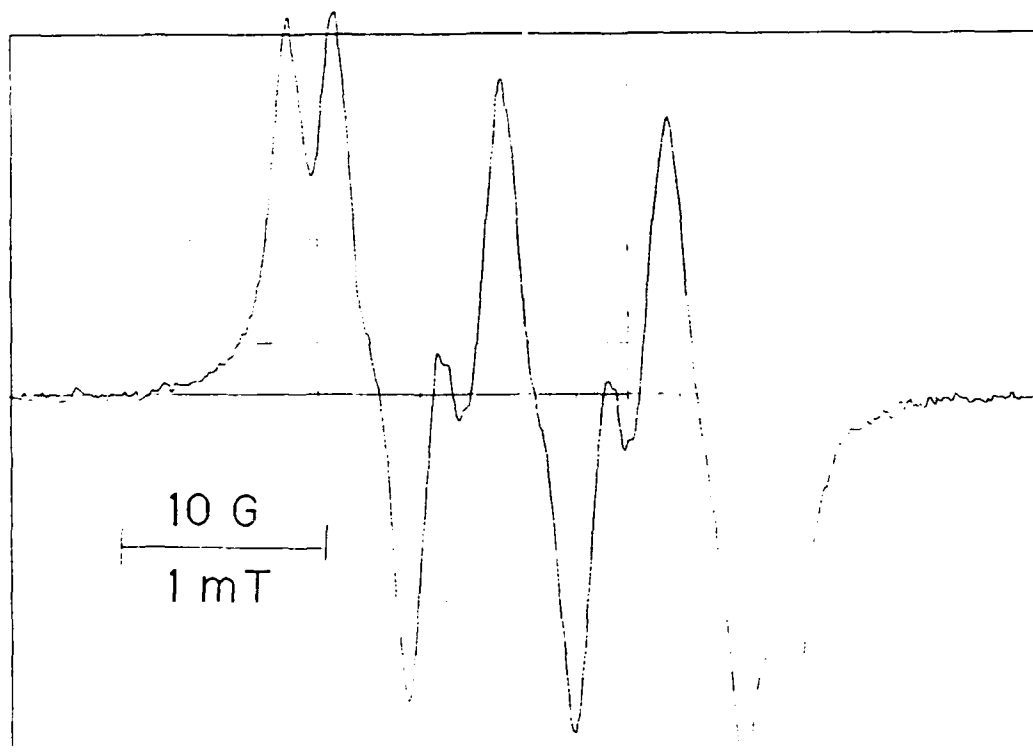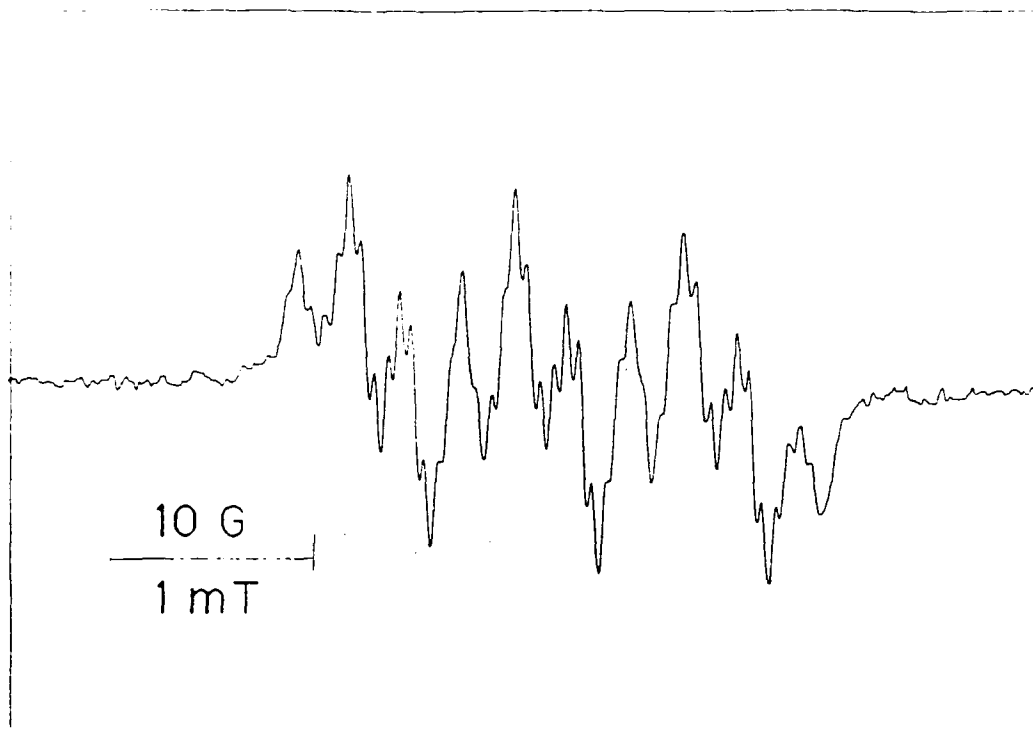
Fig. 56 (Continued)
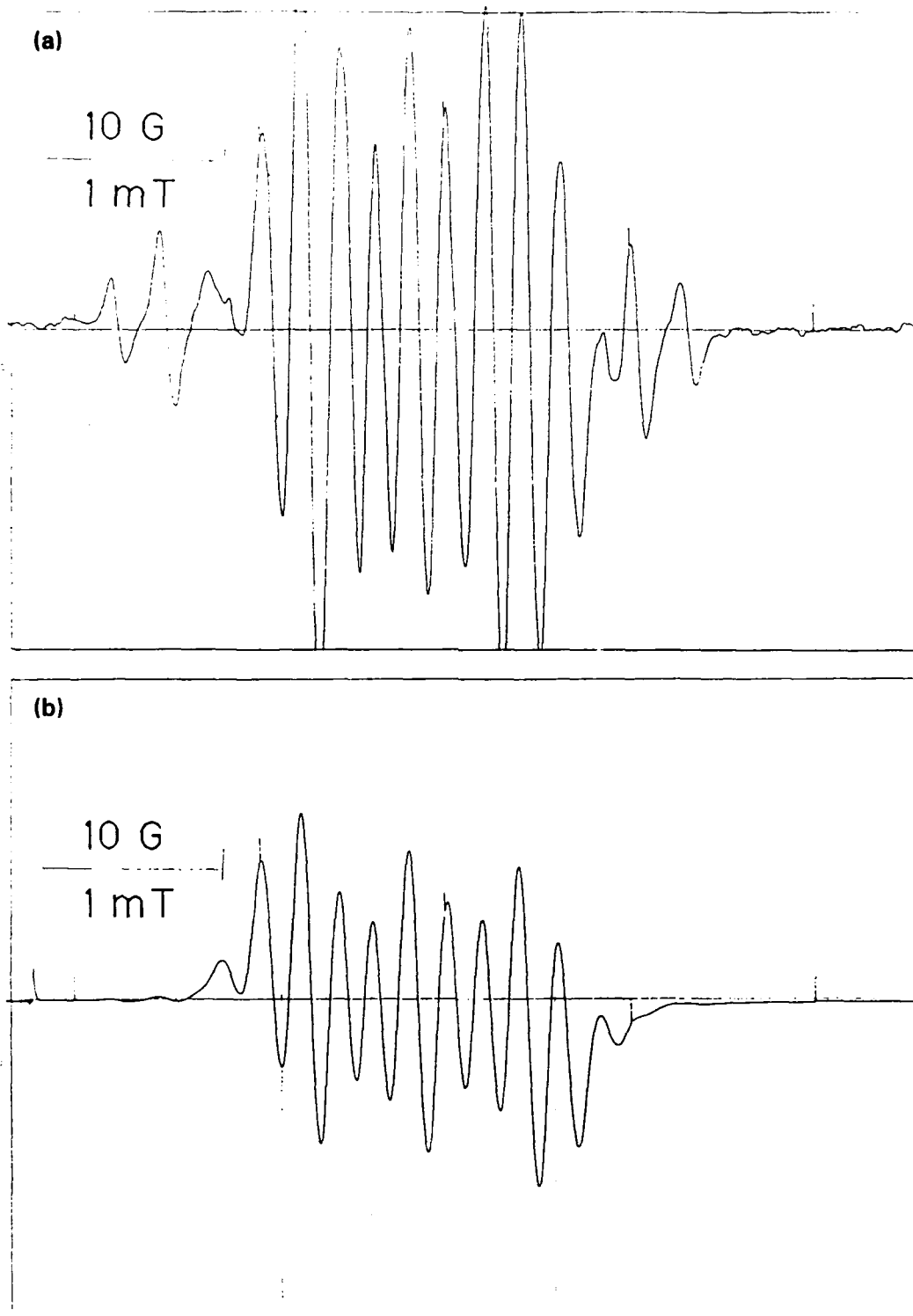
Fig. 57 Time evolution of ESR spectra of TNB-CHO in benzene at 199°C. (a) 4200 s and (b) 7000 s after initiation of experiment.

SC5493.FR
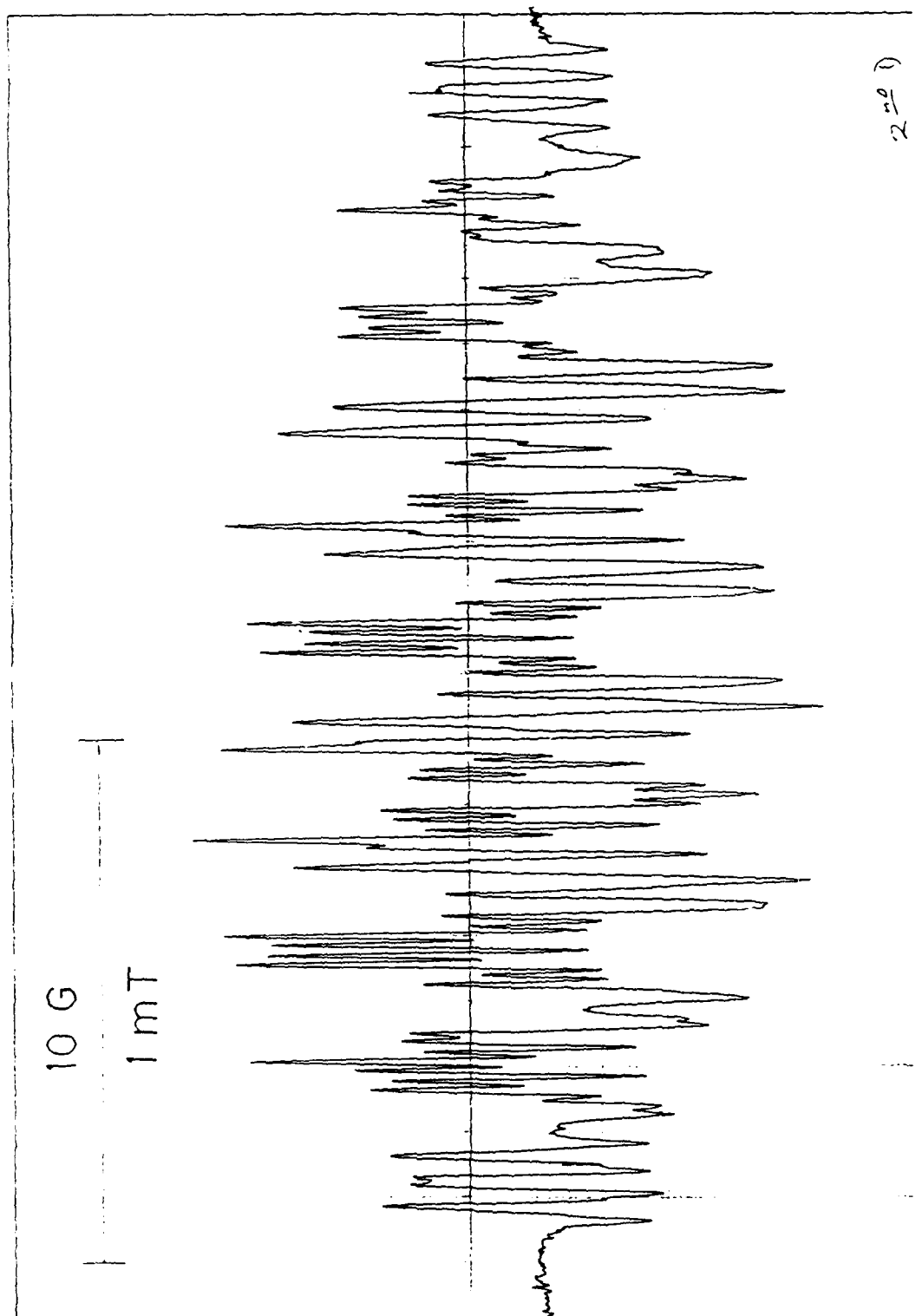
Fig. 58   Second derivative ESR spectrum of radical from TNB-CHO in benzene after heating at 199°C and then cooling to room temperature.

10 G
1 mT

A structure consistent with the observed spectrum is:
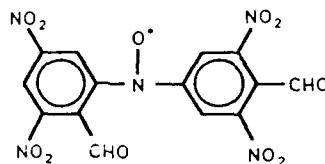
14

On the basis of the relative spans of the two different species it is reasonable to speculate the the "weak" spectrum arises for a familiar type of alkylarylnitroxide radical. Much of the basis for this statement comes from the observation of a 0.26 mT proton splitting which is characteristic of the aromatic hydrogens ortho and para to the "normal" type nitroxide function in the alkylaryl-substituted radicals observed in the condensation of nitroarenes with hydrocarbons containing labile hydrogen.

The nature of the "strong" species is not known. An acyl nitroxide having the linkage R-N(O·)-C(O)-R' is a likely candidate because of the small nitrogen splitting. However it is not possible to derive such a structure having six hydrogens from a simple coupling of two TNB-CHO molecules without invoking additional redox steps. (The structure 14, drawn above, does not account for the small magnitude of the nitrogen splitting, unless unpaired spin density is significantly transferred from the nitroxide to the carbonyl functions.)

In a replicate experiment (Expt 11.A.3) the TNB-CHO/benzene sample was heated initially at 200°C for 1 h without producing any free radicals. The temperature was then stepped to 254°C and a signal appeared after another half hour of heating. The "strong" spectrum appeared first, followed by gradual appearance of the "weak" spectrum. After about 1 h of heating at 253°C the intensity of the spectra diminished abruptly and the heating was interrupted while there was still evidence of radicals present. At room temperature the signal decayed quickly and there was none of the well-resolved species that was noted in the earlier experiment.

Much later in the program additional replicates were run. The TNB-CHO was passed through a chromatographic column to remove any impurities that may have been produced by photodecomposition during storage. In one run (Expt. 7.A.1) the quantity of TNB-CHO exceed solubility in benzene. When the sample was inserted into the 254°C cavity there was an immediate, strong free radical signal. But before a complete

spectrum could be recorded the sample detonated. The experimenter abandoned the laboratory until the benzene vapors had dissipated. When the apparatus was later dismantled it was noted that the force of the explosion had propelled the lower portion of the sample tube deep into the bottom of the dewar and there was much charred material in the tube and on the walls of the dewar. The structure 14 suggested above would require cleavage of an aryl-NO_2 bond which is consistent with the detonation behavior reported here. But the data are too sparse to permit any firm conclusions.

A smaller quantity of TNB-CHO was prepared in benzene, heated for several minutes and shaken to insure complete solution before proceeding with heating at 150°C (Expt. 11.A.4). These conditions produced spectra similar to 11.A.2 in that the pattern was consistent with $a_N \sim 0.6$, $a_{4H} \sim 0.223$, and $a_{2H} \sim 0.0475$ mT but the spectra were not so well-resolved as in the earlier experiment.

A mixture of TNB-CHO and HMB was heated at 138°C (Expt. 11.B.1) and produced a clean nitroxide spectrum consistent with "normal" coupling of the para nitro group with HMB to produce a benzylnitroxide radical. There is evidence in the wing branches of the spectrum for a small doublet splitting, ascribable to the aldehydic proton, Fig. 59.

The situation is far more complicated for reaction of TNB-CHO and TNT (Expts. 11.C.1, 236C and 11.C.2, 100°C). Most striking is the appearance of a transient species whose nitrogen splitting is suggestive of an iminoxyl radical, Fig. 60.

(Aromatic iminoxyls of the type 15

15
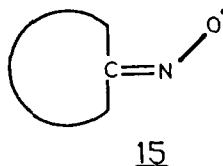
show little unpaired electron delocalization into the ring and have nitrogen splittings on the order of 2.8-3.0 mT [27].) There is another species with a span suggestive of a benzylnitroxide. Yet another set of strong lines is restricted to the central region of this complicated pattern and may indicate presence of another species, similar to the presumed diarylnitroxide observed in the 11.A.n experiments. By 100 s, little remained except the benzylnitroxide and a strong Tar signal.
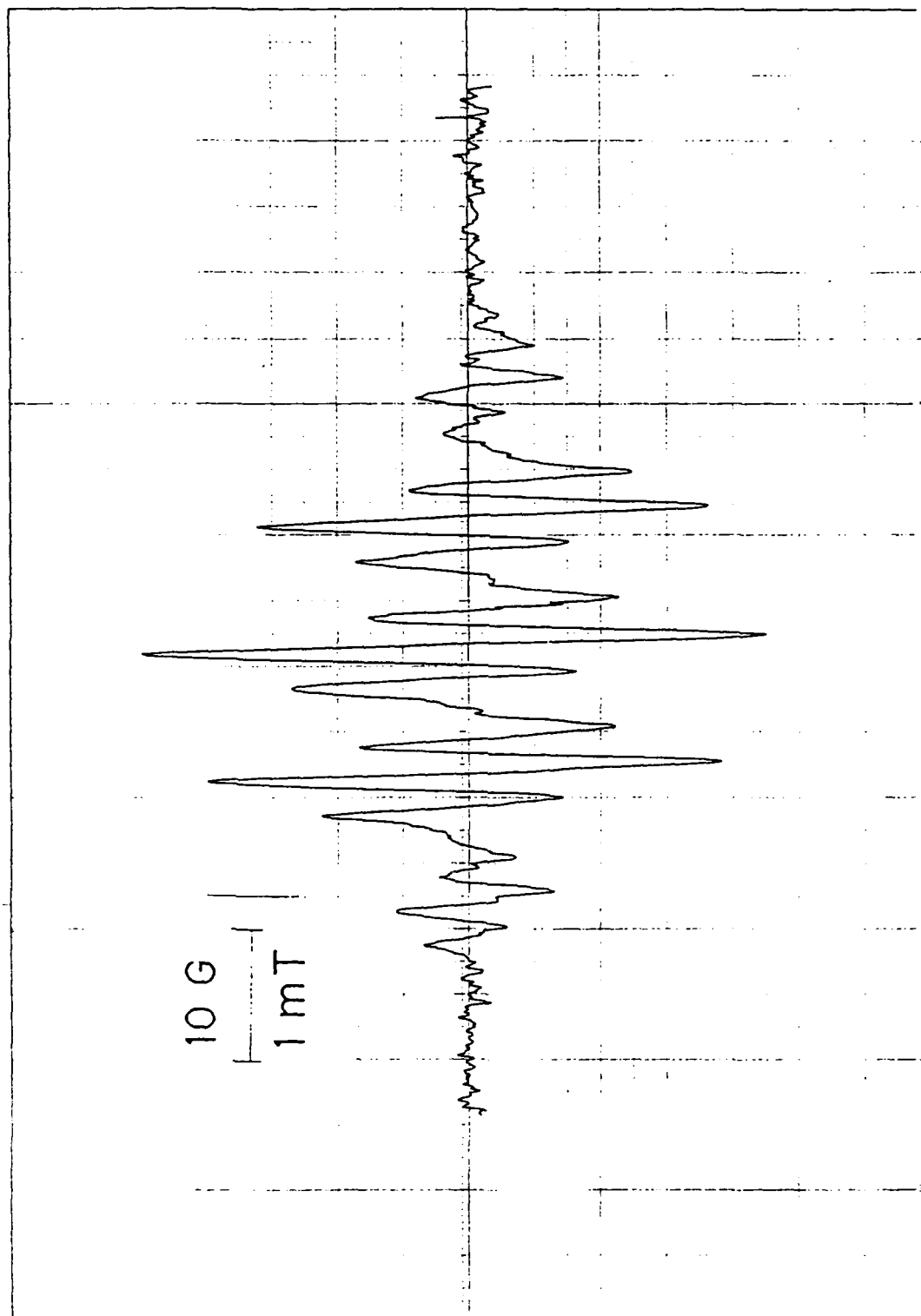
Fig. 59 ESR spectrum of radicals produced by reacting TNB-CHO and HMB at 138°C.
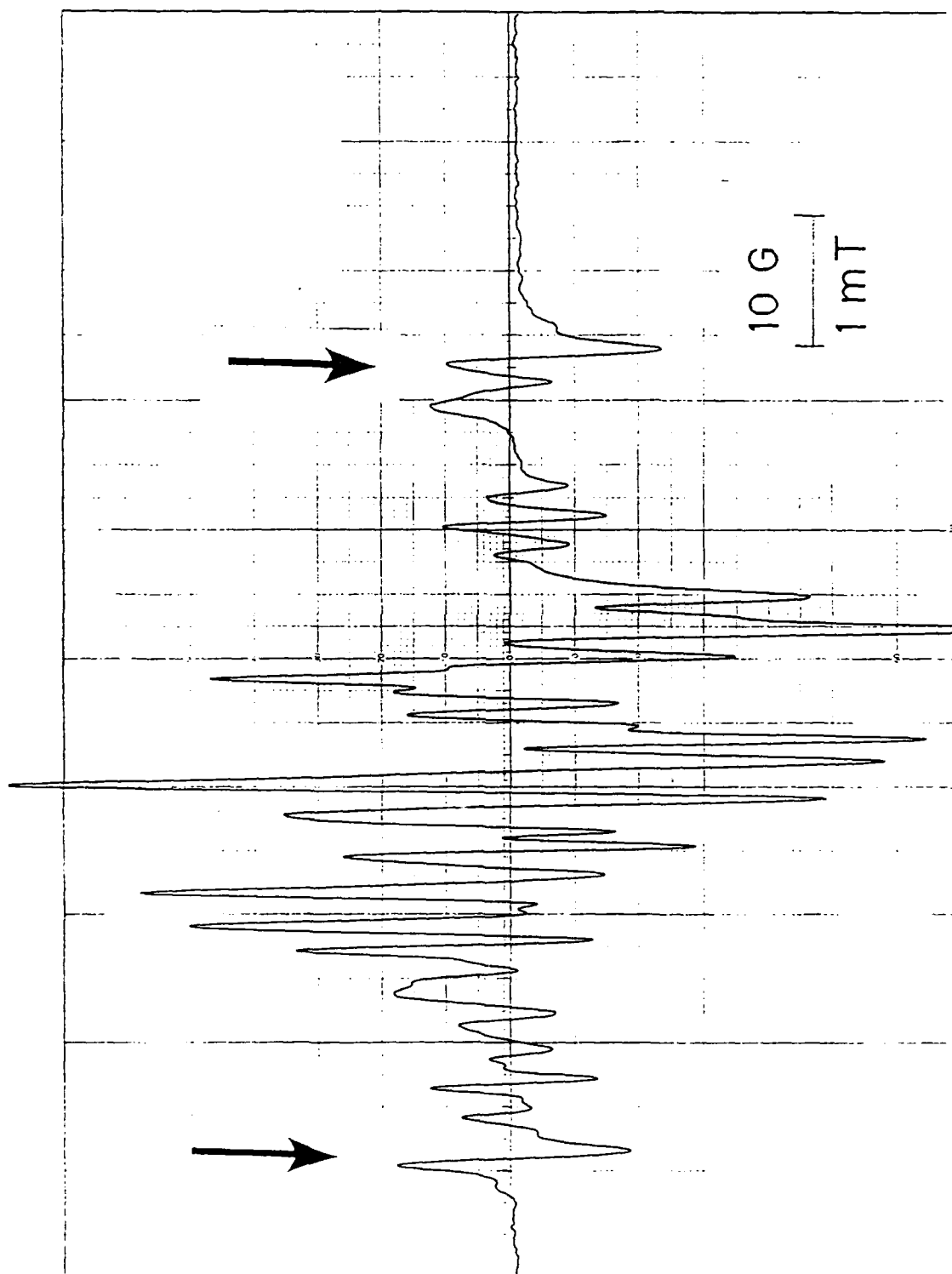
Fig. 60 ESR spectrum of radical species produced by reaction of TNB-CHO and TNT at 236°C. Arrows indicate lines presumed to arise from iminoxyl radicals.

The sample heated at 100°C did not produce any initial iminoxyl nor any terminal Tar. The complex pattern may be ascribed to benzylnitroxide and diarylnitroxide.

A sample of TNB-CHO in excess TNB was heated at 100°C (Expt. 11.D.1). A well-resolved, symmetric spectrum was observed early in the run, Fig. 61, but unfortunately the results are tainted by the fact that the TNB was freshly prepared material that had been stored only overnight under vacuum and still had a faint odor of residual acetic acid used in the recrystallization procedure. The spectrum is readily assigned on the basis of $a_N = 0.921$, $a_{2H} = 1.119$, and $a_{2H} = 0.295$ mT. The g-factor was 2.0048, closer to the values observed in TNT thermolosis than were the g-factors from reactions of TNB-CH$_2$OH.

Very late in the program, a sample of TNB was heated with intentionally added acetic acid to see if radicals could be observed. The resulting spectrum is shown in Fig. 62. The dominant species appears to have splittings due to 3 protons of $a_H = 0.26$ mT and a nitrogen of $a_N = 1.2$ mT but it is difficult to measure the values accurately because of interferences from another radical with a slightly different g-factor which confers overall asymmetry to the spectrum. The g-factor of the main species is approximately 2.0058. Although this data is consistent with a nitroxide derived from trinitrobenzene, there is no clear evidence on the basis of this spectrum as to the nature of the other nitroxide substituent.

A sample of neat TNB-CHO was heated at 140°C (Expt. 11.E.1) and underwent a complex set of spectral transformations. The early species produced an ill-resolved five-branch pattern which then evolved into a three-branch pattern.

3.   Reactions of 2,4,6-Trinitrobenzoic Acid (TNB-COOH)

A number of reactions between TNB-COOH and HMB were carried out. The initial product is consistent with condensation to form the nitroxide 16 followed by decarboxylation to yield nitroxide 7.
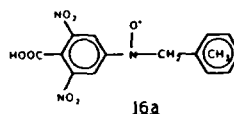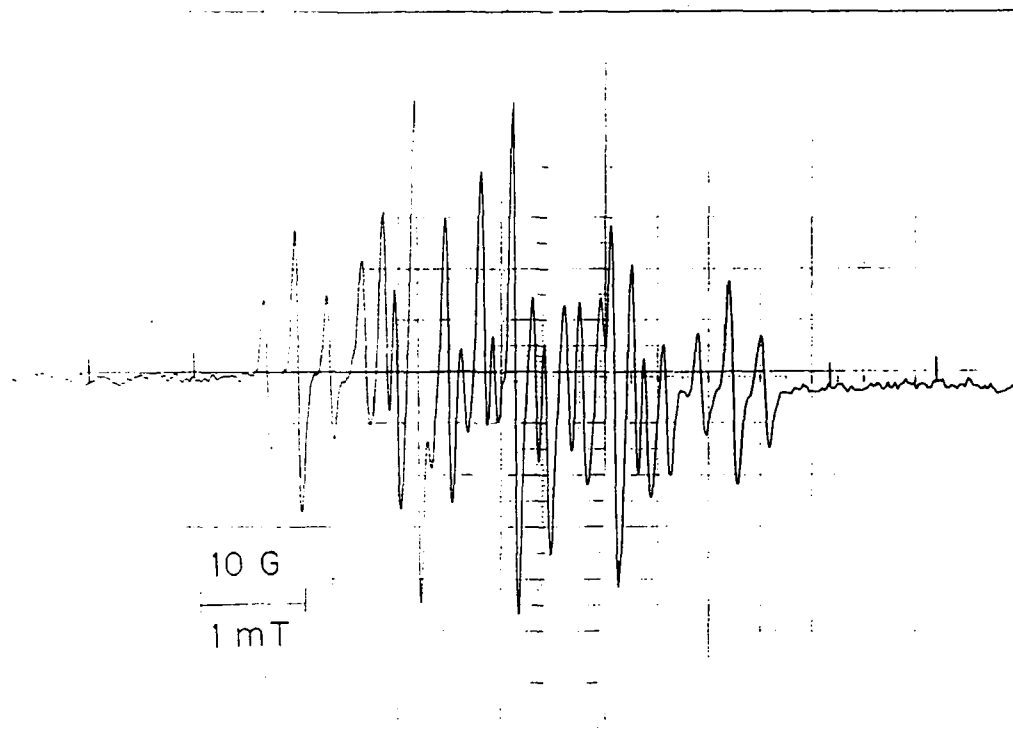
Fig. 61 ESR spectrum observed while heating TNB-CHO in excess TNB at 100°C.
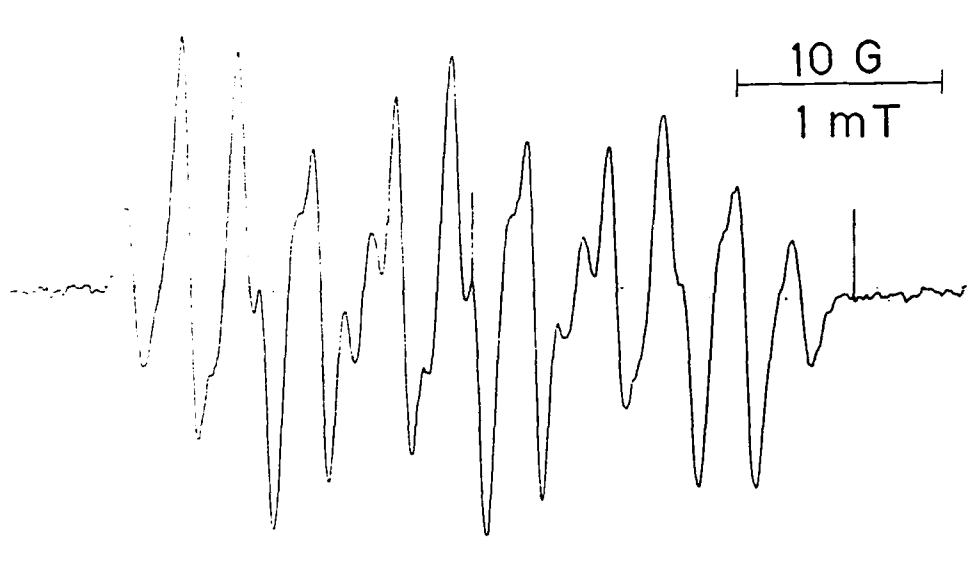
Fig. 62   ESR spectrum observed when TNB was heated with added acetic acid at 161°C.

Deuteration experiments were undertaken to demonstrate that the decarboxylation involves an intramolecular hydrogen transfer involving a cyclic transition state such as:
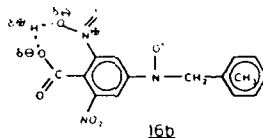
Unfortunately the results were equivocal and the cyclic transition state could not be comfirmed conclusively.

4.   Summary of Reactions of TNT Oxidation Products

Examination of Figs. 50-62 clearly shows that the molecules derived from oxidation of TNT are capable of participating in thermolysis reactions to produce a wide variety of free radical products. It is unfortunate that more time could not have been dedicated to assigning molecular structures to the species responsible for these spectra. However rewarding the results, this would nonetheless be an ambitious undertaking.

It is evident, on the basis of the g-factors reported here and in Appendix B that TNT, TNB-CH$_2$OH, and TNB-CHO react to produce distinctly different types of free radicals. It is conceivable, for instance, that the alcohol might undergo intramolecular condensation with a neighboring nitro group to form another ring; such a distinctly different structure might well explain the different g-factors. But it is useless to speculate on the basis of our limited information.

What is clear, however, is that some of the known, isolable products of TNT thermolysis are capable of producing such distinctly different free radical products. Since the route to the TNT oxidation products is so straightforward (Scheme 2) it is little wonder that that the thermolytic chemistry of TNT is so very complex. Seemingly inconsequential variations in reaction conditions or sample preparation can readily disturb the progression of an incredibly complicated set of interrelated reactions.

III. SUMMARY

2,4,6-Trinitrotoluene (TNT) undergoes thermal decomposition by a process that permits ESR observation of two distinctly different free radical species. Generally, the first spectrum increases to a steady state value and then ultimately decreeases. Meanwhile the second spectral component appears gradually, initially as an asymmetry in the first spectrum, and ultimately as the dominant spectral component.

The initial free radical has been ascribed to intermolecular condensation of two TNT moieties to produce a nitroxide with distinctive hyperfine structure. The hyperfine splittings arise from one nitrogen (a_N = 1.1 mT), two benzylic hydrogens (a_H = 1.1 mT) and the five hydrogens copmprising the methyl group and aromatic ring (a_H = 0.26 mT); the g-factor is 2.0058. The other species has a single featureless absorption line with a g-factor of 2.0035. It appears to arise from a polymeric material which we call "Tar."

Many other nitroxides are derived from intermolecular condensation of nitroarenes and hydrocarbons. The g-factors are similar to that of the nitroxide derived from TNT.

A new approach to analysis of the ESR spectrum of thermolysed TNT permits separation of the nitroxide and Tar contributions long before the Tar absorption becomes evident as a spectral asymmetry. This analysis reveals that Tar is produced at an accelerated rate early in the reaction, as compared to the autocatalytic (i.e., pseudo-first order with respect to Tar) rate observed later.

A series of reactions is proposed :
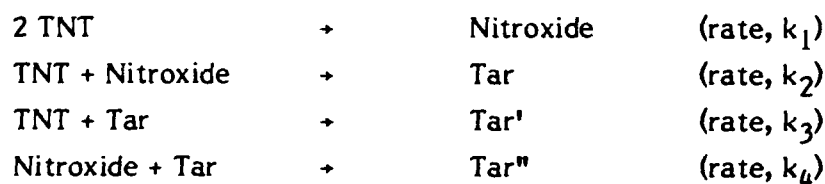
2 TNT	→	Nitroxide	(rate, k_1)
TNT + Nitroxide	→	Tar	(rate, k_2)
TNT + Tar	→	Tar'	(rate, k_3)
Nitroxide + Tar	→	Tar"	(rate, k_4)

Numerical simulations based on rate expressions for this set of simultaneous processes yield concentration-time curves with the same characteristics as the experimental curves. In the simulations Tar appears to form at an accelerated rate early in the

process, in agreement with experiment. Consequently, experiments and simulations share the property that the linear portions of the log[Tar] vs time plots extrapolate back to a Tar concentration greater than zero at the start of the process.

Experimentally, the nitroxide concentration is never very large and behaves as if nitroxide is present as a reactive intermediate. It is possible for nitroxides to disproportionate to produce a nitrone and a hydroxylamine. The nitrone is a likely candidate for an intermediate in the formation of Tar. while the hydroxylamine can readily cycle back to a nitroxide. This chemistry is consistent with the experimental behavior of the nitroxide concentration as monitored by ESR.

It was demonstrated that the nitroxide formed by TNT thermolysis can be observed in benzene or toluene extracts at room temperature. The material undergoes slow decomposition. Different radicals with hyperfine splittings are distinguished by different g-factors that are close to those observed for nitroxide and Tar in molten TNT.

The presence of moisture in TNT promotes high nitroxide concentrations under relatively mild thermolysis conditions. It is not clear whether water enhances nitroxide production or inhibits nitroxide destruction. Moisture has a negligible effect on the development of Tar.

Since the nitroxide formed in TNT thermolysis results from intermolecular condensation of the methyl group of one molecule with a nitro group of another, considerable effort was expended to find model systems to provide additional insights into this process.

Hexamethylbenzene (HMB) and TNT react to form mixtures of spectrally simi-lar nitroxide radicals. This greatly complicates the extraction of kinetic information from the experimental data. The shapes of the kinetic curves are quite different from those for TNT alone. But the curves for TNT/HMB can be simulated on the basis of a set intermolecular condensation reactions analogous to that used for TNT simulations and the results accord with the experimental curves.

Hexamethylbenzene and 2,4,6-trinitrobenzene (TNB) should provide a clean model system for the TNT reaction. However many different nitroxide-like radicals are observed. The proportions depend on reactant ratios as well as temperature of

formation. The effect of charge transfer intermediates is considered to be an important route to formation of secondary nitroxides in systems containing HMB.

Almost any material added to TNT affects the course of thermal decomposition. This fact exacerbates the problem of kinetic and mechanistic studies of TNT thermolysis because seemingly inconsequential changes in experimental conditions such as trace moisture may have a significant impact on experimental reproducibility. A number of different materials were intentionally added in efforts to learn more about the nature and process of Tar production.

TNT can undergo several well-characterized reactions that are initiated by nuceophiles. Meisenheimer complexes are covalently bonded additives of the nucleophile to a carbon atom of the TNT aromatic ring. In addition, the methyl group of TNT can undergo acidic dissociation; the resulting conjugate base can behave as a Meisenheimer nucleophile and bond to a ring carbon of another undissociated TNT molecule to produce a compound known as a Janovsky complex. Consequently, bases have a profound effect on TNT decomposition. Tar formation is enhanced but the nature of the Tar, as reflected by the g-factor, depends on the individual nucleophile.

Acids on the other hand appear to retard radical and Tar formation. The effect is most pronounced with phosphoric acid. This may warrant further investigations as a means for desensitizing TNT and extending its storage life.

Oxidants, reductants, and spin traps were also studied.

Some of the known products of TNT oxidation were added to TNT and also studied in other mixtures. These included trinitrobenzyl alcohol, trinitrobenzaldehyde, and trinitrobenzoic acid. As expected, these materials complicated the appearance of spectra observed in the course of reactions with TNT, TNB, or HMB.

Benzene solutions of the alcohol and the aldehyde yielded ESR spectra with remarkably rich and symmetric hyperfine structure. The spectra are probably from nitroxide species, but the radicals produced from the alcohol in benzene have an unusual g-factor of about 2.0040 which is significantly lower than for the nitroxides resulting from TNT thermolysis. When a sample of the neat alcohol was heated, a different radical species was observed and its g-factor of 2.006 was closer to the usual nitroxide

value. This may be a means for distinguishing radicals produced from intermolecular versus intramolecular condensations.

Radicals resulting from thermal reaction of benzene solutions of the aldehyde exhibited remarkably sharp lines and resolution. As in the case of spectra from the alcohol-derived radicals, it was possible to assign the ESR spectra in terms of number and kinds of nuclei. However the actual molecular structures responsible for these spectra remain speculative.

Nitroxide radicals produced from condensation of trinitrobenzoic acid and HMB were observed to undergo decarboxylation at the elevated temperatures of the reaction conditions.

IV. REFERENCES

1. E.G. Janzen, J. Amer. Chem. Soc. 87, 3531 (1965).

2. R.M. Guidry and L.P. Davis, Thermochem. Acta 32, 1 (1979).

3. L.P. Davis, A.G. Turner, W.R. Carper, J.S. Wilkes, R.C. Dorey, H.L. Pugh, and K.E. Siegenthaler, "Thermochemical Decomposition of TNT: Radical Identification and Theoretical Studies," Report No. FJSRL-TR-0002, April 1981, NTIS ADA 099044.

4. T.M. McKinney, L.F. Warren, I.B. Goldberg, and J.T. Swanson, J. Phys. Chem. 90, 1008 (1986).

5. (a) T. Nishikawa and K. Someno, Bull. Chem. Soc. Jpn., 47, 2881 (1974); (b) P.H.H. Fischer and F.A. Neugebauer, Z. Naturforsch. A, 19, 1514 (1964); (c) F.A. Neugebauer and P.H.H. Fischer, Z. Naturforsch. B, 21, 1036 (1966)

6. A.R. Forrester in Landolt-Bornstein, Zahlenwerte u. Funkt. Naturwiss u. Technik., Neue Ser., Gr. II, 9c1, 1979, 193.

7. W.P. Colman and F.P. Rausch, DTIC Contract No. DAAA21-70-0531, February 1971.

8. J.C. Dacons, H.G. Adolph and M.J. Kamlet, J. Phys. Chem. 74 3035 (1970).

9. R.N. Rogers, Anal. Chem. 39, 730 (1967).

10. A.R. Forrester, J.M. Hay and R.H. Thomson, Organic Chemistry of Stable Free Radicals, Academic Press, New York, 1968, Chapter 5.

11. J.W. Linnett, H. Am. Chem. Soc. 83, 2643 (1961).

12. J.W. Linnett, The Electronic Structure of Molecules, Methuen, London, 1964.

13. J.C. Baird and J.R. Thomas, J. Chem. Phys. 35, 1507 (1961).

14. G. Chapelet-Letourneaux, H. Lemaire, and A. Rassat, Bull. Chim. France, 3283 (1965).

15. D.F. Bowman, T. Gillan, and K.U. Ingold, J. Am. Chem. Soc. 93, 6555 (1971).

16. D.J. Cowley and W.A. Waters, J. Chem. Soc. B 60 (1970).

17. Landolt-Boernstein, Zahlenwerte u. Funkt. Naturwiss. u. Technik., Neue Ser., Gr. II, 13c, 1988, p. 170.

18. E.S. Huyser, Free-Radical Chain Reactions, Wiley-Interscience, New York, 1970, Chapter 12.

19.   R. Meyer, Explosives, 2nd Edition, Verlag Chemie, Deerfield Beach. Florida, 1981, 358.

20.   E. Buncel, "The role of Meisenheimer or (sigma)-complexes in nitroarene-base interactions", in The Chemistry of Functional Groups, Supplement F, The Chemistry of Amino, Nitroso, and Nitro Compounds and Their Derivatives, Saul Patai, Ed., John Wiley, New York, 1982, p 1225.

21.   M.R. Crampton, :"Meisenheimer Complexes," Adv. Phys. Org. Chem., 7, 211 (1969).

22.   C.F. Bernasconi, J. Org. Chem., 36, 1671, (1971).

23.   C.A. Fyfe, C.D. Malkiewich, S.W.H. Damji, and A.R., Norris, J. Amer. Chem. Soc., 98, 6983, (1976).

24.   J.T. Swanson, S.R. Bosco, C.Y. Kruit, R.D Murphy, and W.R. Carper. "An EPR Study of the Thermal Decomposition of TNT/HMB Mixtures." F.J. Seiler Research Laboratory, Technical Report-85-0004, August 1985

25.   T.M. McKinney and I.B. Goldberg, unpublished results.

26.   J.T. Edwards, J. Chem. Ed., 64, 599 (1987).

27.   F.A. Neugebauer, in Landolt-Bornstein, Zahlenwerte u. Funkt., Naturwiss. u. Technik., Neue Ser., Gr. II, 9c1, 1979 ,5 (specifically, section 5.12.1.3).

V. APPENDICES

- Appendix A. Log of reactions studied in this program.

Table 1, in the main body of this Report, is a convenient guide to the different classes of experiments that were performed during this program. The more complete listing of experiments in Appendix A provides a better summary of the individual experimental conditions.

- Appendix B. Summary of some important reactions studied during this program as well as additional reactions studied independently.

Experiments with code designations that refer to Appendix A were carried out in this program. Experiments without such designations were carried out under Independent Research and Development programs. The consolidation of these results is potentially useful for correlating conditions that do and do not lead to Tar formation. Comparison of the tabulated g-factors for the various radicals may also be useful in forming a better assessment of the nature of Tar radicals.

Appendix A. Log of reactions performed.

CATEGORY	MATERIALS	EXPT. CODE	TEMPERATURE
CLASS 1	A: Neat TNT(old)	1.A.0	163
		1.A.1	228
		1.A.2	253
		1.A.3	242
		1.A.4	246
		1.A.5	243
		1.A.6	225
		1.A.7	224
		1.A.8	234
		1.A.9	240
		1.A.10	253
		1.A.11	240
		1.A.12	230
		1.A.13	100
	B: Neat TNT(new, recrystallized)		
		1.B.1	240
		1.B.2	240
		1.B.3	216
		1.B.4	210
		1.B.5	258
		1.B.6	244
		1.B.7	242
		1.B.8	261
		1.B.9	232
		1.B.10	220
		1.B.11	204
		1.B.12	227
		1.B.13	242

Appendix A. Log of reactions performed.

CATEGORY	MATERIALS	EXPT. CODE	TEMPERATURE
CLASS 2	A: TNT/H20 (old)	2.A.1	161
		2.A.2	152
		2.A.3	170
		2.A.4	156.5
		2.A.5	228
		2.A.6	261
		2.A.7	249
		2.A.8	243
		2.A.9	222
	B: TNT/H20(new)	2.B.1	241
		2.B.2	240
		2.B.3	218
		2.B.4	(~261)
		2.B.5	262
		2.B.6	233
		2.B.7	221
		2.B.8	222
		2.B.9	245

Appendix A. Log of reactions performed.

CATEGORY CLASS 3	MATERIALS TNT/HMB	EXPT. CODE	TEMPERATURE
	A: 5%TNT	3.A.1	238
		3.A.2	227
		3.A.3	174
		3.A.4	208
	B: 10%TNT	3.B.1	163
			240
		3.B.2	140
		3.B.3	240
		3.B.4	250
		3.B.5	230
		3.B.6	220
		3.B.7	199
	C: 10%TNT+H20	3.C.1	220
		3.C.2	251
	D: 20%TNT	3.D.1	240
		3.D.2	233
		3.D.3	220
		3.D.4	211.5
		3.D.5	175
	E: 50%TNT	3.E.1	176
		3.E.2	223
		3.E.3	234
		3.E.4	218
	F: TNT/HMB-d18	3.F.1	167
			190
		3.F.2	210

Appendix A.   Log of reactions performed.

CATEGORY CLASS 4	MATERIALS TNB/HMB	EXPT. CODE	TEMPERATURE
	A: 5%TNB	4.A.1	175 244
		4.A.2	170 203
		4.A.3	220
	B: 95%TNB	4.B.1	220
	C: 40% TNB	4.C.1 4.C.2 4.C.3	223 180
	D: 40% TNB/80 % HMB-d18	4.D.1	220, 200, 180, 160, 120

Appendix A.   Log of reactions performed.

CATEGORY	MATERIALS	EXPT. CODE	TEMPERATURE
CLASS 5	A: MISCELLANEOUS ADDITIVES		
	Coke residue	5.A.1	258
	Practical grade	5.A.2	239
	Benzene insol. res.	5.A.3	164
	Benzene insol. res.	5.A.4	240
	m-Terphenyl	5.A.5	170
			237
	CuSO4.5H2O	5.A.6	181
	B: TNT/"SOLVENTS"		
	Acetone	5.B.1	180
	Ethanol	5.B.2	181
	m-Terphenyl	5.B.3	164
	neat	5.B.4(1.A.0)	163
	Tetrahydrofuran	5.B.5	163
	Acetonitrile	5.B.6	163
	Boric acid	5.B.7	162
	Boric acid	5.B.8	253
	Benzene		150
	Benzene	(14.A.1)	253
	C: TNT/REDUCTANTS, NUCEOPHILES, BASES		
	NaCl	5.C.1	258
	Oxalic acid	5.C.2	242
	NaCl	5.C.3	240
	Sodium dithionite	5.C.4	240
	Calcium hydrozide	5.C.5	232
	Sodium borohydride	5.C.6	232
	Sodium borohydride	5.C.7	100
	Sodium sulfide	5.C.8a	100
	Sodium sulfide	5.C.8b	unheated
	Calcuim hydride	5.C.9	unheated
	Calcuim hydride	5.C.10	100
	Calcium hydroxide	5.C.11	100
	SEE ALSO:		
	PBN/dithionite	8.A.3	96
	PBN/dithionite	8.A.4	103
	PBN/dithionite	8.C.2	103

Appendix A. Log of reactions performed.

CATEGORY	MATERIALS	EXPT. CODE	TEMPERATURE
CLASS 5	D: MINERAL ACIDS		
	Hydrochloric	5.D.1	240
	Hydrochloric	5.D.2	249
	Hydrochloric	5.D.3	245
	Nitric	5.D.4	245
	Nitric	5.D.5	245
	Nitric (conc.)	5.D.6	245
	Sulfuric (conc.)	5.D.7	245
	Sulfuric	5.D.8	245
	Phosphoric	5.D.9	245
	Phosphoric	5.D.10	245

Appendix A.   Log of reactions performed.

CATEGORY	MATERIALS	EXPT. CODE	TEMPERATURE
CLASS 6	Systems with 4,6-Dinitroanthranil		

A: NEAT

		EXPT. CODE	TEMPERATURE
		6.A.1	245
		6.A.2	R. T.

B: BENZENE SOLUTION

		EXPT. CODE	TEMPERATURE
		6.B.1	250
		6.B.2	248
		6.B.3	250

C: TRINITROBENZENE SOLUTION (20% DNAnth)

		EXPT. CODE	TEMPERATURE
		6.C.1	252
		6.C.2.	230
		6.C.3	230
		6.C.4	230
		6.C.5	230

D: TNT/DNAnth   (20% DNAnth)

		EXPT. CODE	TEMPERATURE
		6.D.1	252
		6.D.2	
		6.D.3	220
		6.D.4	230
		6.D.5	240
		6.D.6	211

E: TNT/DNAnth   (50% DNAnth)

		EXPT. CODE	TEMPERATURE
		6.E.1	222
		6.E.2	230
		6.E.3	240
		6.E.4	250
		6.E.5	200
		6.E.6	211

F: TNT/DNAnth   (10% DNAnth)

		EXPT. CODE	TEMPERATURE
		6.F.1	220
		6.F.2	231
		6.F.3	241

G: HMB/DNAnth (10% DNAnth)

		EXPT. CODE	TEMPERATURE
		6.G.1	172

Appendix A. Log of reactions performed.

CATEGORY	MATERIALS	EXPT. CODE	TEMPERATURE
CLASS 7	DETONATION MIXTURES		
	A: TNB-CHO/ Benzene	7.A.1	250
	B: TNT/DNAnth/ Benzene	7.B.1	250
	C: TNB-CH2OH/ Benzene	7.C.1	240
CLASS 8	PHENYL t-BUTYL NITRONE (PBN)		
	A: TNT		
		8.A.1	92
		8.A.2	90
		8.A.3	96
		8.A.4	103
	B: m-Terphenyl		
		8.B.1	90
	C: TNB		
		8.C.1	102
		8.C.2	103
CLASS 9	TNB reactions		
	A: neat		
		9.A.1	172
	B: TNB/Ca(OH)2		
		9.B.1	172
		9.B.2	244
		9.B.3	168
		9.B.4	166
		9.B.5	166
	C: TNB/DITHIONITE		
		9.C.1	236

Appendix A.   Log of reactions performed.

CATEGORY	MATERIALS	EXPT. CODE	TEMPERATURE
CLASS 10	TNB-CH2OH REACTIONS		
	A: IN BENZENE		
		10.A.1	100
		10.A.2	150
		10.A.3	(R.T.)
	B: WITH HMB		
		10.B.1	198
		10.B.2	150
	C: WITH TNT		
		10.C.1	100
CLASS 11	TNB-CHO REACTIONS		
	A: IN BENZENE		
		11.A.1	
		11.A.2	199
		11.A.3	253
		11.A.4	
	B: WITH HMB		
		11.B.1	138
	C: WITH TNT		
		11.C.1	226
		11.C.2	100
	D: WITH TNB		
		11.D.1	99
	E: NEAT		
		11.E.1	137

Appendix A.   Log of reactions performed.

CATEGORY	MATERIALS	EXPT. CODE	TEMPERATURE
CLASS 12	MISC. HMB REACTIONS		
	A: HNO3		
		12.A.1	190
		12.A.2	190
CLASS 13	ACCIDENTAL TOLUENE SOLVENT		
		13.A.1 TNB-CHO	
			204
		13.B.1 TNT	
			249
CLASS 14	TNT IN BENZENE		
		14.A.1	253

Product A   R.T.

Appendix B.   Correlation of reaction conditions and presence or absence of Tar.

	A	B	C	D	E	F
1	Mixture		hfsc's	g Radical	g Tar	COMMENTS
2						
3	CONDITIONS WHERE TAR WAS OBSERVED. (Compare with Line 392ff.)					
4						
5	TNT/HMB-d18					Little sign of Tar until T was raised to ~250; then, quick conversion
6						
7		Temp	200-250			
8		Time 4300s				
9						
10	TNT/TNT/HMB-d18					Dropping T made Tar line very evident @2260 s; less so @ 198/3300s
11						
12		Temp	235-90-235			
13		Time				
14						
15	NB-d5/Cyclohex					Some initial asymmetry; then something like a Tar line appeared
16						
17		Temp	250			
18		Time 3220s				
19						
20	NB-d5/Tetralin					Evolving species ratios; not quite sure if Tar is present. Not really sure about purity of starting tetralin.
21						
22		Temp	203-70-250			
23		Time 7350s				
24						
25	NB-d5/Decalin					Clearly two different g-values (dB= 1.7G); not sure if Tar contributes to spectral asymmetry
26						
27		Temp	200			
28		Time 2660s				
29						
30	TNT/K'guhr-d?					Complete conversion to Tar.
31						
32		Temp	240			
33		Time 1800s				
34						

Appendix B. Correlation of reaction conditions and presence or absence of Tar.

	A	B	C	D	E	F
1	Mixture		hfsc's	g Radical	g Tar	COMMENTS
35	2,6-DNT/HMB-d18					Standard "weird" 4-branch pattern; hi-field most intense initially
36						Line #3 got relatively much stronger, but g-value is too high for Tar
37	Temp	248				
38	Time 6400s					
39						
40	TNT/K'guhr-d?					Little Tar early in run; then exponential growth as
41						nitroxide diminished.
42	Temp	200-RT-200				
43	Time 5600s					
44						
45	NB-d5/Decalin-d18					Multiple species, changing ratios; different g's and aN's
46						Tar-like line became obvious at the end, particularly in
47	Temp					2nd derivative.
48	Time					
49						
50						
51	NB-d5/Tetralin-d12					Very revealing transformations: Initially just 3 lines
52			aN			Then another species (2≠ N's)grew at lower g-value: aN=4.7&6.0
53	Temp	200	0.47			Tar-like absorption grew into the middle of this pattern
54	Time 7400s		0.6			This data may be quite significant.
55						Field center values differ by ~4.5G (no NMR markers)
56						
57	NB-d5/Toluene-d8					Ill-defined spectrum--Too many lines that can't be explained by
58						a deuterium splitting (far too large magnitude)
59	Temp	250				Tar-like line evident by 600 sec.
60	Time 2700s					
61						
62	NB-d5/HMB-d18					Nice deuterium splitting, correct magnitude.
63						Tar evident on first scan; sort of grew to a constant level and stayed
64	Temp	200				
65	Time 8450s					
66						

Appendix B. Correlation of reaction conditions and presence or absence of Tar.

	A	B	C	D	E	F
1	Mixture		hfsc's	g Radical	g Tar	COMMENTS
67	"d3"-TNT/K'guhr					Extra species; rapid Tar conversion.
68						
69	Temp	200				
70	Time					
71						
72	2-NT/o-Xylene					Ill-resolved spectra; weak
73						Some asymmetry that may possibly arise from Tar, but not sure.
74	Temp	200-250				
75	Time	14850s				
76						
77	2-NT/m-Xylene					Ill-resolved spectra; weak
78						Some asymmetry that may possibly arise from Tar, but not sure.
79	Temp	243				
80	Time	4650s				
81	2,6-DNT/o-Xylene					"Normal" weird 4-branch pattern
82						Line #3 grew exhorbitantly, Tar-like, but wrong g-value.
83	Temp	253				
84	Time	4400s				
85						
86						Unusual nitroxide spectra: line "7" was unusually intense early-on.
87	TNT/TNB					Extra species present in the early spectra.
88						Toward the end of the run, line"8" started to look like a Tar line.
89	Temp	221				
90	Time	9450s				
91						
92	TNT/xsTNB					Tar present from 200 sec.
93						Became more evident at lower temperatures.
94	Temp	222 & lower				
95	Time	5700				
96						
97	2-NT/THQuinoline					Usual "weird" 4-branch pattern
98						Lots of HFS, but Tar evident by 850s.
99	Temp	250				
100	Time	2180s				

Appendix B. Correlation of reaction conditions and presence or absence of Tar.

	A	B	C	D	E	F
1	Mixture		hfsc's	g Radical	g Tar	COMMENTS
101	NB-d5/Cyclohex-d12					
102						Nitrogen triplet plus two transient satellites; the one at low field
103			aN	2° corr.		disappeared quickly while the one at higher field took on
104	Temp	251				characteristics of Tar.
105	Time 4100s					
106						
107	NB-d5/Cyclohex-d12					
108			aN	2° corr.		Similar evolution, but experiment was interrupted
109	Temp	250	1.121	2.0058	2.0032	before Tar line got very intense.
110	Time 1150s			2.0058	2.0032	
111						
112	NB-d5/Cyclohex					Messy, multiple species, plus Tar growth.
113						
114	Temp	254				
115	Time 4200s					
116						
117	NB-d5/Cyclohex-d12					Nitrogen triplet plus two transient satellites; the one at low field
118			aN	2° corr.		disappeared quickly while the one at higher field first decreased,
119	Temp	251	1.12	2.0059	2.0033	then took on characteristics of Tar.
120	Time 3100s			2.0059	2.0033	
121						
122	NB-d5/Cyclohex-d12					Decent kinetic data on Tar growth.
123						
124	Temp					
125	Time 14700s					
126						
127	TNB/Anthracene					Early TNB-nitroxide plus another species which was centered
128				uncorr.		at the Tar g-value, but had 1:2:1-structure
129	Temp	201		2.0059	2.0034	Is this Tar related or not?
130	Time 11280s			2.0061	2.0034	Additional, symmetric fine structure appeared toward end of run.
131						

Appendix B.   Correlation of reaction conditions and presence or absence of Tar.

	A	B	C	D	E	F
1	Mixture		hfsc's	g Radical	g Tar	COMMENTS
132	TNB/Anthracene					Unheated sample showed charge transfer color and also exhibited
133						a wide ESR absorption.
134	Temp	RT				Line broadened when temperature was increased and the normal
135	Time					spectrum appeared.
136						
137	TNB-COOH/TNT					Weak absorption at Tar g-value at 200; no other structure
138						At 240, got iminoxyl-type spectrum plus nitroxide and Tar
139	Temp	242				
140	Time 4000s					
141						
142	TNB-COOH/HMB					Decarboxylation transformations.
143						Tar evident in final scans (Line C- Line B evaluation).
144	Temp	200				
145	Time 2300s					
146						
147	TNB-COOH/PhCl6				2.0035	Looks like only Tar material was observed
148						(Purified hexachlorobenzene.)
149	Temp	236				
150	Time 3050s					
151						
152	TNB-COOH/PhCl6/TNT				2.0034	Looks like only Tar material was observed.
153						
154	Temp	239				
155	Time 500s					
156						
157	TNT-d5/K'guhr				2.0037	Initial 3-line nitroxide; normal aN ~ 10 G
158					2.0036	Rapid appearance of Tar.
159	Temp	242				
160	Time 1050s					
161						
162	TNB-CHO/TNT		2 Iminoxyls			Iminoxyls plus nitroxide at 195; both got stronger at 235.
163			aN			Iminoxyls were quite long-lived.
164	Temp	195-23	2.931	2.0041		Tar quite evident at end.
165	Time 1750s		3.03	2.0035	2.0032	

Appendix B. Correlation of reaction conditions and presence or absence of Tar.

#	A	B	C	D	E	F
1	Mixture		hfsc's	g Radical	g Tar	COMMENTS
166						
167	TNB-CHO/TNB		Iminoxyls			Weak spectra at 150; nitroxide plus 3 or 4 iminoxyls at 196.
168			aN			Iminoxyls were quite long-lived and underwent complex evolution.
169	Temp 150-200		3.26	2.0035		Impossible to be certain which iminoxyl wing lines are paired
170	Time 6650s		3.03	2.0034	2.0036	so iminoxyl splitting values are not firm. Raised T to 236;
171						iminoxyls decayed quickly and Tar-like system remained.
172						
173	TNB-COOH/TNT					Messy spectra early, at lower temperatures; nitroxide became better
174						defined as temp. was raised, but Tar also became more evident.
175	Temp 200-250					
176	Time 3785s					
177						
178	TNB-COOH/TNB					Did not expect this experiment to yield radicals!
179						Observed messy, asymmetric spectra with strong evidence of Tar.
180	Temp 250					
181	Time 1040s					
182						
183	HPic/m-Ph3				2.0035	Tar-like behavior from the start, but also satellite lines
184						
185	Temp 240					
186	Time 1830s					
187						
188	neat HPic		Iminoxyl			Short-lived iminoxyl; replaced quickly by Tar.
189			uncorr			
190	Temp 240		2.0043		2.0036	
191	Time					
192						
193	HPic/TNB-COOH		Iminoxyl			Weak signal at 200; strong iminoxyl at 242
194						Decayed somewhat and then stabilized
195	Temp 200-243-279		uncorr 2.0041			Kicked T 'way up and iminoxyl converted to Tar.
196	Time 4130s					
197						

Appendix B. Correlation of reaction conditions and presence or absence of Tar.

	A	B	C	D	E	F
1	Mixture		hfsc's	g Radical	g Tar	COMMENTS
198	neat TNB-CHO		Nitrox midpoint	uncorr		Multiple iminoxyl species plus nitroxide
199				2.0054	2.0039	Tar-like structure toward end of run.
200	Temp	200				
201	Time 1730s					
202						
203	TNB-CHO/TNT		Iminoxyl			Iminoxyl plus nitroxide plus Tar
204			3.06			
205	Temp	202				
206	Time 1180s					
207						
208	TNB-CHO/TNT					Quite transient iminoxyl plus nitroxide and Tar
209						
210	Temp	236				
211	Time 565s					
212						
213	neat TNB-COOH					Transient iminoxyl plus messy nitroxide plus Tar
214						
215	Temp	242				
216	Time 1250s					
217						
218	neat TNT-d5		Nitrox 2°corr			3-branch pattern, aN=8.4; unequal intensities (weak low-field line).
219			0.793	2.0037	2.0035	Multiple species suggested. With time, center line got relatively more intense, but not at all sure if it is due to Tar. Does not look like TNT-nitroxide! g-Factor is too low.
220	Temp	240				
221	Time 5400s					
222				uncorr		
223	2-NT/HMB			2.0059		5-branch pattern plus other species; eventually kicked over to Tar.
224				secondary		
225	Temp	240		radical	Tar	
226	Time 18050s			2.0037	2.0031	
227					2.003	
228						
229						

Appendix B. Correlation of reaction conditions and presence or absence of Tar.

	A	B	C	D	E	F
1	Mixture		hfsc's aN aCH2	g Radical	g Tar	COMMENTS
230	NB-d5/HMB					"Textbook" 1:3:4:3:1 pattern that lasted quite well
231						After T was increased to 250, started getting Tar.
232	Temp 195-177-252		1.101	2.0056		Line separations not exactly equal, but cannot justify by
233	Time 11700s		1.106	2.0055	2.0026	saying aN ≠ aCH2. May be observing some T-effect on g,
234				2.0057	2.003	but not at all sure.
235			1.103	2.0057	2.003	
236						
237	NB/Cyclohex-d12		1.102	2.0057	2.0031	Tar evident in 2nd derivative at 2450 sec.
238						
239	Temp	250				
240	Time 4200s					
241						
242	TNT/FEFO		2 Iminoxyls			Iminoxyl-type radicals; then Tar-like behavior.
243			2.932			
244	Temp	140	3.057	2.0035	2.0037	
245	Time 10200s					
246						
247	FEFO/HMB					Iminoxyl? plus Tar.
248					2.0033	
249	Temp	165			2.0034	
250	Time	2880				
251						
252	FEFO/HMB		0.776	2.0069	2.0031	Evaporated CH2Cl2 before starting. Good 1:3:4:3:1 pattern at 165
253						At 202, Tar started forming.
254	Temp	165				
255	Time 5640s					
256						
257	FEFO/HMB-d18					No D splittings resolved. Tar-like line dominated hi-field nitrogen lin
258			0.743	2.0067	2.0026	late in run.
259	Temp	164			2.0033	Note consistently high g-values with FEFO: fluorine effect?
260	Time 5345s					
261						
262						

Appendix B. Correlation of reaction conditions and presence or absence of Tar.

	A	B	C	D	E	F
			hfsc's	g Radical	g Tar	COMMENTS
263	FEFO/TNB					Iminoxyl, followed by Tar plus 8G satellites.
264			Iminoxyl			Seen also in methyl-oxidized systems
265	Temp	164-2	3.044	~2.0038		
266	Time 13730s				2.0037	
267						Hfs radical+Tar+nitrone product: Difficult to judge Tar position
268	TNB/PBN		aN			amongst all the other structure. If Tar was indeed present,
269	(8.C.2)		1.447	2.0057	2.0052	it was a broad envelope underlying the center of the
270	Temp	103		2.0058	2.0052	nitrone-nitroxide spectrum and g-value is unusually high.
271	Time 5100s			2.0058	2.0052	
272						Initially observed radical with hfs. But
273	TNT/BH4-					within 250 sec, Tar was dominant species.
274	Page (5.C.6)				2.0038	
275	Temp	232			2.0035	
276	Time 479s					
277						No radical hfs observed; only Tar seen from
278	TNT/BH4-					earliest spectrum at 43 sec.
279	(5.C.6)				2.0053	This radical is quite different from "normal" tar; unusually high g-
280	Temp	100			2.005	
281	Time 850s					
282						
283	TNT/NA2S.9H2O				2.0062	Additional anisotropic components present (total number >3).
284	(5.C.8)				2.006	Radical present in unheated mixture
285	Temp	25				Unusually high g-value, but average of anisotropic
286	Time 0s; no heating					components was not calculated.
287						
288	TNT/NA2S.9H2O				2.0038	One broad, asymmetric line
289	(5.C.8)				2.0038	
290	Temp	100				
291	Time 1000s				2.0049	Room temp. value at end of heating run. Additional anisotropic
292						components visible at low-field.
293						
294						

Appendix B.   Correlation of reaction conditions and presence or absence of Tar.

	A	B	C	D	E	F
1	Mixture		hfsc's	g Radical	g Tar	COMMENTS
295	TNT/CaH2 (5.C.9)					
296					1.9999	Single line observed in the unheated mixture
297	Temp	25			1.9999	20 h later, w/o any heating.
298	Time 0 s; no heating					Extraordinarily low g-values.
299						
300	TNT/CaH2					
301	(5.C.9)		CaH2 line	1.9999		Complex mixture of species: TNT-nitroxide, Tar, and CaH2 line;
302	Temp	100		1.9994		eventually decayed to just Tar and CaH2 line. Very low g-values.
303	Time 4200s		Tar line		2.0049	
304					2.0048	
305						
306	TNT/Ca(OH)2 (5.C.11)					
307					2.0048	Strong Tar line initially; then TNT nitroxide became clearly
308	Temp	100	nitrox	2.0056	2.0048	evident (350s), but then gradually faded.
309	Time 2450s				2.0049	
310					2.0048	Room temp. spectrum, after heating. No nitroxide evident.
311						
312	TNT/HCl (5.D.1)					
313					2.0037	Weak nitroxide spectrum eventually replaced
314	Temp	242				by this Tar line at 9000 sec.
315	Time 9000s					
316						
317	TNT/HCl (5.D.2)					
318						Respectable TNT nitroxide spectrum, with slow growth
319	Temp	249				of Tar line.
320	Time 5100s					
321						
322	TNT/HCl (5.D.3)					
323			1.081	2.0056		Unremarkable growth of Tar-asymmetry into the
324	Temp	244				nitroxide spectrum.
325	Time 5200s					
326						

Appendix B.   Correlation of reaction conditions and presence or absence of Tar.

	A	B	C	D	E	F
1	Mixture		hfsc's	g Radical	g Tar	COMMENTS
327	TNT/HNO3 (5.D.4)		0.831	2.0037		Early three-line spectrum: NOTE low g-value! (Could this suggest NO2 + H3CAr ---> Tar?)
328						
329	Temp	245	1.087	2.0057	2.0034	Replaced with TNT-nitroxide plus (eventually) Tar.
330	Time 5700s				2.0035	
331						
332	TNT/HNO3 (5.D.5)				2.0033	Normal nitroxide + Tar.
333					2.0033	
334	Temp	245				
335	Time 1730s					
336						
337	TNT/HNO3 (conc) (5.D.6)		0.808	2.0037		Three-branch radical; NOTE low g-value.
338						
339	Temp	245			2.0038	Superceded by (TNT nitroxide?) + Tar.
340	Time 4380s				2.0036	
341						
342	TNT/H2O (2.B.9)		1.083	2.0057	2.0033	Standard growth of Tar into nitroxide spectrum.
343						
344	Temp	245				
345	Time 2170s					
346						
347	TNT/H2SO4 (5.D.7)		iminoxyl 3.03	2.00367		Transient iminoxyl that barely lasted into second sweep.
348						
349	Temp	245			2.0035	Rapidly superceded by asymmetric Tar line.
350	Time 2115s				2.003	
351					2.0035	
352						
353	TNT/H2SO4 (5.D.8)		iminoxyl 3.018	2.0037		Transient iminoxyl that barely lasted into second sweep.
354						
355	Temp	245			2.0036	Rapidly superceded by asymmetric Tar line.
356	Time 3845s				2.0036	
357						

Appendix B. Correlation of reaction conditions and presence or absence of Tar.

	A	B	C	D	E	F
1	Mixture		hfsc's	g Radical	g Tar	COMMENTS
358	TNT/H3PO4					TNT nitroxide + another sharp HFS species, but could not isolate
359	(5.D.9)		1.087	2.0056	2.0032	sufficiently to characterize.
360	Temp	245	1.083	2.0057	2.0034	Very slow appearance of Tar; but when it finally dominated,
361	Time 13,310s				2.0036	sample started "popping".
362						
363						Early appearance of TNT-nitroxide. Plus another transient species.
364	TNT/H3PO4					having extremely sharp lines and spanning only about 20G.
365	(5.D.10)					Not possible to extract a g-value
366	Temp	245				
367	Time 7940s		1.082	2.0057	2.0033	Eventually, TNT nitroxide dominated and ultimately, Tar.
368						
369	TNB/Ca(OH)2					Nitroxide-like radical HFS; with strong Tar-asymmetry.
370	(9.B.2)			2.006	2.005	Suggests that Meisenheimer may play important role in all this chen
371	Temp	244			2.005	But intermediate g-value suggest Meisenheimer-Tar is unusual.
372	Time 1100s					
373						
374	TNB/Ca(OH)2					Nitroxide-like radical HFS; with strong Tar-asymmetry.
375	(9.B.3)					Suggests that Meisenheimer may play important role in all this chen
376	Temp	168		2.006	2.005	But intermediate g-value suggest Meisenheimer-Tar is unusual.
377	Time 3300s				2.0037	(late value of Tar g-value)
378						
379	TNB/Ca(OH)2/H2O					Mixture of nitroxide-type species plus Tar.
380	(9.B.4)					
381	Temp	166				
382	Time 2560s					
383						
384	TNь/Ca(OH)2/H2O			2.0059	2.0049	Initial spectrum has span of only 18.14 G: Looks like
385	(9.B.5)					aN = 8.46; a1H = 11.44; a3H = 2.64.
386	Temp	166				Then Tar asymmetry grew in at a rather high g-value.
387	Time 6000s					But intermediate g-value suggest Meisenheimer-Tar is unusual.
388						
389						
390						
391						

Appendix B.   Correlation of reaction conditions and presence or absence of Tar.

	A	B	C	D	E	F
1	Mixture	hfsc's	g	Radical	g Tar	COMMENTS
392	CONDITIONS OF LITTLE OR NO TAR CONVERSON					
393						
394	"PRODUCT A"	aN				Material isolated by benzene extraction of bulk TNT thermolysis.
395		0.907 2.0054				
396		a2H				
397		0.32				
398						
399	HMB/HNO3	aN				Three-line spectrum, plus other weak structure; intensities are not
400	(12.A.1)	1.41 2.0059				textbook-perfect; some posible hint of Tar as well, but not sure.
401						
402	4-NT/HMB-d18					Spectral asymmetry; anomolous broadening @ hi temp, less @ low T
403						(Reverse of normal expectations.)
404	Temp 230-200-180					
405	Time 11100s					
406						
407	3-NT/HMB-d18					Symmetric spectrum; anomolous broadening @ hi temp, less @ low T
408						(Reverse of normal expectations.)
409	Temp 220-200-160					
410	Time 11050s					
411						Early, familiar, weird 4-branch spectrum lost lo-field line at lo temp;
412	2-NT/HMB-d18					This is an important observation;
413						two species; aN(residue) = 8.3 G.
414	Temp 260-195-160					Early spectrum like 2,6-DNT on P1657.
415	Time 3650s					
416						
417	NB-d5/Toluene					Low-level secondary species--fairly constant.
418						
419	Temp 250					
420	Time 920s					
421						
422	NB-d5/MeCyclohex					Evolving spectra, but no clear sign of Tar.
423						Nitroxide nitrogen attached to ring, rather than methyl group.
424	Temp 204					
425	Time 2300s					

Appendix B. Correlation of reaction conditions and presence or absence of Tar.

	A	B	C	D	E	F
I	Mixture		hfsc's	g Radical g	Tar	COMMENTS
426						
427	NB-d5/Tetralin					Evolving species ratios; not quite sure if Tar is present. Not really sure about purity of starting Tetralin.
428						
429	Temp	203-70-250				
430	Time 7350s					
431						
432	NB-d5/Decalin					Clearly two different g-values (dB= 1.7G); not sure if Tar contributes to spectral asymmetry
433						
434	Temp	200				
435	Time 2660s					
436						
437	NB-d5/isoOctane					Multiple species; evolving ratios; different g's and aN's; low temperatures; no Tar evident.
438						
439	Temp	224				
440	Time 3000s					
441						
442	2,4-DNT/HMB-d18					3-Branch pattern; "normal" anomalous broadening--worse at No signs of Tar, even at lo temp.
443						
444	Temp	222-200-98				
445	Time 6800s					
446						
447	NB/HMB-d18					No signs of Tar; pronounced anomalous linewidth effect
448						
449	Temp	200				
450	Time	6400				
451						
452	NB-d5/o-Xylene					Assignable spectra, but also two extra, symmetric lines in wings. No strong evidence of Tar Nitroxide spectrum very weak at 150, but came back at 250C.
453						
454	Temp	250-150-250				
455	Time 5100s					
456						

Appendix B.   Correlation of reaction conditions and presence or absence of Tar.

#	A	B	C hfsc's	D g Radical g	E Tar	F COMMENTS
1	Mixture					COMMENTS
457	2-NT/o-Xylene					Ill-resolved spectra; weak Some asymmetry that may possibly arise from Tar, but not sure.
458						
459		Temp	200-250			
460		Time 14850s				
461						
462	2-NT/m-Xylene					Ill-resolved spectra; weak Some asymmetry that may possibly arise from Tar, but not sure.
463						
464		Temp	243			
465		Time 4650s				
466						
467	2,4,6-TriPhNB/HMB-d18					Symmetric, clean nitroxide spectra; no signs of Tar.
468			aN			Still present 4 days later; anisotropic g values measured as:
469		Temp	230 1.373	2.0061		<2.02081, 2.004581, 1.984519> = <2.0033>
470		Time 12750s				<2.020998, 2.004556, 1.984168> = <2.0032>
471						It is strange that these averages are so much lower than measured
472						isotropic value--unless it converted to Tar during 4 day storage.
473						
474						
475						
476	TNB/HMB-d18		aN			No signs of Tar until temp was reduced below 100. Then anisotropy
477			1.008	2.0058		became so strong that it sort of looks like Tar.
478		Temp 220-200&lower				
479		Time 800s				
480						
481	neat TNB					Possible weak line toward end of run--otherwise, so signals
482						
483		Temp	244			
484		Time 7200s				
485						
486	TNB/Anthracene					Early TNB-nitroxide plus another species which was centered
487						at the Tar g-value, but had 1:2:1-structure
488		Temp	201			Is this Tar related or not?
489		Time 11280s				Additional, symmetric fine structure appeared toward end of run
490						

Appendix B.   Correlation of reaction conditions and presence or absence of Tar.

	A	B	C	D	E	F
1	Mixture	hfsc's	g	Radical g	Tar	COMMENTS
491	TNT-d5/KG/HMB-d18					Well behaved, clean spectra; rather large aN (12G)
492		aN				High g-value!
493	Temp	167	1.201	2.006		
494	Time 2280s	aD				
495		0.158				
496	HPic/TNT					Multiple species of iminoxyl-type radicals
497		Iminoxyl				Some low-level (nitroxide?) during experiment.
498	Temp 200-24	aN			2.0043	Only one iminoxyl at end of run (plus two satellites).
499	Time 3050s	2.871				
500						
501	2,6-DNT/xsHMB			2° corr		Remarkably clean nitroxide spectra; stable over long period; no Tar
502				2.0061		evident. aN=12.88; aCH2 10.17; aH=1.07;a3H=1.16
503	Temp 195					
504	Time 11000s					
505						
506	2-NT/xsHMB			uncorr		5-Branch nitroxide plus another asymmetrically placed species
507				2.0061		Compare these spectra to those
508	Temp 256-237				2.0041	with the "weird" 4-branch patterns
509	Time 2470s					
510						
511	neat TNT-d5	Nitrox	2°corr			3-branch pattern, aN=8.4; unequal intensities (weak lo-field line)
512		0.793	2.0037		2.0035	Multiple species suggested. With time, center line got relatively more
513	Temp 240					intense, but not at all sure if it is due to Tar.
514	Time 5400s					Unusually low g-value for TNT--not TNT?
515						
516	4,6-DNAnth/Benzene					Weak multiple line spectrum at 250; never got very strong;
517						survived cooling and re-heating; never developed into Tar.
518	Temp 100-250					
519	Time 17000s					
520						
521	NB-d5/Toluene-d8					Multiple species; but no Tar.
522						
523	Temp 250					
524	Time 3440s					

Appendix B.   Correlation of reaction conditions and presence or absence of Tar.

	A	B	C	D	E		F
	Mixture		hfsc's	g	Radical g	Tar	COMMENTS
1							
525							
526	TNT/PBN/S2O4=						Observed only the nitrone nitroxide.
527	(8.A.4)	aN					
528	Temp		103	1.466	2.0058		
529	Time		4625	1.464	2.0058		
530							
531	TNB-CH2OH/Benzene						Nice, symmetric nitroxide spectrum while heating.
532	(10.A.1)	aN					One week later, sealed tube still had intense signal; lines were quite
533	Temp		149	0.808	2.0039		sharp and symmetric spectrum exhibited extraordinary resolution.
534	Time 1500s +1 wk						Note that this nitroxide-like radical has tar-like g-value.
535							
536	TNB-CH2OH/Benzene						Spectrum started out with rich fine structure; broadened
537	(10.A.3)	aN					when temperature was reduced; returned when elevated.
538	Temp		254	0.788	2.0039		Radical persisted at room temperature, when g-values were
539	Time						measured. Note that this nitroxide-like radical has tar-like g-value.
540							
541	TNB-CH2OH/TNT						Initially complex mixture of radicals evolved to a fairly clean nitrixid
542	(10.C.1)	aN					species at 1300s.
543	Temp		100	0.817	2.0039		Note that this nitroxide-like radical has tar-like g-value.
544	Time 3700s						
545							
546	TNB-CHO/TNB						Aldehyde had a faint odor of acetic acid from purification procedure.
547	(11.D.1)	aN		2.0048			
548	Temp		100	0.921			
549	Time 2600s		a(2H) 1.119				
550			a(2H)				
551			0.295				
552							